Developing a Single Dressing Containing both Antifungal and Antibacterial Drugs for Treating Mixed Infections in Diabetic Foot Ulcers

ASIF AHMED

A thesis submitted in partial fulfilment of the requirements of the University of Greenwich for the Degree of Doctor of Philosophy.

March 2018

DECLARATION

"*I certify that the work contained in this thesis, or any part of it, has not been accepted in substance for any previous degree awarded to me, and is not concurrently being submitted for any degree, other than that of Doctor of Philosopy being studied at the University of Greenwich. I also declare that this work is the result of my own investigations, except where otherwise identified by references and that the contents are not the outcome of any form of research misconduct.*"

_____   Mr. Asif Ahmed (Candidate)

_____   Dr J.S. Boateng (First supervisor)

ACKNOWLEDGMENTS

This thesis is dedicated to:

My baby daughter Asiya Ahmed and my wife Kaniz Fatema

ABSTRACT

The prevalence of chronic wounds such as diabetic foot ulcers (DFUs) is growing at an epidemic rate in the United Kingdom, with a high cost burden for the National Health Service and are prone to infections. Mixed bacterial-fungal infections are more complicated than single microbe infections with enhanced severity of DFUs. Moreover, recently developed medicated dressings target only either bacterial or fungal infection. This study therefore aims to develop advanced bioactive calcium alginate-based dressings that will deliver therapeutically relevant doses of broad-spectrum antibiotic and antifungal drugs to target mixed infections in DFUs. The therapeutic calcium alginate (CA) based dressings were prepared as films and wafers by solvent casting and freeze-drying technique respectively, with ciprofloxacin (CIP) and fluconazole (FLU) as model antibacterial and antifungal drugs respectively. The dressings were physically characterized by scanning electron microscopy (SEM), X-ray diffraction (XRD), Fourier transform infrared spectroscopy (FTIR) and texture analysis. Further functional characterization for exudate handling properties included porosity, water absorption (Aw), equilibrium water content (EWC), swelling index (Is), water vapour transmission rate (WVTR), evaporative water loss (EWL) and moisture content, drug dissolution by HPLC, *in vitro* antimicrobial and cell viability (biocompatibility) studies. Further, the exudate handling, antimicrobial and cell viability properties of the dressings were compared with commercial silver and CA based Algisite Ag® and hydrogel Actiformcool®. The drug loaded films were transparent, flexible, uniform, durable and elastic while drug loaded wafers were soft, uniform texture and thickness, and pliable in nature. SEM investigation showed differences in surface morphology between films (continuous sheets) and wafers (porous matrix). XRD confirmed the presence of calcium carbonate in the dressings and FTIR showed that the addition of drug caused the shift of peaks towards a higher wavenumber due to hydrogen bonding formation. Wafers showed better wound dressing properties than films and the commercial dressings for swelling, EWC (91 − 95%), Aw (1085 − 2377%) and moisture content (9 − 17%) due to high porosity. The dressings showed initial fast release followed by sustained drug release which completely eradicated all causative bacteria (*Escherichia coli, Pseudomonas aeruginosa* and *Staphylococcus aureus*) and reduced fungal load (*Candida albicans*) 10 fold within 24 h. Moreover, the medicated dressings were found to be highly biocompatible ($> 70\%$ cell viability over 72 h) with human primary adult keratinocytes and showed maximum wound closure (*in vitro* scratch assay) within 7 days. CA wafers and films appeared to be potential delivery systems for delivering antimicrobial agents to mixed infected DFUs.

CONTENTS

CHAPTER 3: FUNCTIONAL (FLUID HANDLING AND DRUG   **98-142**
RELEASE) CHARACTERISTICS OF CALCIUM ALGINATE
BASED DRESSINGS

CHAPTER 4: ANTIMICROBIAL PROPERTIES OF DRUG LOADED CALCIUM ALGINATE DRESSINGS TARGETTING BACTERIAL, FUNGAL AND MIXED INFECTIONS IN CHRONIC DIABETIC FOOT ULCERS

FIGURES

TABLES

ABBREVIATIONS

Abbreviation	Meaning
AGEs	Advanced glycation end-products
Amp B	Amphotericin B
ANOVA	Analysis of varience
API	Active pharmaceutical ingredient
ASTM	American Society for Testing and Materials
ATP	Adenosine triphosphate
Aw	Water absorption
bFGF	Basic fibroblast growth factors
BET	Brunauer-emmett teller
BLK	Blank
BSA	Bovine serum albumin
CA	Calcium alginate
CFU	Colony forming units
CIP	Ciprofloxacin
CMC	Carboxymethyl cellulose
DCU	Drug content uniformity
DFI	Diabetic foot infection
DFUs	Diabetic foot ulcers
DL	Drug loaded
DMSO	Dimethyl sulfoxide
D-PBS	Dulbecco's phosphate buffered saline
ECM	Extracellular matrix
EGF	Epidermal growth factor
EP	Electrophysical therapies
EPS	Extracellular polymeric substances
ES	Electrical stimulation

EWC	Equilibrium water content
EWL	Evaporative water loss
FBS	Foetal bovine serum
FLU	Fluconazole
FTIR	Fourier transform infrared spectroscopy
GLY	Glycerol
HA	Hyaluronic acid
HBOT	Hyperbaric oxygen therapy
HCl	Hydrochloric acid
HIF	Hypoxia-inducible factors
HLGY V	ɤHemolysin V
HPLC	High performance liquid chromatography
HPMC	Hydroxypropyl methycellulose
IGF-1	Insulin like growth factor-1
IL	Interleukin
IMS	Industrial methylated spirits
IR	Infrared
ISO	International Organization for Standardization
IUPAC	International Union of Pure and Applied Chemistry
IV	Intravenous
LB	Luria Bertani
LLL	Low level laser
M block	Mannuronic acid block
MBC	Minimum bactericidal concentration
MCP-1	Monocytes chemoattractant protein-1
MFC	Minimum fungicidal concentration
MH	Muller-Hinton
MIC	Minimum inhibitory concentration
MMPs	Matrix metallo-proteinase

MPCA	Methyl-phenazine-1-carboxylic acid
MRSA	Meticillin-resistant *staphylococcus aureus*
MTT	Methylthiazolyldiphenyl-tetrazolium bromide
Na-CMC	Sodium carboxymethyl cellulose
NCCLS	National Committee for Clinical Laboratory Standards
NPUAP	National pressure ulcer advisory panel
NPT	Negative pressure therapies
OD	Optical density
PAD	Peripheral arterial diseases
PCR	Polymerase chain reaction
PDGF	Platelet derived growth factor
PEG	Polyethylene glycol
PEMF	Pulsed electromagnetic field
PEK	Primary epidermal keratinocytes
PQS	*Pseudomonas* quinolone signal
PVP-I	Povidone iodine
PVD	Peripheral vascular diseases
RCW	Removal cast walzers
ROS	Reactive oxygen species
SB	Sabouraud dextrose
SEM	Scanning electron Microscopy
STP	Streptomycin
SWF	Simulated wound fluid
TCC	Total contact cast
T_g	Glass transition temperature
TGA	Thermogravimetric analysis
TGFβ	Transforming growth factor beta
TIMMPs	Tissue inhibitors matrix metallo-proteinase
TNF	Tumour necrosis factors

UATR	Universal attenuated total reflectance
UK	United Kingdom
US	United States
UV	Ultra violet
VEGF	Vascular endothelial growth factors
VLUs	Venous leg ulcers
WOA	Work of adhesion
WVTR	Water vapour transmission rate
XRD	X-ray diffraction
ZOI	Zone of inhibition

PUBLICATIONS

1. **Asif Ahmed**, Joshua Boateng. (2018). Calcium alginate-based antimicrobial dressings for potential healing of infected foot ulcers. *Therapeutic Delivery*, 9(3), 185-204. DOI: 10.4155/tde-2017-0104.

2. **Asif Ahmed,** Giulia Getti, Joshua Boateng. (2017). Ciprofloxacin loaded calcium alginate wafers prepared by freeze-drying technique for potential healing of chronic diabetic foot ulcers. *Drug Delivery and Translation Research,* ISSN 2190-3948, 1-18. DOI: 10.1007/s13346-017-0445-9.

3. Omar Sarheed, **Asif Ahmed**, Douha Shouqair, Joshua Boateng. (2016). Antimicrobial dressings for improving wound healing. In: Alexandrescu; (Ed) "Wound Healing", *Intech Publishers*, Croatia, (ISBN 978-953-51-4810-4)". DOI: 10.5772/63961

CONFERENCE PROCEEDINGS AND SYMPOSIA

1. **Asif Ahmed**, Joshua Boateng. "Calcium alginate dressings containing both antifungal and antibacterial drugs for potential treatment of mixed infection in diabetic foot ulcers." At the Research and Enterprise Training Institute launch event, University of Greenwich, UK, 6 December, 2017.

2. **Asif Ahmed**, Joshua Boateng. "Calcium alginate dressings containing both antifungal and antibacterial drugs for potential treatment of mixed infection in diabetic foot ulcers." At the 13th National Conference of the Primary Care diabetes society, Birmingham, England, 23-24 November, 2017.

3. **Asif Ahmed**, Giulia Getti, Joshua Boateng. "Ciprofloxacin loaded calcium alginate based dressings for potential healing of chronic diabetic foot ulcers." at the European Wound Management Association (EWMA) conference, Amsterdam, Netherland, 3-5 May, 2017, Abstract ID: 663.

4. **Asif Ahmed**, Giulia Getti, Joshua Boateng. 'Morphological and *in-vitro* biological property characterization of ciprofloxacin loaded lyophilized wafers to heal chronic leg and diabetic foot ulcers.' at the 2nd Microscopy Congress, London, UK (14-15 November 2016).

5. Ovidio Catanzano, **Asif Ahmed**, Giulia Getti, Rachel Docking, Patricia Schofield, Joshua Boateng. 'Composite Wafer Dressing for Dual Delivery of Lidocaine and Silver Nanoparticles in Chronic Wounds.' Proceedings of the American Association of Pharmaceutical Scientists (AAPS) Annual Meeting and Exposition, Denver, Colorado, November 2016, 29M0830.

6. **Asif Ahmed**, Joshua Boateng. 'Calcium Alginate Based Dressings for Healing of Diabetic Foot Ulcers.' Academy of Pharmaceutical Sciences UKPHARMSCI Conference, (5-7 September 2016).

7. **Asif Ahmed**, Joshua S. Boateng. 'Calcium Alginate Based Films for Healing of Diabetic Foot Ulcers.' 4th Faculty Research Symposium, University of Greenwich, (April 2016).

CHAPTER 1:   GENERAL INTRODUCTION AND LITERATURE REVIEW

1.1   Background and overview

The prevalence of chronic wounds, including diabetic foot ulcers (DFUs), leg ulcers, pressure ulcers and arterial ulcers are increasing rapidly in the United Kingdom (UK). It is predicted that in 20 years from 2005 to 2025, the number of patients with chronic wounds will be increased by 3.4 million from 60.4 million to 63.8 million (Posnett *et al*., 2008). DFUs are one of the most common causes of morbidity and high risk of lower extremity amputation (Singh *et al*., 2005) in diabetic patients. Globally, an estimated 15% of diabetic patients are affected by DFUs in their lifetime and this has a high cost burden for national health providers (Ravichandran *et al*., 2015). For example, in England alone, DFUs and associated amputations cost taxpayers approximately £972 million to £1.13 billion in 2014-15, which is equivalent to 0.72-0.83% of the entire budget of the National Health Service (Kerr, 2017). However, the care of all chronic wounds in 2014 was estimated at £2.17 billion and this figure is predicted to rise to about £2.38 billion by 2019 (Dowsett *et al*., 2014). The annual cost of wound dressing and other materials in wound care was £420 million in 2014, and will increase by £41 million from 2014 to 2019 (Dowsett *et al*., 2014). Therefore, the demand of developing wound dressings is increasing day by day. Medicated dressings such as lyophilized wafers and solvent cast films can reduce the cost burden because of relatively low manufacturing costs (Morales *et al*., 2011; Nagesh *et al*., 2016) compared to other advanced dressings such as tissue engineered substitutes.

Traditional wound dressings such as gauze, cotton, wool, plasters, fibres, lint and bandages were widely used in the past, and though reduced in frequency of use, they are still employed in acute wound care because of certain benefits such as absorbency and cheap cost. However, these dressings are unable to absorb adequate amounts of wound fluid and create leakage and skin maceration, which leads to inconvenience and poor patient compliance. Moreover, these dressings are unable to provide a moist environment for wound healing (Boateng and Catanzano, 2015). Therefore, there is increased demand for developing more effective advanced dressings. Modern dressings such as films, hydrogels, hydrocolloids, lyophilized wafers, and foams can create and maintain a moist environment around the wound to facilitate wound healing (Pawar *et al*., 2014; Boateng *et al*., 2015a). In addition to maintaining a moist environment, these dressings can play major roles in different stages of wound healing. For example, lyophilized wafers containing both antibacterial and anti-

inflammatory / analgesic drugs can eradicate bacterial load and at the same time reduce pain (Pawar *et al*., 2014; Catanzano *et al*., 2017).

There are some factors such as oxygenation, wound bioburden and infection, mixed infection, biofilm formation and high exudates, which impair healing of chronic ulcers. Some other patient related factors including age, physiological stress, diabetes (hyperglycaemia), obesity, smoking, alcohol consumption, medications and poor nutrition can impair wound healing (Guo and Dipietro, 2010). These inhibiting factors in wound healing can be overcome by proper diagnosis and treatment. The treatment of chronic leg and DFUs involves off-loading of the foot, revascularization, debridement, applying wound dressings and antimicrobial therapy (Burns and Kuen, 2012; Leese *et al*., 2009). Depending on the severity and condition of the patients, advanced therapies such as hyperbaric oxygen therapy (HBOT), negative pressure therapies (NPT), electrophysical therapy (EP), pulsed electromagnetic therapy and low-level laser therapy may also be required for the treatment of chronic DFUs (Braun *et al*., 2014; Boateng and Catanzano, 2015).

Wound dressing is one of the most widely used therapies in DFUs. These wound dressings can be prepared using natural and synthetic polymers through solvent casting and freeze-drying method in the form of films and wafers respectively (Pawar *et al*., 2014; Kianfar *et al*., 2013a; Boateng *et al*., 2013a; Pawar *et al*., 2013). Film dressings have been widely used in the past for the management of wounds and are currently used in health care centres. Films can be used as a primary or secondary dressing and can also be combined with other types of dressings including hydrogels, hydrocolloids and foams (Mayet *et al*., 2014). The ideal film should be transparent, flexible and pliable, with transparency allowing visual examination of the wound bed without removal whilst flexibility permits ease of application around the knees ankles and other difficult areas of the body. The semi-permeable properties allow gaseous and water vapour exchange but impermeable to liquid and bacterial contamination. However, these dressings are not suitable for highly exuding wounds such as DFUs and venous leg ulcers (VLUs) because of inability to absorb high amounts of exudates. Inappropriate use of films can cause exudate accumulation, skin maceration and fluid tapping (Fonder *et al*., 2008). The problem of maceration of exudates can be overcome by lyophilized wafers, which are highly porous in nature and have greater fluid handling capacities than films. Therefore, it can accumulate large volumes of exudate within its polymeric matrix and able to maintain moist environment without damaging newly formed tissue (Matthews *et al*., 2006).

The prevalence of mixed infections in DFUs is now becoming a challenge in healing of these chronic wounds and investigations of mixed infection in DFUs suggests that the treatment outcomes are very poor. Current studies target either only bacterial infection or fungal infection. Systemic antibiotics are mainly prescribed in this regard (Leese *et al*., 2009), however, poor blood circulation at the lower extremities of diabetic patients makes oral and intravenous (IV) administered antibiotics ineffective. Systemic antibiotics therapies are also associated with several systemic side effects such as nausea, vomiting, dizziness, erythema, tenderness, thrombocytopenia, headache and allergic reactions (Sarheed *et al*., 2016).

Ciprofloxacin (CIP) and fluconazole (FLU) are used as model drugs in this project. It is reported (Leese *et al*., 2009) that oral or IV dosage forms of CIP have been used in moderate to severe diabetic foot infection (DFI). The therapy recommended is 400 mg CIP parenterally three times a day or 500-700 mg CIP orally two times a day for moderate DFI. For severe infection, IV CIP 400 mg two times a day or oral CIP 500-750 mg two times a day along with other drugs such as metronidazole is recommended. Due to this high dose, severe side effects were reported in the clinical study (Peterson *et al*., 1989). In other clinical study (Chellan *et al*., 2012), FLU combined with standard care for fungal infection in DFUs has been shown to be superior to standard care alone. In this study, 150 mg FLU tablet was given to the patients daily and mild gastrointestinal symptoms were reported. Therefore, direct application of these therapies to the wound site appears to be a more effective alternative to systemic drug administration. In addition, medicated wound dressings require lower amounts of drug to kill or inhibit causative organisms and these act directly on the wound site thus able to avoid systemic side effects. In addition to preventing infection, the drug loaded dressings can play multiple roles at the same time such as absorbing exudate, promoting angiogenesis and cell proliferation, whereas, systemic treatments only target infections. Therefore, multifunctional wound dressings are required to tackle the complications in chronic DFUs.

This chapter describes different types of chronic wounds and reviews DFUs in more detail. Different stages of wound healing and complications at each stage have been illustrated (**Figure 1.1**). Factors associated with impaired healing of chronic leg, DFUs are also discussed and the prevalence of polymicrobial and mixed infections is elucidated. Wound management protocols of DFUs are clarified along with describing possible therapies. Different types of wound dressings available for DFUs, their advantages and drawbacks, and ideal characteristics of these dressings are critically discussed. Commercially available dressings for treating DFUs are summarised to get an idea about the choice of dressings. Advantages of medicated wound

dressings are compared with systemic antibiotic treatment in order to understand the need for developing antimicrobial dressings. The chemistry and roles of calcium alginate, (CA), CIP and FLU in wound healing are discussed to clarify the reason behind choosing the polymer and drugs. The effects of plasticizer on the dressings are also reviewed while formulation processes and techniques are described to inform the preparation of the dosage forms.

1.2   Wound healing process

Wound healing is generally considered to be a complex but much arranged process, which involves a series of interdependent and overlapping biochemical, physiological and molecular phases. These are described as haemostasis/coagulation, inflammation, proliferation (granulation tissue formation) and re-epithelialization/remodelling shown in **Figure 1.1** (Falanga, 2005). Each phase is regulated by specific biological markers and has a well-defined period during the normal healing process. The cell to cell and cell to extracellular matrix interactions are required in every phase of wound healing. These interactions are mediated by several growth factors, proteases and cytokines. Alterations in one or more of these components could account for impaired healing of chronic wounds. Each cytokine has a vital role at different phases of wound healing and their effects are not restricted in one phase of wound healing (Jurjus *et al*., 2007). The transition between wound healing phases depends on the differentiation and maturation of different types of essential cells such as keratinocytes, fibroblast, mast cells and macrophages (Guo and Dipietro, 2010). The wound healing stages summarized below need to be well understood to develop formulations (dressings) and novel technologies.
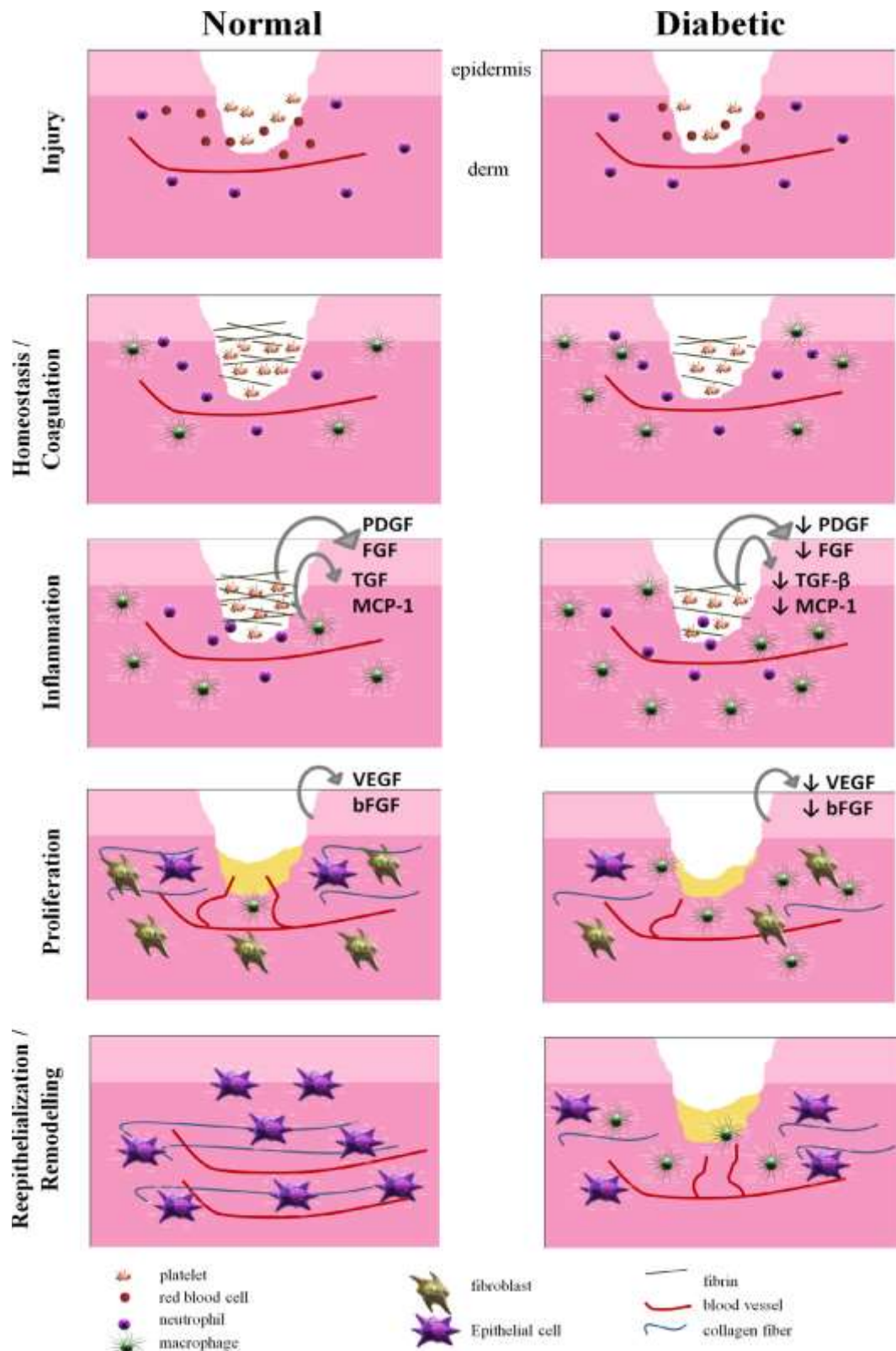
Figure 1.1   Differences in healing process of normal and diabetic wounds (adapted from Moura *et al*., 2013). [Platelet derived growth factor (PDGF), transforming growth factor beta (TGF-β), monocytes chemoattractant protein 1 (MCP-1), epidermal growth factor (EGF), vascular endothelial growth factors (VEGF) and basic fibroblast growth factor (bFGF)].

1.2.1 Haemostasis/coagulation

Immediately after injury, bleeding occurs to flush out bacteria and/or antigens from the wound site and triggers haemostasis which is initiated by formation of a fibrin plug (coagulation) consisting of platelets and provides an instant protection from the external environment and primary coverage of wound (Falanga, 2005). Aggregated platelets secrete cytokines (including leukotriene B4, platelet factor IV) and several growth factors such as PDGF, TGF-β, MCP-1), IGF-1 and EGF that recruit neutrophils and monocytes to the wound area which are extremely important for the first phase of new tissue formation process (Enoch and Price, 2004).

1.2.2 Inflammation

The inflammatory phase is initiated simultaneously with haemostasis, sometimes from a few minutes after injury up to 24 h and continues for about 3 days (Boateng *et al*., 2008). Once haemostasis has been achieved, the blood vessels dilate (vasodilation) to allow pro-inflammatory substances (growth factors) such as PDGF, TGF-β, MCP-1, IGF-1 and EGF which attract the migration of leukocytes, macrophages and lymphocytes into the wound site (Demidova-Rice *et al*., 2012). This leads to a rise in exudation of fluid into the extravascular space, therefore there may be a chance of maceration to surrounding healthy skins. Leukocytes as phagocytic cells secrete reactive oxygen species (ROS) which are antimicrobial and protease that remove bacteria, foreign bodies and damaged tissue from the wound site. The resolution of inflammatory phase is accompanied by anti-inflammatory cytokines such as TGF A1 and interleukin 1 followed by bioactive lipids such as cyclopentenone prostaglandin, lipoxins and resolvins (Grinnell, 1994). This process is completed by prevalence of macrophages which are the most important cells in the late inflammatory phase (48-72 h) that further release cytokines and growth factors such as TGF-β, PDGF and MCP-1 into the wound site, recruiting fibroblasts, keratinocytes and endothelial cells to repair the damaged blood vessels. Finally, the lymphocytes entering the wound during inflammatory phage (> 72 h after injury) may subsequently be involved in collagen and extracellular matrix (ECM) remodelling (Enoch and Price, 2004) during the next phase.

1.2.3 Proliferation

The proliferative phase occurs just after 72 h and lasts for 2-4 weeks after injury. The phase is characterized by fibroblast migration, collagen synthesis, angiogenesis and granulation tissue formation (Enoch and Price, 2004). The migration of fibroblasts activated by TGF-β and PDGF produces the matrix proteins fibronectin, hyaluronan and later collagen and proteoglycans; subsequently rebuilding the ECM to determine the synthesis and remodelling of the tissue (Grinnell, 1994). The synthesis of collagen plays a central role in wound repair because of fibroblasts migration. After injury, the collagen is exposed to blood that promotes and activates platelet aggregation and chemotactic factors. Later, synthesis of collagen becomes the foundation for ECM deposition in response to the injury (Brett, 2008). The process of forming new blood vessels usually happens simultaneously during all stages of the healing process and is called angiogenesis. The angiogenic factors such as VEGF, bFGF, PDGF, tumour necrosis factor (TNF-α) and TNF-β induce angiogenesis by macrophages (Schreml *et al.*, 2010). In addition, protease expression and activity are essential for the angiogenesis process (Singer and Clark, 1999). When the wound site is filled with new blood vessels, the demand for oxygen increases and oxygen binds to hypoxia-inducible factors (HIF), blocking its activity and stopping angiogenesis. The newly formed blood vessels will contribute to formation of granulation tissue (composed of collagen and ECM). Disturbance of this dynamic process may prolong the healing process and leads to chronic wounds (Lauer *et al.*, 2000).

1.2.4 Reepithelization/remodelling

The last phase of wound healing is reepithelization or remodelling, also known as maturation. It occurs simultaneously with the development of granulation tissue and continues for several months up to 2 years after wound closure (Boateng *et al.*, 2008). Regeneration (remodelling) of the tissue is characterized by continuous collagen synthesis and its breakdown as ECM. This molecular event is maintained by matrix metallo-proteinase (MMPs) and tissue inhibitors of matrix metallo-proteinase TIMMPs (Enoch and Price, 2004). The three major types of MMPs such as MMP-1 (collagenase), MMP-2 and MMP-9 (gelatinase) are produced by macrophages, fibroblasts and endothelia cells that facilitate formation and strengthening of collagen fibre resulting in rigid, thicker and scar tissue (Mannello and Raffetto, 2011; Schultz *et al.*, 2005). As remodelling in the wounded area establishes, the MMPs activity increases and TIMPs activity decreases (Enoch and Price, 2004).

1.2.5 Impaired wound healing

Although acute wounds usually heal linearly through the different wound healing phases, in the case of chronic wounds such as DFUs, the normal healing process is disrupted in one or more of the above-mentioned healing stages (Falanga, 2005). In the case of DFUs, the healing impairment is caused by extrinsic factors [(neuropathy, ischemia, infections) and intrinsic factors (altered bioavailability of growth factors, excess exudates, and abnormalities of ECM and tissue protease activity) (Jeffcoate *et al*., 2004)]. In addition, healing of DFUs may be impeded by the accumulation of necrotic and unhealthy tissue, slough and failure of reepithelization.

1.3   Types of wounds

According to the Wound Healing Society, a wound can be defined as the breakdown or disruption of normal anatomical structure of skin and a disturbance to its function to the immune system leading to serious morbidity and mortality (Boateng *et al*., 2008). Depending on the healing process and the clinical perspective, wounds can be broadly classified as acute and chronic.

1.3.1   Acute wounds

This kind of wound caused by mechanical injuries is superficial involving both the epidermis and superficial dermis comprising the subcutaneous layer. Mechanical injuries are associated with surgical incisions, abrasions, tears and lacerations. Acute wounds heal within the expected time, usually 8-12 weeks (Boateng and Catanzano, 2015) due to sufficient blood supply to the infected area. This wound progresses through an orderly sequential trajectory of haemostasis, proliferation, maturation and remodelling. Haemostasis is initiated by platelet aggregation and fibrin clot formation. The release of macrophages and neutrophils prevent bacterial infection and initiates wound healing (Dreifke *et al*., 2015). As healing progresses, new healthy tissues as well as collagen are synthesized and hence promoting wound closure (Nicks *et al*., 2010).

1.3.2   Chronic wounds

Chronic wounds arise from tissue destruction of all layers in the skin including epidermis, dermis and subcutaneous fat tissue that causes prolonged healing times beyond 12 weeks and may linger for months or years. They are associated with predisposing factors such

as diabetes, shock, chronic renal and hepatic failure that might disturb the balance between wound bioburden and the patient's immune system or hinder the wound healing cycle (Sarheed *et al.*, 2016; Nawazz, 2011). In addition, prevalence of polymicrobial and mixed infections, and poor initial treatment also contribute towards retardation in healing of chronic wounds (Roudbary *et al.*, 2014; Dowd *et al.*, 2011). The incidence of chronic wounds including DFUs, leg ulcers, pressure ulcers, venous ulcers, arterial ulcers and trauma, is increasing dramatically due to obesity, aging population, alcoholism, smoking, stress, poor nutrition, ischemia, venous stasis disease, or prolonged pressure (Guo and Dipietro, 2010). Different types of chronic wound are illustrated (**Figure 1.2**) and discussed in detail.

Figure 1.2   Different types of chronic wounds such as arterial ulcer (A), venous ulcer (B), diabetic foot ulcer (C) and pressure ulcer (D) (Reproduced from Fonder *et al.*, 2008).

1.3.2.1 Diabetic foot ulcers (DFUs)

Diabetic patients are susceptible to infections of foot ulcers due to peripheral neuropathy followed by ischemia from peripheral vascular disease (PVD) resulting in poor circulation and weakened neutrophil function (Alavi *et al.*, 2014). Neuropathy in diabetic patients plays a major role in impairing sensations and motor functions and disturbances in autonomic components of the nervous system leading to ulceration. The loss of sensation produces anatomic foot deformities which gradually cause skin breakdown and exacerbates the development of ulceration (Pendse, 2010). Therefore, the underlying tissues are susceptible to bacterial and fungal colonization leading to foot infection. Further, autonomic neuropathy is associated with diminishing sweat and moisturizing factors, leading to dry skin which is increasingly vulnerable to fissures and a subsequent development of infection (Mousley, 2007). The PVD is due to atherosclerosis in which blood vessels become narrowed which limits the flow of blood and oxygen resulting in ischemia. The severity of PVD depends upon several factors such as severity of diabetes and dyslipidemia, obesity, smoking, hypertension and a family history of atherosclerosis (Kevin *et al.*, 2013).

Many of the other issues related to the occurrence of DFUs are progressive atrophy of skin connective tissue, reduced pro-collagen synthesis, proliferative capacity and number of fibroblasts and a high level of tissue degrading MMPs. Furthermore, hyperglycaemia and oxidative stress contribute to nerve dysfunction and ischemia concerning abnormal glycation of nerve proteins and inappropriate activation of protein kinase C (Farzamfar *et al.*, 2013). ECM deposition is another complication of DFUs. ECM is an essential cellular component, which initiate biochemical and biomechanical cues required for tissue morphogenesis, differentiation and homeostasis. In addition to ECM dysfunction, the excess of MMPs and lack of TIMMPs cause impaired keratinocyte migration and leukocyte function leading to inadequate repair of tissue during wound closure resulting in subsequent development of foot infection (Dreifke *et al.*, 2015). Classification of DFUs is needed to better describe the condition of a foot ulcer to facilitate the choice of appropriate dressing for improving wound healing. Various classifications have been used to describe diabetic foot lesions, but none of them has been recognised universally. Amongst all these systems, the Wagner-Meggitt is the most accepted method and described by Meggitt (1976) and Wagner (1982) as shown in **Table 1.1** (Jain, 2012; Ahmad J, 2015).

Table 1.1. Classification of DFUs by Wagner-Meggitt method

Grade	Characteristics	
Grade 0	No breakdown of skin (foot symptoms like pain only)	
Grade 1	Superficial ulcers	
Grade 2	Deep ulcer to tendon, bone or joint	
Grade 3	Ulcers with bone or osteomyelitis	
Grade 4	Forefoot gangrene	
Grade 5	Entire foot gangrene	

The University of Texas, US further developed an advanced classification based on stages using the traditional grading system. This system is now broadly used in many diabetic foot centres and clinical trials as illustrated in **Table 1.2** below (Jain, 2012).

Table 1.2. University of Texas grades for DFUs classification

Stage	Grade			
	Grade 0	Grade 1	Grade 2	Grade 3
Stage A	Pre-ulcerative site or healed ulcers (completely epithelized	Superficial ulcers (including epidermis and dermis, but not to tendon, capsule or bone)	Ulcers penetrating to capsule or tendon	Ulcers penetrating to bone or joint.
Stage B	Infection present	Infection present	Infection present	Infection present
Stage C	Ischemia present	Ischemia present	Ischemia present	Ischemia present
Stage D	Infection and ischemia present	Infection and ischemia present	Infection and ischemia present	Infection and ischemia present

1.3.2.2 Pressure ulcers

Pressure ulcers are caused by constant pressure occurring in the lower regions of the body such as sacrum, coccyx or hip areas and on the lower extremities. The prevalence of pressure ulcers in bony prominence of the body such on the heel is increasing day by day. About 70% of all pressure ulcers occur in elderly people between 70-80 years of age (Agale, 2013). However, around 10% of pressure ulcers are caused by multiple medical devices such as feeding tubes, endotracheal tubes, tracheostomy tubes, cervical collars and positive pressure airway masks. The development of pressure ulcers depends on multiple factors such as

sustained compression of soft tissue, localized pressure, interface pressure, shear, moisture and friction (Monfre, 2016). Once pressure ulcers have been identified, the ulcers are categorized into different stages to determine the treatment plan. The National Pressure Ulcer Advisory Panel (NPUAP) has defined the different stages of pressure ulcers (NPUAP, 2016) and these are summarised and illustrated in **Table 1.3** and **Figure 1.3** respectively.

Table 1.3. Classification of pressure ulcers by NPUAP.

Stage	Characteristics
Stage 1	Non-blanchable erythema in which skin breakdown does not occur but it may appear as darkly pigmented with slight pain.
Stage 2	Partial thickness of skin loss from epidermis or dermis presenting as shallow open ulcers with red pink wound bed but without slough.
Stage 3	Further destruction of skin in which adipose (fat) is visible in the ulcers categorized by full thickness skin loss.
Stage 4	Full thickness tissue loss with exposed bone, tendon and muscle.
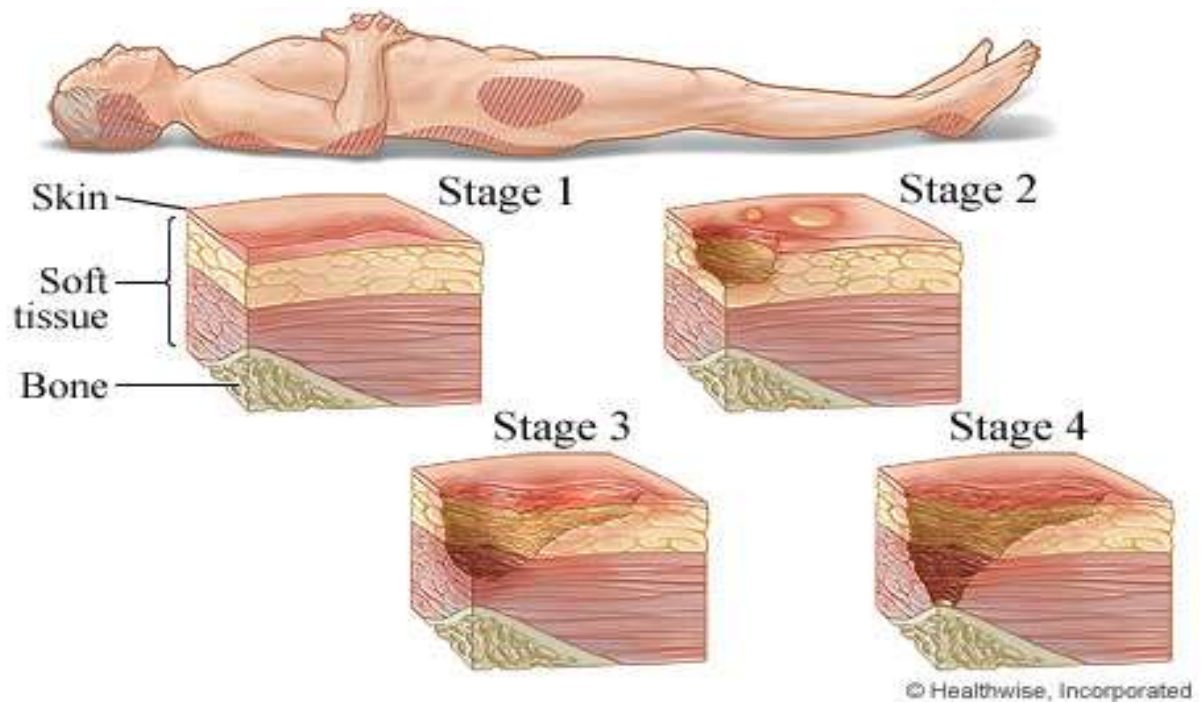
Figure 1.3 Stages of pressure ulcers (adapted from http://www.webmd.com/skin-problems-and-treatments/four-stages-of-pressure-sores).

1.3.2.3 Venous leg ulcers

Venous leg ulcers (VLUs) are open skin lesions that occur between the ankle and the knee because of chronic venous insufficiency (Kerin, 2013). The prevalence of VLUs is more common in women and older (60-80 years) people. In the UK, the prevalence of VLUs is about 1-2% of the general population and it costs £400-600 million per year (Kerin, 2013). In the United States (US) approximately 1 million people develop VLUs and the treatment budget is about 2.5 billion dollars annually (Agale, 2013; Cerman *et al.*, 2016). Venous insufficiency is the most common cause of lower extremity ulceration and responsible for 80% of all leg ulcers (Agale, 2013). VLUs are also associated with venous hypertension, in which venous pressure in deep veins, is reduced below normal pressure during ambulation and raised in orthostatic position. The venous hypertension is attributed to leakage of fluid out of the stretched vein into the tissue, leading to accumulation of brownish/red pigment in the gaiter area of the leg. Other risk factors of VLUs include age, sex, race obesity, family history, lifestyle, phlebitis, congenital vein dysfunctions, varicose veins, calf muscle pump failure and number of pregnancies (Agale, 2013). VLUs are explained by three major theories such as fibrin cuff theory, leukocyte entrapment theory and microangiopathy theory (Irving and Hargreaves,

2009). Chronic VLUs take a long time to heal, which is attributed to physical and psychological imbalance and negatively affect patient's social status (Faria *et al*., 2011).

1.3.2.4 Arterial ulcers

Arterial ulcers are the result of reduced blood supply to the lower limb due to arterial insufficiency. The ulcers can develop when arteries become narrowed or blocked and therefore the skin becomes starved of oxygen and nutrients. This hypoxic condition is called ischaemia which might lead to ulceration (Agale, 2013). The most common cause of ischaemic leg ulcers is atherosclerosis of medium and large sized arteries. Some other risk factors of atherosclerosis include diabetes, tobacco use, dyslipidaemia, hypertension, thromboangitis, vascilities, pyoderma gangrenosum, thalassaemia and sickle cell disease (Grey *et al*., 2006). Further damage to arterial system occurs with thrombotic and atheroembolic episodes which may be attributed to tissue necrosis and ulcer formation. Unlike VLUs, which arise generally between the legs and ankle, arterial ulcers are often seen over toes, heels and bony parts of the foot. The ulcerations are often painful, unless the patient has lost sensation. Arterial ulcers can be improved by restoration of arterial functions through revascularization and failure of revascularization leads to limb amputation in patients with arterial ulcers. However, stem cell therapies are now under investigation for treating arterial ulcers (Demidova-Rice *et al*., 2012).

1.4   Factors affecting healing of chronic leg and DFUs

Multiple factors that impair chronic wound healing can be classified as local and systemic factors. Local factors such as oxygenation, infections (poly-microbial and mixed infections), foreign bodies and venous insufficiency directly influence the repair of wounds, while systemic factors such as age, gender, sex hormones, stress, ischaemia, diabetes, obesity, medications, alcoholism and smoking and nutrition affect the individual's ability for wound healing (Gua and Dipietro, 2010). Both factors are correlated and can act synergistically to impair wound healing.

1.4.1   Oxygenation

Oxygen is an important element, which plays a vital role in every stage of wound healing by stimulating angiogenesis, keratinocyte differentiation, migration and reepithelization, increasing fibroblast proliferation and collagen synthesis, and promoting wound closure (Rodriguez *et al*., 2008). The basic role of oxygen is to produce adenosine triphosphate (ATP) by oxidative phosphorylation and the ATP provides energy, which is essential for proper

regulation of cellular functions (Semenza, 2000). After tissue injury, the blood vessels cannot provide oxygen and the wound becomes hypoxic. In normal wound healing, oxygen promotes production of cytokines and growth factors from macrophages, keratinocytes and fibroblasts (Sarheed *et al.*, 2016). In chronic ulcers, the transcutaneous oxygen tension is very low ranging from 15-27 mm Hg as compared to control levels of 45-52 mm Hg (Mani *et al.*, 1986). This hypoxic condition in chronic DFUs is associated with systemic factors such as age and hyperglycaemia, which induce poor oxygenation through impaired vascular flow and retard the healing process. Aged skins are less mobile to fibroblasts, which reduce turnover of keratinocytes to the epidermis and promote low response to simulation from growth factors. Therefore, the impaired cellular activity results in shrinking granulation tissue formation and reepithelization, hence preventing wound healing (Enoch and Price, 2004).

1.4.2 Wound bioburden

Wound bioburden refers to the microbial load, microbial diversity and prevalence of pathogenic organisms in the wound (Gardner and Frantz, 2008). Wound bioburden is very common in chronic leg and diabetic foot ulcers due to loss in integrity of tissue structure, which become susceptible to microbial colonization. It has been reported that a microbial load greater than 10^5 colony forming units (CFU) per gram (g) of host tissue represents increased bioburden or critical colonization (Spichler *et al.*, 2015). This microbial load may be higher in DFUs and other chronic wounds. According to wound care guideline, the microbial load in chronic wounds such as VLUs, DFUs, pressure and arterial ulcers is greater than 10^6 CFU/g of tissue (Chronic Wound Care Guidelines (web), 2006). Increased bioburden may engulf the host defence ability without triggering a generalized immunological reaction and may lead to infection (Richard *et al.*, 2012). However, prevalence of multiple species of pathogenic organisms in chronic wounds could be more crucial than microbial load in promoting infection. It has been reported that chronic wounds may contain several species of microbial organisms in a single wound bed and that induces poor healing rate (Bowler, 2003; Trengove *et al.*, 1996). According to experts and clinical studies, foot ulcerations are highly prone to colonization by various pathogenic organisms including *Staphylococcus aureus* (*S. aureus*)*, Streptococcus* spp*, Enterococcus* spp*, Clostridium perfringens* (*C. perfringens*)*, Enterobacteriaceae* spp, *Pseudomonas aeruginosa* (*P. aeruginosa*) and *Stenotrophomonas maltophilia* (*S. maltophilia*) that may cause delayed wound healing and infection (Bowler *et al.*, 2001; Edmonds, 2009).
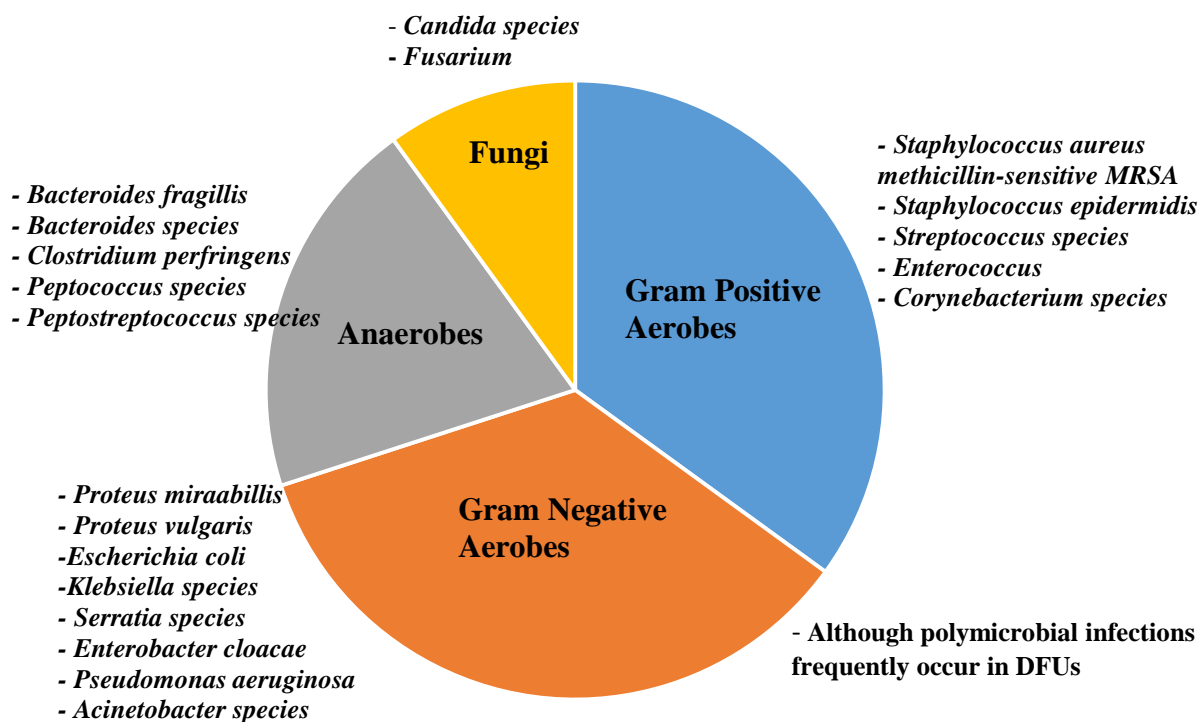
Figure 1.4 The prevalence of causative microorganisms in DFUs (adapted from Frykberg *et al.*, 2006).

1.4.3 Wound Infection

Human skin can resist 10^5 colonies of microflora without any clinical problems (Kerr, 2012). However, further increments in the number of microbial colonies overwhelm host resistance, resulting in invasion and multiplication of the organisms. Depending on the state of infection and replication of microorganisms, wounds can be classified as contaminated, colonized, local /critical colonized and invasive infected (Guo and Dipietro, 2010). Contaminated wound refers to the presence of microorganisms on the wound surface without any replication, while colonized wound is the multiplication of microorganisms on the wound surface without invading underlying tissue. Local infection/critical colonization is defined as the multiplication of microorganisms on the wound surface and initiation of local tissue response, while invasive infection is the prevalence of replicating microorganisms within a wound which leads to inflammatory responses with tissue damage (Guo and Dipietro, 2010; Gardner and Frantz, 2008).

In the case of chronic leg ulcers, microorganisms start replicating rapidly and infection will arise once tissue is damaged. This high microbial load will prolong inflammation due to

17

prolonged elevation of pro-inflammatory cytokines such as interleukin-1 and TNF-α, which causes delay in wound healing beyond 12 weeks (Menke *et al*., 2007). The prolonged inflammation is also associated with inhibiting ECM formation by upregulating MMPs. The degradation of ECM subsequently retards proliferation and cell migration, which impairs wound healing. From a microbiological perspective, the healing of chronic ulcers is overwhelmed by both bacteria and endotoxins, and exhibits signs and symptoms of infection. There are several risk factors associated with increased incidence of infection in DFUs compared to other chronic wounds. It has been reported that the role of stress and compressive force leads to overgrowth of bacteria and therefore results in reduced function of macrophages and neutrophils (Falanga, 2005). In addition, hyperglycaemia and other metabolic factors favour hypoxic conditions in the wound, which adversely affects neutrophil and macrophage function (Sharma *et al*., 2006).

1.4.3.1 Bacterial and polymicrobial infection

Chronic leg and DFUs are usually highly exuding wounds with protein rich wound bed, which is highly susceptible to bacterial growth. The most predominant bacterial species in DFUs are *S. aureus*, together with other aerobes including *S. epidermidis*, *Streptococcus* spp, *P. aeruginosa*, *Enterococcus* spp (Gardner and Frantz, 2008). Several clinical studies have reported that *S. aureus* is the most prevalent bacteria in DFUs. Sharma and co as well as Abdulrazak and co-workers reported that *S. aureus* was isolated from DFI in about 38.4% of cases, whilst *P. aeruginosa* and *Proteus mirabillis* (*P. mirabillis*) were about 17.5% and 18% respectively (Sharma *et al*., 2006; Abdulrazak *et al*., 2005). In another study, Sotto *et al* investigated DFUs infected only by *S. aureus* and they identified five virulence genes isolated from *S. aureus* strain by polymerase chain reaction (PCR) method. The virulence genes were capsular type 8 (cap8), Staphylococcus enterotoxin A, Staphylococcus enterotoxin I, LukDE leukocidin (lukD/lukE) and ʏhemolysin V. Finally, they concluded that amongst the five genes, LukDE was the most favourable outcome for infection resolution or healing of uninfected DFUs (Sotto *et al*., 2008).

The prevalence of methicillin-resistant *S. aureus* (MRSA) is significantly higher in DFUs (Tentolouris *et al*., 2006). In a study, 84 patients with infected DFUs were investigated and it was found that the prevalence of *S. aureus* was the most common and approximately 50% of the isolates were resistant to methicillin (Chita *et al*., 2013). MRSA infections can be acquired by prolonged and repeated hospitalizations, community, pre-broad-spectrum antibiotic therapy and the presence of surgical wounds and are associated with worse outcomes

in patients with DFUs (Lipsky *et al.*, 2004). Another severe infective bacterium is *P. aeruginosa*, which causes extensive tissue damage in DFUs, including osteomyelitis, septic arthritis and bacteremia (Edmonds, 2009).

Polymicrobial infection is another factor that impairs chronic wound healing and DFUs are usually associated with this type of infection. It is reported that polymicrobial infection is responsible for approximately 85% of the amputations among patients with DFI. This can be explained by the prevalence of both Gram-positive and Gram-negative bacteria present together in the wound bed. Several risk factors such as hyperglycaemia, loss in immunogenic response, neuropathy and peripheral arterial disease leads to limb-threatening DFI (Frykberg *et al.*, 2006). In a recent microbiology study of 427 positive cultures, it was found that about 84% of the infections were polymicrobial (Imirzalioglu *et al.*, 2014). Polymicrobial infection can be induced by microbial interference where one microorganism suppresses and/or outbreeds the growth of other microorganisms (Imirzalioglu *et al.*, 2014).

1.4.3.2 Mixed infections

Mixed infection refers to the presence of both bacteria and fungi in the wound bed. Mixed bacterial and fungal infections have been reported in 21.4% of patients and fungal infections alone in 5.8% of patients with diabetic foot wounds (Chellan *et al.*, 2010). In another study, mixed (fungal-bacterial) infections were found in about 68.2% (of 22 patients) of cases and fungal infection alone was 31.8% (Missoni *et al.*, 2005). In another clinical study, fungal and mixed foot ulcer infections were reported in about 14.9% of diabetic patients (Missoni *el al.*, 2006). This study identified 15 yeast species from genera Candida, Cryptococcus, Trichosporon and Rhodotorula. They revealed that *Candida parapsilosis* (in 61.5% of patients), and *Candida albicans* (*C. albicans*) and *C. tropicalis* (in 10.8% of patients each) were the most causative agents of fungal and mixed infections. Fungal infection alone has now become severe in inducing onychomycosis in the toes and nails of diabetic patients, as well as the association of these infections with the development of severe and deep inflammatory process in the feet (Winston and Miller, 2006; Mohamed, 2013). In a survey, it was found that onychomycosis was associated with 82% of dermatophytes (primarily *Trichophyton rubrum*) and 7% C. *albicans* isolates (Kemna and Elewski, 1996).

The non-treatment of fungal infection may lead to secondary bacterial infection creating mixed infection and subsequently cause foot ulceration, paronychias, cellulitis, gangrene, osteomyelitis and lower limb amputation (Chadwick, 2013). The mixed infection can be

developed through initial fungal infection, leading to fissures in the epidermis, facilitating bacterial entry and may work synergistically to create a deep-seated infection (Chadwick, 2013). The complication of mixed infection in DFUs can be severe, with the patients being unaware of fungal infection due to loss of sensation (neuropathy). Moreover, peripheral arterial disease and vascular insufficiency can supress tissue viability and subsequently stop wound healing. As shown by epidemiologic data, 85% of the amputations among the patients with DFUs have been attributed to mixed infections (Chadwick, 2013). It is reported that bacteria and fungi can communicate among themselves by physical interaction and induce biosynthesis genes (Schroeckh *et al*., 2009). For example, the interaction between C. *albicans* and *P. aeruginosa* in the respiratory tract can increase the risk of ventilator-associated pneumonia and candidaemia (Peleg *et al*., 2010).

1.4.4 Biofilm

According to Donlan and Costerton, a biofilm is defined as "a microbially derived sessile community, characterized by cells that are irreversibly attached to a substratum, an interface or to each other. These cells are encased in a matrix of extracellular polymeric substances (EPS) which they have produced and exhibit an altered phenotype with respect to growth rate and gene transcription" (Donlan and Costerton, 2002). The first step of biofilm development is the attachment of pioneering bacteria in which a solid surface (composed of protein and polysaccharide) and blood or water provides a suitable environment for bacterial attachment and growth. After that, the bacterial cells initiate approach to and adherence onto the surface by van der Waals forces. The cells then start proliferating and produce small aggregates or micro-colonies within the biofilm under construction (Sarheed *et al*., 2016). In the next step, bacterial cells start communicating to each other, which is essential for biofilm formation, including EPS production, synergistic or antagonistic interactions between cells and alteration in bacterial phenotypic characteristics. This communication by auto-inducers is known as quorum sensing, which is responsible for the regulation of gene expression and in response to fluctuations in cell density (Richard *et al*., 2012). Finally, bacteria are embedded in EPS polymeric matrix and form three-dimensional mushroom like architecture called mature biofilm. At this stage biofilm shows maximum resistance to antibiotics.

Biofilm formation is a very common complication in the healing of DFUs. It was found in 38% (of 82 patients) patients with DFUs and 20% of this was caused by *S. aureus* (Banu *et al*., 2015). There are also several organisms associated with biofilm formation in DFUs such as

C. albicans, C. parapsilosis, and *C. parapsilosis, S. aureus, P. aeruginosa, E. coli, Klebsiella pneumoniae, Klebsiella Oxytoca, Proteus vulgaris* (Guo and Dipietro, 2010; Roudbary *et al*., 2012; Zubair *et a*l., 2011a; Malik *et al*., 2013). Current antibiotic therapies are struggling to overcome biofilms, as it requires about 100 to 1000 times' higher doses than the minimum inhibitory concentration and minimum bactericidal concentration of antibiotics (Hoiby *et al*., 2010). Several mechanisms are involved in the development of resistance of antibiotics to biofilms including:

i) Biofilm forms rigid physico-chemical layer prevents antibiotics from passing through the resulting barrier (Richard *et al*., 2012);

ii) Due to high density of bacteria into biofilm, there is increased horizontal gene transmission and therefore transfer of resistance genes;

iii) Bacterial cells simultaneously release endotoxins that may degrade antibiotics (Hoiby *et al*, 2010);

iv) Change in microenvironment may alter the potency of antibiotics;

v) The presence of persister cells in biofilms may account for resistance (Stewart, 2002). However, biofilm protects the bacteria from host defences by wrapping themselves in glycocalyx while bacteria secrete products within the film that makes phagocytic penetration poor (Sarheed *et al*., 2016).

1.4.5 High exudates (wound fluid)

Exudate is a high protein rich fluid which is derived from serum by extravasation in the inflammatory phase (Speak, 2014). It plays an essential role in wound healing process by maintaining a moist environment, promoting migration of tissue repairing cells, facilitating diffusion of nutrients, growth factors and assisting with autolysis (Romanelli *et al*., 2010; Chadwick and McCardle, 2014). However, in case of DFUs, overproduction of exudate can slow down cell proliferation, interfere with growth factor availability as well as may contain high levels of both inflammatory mediators and MMPs. Therefore, it can damage peri-wound skin, cause skin weakening and maceration, and increases risk of tissue damage (excoriation) and enlargement of the wound which slows down healing of DFUs (Speak, 2014). Furthermore, excess exudate is also attributed to risk of infection, amputation and poor quality of life of patients with DFUs.

Both excessive and very low exudate volumes can hinder the wound healing process. It is reported that third degree burns, donor sites and unspecified granulating wounds release exudates between 3.4 to 5.1 g/10 cm^2/ 24 h (Thomas (web), 2007). It was further reported that patients with chronic leg ulcers generate about 5 g/10 cm^2 exudate in a day (Thomas (web), 2007). High viscous exudate indicates high protein contents due to infection, inflammation and presence of necrotic tissue, while low exudate is also associated with ischemic ulcers and dehydration (Grey et al., 2006; White and Cutting, 2006). The management of high exudate may create high burden for health care provision by extending the healing time and increasing frequency of dressing changes that impact heavily on clinical time and use of resources. The colour of exudate may indicate type of tissue and type of bacteria present in the wound bed. **Table 1.4** below shows different types and colour of exudate and their significance to healing.

The healing of chronic leg and DFUs also depends on the pH of the wound fluid. The pH of exudate in chronic wounds is about 7.5 and reducing the pH of wound bed (weakly acidic environment) promotes wound healing. MMPs are inactivated at lower pH and therefore, suppress the inflammatory processes and promoting increased rate of epithelialization (McArdle *et al*., 2014). It is also reported that oxyhemaglobin releases more oxygen in an acidic environment, facilitating angiogenesis, keratinocyte differentiation, migration and reepithelization (Leveen *et al*., 1973). Furthermore, in acidic wound bed, the rate of bacterial replication is low and hence enhancing efficacy of antibiotics (Percival *et al*., 2014).

Table 1.4.   Colour, types of exudate and its significance (Nicholas, 2016).

Type	Consistency	Colour	Significance
Serous	Thin, watery	Clear, straw-coloured	Normal, but increase in volume may indicate infections associated with *S. aureus, P. aeruginosa, Streptococci* Spp.
Fibrinous	Thin, watery	Cloudy	Fibrin protein strands present which may indicate a response to inflammation
Serosanguineous	Thin, slightly thicker than water	Clear, pink	Indicates presence of red blood cells and indicate capillary damage
Sanguineous	Thin, watery	Reddish	Low protein content due to trauma to blood vessels
Purulent	Thick, sticky	Yellow, milky, creamy	Bacterial infection associated with *P. aeruginosa,* may contain inflammatory cells
Haemopurulent	Viscous, sticky	Reddish, milky	Presence of dead bacterial cells, neutrophils and inflammatory cells. Consequent damage to dermal capillaries leads to blood leakage.
Haemorrhagic	Thick	Dark red	Infection, Trauma, Spontaneous bleeding due to fragile dermal capillaries

1.4.6   Other factors

Age could be a major risk factor for wound healing due to altered inflammatory response such as delayed T-cell infiltration into the wound area, reduced capacity of macrophage

23

phagocytosis and reduced secretion of growth factors (Guo and Dipietro, 2010). Moreover, some other complications in aged people such as delayed re-epithelization, collagen synthesis, and angiogenesis influence can impair wound healing (Gosain and DiPietro, 2004).

Sex hormones and gender differences: Sex hormones play an important role in processing and functioning physiological system and has an impact on delaying wound healing especially in geriatric patients (Oh and Phillips, 2006). Female sex hormones such as oestrogens appear to have significant effects on wound healing (Gilliver *et al*, 2007) process including neoangiogenesis, reepithelialization and cell proliferation (Khaksar *et al*., 2010). In aged women, the oestogen production is decreased which reduces collagen synthesis and therefore, delays wound healing (Oh and Phillips, 2006). It has been reported in clinical studies on both animals and humans that topical application of oestrogens promoted wound healing significantly (Khaksar *et al*., 2011; Ashcroft *et al*., 1999). Androgens are present mainly in the male testes but also present in female ovaries and adrenal glands. Androgens play a vital role in regulating immune response and studies have revealed that it reduced the inflammatory phase in cutaneous wound healing of male mice and increased ECM deposition (Oh and Phillips, 2006, Ashcroft *et al*., 2002). Moreover, gender has also influences on healing DFUs. In many clinical studies, it has been reported that the incidence of lower extremity amputation is higher in men than women (Armstrong *et al*., 1997; Gonsalves *et al*., 2007; Otiniano *et al*., 2003). The reasons behind this observation is that men are more likely to have peripheral neuropathy, sensory neuropathy, reduced joint mobility and higher foot pressure (Peek, 2011). However, the mortality rate after lower extremity amputation is higher in diabetic women than men (Lavery *et al*., 1997a; Helaine *et al*., 2004) due to atherosclerotic complications (Pyorala *et al*., 1987) and congestive heart failure (Hambleton *et al*., 2009).

Psychological stress is also associated with impaired wound healing. Stress upregulates the secretion of glucocorticoid and cortisol hormones from hypothalamic-pituitary-adrenal gland, which results in deregulation of the immune system. The release of epinephrine and norepinephrine from sympathetic-adrenal medullary is also increased resulting in hyperglycaemia, which causes a significant delay in the healing process (Guo and Dipietro, 2010).

Diabetes is the major factor for non-healing DFUs and diabetic feet are normally hypoxic. The prolonged hypoxia can amplify the early inflammatory response, thereby leading to insufficient perfusion and insufficient angiogenesis causing impaired wound healing.

Hyperglycaemia upregulates the production of reactive oxygen species (ROS) and advanced glycation end products (AGEs) which are responsible for impaired wound healing. Neuropathy, high levels of MMPs, keratinocytes and fibroblasts dysfunction in diabetes influence delayed wound healing (Guo and Dipietro, 2010).

Medications such as corticosteroids, nitrofurantoin, neomycin sulphate, povidone iodine, chlorhexidine 2% and hydrogen peroxide interfere with platelet aggregation, inflammatory responses and cell proliferation, thereby affecting wound healing (Damir, 2011). Systemic corticosteroids heal the wounds by supressing cellular responses including collagen synthesis and fibroblast proliferation but might have the risk of wound infections (Guo and Dipietro, 2010). Though systemic administration of ibuprofen (non-steroidal anti-inflammatory drug) reduces pain and inflammation, it has negative effects on wound healing, including reduced number of fibroblast synthesis, weakened breaking strength, delayed epithelialization and therefore poor wound contraction (Krischak *et al*., 2007). Chemotherapeutic drugs such as adriamycin and bevacizumab have been reported as risk factors for impaired wound healing (Gulcelik *et al*., 2006; Gordon *et al*., 2009). Adriamycin weakens the immune function of the patients and delays inflammatory phase of healing and increases risk of infections. In addition, this agent delays cell migration into the wound site, lowers fibrin deposition and collagen production and therefore, inhibits wound constructions (Anderson *et al*., 2014). Another chemotherapeutic drug, bevacizmab acts an angiogenesis inhibitor and VEGF neutralizers that limit the nutrients, oxygen and cells' supply to the wound site, resulting in wound dehiscence and infection (Guo and Dipietro, 2010; Lemmens *et al*., 2008).

Obesity is closely connected to oxygenation that influences impair wound healing. It increases the workload of the heart resulting in reduced oxygen supply into the blood and therefore creates hypoxic condition to the body tissue (oxygenation). The hypoxic tissues near the wound site are unable to form fibroblasts from collagen and retard oxygen-dependant cellular repair (Goldman, 2009). Obese patients have the high risk of infections due to avascularity of the surrounding adipose tissue that decrease the body's ability to defend against infection. This is because, the lack of oxygen numbs the neutrophils ability to phagocytise the invading microorganisms leading to high microbial load in the wounds (Goldman, 2009; Kranke *et al*., 2012).

Socio-environmental risk factors such as smoking, alcohol consumption, improper diabetes education, poverty, racial distribution and poor personal hygiene and nutrition

contribute to impair healing of DFUs (Farzamfar *et al*., 2013). Alcohol consumption in diabetic patients increases insulin resistance, blood sugar levels and the risk of protein energy malnutrition (Markuson *et al*., 2009) due to poor eating habits. Therefore, the inflammatory and immune responses are altered including decreased neutrophil chemokines with reduced neutrophil infiltration, decreased interleukin-8 (IL-8), TNF-α production and monocytes functions and reduced macrophage function to microbes (Anderson *et al*., 2014). The above phenomena cause impaired wound healing by perturbing angiogenesis, collagen production and fibroblasts migration, increasing rate of infection and weakening scar tissue during remodelling (Anderson *et al*., 2014).

Smoking has been reported (Manassa *et al*., 2003) as one of the highest risk factors in wound healing complications. Tobacco products contain some poisonous substances such as nicotine, carbon monoxide and hydrogen cyanide. Nicotine interferes with the oxygen supply into the blood and decreases the blood flow to the tissue by narrowing blood vessels (vasoconstriction), inducing tissue ischaemia (Ahn *et al*., 2008; Sorensen *et al*., 2009). It increases the release of epinephrine by stimulating the sympathetic nervous system, resulting in peripheral vasoconstriction. Carbon monoxide present in tobacco is also responsible for tissue hypoxia. It induces deoxygenated haemoglobin into the bloodstream because it has higher binding affinity with haemoglobin than oxygen. In addition, hydrogen cyanide has the negative effect on oxygen metabolism that promotes the risk of atherosclerosis (Guo and Dipietro, 2010). In the inflammatory phase, these substances retard white cell migration, resulting in reduced number of monocytes and neutrophils that lowers host's defence against microorganisms. Therefore, it increases the risk of infection and impairs wound healing. In the proliferative stage of wound healing, these effects perturb epithelialization, fibroblasts migration, ECM deposition and hinder wound contraction (Ahn *et al*., 2008).

1.5   Wound management in chronic leg and DFUs

The basic aim of wound management is wound closure by offloading, revascularization, debridement, infection control and advanced wound care therapies (e.g. NPT, HBOT and EP methods (Chadwick *et al*., 2014; Burns and Kuen, 2012). It is very important to start treatment in the early stage of wound healing to aid prompt healing. In addition, it is also essential to identify whether the DFUs is neuropathic, ischaemic or neuroischaemic to inform the choice of appropriate treatment (Chadwick *et al*., 2014). Other extrinsic factors such as hyperglycaemia,

hypertension, hyperlipidaemia and proper nutrition need to be controlled alongside using advanced dressings.

1.5.1 Off-loading

Off-loading means removal of pressure or pressure modulation and is one of the most important techniques to manage neuropathic ulcers in diabetic patients (Yazdanpanah *et al*., 2015). Wheelchairs or crutches can be useful offloading devices to heal foot ulceration (Kruse and Edelman, 2006). There are also several other off-loading approaches such as total contact cast (TCC), removal cast walkers (RCW), scotch cast boots, windowed casts and custom splints. Among all these approaches, TCC is the gold standard and most effective off-loading technique for the healing of neuropathic DFUs (Burns and Kuen, 2012; Yazdanpanah *et al*., 2015). However, Achilles tendon lengthening with TCC showed more potential than TCC alone (Speak, 2014). TCC also has adverse effects such as skin irritation, intolerable in hot weather, difficulty in taking baths, disturbance during sleep, and high cost, which have resulted in a decline in its use (Chadwick *et al*., 2014).

1.5.2 Revascularization

DFUs are associated with peripheral arterial disease (PAD) which is characterized by both micro- and macrovascular complications (Burns and Kuen, 2012). Microvascular complications are very common in diabetic patients because of the thickening of capillary basement membrane due to inhibition of leukocyte migration, while macrovascular dysfunctions attributed to atherosclerosis in peripheral, coronary and cerebral arteries cause 80% mortality and 75% hospitalization in diabetic patients (Faries *et al*., 2004; Zibaeenezhad *et al*., 2012). Reestablishment of pulsatile arterial flow to the infected foot can be achieved by surgical revascularization which subsequently heals ischemic and neuroischemic ulcers (Burns and Kuen, 2012). However, surgical revascularization has been reported to be unfavourable for diabetic patients because of some co-morbidities such as hypertension, dyslipidaemia, systolic and diastolic heart failure, autonomic dysfunction, PAD, cerebrovascular disease, microvascular disease and nephropathy (Smith *et al*., 2002).

1.5.3 Debridement and cleansing

Debridement is an essential approach to heal DFUs promptly. It is the removal of dead tissue, peri-wound callus and foreign bodies, which creates a healthier wound bed and allows better visualization of the wound site. Debridement of tissue also significantly reduces the microbial load and stimulates release of growth factors (Burns and Kuen, 2012). There are several debridement methods applied in wound care including: surgical sharp debridement, enzymatic debridement, larval therapy and autolytic removal by rehydration of necrotic tissue. Leaper stated that "debridement, surgical debridement involving continuous tissue removal using sharp scalpel was the gold standard" (Leaper, 2002). A Cochrane review also noted that autolytic debridement with hydrogels was most effective in DFUs management based on differences in healing rates as compared to gauze or standard care (Edwards and Stapley, 2010). Maggot therapy is an enzymatic therapy in which the necrotic tissues are dissolved by proteolytic enzymes such as collagenase, serine proteases (trypsin-like and chymotrypsin-like enzymes), metalloproteinase and aspartyl proteinase secreted by the maggots (*Lucilia sericata*) (Gottrup and Jorgensen, 2011). These enzymes dissolve the necrotic tissue and allow absorption in semi-liquid form gradually over time (Boateng *et al.*, 2008). The larvae of *Lucilia sericata* do not digest living human tissue as it spares the healthy tissues necessary for wound healing (Gottrup and Jorgensen, 2011). The healthy tissues of the host are unaffected, because ECM components (such as collagen and fibronectin) of living cells are resistant to those proteolytic enzymes secreted by *Lucilia sericata* thus preventing healthy tissue degradation (Chambers *et al.*, 2003). Maggot therapy has been reported to be more effective in healing of chronic leg and DFUs than conventional surgical therapy (Sherman, 2003). The better healing properties of maggot may be due to its ability to stimulate granulation tissue production as well as to kill bacteria (Prete, 1997; Nigam *et al.*, 2006). However, in a recent review, Hinchliffe *et al* noted that, larvae therapy did not significantly improve healing time, and can lead to risk of amputation in patients with DFUs (Hinchliffe *et al.*, 2008).

After debridement, the wound bed needs to be irrigated with saline and cleansing agents such as povidone iodine, ionized silver, acetic acid, chlorhexidine, hydrogen peroxide, polyhexanide/betaine, alcohol, sodium hypochlorite and N-chlorotaurine (Winston and Miller, 2006), and an ideal dressing should be applied to absorb blood and exudates that will help accelerate initial stages of wound healing. A detailed discussion of the different types of dressings is found in the following sections.

1.5.4 Wound dressings

Wound dressings play a key role in the management of chronic DFUs. The choice of wound dressings depends on several factors that affect wound healing such as heavy exudate, microbial load, biofilms, severity of pain and infection. Generally, dressings should possess certain ideal characteristics as follows.

i.   Dressings should maintain a moist wound environment that can facilitate proliferation and migration of fibroblast and keratinocytes, transport enzymes, growth factors and hormones, promote collagen synthesis and decrease scar formation (Sarheed *et al*., 2016).

ii. Dressings should permit the observation of wounds and allow mechanical protection to the periwound area, comfortability to the patients and conformability to the wound shape (Hilton *et al*., 2004).

iii. It must absorb excess exudates and allow drainage to prevent maceration (Hilton *et al*., 2004).

iv. It should allow gaseous exchange between wounded tissue and the environment (Dhivya *et al*., 2015).

v.   It should be non-adherent to the wound and can be changed frequently and easily without causing trauma to the healing wound (Jones *et al*., 2006).

vi. It must be sterile, non-toxic, non-allergic, and inexpensive and have long shelf life (Dhivya *et al*., 2015).

vii. It should be able to inhibit microbial colonization and must be impermeable to bacteria by creating an effective barrier (Sood *et al*., 2014).

viii. It should maintain optimal temperature and pH in the wound (Sood *et al*., 2014).

However, no single dressing can fulfil all the requirements of healing due to complexities of DFUs. The classification of dressings is discussed below.

1.5.4.1 Traditional dressings

Traditional wound dressings include gauze, lint silk, cotton wool, plasters and bandages. The dressings are commonly made of natural, synthetic or semisynthetic materials and may be used as passive or secondary dressings for protecting the wound from contaminants (Dhivya *et al*., 2015). These dressings are used in low exuding wounds and are limited to simple, clean, superficial and minor burn wounds. Therefore, these dressings have been largely replaced by

more modern and advanced dressings because of the need for healing of chronic wounds such as DFUs. However, these dressings are still used sometimes because of ready accessibility in most of the surgical centres and clinics, they are cheaper and can provide some bacterial protection (Boateng and Catanzano, 2015). For example, gauze dressings made of woven or nonwoven fibres of cotton, rayon polyester or a combination of both are used in the packing of open surgical and cavity wounds (Boateng *et al*., 2008). Sterile gauze pads are also used as packing for open wounds to absorb exudates and fluids. It is reported to be used as a standard treatment for DFUs in conjunction with antibiotic treatments (Hilton *et al*., 2004). The use of these dressings is limited when the outer surface becomes moistened by heavy exudate and external fluids thus resulting in maceration to the wound sites. In addition, it is painful during changing of the dressings when dry thus causing patients discomfort (Chang *et al*., 1998; Boateng *et al*., 2008). The removal of this dressing can promote cross-contamination of the wounds by dispersion of bacteria into the air.

Gauze and bandage dressings can be therapeutically improved by incorporating antimicrobials such as povidone iodine (PVP-I), chlorine releasing solutions (Dakin's and sodium hypochlorite solutions), hydrogen peroxide, silver releasing agents, honey, chlorhexidine and acetic acid (Boateng and Catanzano, 2015). In addition, incorporation of zinc, petroleum, bismuth and iodine can make these dressings non-adherent and moderately occlusive (Sood *et al*., 2014). However, bandages made of natural cotton wool are used for retention of light dressings, whilst high and short stretch compression bandages facilitate prolonged compression in case of venous ulcers (Dhivya *et al*, 2015). Using creams and gels as wound dressing has major limitations due to their inability to maintain effective drug concentration for a prolonged period at the moist wound surface because of short residence time. These semi solid formulations (creams and gels) absorb fluid rapidly and therefore, become mobile due to loss of rheological properties (Boateng *et al*., 2008).

1.5.4.2 Modern and advanced medicated dressings

Modern dressings in the form of hydrogels, hydrocolloids, foams, films and wafers, have been developed to overcome the limitations of traditional dressings described above. These modern dressings provide the ideal characteristics of wound dressings such as maintaining moist environment in the wound, which helps in proliferation and migration of fibroblasts and keratinocytes to promote wound healing. Moreover, the addition of antibiotics and antiseptics into the modern dressings make them advanced medicated wound dressings

(Pawar *et al*., 2014; Boateng *et al*., 2015a). These advanced medicated wound dressings can kill or inhibit bacteria, fungi and protozoa. In addition, these dressings can drain exudate and also have the ability to release drugs effectively onto the target site without damaging host tissues (Phoudee and Wattanakaroon, 2015; Cutting, 2010). Finally, the dressings reduce malodour and are cost effective (Cutting, 2010).

1.5.4.2.1 Hydrogels

Hydrogel dressings are three-dimensional networks of insoluble synthetic or semisynthetic polymers or an appropriate combination, which possess hydrophilic and swellable properties (Lloyd *et al*., 1998; Skorkowska *et al*., 2013). To maintain three-dimensional networks, the hydrophilic polymer chains are crosslinked either by covalent bonds or non-covalently by electrostatic, hydrophobic or van der Waals interactions (Moura *et al*., 2013). The synthetic and semisynthetic polymers include poly(hydroxyethyl methacrylate), polyethylene glycol and derivatives, poly(vinyl alcohol), polyvinylpyrrolidone, polyacrylamide, polyacrylate and polyurethane (Gibas and Janik, 2010). Hydrogels contain up to 96% water, which enables them to release water molecules to the wound surface and provides a moist environment inside the wound thus stimulating the growth of new tissue and the migration of epithelial cells (Jones *et al*., 2006; Skorkowska *et al*., 2013). As a result of high water content, the dressings cannot absorb much exudate from highly exuding wounds, which can lead to skin maceration and bacterial proliferation and therefore produce bad odour in the infected wounds. Therefore, their use in DFUs should be as an adjunct to sharp debridement of necrotic scare tissue.

However, a Cochrane Review (Dumville *et al*., 2013a) reported that hydrogels are more effective for healing DFUs than basic wound contact dressing. Hydrogels are easily permeable to moisture vapour, oxygen and metabolites, which can facilitate healing of ischemic DFUs. In addition, it enhances autolytic debridement of slough and necrotic tissue. Hydrogels are also prescribed for chronic leg, pressure, and vascular ulcers because it can easily be applied/removed without interfering with the wound beds as well as by promoting rapid epithelialization (Moura *et al*., 2013; Sood *et al*., 2014). Morgan reported that hydrogel dressings are suitable for use in all four stages of wound healing with the exception of infected and heavy drainage wounds (Morgan, 2002). Hydrogels can be applied as amorphous gels (thick, viscous gels) or as elastic, sloid sheet or film.

1.5.4.2.2   Hydrocolloids

Hydrocolloid dressings consist of an external layer (e.g. semi-permeable films, foams or non-woven polyester fibres) and a hydrophilic internal layer that may contain biocompatible colloidal gels made of proteins (e.g. collagen, gelatine) or polysaccharides (e.g. cellulose and its derivatives) (Moura *et al*., 2013). The semipermeable external layer protects the wound bed against debris and microbial penetration but permeable to water vapour and oxygen. The active internal layer contains hydrophilic colloidal particles that absorb exudates and swell into a gel-like mass over the wound and therefore provides a moist environment (Skorkowska *et al*., 2013). However, due to possible hypoxic condition and excessively moist environment, it could facilitate necrotic tissue autolysis and subsequently increase the risk of maceration and infection at the wound site (Hilton *et al*, 2004).

It has been reported that hydrocolloid dressings are useful in the treatment of venous leg ulcers where compression therapy alone doesn't work (Koksal and Bozkurt, 2003). It is also noted that hydrocolloid dressing is the second most popular choice for the treatment of DFUs in a study of British diabetic specialist nurse chiropodists (Boateng *et al*., 2015). These dressings can release drug in a sustained manner over than 7 days in DFUs. They are also indicated for pressure ulcers, necrotic wounds and minor burns (Sood *et al*., 2014). The microbial load of chronic ulcers can be managed by hydrocolloid dressings due to its acidic properties. These dressings make the wound bed acidic, which inhibits bacterial growth and maintain optimum stable temperature and moisture level (Sood *et al*., 2014). Therefore, it promotes the successive phases of wound healing such as clearing, proliferation, angiogenesis and epidermisation. The acidic pH also reduces the production of prostaglandin E2 and acts as an analgesic by decreasing pain (Skorkowska *et al*., 2013). These dressings can be used in paediatric wound care management because of easy removal without any pain (Dhivya *et al*., 2015).

1.5.4.2.3   Foam dressings

Foam dressings are hydrophilic materials, usually composed of polyurethane or polymethylsiloxane and retain a porous structure (Skorkowska *et al*., 2013). Foam dressings can be used as an alternative to hydrocolloid dressings for DFUs treatment due to its high absorbency of exudates, thereby preventing maceration, facilitating removal of slough, thermal insulation, easy to cut to shape, cushioning, protective and conformable to body surfaces. Their wound exudate absorbance capacity depends on the polymers employed in the formulation of

foam and on the foam thickness. Due to its protective and absorbency properties, this type of dressings can be left on the wound for up to 7 days which is very effective in DFUs treatment (Moura *et al*., 2013; Kavitha *et al*., 2014). Examples of foam dressings indicated for chronic leg and DFUs are listed in **Table A1.1 (Chapter 8)**.

There are very few clinical studies on foam dressings for use in DFUs. A Cochrane Review (Dumville *et al*., 2013b) of foam dressings for healing DFUs suggests that any type of foam and other dressings such as hydrocolloid and alginate dressings have no statistically significant difference in efficacy. However, their absorbency, comfortability, high moisture vapour permeability, angiogenesis and autolysis ability would theoretically make them a suitable choice for healing chronic wounds (Hilton *et al*., 2004). The outer layer (hydrophobic) protects the wound from external liquid and further damage but allows gaseous and water vapour exchange (Dhivya *et al*., 2015). The inner (hydrophilic) layer facilitates formation of moisture absorbing capillaries that keep the wound at optimum moisture level thus promoting wound healing (Skorkowska *et al*., 2013).

1.5.4.2.4 Semipermeable adhesive films

Films are semipermeable thin, flexible sheets of clear polyurethane incorporating an adhesive coating to one side to allow adherence to the skin. The adhesive reacts with wound fluid to prevent adhesion to the wound bed while allowing the dressing to stick to the dry periwound skin. Film dressings are made of natural synthetic or semi synthetic polymers such as chitosan, collagen, gelatine, polyvinyl alcohol, polyethyleneoxide and polyethyleneglycol (Mayet *et al*., 2014). They are highly elastic, conform to any contour of the body and are suitable for use as primary or secondary dressings. The transparent nature of film dressings allows useful visualization of the wound bed as it is healing without the need for its removal. These dressings are permeable to water vapour, oxygen and carbon dioxide but impermeable to bacteria and water. This means that oxygen is allowed into the wound to promote healing while, the water vapour and carbon dioxide produced can escape (Sood *et al*., 2014). The dressing also acts an effective barrier to external water and bacteria. The semipermeable nature of film dressings helps to achieve lower overall infection rate than traditional dressings.

Film dressings are suitable for superficial, lightly exuding or epithelializing wounds but they are not suitable for wounds with heavy drainage or patients with frail skin (Sood *et al*., 2014). They are avoided for heavily exuding wounds because excess fluids tend to accumulate beneath the dressings and therefore lead to skin maceration, bacterial proliferation and

infection. This shortcoming tends to result in frequent dressing changes, which is a compliance challenge for the patients (Boateng *et al*., 2008). In a clinical study, it was reported that films promote rapid wound healing, decrease pain, less scaring, visual wound assessment and facilitate patient mobility and hygiene (Rubio, 1991).

1.5.4.2.5 Lyophilized wafers

Lyopilized wafers are reported as one of the most advanced wound drug delivery dressings (Pawar *et al*., 2014; Boateng *et al*., 2015; Labovitiadi *et al*., 2012). They are prepared by freeze-drying technique in which polymer solutions or gels are freeze dried to give solid porous structures that can easily be applied to highly exuding wound surface (Pawar *et al*., 2014). Due to its highly porous nature, it can absorb large amounts of heavy exudate whilst maintaining a moist environment without damaging newly formed tissue that improves wound healing (Pawar *et al*., 2014). In addition, the porosity of the wafers also allows gaseous (water vapor) exchange which enables evaporation of wound exudates through the polymeric matrix to the surrounding environment, thus preventing fluid accumulation under the dressing and subsequently reducing the risk of skin maceration and controlling infections (Ng and Jumaat, 2014).

It has been reported that wafers have excellent physico-chemical properties in terms of swelling, adhesion, diffusion, drug stability and drug loading capacity (Pawar *et al*., 2014; Boateng *et al*., 2015a, 2010; Matthews *et al*., 2008). However, the adequate water uptake capacity can prevent cellular dehydration and therefore, promote collagen synthesis and angiogenesis to accelerate wound healing (Elsner and Zilberman, 2010). It can be loaded with multiple drugs simultaneously, which imparts multifunctional effects (Boateng and Catanzano, 2015; Kianfar *et al*., 2013a, Pawar *et al*., 2014). Furthermore, wafers are a compatible delivery system to carry both insoluble and soluble antimicrobial drugs to achieve better antimicrobial activity (Labovitiadi *et al*., 2012). Lyophilized formulations generally possess better drug stability compared with a semi-solid hydrogel dosage forms as the size, shape and form of encompassed compounds are preserved by preventing crystal ripening and agglomeration (Matthews *et al*., 2008; Ayensu *et al*., 2012b). Furthermore, the unique characteristics of wafers make them suitable for long-standing chronic suppurating wounds such as third degree burn wounds, DFUs and oral mucosal inflammation (Morgan, 2002).

Some recently developed polymeric based film and wafer dressings reported in literature are summarized in **Table 1.5**.

Table 1.5   Recently developed film and wafer dressings to aid chronic wound healing.

Dressing type	Polymer	Reference
Film	Polyox and carrageenan	Boateng *et al*., 2013
Film	Sodium alginate	Momoh *et al*., 2015
Film	Polyox, hydroxypropylmethyl cellulose (HPMC), carrageenan, sodium alginate and chitosan	Pawar *et al*., 2013
Film	Chitosan and gelatin	TVL *et al*., 2010
Film	Poly(2-hydroxyethyl methacrylate)	Tsou *et al*., 2005
Film	Gelatin, sodium carboxymethyl cellulose (Na‑CMC)	Okoye and Okolie, 2015
Film	polyvinyl alcohol and sodium alginate	Kim *et al*., 2008
Wafer	Sodium alginate and gelatine	Boateng *et al*., 2015
Wafer	Polyox, carrageenan and sodium alginate	Pawar *et al*., 2014
Wafer	Polysaccharide	Labovitiadi *et al*., 2012

1.5.4.2.6 Biological dressings

Biological dressings are made from biomaterials such as collagen, hyaluronic acid, chitosan, alginates and elastin that play an important role in the healing process and new tissue formation (Boateng *et al*., 2008). These types of dressings are also referred as bioactive dressings because of their biocompatibility and biodegradability and ability to take active part in the wound healing process thus making them attractive choices as dressings in wound care. Sometimes these dressings are incorporated with biological agents such as growth factors, nucleic acids and stem cells for delivery to the wound site (Boateng and Catanzano, 2015). Moreover, impregnation of naturally derived agents such as aloe vera, honey, silver, iodine and other antimicrobials into the biomaterials make them advanced therapeutic dressings for healing chronic wounds effectively (Boateng and Catanzano, 2015).

Collagen plays an active role in cell signalling that regulates cell anchorage, migration, proliferation, differentiation and survival (Moura *et al*., 2013). Collagen is enzymatically biodegradable via collagenase, gelatinase and metalloproteinase (Parenteau *et al*., 2010). Its degradability and water uptake capacity can be further improved by freeze-dried technique (Kondo *et al*., 2012). This polymeric matrix can be medicated by incorporating antimicrobials thus serving as a reservoir for drug delivery (Ruszczak *et al*., 2003). It also acts as a tissue engineered skin substitute that accelerate DFUs healing by actively secreting growth factors during repair process (Yazdanpanah *et al*., 2015). Gelatine is a collagen derivative, which has been reported for use by the incorporation of growth factors into its polymer matrix, which accelerated wound healing capacity in genetically healing impaired diabetic mice model (Kawai *et al*., 2005).

Hyaluronic acid (HA) is glycosaminoglycan, which is a major component of ECM of the connective tissue with hydrophilic, biodegradable, biocompatible properties and possesses viscoelastic nature (Boateng *et al*., 2008). The wound healing properties of HA are associated with promoting mesenchymal and epithelial cell migration and differentiation, thus enhancing collagen deposition and angiogenesis (Moura *et al*., 2013). HA is also reported as an essential component, which contributes to all phases of chronic wound healing including inflammation, granulation tissue formation, and reepithelialisation and remodelling (Anisha *et al*., 2013). Chitosan-HA composite sponge dressing containing silver has been reported to be effective for healing of DFUs (Anisha *et al*., 2013). In a clinical study, HA impregnated gauze pad showed better efficacy in venous leg ulcers than neutral gauze pad (Humbert *et al*., 2013).

Chitosan is a cationic biopolymer composed of glucosamine and N-acetyl glucosamine. It is biodegradable, biocompatible, non-antigenic, non-toxic, bioadhesive and antimicrobial with haemostatic properties (Moura *et al*., 2013). Chitosan based dressings have been reported as effective in healing DFUs in many clinical studies (Wang *et al*., 2008; Ben-shalom *et al*., 2008; Zhang *et al*., 2011; Lee *et al*., 2012).

Alginate dressings are made from the sodium and calcium salts of alginic acid found in a family of brown seaweed (Phaeophyceae) (Jones *et al*., 2006). These dressings accelerate wound healing by activating macrophages to produce TNF-α which induces angiogenesis (Dhivya *et al*., 2015). It has good physicochemical properties in terms of mucoadhesivity, absorbency and biocompatibility (Moura *et al*., 2013). Therefore, the dressings can be used in highly exuding wounds such as DFUs. In the wound bed it exchanges ions (sodium ions) present in the exudates and form hydrophilic gels, which cover the ulcers and provides moist environment, and promotes granulation and epithelialization. The dressings also facilitate haemostasis by exchanging calcium ions with sodium ions present in the fluid (Skorkowska *et al*., 2013). These dressings have some antimicrobial activity against pathogenic microorganisms present in DFUs such as *S. aureus*, *P. aeruginosa*, *S. pyogenes* and *Bacteroides fragilis* (Hilton *et al*., 2004).

1.5.5 Systemic antibiotic therapies

It has been reported that about 40-60% of diabetic patients treated for foot ulcers receive antibiotic therapy (Lipsky, 2007). The therapy only targets infection of chronic wounds especially in DFI. Selection of appropriate antibiotics depends on the following factors (Bader and Alavi, 2014; Lipsky, 2007):

i. Clinical severity and extent of the infection

ii. The risk factors for resistant organisms

iii. The recent use of antibiotic and its outcome

iv. Susceptibility test of isolated organisms

v. Vascular condition at infected site

vi. Drug allergy of patients and drug interactions

vii. Physiological conditions such as kidney and liver disease, and gastrointestinal absorption impairment

viii. Frequency of administration and cost

ix. Patient preferences

x.   Published efficacy data

The route of administration and duration of treatment also depend on the above factors. Systemic antibiotics are used to reduce wound bioburden and the treatment regimens of DFI by systemic antibiotics are summarized in **Table A1.2 (Chapter 8).**

1.5.6   Advanced physical therapies
1.5.6.1 Oxygen associated therapies

Oxygenation is a major factor that affects wound healing especially in DFUs, because of poor blood circulation that prevents oxygen transportation to the healing cells. Systemic hyperbaric oxygen therapy (HBOT) is a prominent advanced therapy in the treatment of non-healing DFUs that increases oxygen saturation of plasma thus improving wound tissue hypoxia, enhances perfusion, reduces oedema by promoting fluid absorption into the venous system, down regulates inflammatory cytokines, and promotes fibroblast proliferation, collagen synthesis and angiogenesis (Boateng *et al*., 2008; Yazdanpanah *et al*., 2015). This therapy reduces the major risk of amputation in DFUs and promotes long-term wound improvement (O'Loughlin *et al*., 2010). HBOT is used in Wanger Grade 3 diabetic wounds if the standard treatment fails within 30 days (Farzamfar *et al*., 2013).

Topical wound oxygen therapy is an alternative way of inducing oxygen, where 100 % humidified; pressurized oxygen is directly applied to the ischemic ulcers and has been shown to be effective for wound healing (Blackman *et al*., 2010). However, the HBOT is practiced in only a small number of patients because of high cost and is also time consuming. In recent years, the oxygen is incorporated into the dressings, which makes the therapy more portable, cost effective and effective in rapid healing. Oxyzyme^{TM} (Crawford healthcare Ltd, Knutsford UK) is an oxygen loaded double layered hydrogel dressing that allows oxygen transportation to the wound bed by acting as a form of molecular pump (Brimson and Nigam, 2012). In a multinational case study, 100 patients with different chronic ulcers: VLUs (39), arterial (14), DFUs (13), pressure (13) and mixed (21) were treated with Oxyzyme^{TM}. The study revealed that, 10% wounds healed completely (VLUs: 7%, mixed: 3%), 63% improved (VLUs: 22%, mixed: 11%, arterial ulcers: 11%, DFUs: 10% and pressure ulcers: 9%,) 16% remained static (VLUs: 6%, mixed: 4%, arterial ulcers: 1%, DFUs: 2% and pressure ulcers: 3%), whilst 11% (VLUs: 4%, mixed: 3%, arterial ulcers: 2%, DFUs: 1% and pressure ulcers: 1%) deteriorated (-h *et al*., 2009). OxyBand® (OxyBand Technologies Inc, St Louis Missouri, US) and

Oxygenesys® (Halyard Health Inc, Alpharreta Georgia) are also oxygen loaded hydrocolloid and foam dressings respectively (Boateng and Catanzano, 2015).

1.5.6.2 Negative pressure therapies

Negative pressure therapy (NPT) is widely used in treating about 300 million acute wounds annually (Boateng and Catanzano, 2015). The system uses a controlled, localized negative pressure through a latex-free and sterile polyurethane or polyvinyl alcohol foam dressing. The negative pressure takes out fluid from wound bed and enhances blood circulation to the infected area. Therefore, it decreases microbial load, increases new blood vessel formation and cellular proliferation, and promotes oxygenation (Yazdanpanah *et al*., 2015). NPT is used in Wanger Grade 3 DFUs without ischemia, to prevent amputation or re-amputation and to promote healing by secondary intention (Kevin *et al*., 2013). It has been reported that the rate of secondary amputation was lower in DFUs after NPT (4.1%) as compared to moist wound care (10.2%) (Pendse, 2010). However, treatment costs and further clinical evidence is required to authenticate the use of NPT in regular clinical practice.

1.5.6.3 Electrophysical therapies

Electrophysical (EP) therapies include electrical stimulation (ES), pulsed electromagnetic field (PEMF) and low-level laser (LLL) therapy (Boateng and Catanzano, 2015).

Inducing **ES** promotes wound healing by initiating cell migration including keratinocytes, macrophages, neutrophils and fibroblasts through various signalling mechanisms (Kevin *et al*., 2013). ES also improves blood flow and reduces the risk of infection in DFUs. In a clinical trial, it was reported that the healing rate of DFUs was higher in the ES group (52.68%) who received direct-current cathodal stimulation to the wound compared to placebo group (38.39%) who received zero-intensity electrical stimulation (Asadi *et al*., 2015). It could be a potential advanced therapy for the treatment of DFUs in terms of cost, safety and portability (Yazdanpanah *et al*., 2015). In review studies, **PEMF** has been reported effective in healing of venous leg ulcers (Aziz *et al*., 2013; Ravaghi *et al*., 2006). Clinical and animal studies have been undertaken on healing chronic wounds (diabetic stump wounds and DFUs) and it is reported effective therapy in wound healing by promoting angiogenesis, preventing tissue necrosis and accelerating wound closure (Isakov *et al*., 1996; Callaghan *et al*., 2008). In a pilot study it was demonstrated that PEMF therapy is successful in healing DFUs by decreasing

wound size by 18% in the active PEMF group compared with a 10% decrease in the control group. It also demonstrated the increment of cutaneous capillary blood velocity (by 28%) and capillary diameter (by 14%) to promote wound healing and improve microcirculation (Kwan *et al*., 2015). **LLL** therapy is not an established therapy in treating DFUs. However, many *in vivo*, animal and cell studies suggest that it could be a promising treatment option for DFUs (Minatel *et al*., 2009; Kaviani *et al*., 2011; Jagar *et al*., 2012; Landau *et al*., 2011). LLL therapy works through stimulating molecules and atoms of the body cells by applying light energy to the treatment area from a certain distance (Karu, 1989). Different wavelengths with different depths of penetration are used in this therapy. Red (685 nm) laser has the highest depth of penetration and yellow has the lower depth of penetration than green, blue (405 nm) and violet (Beckmann *et al*., 2014). However, infrared and near infrared light (over 700-1000 nm) have shown deeper penetration than red light (Litscher *et al*., 2004). Blue light has a bactericidal effect on the tissue surface. Cell studies on human keratinocytes, fibroblasts and endothelial cells have been demonstrated to be effective for wound healing with near infrared light (Houreld and Abrahamse, 2010; Danno *et al*., 2001). In these studies, it was revealed that after treatment with laser therapy (with near infrared radiation) the production of TGF-β1 and MMPs-2 (gelatinase) was increased which accelerates wound closure. In chronic wounds, MMPs-2 play a surveillance role in the skin such as control of collagen homeostasis in the tissue resulting in remodelling of scare tissue (Agren, 1994). Morever, MMPs can degrade damaged ECM components which clear wound bed and hence, facilitating interaction between new-born collagen and healthy ECM at the wound edge thus promotes migration of immune cells through uninjured tissue into the wound bed (Rohl and Murray, 2013).

1.6 Need for developing antimicrobial dressings in place of systemic treatment

The delivery of antibiotics through dressings directly to the wound sites may be preferred to the systemic administration because dressings require lower antibiotic dose. Therefore, it has great advantages of avoiding systemic side effects, interference with wound healing and inducing drug resistance (Lipsky *et al*., 2008). Zubair *et al*. performed an interesting clinical study on bacteria isolated from DFUs patients and their resistance to different classes of drugs. They reported that penicillin group exhibited the highest drug resistance (73.5%) followed by cephalosporin group (54%), quinolones and fluroquinolones (52.8%), aminoglycosides group (38.5%), beta lactam inhibitors (32.2%) and carbapenems (18.4%) (Zubair *et al*., 2011b). Serious adverse effects of systemically administered antibiotics have been reported in many clinical studies of DFI as summarized in **Table 1.6**.

Table 1.6 List of antibiotics reported in clinical studies of DFI.

Drugs	Route of administration	Adverse effects	Reference
Clindamycin	Oral	Erythema, pain/tenderness and purulent drainage and mild diarrhoea	Lipsky *et al*., 1990
Linezolid	IV and oral	Thrombocytopenia, rash, anaphylaxis and phlebitis	Lipsky *et al*., 2004b
Cefoxitin	IV	Mild eosinophilia, eosinophiluria, hematuria, leukocyturia, rashes and amputations	File and Tan, 1983; Fierer *et al*., 1979
Cephalexin	Oral	Mild nausea and diarrhoea	Lipsky *et al*., 1990
Ciprofloxacin	Oral and iv	Nausea, vomiting and required amputation therapy	Peterson *et al*., 1989
Ofloxacin	Oral and iv	headache, dizziness, anxiety, insomnia, heartburn, nausea and/or vomiting, gastroenteritis, dyspepsia, constipation, tender sinuses and fever	Lipsky *et al*., 1997
Amphicillin/sulbactam Amoxicillin/clavulanate	Oral and iv	Headache, anxiety, mood swings, nausea, vomiting, diarrhoea, rash, phlebitis, thrush and pruritus	Lipsky *et al*., 1997; Grayson *et al*., 1994
Daptomycin	IV	Nausea, vomiting, vaginosis, arrhythmia, diarrhoea, dermatitis, increased creatinine and creatine	Lipsky and Stoutenburgh, 2005

In addition, poor blood circulation at the extremities in DFUs makes systemic antibiotic therapy ineffective. A final concern is manufacturing cost, with the manufacturing cost of IV or oral products being higher than dressings. The above limitations of systemic antibiotic therapy have resulted in the need for developing antimicrobial dressings for improving wound healing in infected DFUs.

1.7 Materials and drugs used in this study

1.7.1 Calcium alginate

Calcium alginate (CA), a calcium salt of alginic acid, consists of alternating sequences of β-(1-4) D-mannuronic acid (M-blocks) and α-(1-4) L-guluronic acid (G-blocks) (**Figure 1.5**). The proportional distribution of the blocks depends on the origin and the part of the seaweed used (Malafaya *et al*., 2007) with the mannuronic and guluronic acid residues adopting different conformational structures. It has been found by conformational analysis that the di-equatorial mannuronic acid residues in M-block exhibit flat ribbon-like chain conformation whilst the di-axially linked guluronic acid residues in G-block show rigid structures (Daemi and Barikani, 2012).
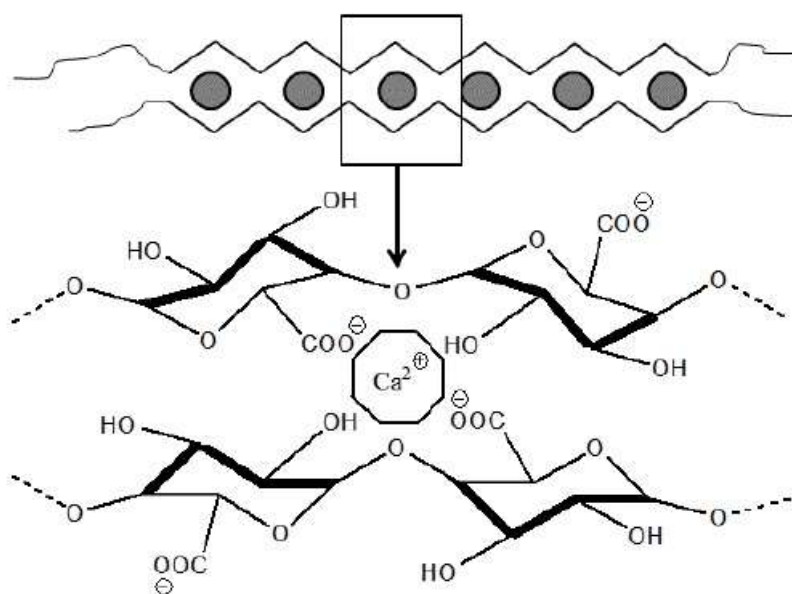
Figure 1.5 "Egg box" model of calcium alginate (adapted from Sharma *et al*, 2016).

Calcium alginate has been widely used in highly exuding wounds such as DFUs, pressure ulcers and leg ulcers due to its haemostatic properties. It exchanges calcium ions with sodium ions present in the blood (wound exudate) and this stimulates growth factors including platelet-

derived growth factors and cytokines, which play a vital role in cell recruitment and extracellular matrix deposition (Taskin *et al*., 2013). It has been reported as biocompatible, bioadhesive, high water absorption capacity, potential carrier for controlled drug release and non-toxic to cells (Shilpa *et al*., 2003; Lloyd *et al*., 1989). *In vitro* wound healing capacity test of calcium alginate based nano fiber bandage in rat model confirmed it as an excellent dressing material (Tarun and Gobi, 2012).

1.7.2 Plasticizer

According to the council of the International Union of Pure and Applied Chemistry (IUPAC) plasticizer is defined as "a substance or material incorporated in a material (usually a plastic or elastomer) to increase its flexibility, workability, or distensibility" (Vieira *et al*., 2011). The functional property of plasticizer is to facilitate the flexibility and processability of polymers by reducing the glass transition temperature (T_g). This is because, reduction of T_g of polymer increases mobility of the polymeric chain. Therefore, intermolecular force between the polymer chains is decreased resulting in polymer matrix flexibility. Plasticizers are normally non-volatile, high boiling, low molecular weight compounds added to polymers to reduce deformation tension, hardness, density, viscosity and electrostatic charge as well as to increase flexibility of polymer chain, resistance to fracture and dielectric constant (Vieira *et al*., 2011). The purpose of adding plasticizers into the polymeric gel is to get improved mechanical properties of films by reducing tensile strength and Young's modulus (Elastic modulus) and increasing elongation, toughness and resistance to cracking (Lim and Hoag, 2013). Other physicochemical properties of polymeric films, such as crystallinity, opacity, biological degradability, swelling capacity and adhesion, are also affected by plasticizer (Vieira *et al*., 2011). However, the above physicochemical properties of films depend on the concentration of plasticizer and its biocompatibility with the polymer. A low concentration of plasticizer results in increasing rigidity of the polymer instead of softening effect whilst high amounts of plasticizer affects the biocompatibility of polymer resulting in phase separation with leaching effect (Vieira *et al*., 2011; Chamarthy and Pinal, 2008).
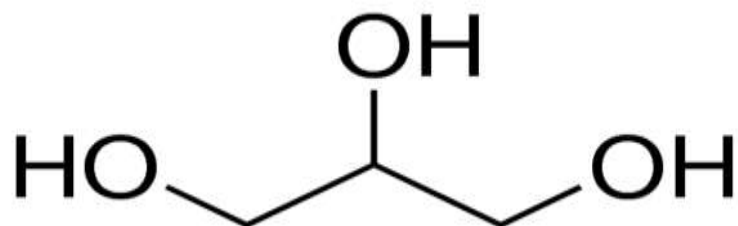
Figure 1.6   Chemical structure of glycerol.

Glycerol (GLY) is noted as a good plasticizer for polymeric films in several studies as it produces transparent, flexible, uniform, durable and elastic films (Momoh *et al*., 2015; Boateng *et al*., 2009; Puoci *et al*., 2012). GLY is a hydrophilic compound that contains three hydroxyl groups (**Figure 1.6**) which increases solubility in water and moisture content. The hydrophilic nature increases permeability, sorption capacity and the mobility of the polymers, which prevent the recrystallization and increase the film flexibility. GLY has been shown compatible with many polymers such as carrageenan, amylose, chitosan, carboxymethyl cellulose (CMC), hydroxypropyl methycellulose (HPMC), alginates and polyox (Momoh *et al*., 2015; Boateng *et al*., 2009; Vieira *et al*., 2011)

1.7.3   Model drugs

1.7.3.1 Ciprofloxacin

Ciprofloxacin (CIP), a second-generation fluoroquinolone derivative, has been shown to be highly effective against both Gram positive and Gram negative bacteria both of which are commonly found in infected wounds. The chemical structure of CIP (**Figure 1.7**) is 1-cyclopropyl-6-fluoro-4-oxo-7-(piperazin-1-yl)-1,4-dihydroquinoline-3-carboxylic acid with the 6-fluoro substituent being responsible for antibacterial activity. In addition, 7-piperazino group found to be responsible for inhibiting *Pseudomonas* where the cyclopropyl substituent contributes the CIP's high antibacterial activity.
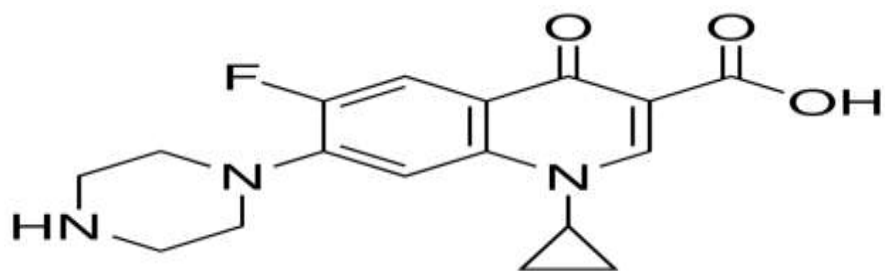
Figure 1.7   Chemical structure of ciprofloxacin.

The bactericidal effect of CIP is associated with the inhibition of topoisomerase II (DNA gyrase) and topoisomerase IV, which are responsible for ATP-dependent negative supercoiling of bacterial DNA replication, transcription, repair and recombination (LeBel, 1988). It is now widely used in the treatment of chronic wounds because of its low minimum inhibitory concentration (MIC) (Jannesari *et al*., 2011; Okoye and Okolie, 2015; Puoci *et al*., 2012). The MIC for CIP is reported in the literature for *E. coli*, *S. aureus* and *P. aeruginosa* as 0.015 µg/ml, 0.5 µg/ml and 0.25 µg/ml respectively (Andrews, 2001).

1.7.3.2 Fluconazole

Fluconazole (FLU) is a synthetic triazole derivative antifungal agent that is effective against a wide range of systemic and superficial fungal infections. The structural formula of FLU is 2-(2,4-Difluorophenyl)-1,3-bis(1H-1,2,4-triazol-1-yl) propan-2-ol (**Figure 1.8**) (Oliveira *et al*., 2015). FLU acts by inhibiting 14-α demethylase, a cytochrome P-450 enzyme which catalyses the conversion of ergosterol from lanosterol. However, ergosterol is an essential component of the fungal cell membrane and depletion of its synthesis results in increased cellular permeability causing leakage of cellular contents (Ghannoum and Rice, 1999). FLU is highly effective against Candida spp. such as *C. albicans, C. parapsilosis,* and *C. Tropicana*, which are the main causative agents for DFUs (Cordeiro *et al*., 2013; Missoni *et al*., 2006). FLU has desirable pharmacological properties including a relatively long half-life of 30 h, renal excretion of over 80% of the unchanged drug, 12% binding plasma protein, ability to be administered either orally or parenterally, and over 90% oral bioavailability (Oliveira *et al*., 2015).
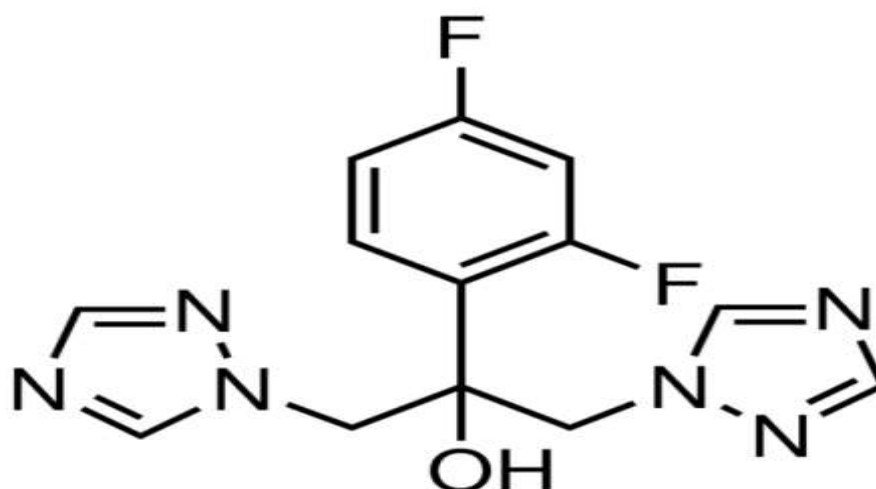
Figure 1.8   Chemical structure of fluconazole.

1.8   Hypothesis, aims and objectives

As discussed above, mixed infection is one of the major risk factors, which impairs healing of chronic DFUs. Management of mixed infections in DFUs is not well studied. Current treatment is mostly based on the systemic delivery of antibacterial and antifungal drugs. However, recently developed dressings target only either bacterial or fungal infection. The hypothesis for this research project is that CA based films and wafers can simultaneously deliver antibacterial (CIP) and and antifungal (FLU) drugs for effective healing of mixed infected DFUs.

Therefore, the project aims to develop, formulate, characterize and optimize advanced therapeutic (medicated) dressings containing broad spectrum antibacterial and antifungal drugs to target mixed infections in DFUs. The dressings will be manufactured by solvent cast and freeze-drying technique. The optimum amount of antibacterial and antifungal drug will be incorporated into the formulations separately and combined to eradicate bacterial and fungal load, and mixed infections in a diabetic foot.

The key objectives are as follows:

1.   **Pre-formulation and physicochemical studies of model antibacterial and antifungal drug, and polymer:** This will be undertaken to identify and characterize physico-chemical compatibility of the two model drugs with CA polymeric excipient. Further studies will be performed to develop stable and biodegradable CA based films and wafers to deliver CIP and FLU simultaneously for healing of chronic DFUs.

2.   **Formulation development:** CA based dressings will be prepared with different amounts of GLY as plasticizer to optimize films by solvent casting method while unplasticized gels will be freeze-dried to obtain wafer.

3.   **Characterization of the formulations:** The dressings will be physically characterized by SEM, XRD, FTIR and texture analysis (for mechanical properties and *in-vitro* adhesion). The dressings will be further characterized for functional properties for porosity, water absorption (Aw), equilibrium water content (EWC), swelling index, water vapour transmission rate (WVTR), evaporative water loss (EWL), moisture content and *in vitro* drug release studies.

4. **Biological testing the optimized formulations targeting chronic diabetic foot ulcer:** Initially, *in vitro* antibacterial and antifungal inhibition assays will be carried out separately to test the release of the drugs from the proposed dressings and in enough quantities to inhibit or kill both common wound bacteria and fungi. In antibacterial assay the dressings will be tested against causative microbes commonly found in infected chronic wounds i.e. *E. coli*, *S. aureus* and *P. aeruginosa* followed by *C. albicans* in antifungal assay. After that, *C. albicans* will be cultured with either *E. coli*, and/or *P. aeruginosa* and/or *S. aureus* to represent mixed infection and there after the optimized dressings will be tested.

- *In vitro* cell viability (MTT assay) and migration study (wound healing scratch assay) of the final optimized dressings will be investigated to elucidate the wound healing action.

5. The fluid (exudate) handling and biological properties (antimicrobial, cell viability and migration) of the dressings will be compared with commercial CA based antimicrobial dressings currently available on the market.

CHAPTER 2: FORMULATION DEVELOPMENT AND PHYSICO-CHEMICAL CHARACTERIZATION OF CALCIUM ALGINATE BASED DRESSINGS

2.1 Introduction

Chronic wounds arise from tissue injuries or disruption to anatomical structures that do not heal within 12 weeks. They are associated with predisposing factors that might disturb the balance between wound bioburden and the patient's immune system or hinder the wound healing cycle (Sarheed *et al.*, 2016). The incidence of chronic wounds including diabetic foot ulcers (DFUs), leg ulcers, pressure ulcers, venous ulcers, arterial ulcers and trauma, has increased dramatically in recent years and the development of more effective therapies have lagged behind this increase. The estimated prevalence of diabetes in the United Kingdom for 2015 was 4.5 million and estimated to rise to 5 million by 2025 (Diabetes UK, 2016) with about 12 to 25% of diabetic patients affected by DFUs during their lifetime (Ravichandra and Chitti, 2015). DFUs are caused by ischaemia, neuropathy and infection and are one of the most common causes of morbidity with high risk of lower extremity amputation (Singh *et al.*, 2005).

Natural and synthetic polymers are widely used in chronic leg and DFUs (Moura *et al.*, 2013) and play multiple roles in wound healing (Moura *et al.*, 2013; Sood *et al.*, 2014). Alginate based dressing is one of the most studied and applied in DFUs. Alginate is highly biocompatible, with low toxicity and good mucoadhesive characteristics (Lee and Mooney, 2012). Calcium alginate (CA) is highly efficient to absorb wound exudates, hence facilitating debridement and promoting wound healing in DFUs (Tarun and Gobi, 2012).

Wound dressings are one of the most practical ways of treating DFUs. There are several types of dressings available on the market for the treatment of DFUs. However, films and wafers are one of the most commonly used therapeutic dressings amongst all due to some distinct advantages in terms of physico-chemical and wound healing properties as well as relatively cheaper costs. Solvent casting and lyophilisation techniques have been used to prepare films and wafers respectively (Boateng *et al.*, 2010). Though films can also be prepared by hot melt extrusion method, this technique is limited due to high temperature required which can cause thermal degradation of labile film ingredients (Morales and McConville, 2011). Lyophilized wafers have the unique advantage of being highly porous which enables them to absorb more exudate from highly exuding wound and high drug loading as compared to films (Sarheed *et al.*, 2016; Boateng *et al.*, 2009).

In this research, ciprofloxacin (CIP), has been used a model antibacterial drug. CIP is a second-generation fluoroquinolone derivative, which has been shown to be highly effective against Gram positive and Gram negative bacteria both of which are commonly found in infected wounds. Due to its low minimum inhibitory concentration (MIC), it has become a promising drug to incorporate into polymeric dressings for the potential treatment of chronic wounds (Puoci *et al*., 2012; Jannesari *et al*., 2011; Okoye and Okolie, 2015; Kataria *et al*., 2014; Ozturk *et al*., 2006; Roy *et al*., 2015; TVL et al., 2010; Shi *et al*., 2015). Antibiotic loaded dressings have the advantages of avoiding systemic side effects and interference with wound healing as well as reducing incidents of drug resistance (Lipsky *et al*., 2008). Serious adverse effects of systemically administered CIP have been reported (Beberok *et al*., 2011), which creates the need to develop CIP loaded dressings as an alternative way for healing of DFUs. Furthermore fluconazole (FLU) has been used as a model antifungal drug to evaluate the efficacy of the delivery systems. FLU has advantages of retaining extended half-life, low molecular weight and protein binding, and high level of penetration ability (Karthikeyan *et al*., 2015). FLU is reported to be effective against *Candida* infection in DFUs (Missoni *et al*., 2005). FLU was also prescribed (300 mg once a week for 6 month) in the treatment of onychomycosis in diabetes (Winston and Miller, 2006). However, FLU loaded dressings have not been well established in chronic wound healing. In a study FLU loaded Eudragit nanofiber dressing demonstrated effectiveness in inhibiting fungal growth (Karthikeyan *et al*., 2015). Therefore, in this study FLU loaded dressings have been developed for effecting healing of DFUs.

This chapter describes the formulation development and evaluation of the physico-chemical characteristics of therapeutic CA based solvent cast films and lyophilized wafers that will deliver therapeutically relevant doses of broad-spectrum antibiotic (CIP) and antifungal (FLU) drugs directly to the wound site of infected DFUs. The films were initially plasticized with different amount of glycerol (GLY) to achieve ideal physical properties for drug loading. Further, the formulated films and wafers were physically characterized by scanning electron microscopy (SEM), X-ray diffraction (XRD), Fourier transform infrared spectroscopy (FTIR) and texture analysis (for mechanical properties and *in-vitro* adhesion). The purpose of these physico-chemical studies was to understand the drug polymer interaction and compatibility.

2.2 Materials

Calcium alginate (mannurronic acid: guluronic acid (59:41), molecular weight: 398.32 g/mol) [CA, (lot number: BCBM8132V)], Ciprofloxacin (lot number: LRAA6508), Fluconazole (lot number: LRAA6502) and tris(hydroxymethyl)aminomethane (lot number: SLBH9329V) were purchased from Sigma-Aldrich (Gillingham, UK). Sodium carbonate (lot number: 1546575), sodium chloride (lot number: 1560652), bovine serum albumin [BSA, (lot number: 1158022)], hydrochloric acid [HCl, (lot number: 1480980)], ethanol (batch number: 0933421) and glycerol [batch number: 1340773] were ordered from Fisher Scientific (Loughborough, UK).

2.3 Methods

2.3.1 Preliminary formulation development of blank plasticized and unplasticized films

CA was used as a starting material due to its haemostatic effect. It exchanges calcium ions with sodium ions present in the blood (wound exudate) and this stimulates growth factors including platelet-derived growth factors and cytokines, which play a vital role in cell recruitment and extracellular matrix deposition (Taskin *et al*., 2013). Morever, antibacterial activity of CA (Shilpa *et al*., 2003; Tarun and Gobi, 2012; Hilton *et al*., 2004) make it an ideal choice for formulating an advanced medicated dressing for treating DFUs. CA is water insoluble but dissolved in sodium carbonate solution (Tarun and Gobi, 2012). The chemistry behind this is that CA forms a gel via ion exchange method. During formulation, calcium ions present in β-D mannuronic acid (M block) of CA exchange with the sodium ions of the sodium carbonate thus form sodium alginate and calcium carbonate as a biproduct. The advantage of this method is that the residual calcium carbonate also has haemostatic effect in the early stage of wound healing (Lansdown, 2002). Calcium ions act as a clotting factor (factor IV) which induces synthesis and release of other clotting factors (VII, IX and X) and catalyse the conversion of prothrombin to thrombin resulting in platelet formation (Lansdown, 2002). Moreover, influx of calcium ions into the cells regulate inflammatory cell filtration, fibroblast proliferation and keratinocyte migration (Kawai *et al*., 2011). Furthermore, antibacterial activity of calcium carbonate has also been reported (Ataee *et al*., 2011). Therefore, the presence of some amount of residual calcium carbonate will be expected to play a partial role in closure of DFUs.

Initially, different (0.5-2.5% w/w) aqueous gels of CA were prepared to determine suitable concentration of gels for further formulation development. Selection of suitable gel concentration of CA was based on the gel uniformity, transparency, lump formation of undissolved polymer, ease of pouring and air entrapment (Boateng *et al.*, 2009). The gels were prepared by adding the CA powder slowly and stirring on a magnetic stirrer at 50 ℃ to assist complete dissolution**.** 20 g of the resulting gels were poured into Petri dish (86 mm diameter) as a casting container and dried in a fan oven at 30 ℃ for18 h to obtain films. These films were checked visually for morphological defects.

Based on initial observations, different 1% w/w gels were prepared by dissolving CA in different concentrations (0.005-0.028 M) of sodium carbonate solutions. Furthermore, different amounts of GLY based on the total polymer weight (w/w) were added to the 1% w/w gels to prepare plasticized film dressings as summarized in **Table 2.1.**

Table 2.1   Composition of CA and GLY (amounts based on total dry weight) in gels used for plasticized film dressings.

CA (g)	GLY (g)	Total weight (g)	GLY content in final film (%)
1.00	0.00	1.00	0.00
1.00	0.10	1.10	9.09
1.00	0.25	1.25	20.00
1.00	0.50	1.50	33.33
1.00	0.75	1.75	42.86
1.00	1.00	2.00	50.00

2.3.2   Preparation of drug loaded (DL) films

Based on preliminary observation of the films prepared in **Table 2.1**, drugs were loaded into the optimized film containing 33.33% (w/w) GLY. CIP was dissolved in 0.014 M sodium carbonate solution at a concentration of 0.25 mg/ml (w/v) and FLU was dissolved in ethanol at the concentration of 50 mg/ml (w/v) as stock solutions respectively. Different volumes of the stock drug solutions were added to the plasticized gels (CA-33.33% GLY) to achieve drug

concentrations of 0.005, 0.010 and 0.025% w/v for CIP and 0.05, 0.10 and 0.20% w/v for FLU respectively in the gels. To prepare combined DL (CIP and FLU) films, the drugs were mixed at the ratio of 1:10 and 1:20 (CIP: FLU). To obtain the plasticized DL films, GLY was dissolved in sodium carbonate solution by stirring at 50 ℃ for 10 min and then solutions of the drug were added to the hot solution with continuous stirring. After that, CA powder was added in tiny amounts to avoid lump formation with continuous stirring at 50 ℃ for 3 h. Finally, 20 g of resulting gels were poured into Petri dish and oven dried at 30 ℃ for 18 h. **Figure 2.1** illustrates the preparation of BLK and DL films by solvent cast method. All dried films were wrapped with parafilm and kept in a desiccator until required.
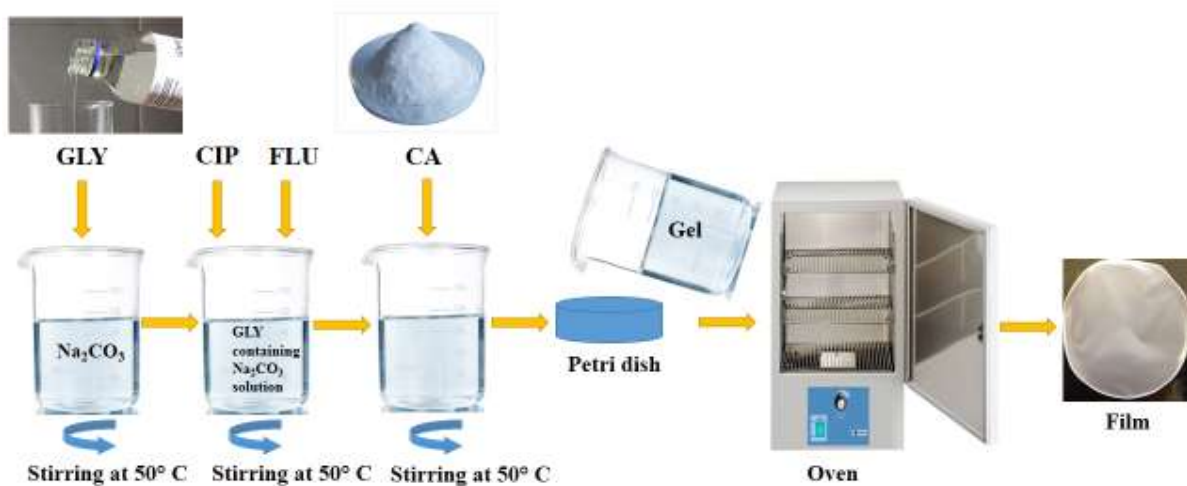
Figure 2.1   Schematic representation of preparation of solvent cast polymeric films (BLK and DL).

2.3.3   Preparation of polymer gels for lyophilized wafers

The blank (BLK) polymeric gels comprising of CA (0.5 - 2% w/w) were prepared by adding the polymer powder in tiny amounts into the vortex of a vigorously stirred 0.014 M sodium carbonate solution at 50 ℃ to avoid lump formation. In the case of CIP loaded gels, stock solution of CIP was initially prepared at the concentration of 20 mg/ml in 0.1 N hydrochloric (HCl) solution. The stock solution was further diluted with 0.014 M sodium carbonate to achieve working stock solution at a concentration of 1 mg/ml. On the other hand, same stock solution of FLU as previously prepared for films was used for the FLU loaded wafers. Different volumes of working stock of CIP were added to the BLK gels (1% w/w) to

achieve drug concentrations of 0.0001-0.0400% w/v in the gel. For FLU loaded wafers, the drug concentrations of 0.05-0.40% w/v were obtained in the gel. Wafers formulated with combined drugs were prepared by adding both drugs (CIP and FLU) at the ratio of 1:10, 1:20 and 1:30 (CIP: FLU) into the BLK gels.

2.3.4   Preparation of lyophilized wafers

The lyophilized wafers were prepared by the freeze-drying technique illustrated in **Figure 2.2 (a)**. Each of formulated gel (1 g per well) was poured into 24 well plates (diameter 15.6 mm) (Corning® Costar® cell culture plates; Sigma-Aldrich) and freeze-dried using a Virtis Advantage XL 70 freeze dryer (Biopharma Process Systems, Winchester, UK) in automatic mode. Previously reported lyophilisation cycle with slight modification was adapted to prepare wafers (Pawar *et al*., 2014) (illustrated in **Figure 2.2 b**). In brief, the samples were cooled to -5 ℃ from room temperature for 1 h, and further frozen at -50 ℃ for 8 h (at 200 mTorr). The frozen samples were then primary dried to -25 ℃ (at 50 mTorr) in a sequence of thermal ramps for 24 h, followed by secondary drying at 20 ℃ (at 10 mTorr) for 7 h.
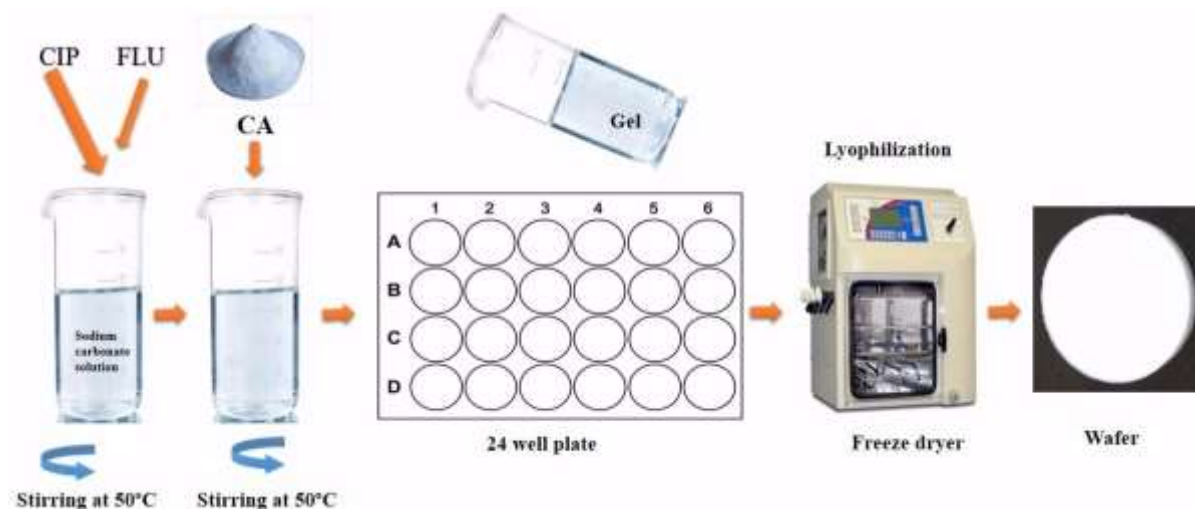
Figure 2.2 (a) Illustration of the preparation of lyophilized wafers (BLK and DL).
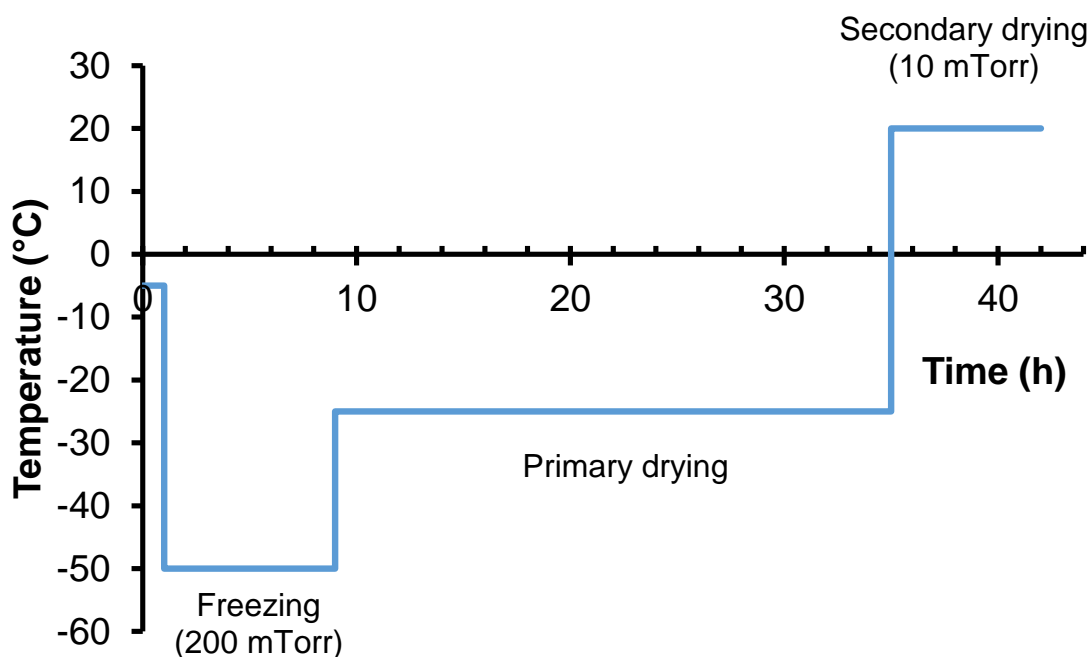
Figure 2.2 (b) Graphical representation of freeze drying cycle used for the preparation of BLK and DL wafers.

2.3.5 Scanning electron microscopy (SEM)

SEM was used to analyse the surface morphology of the dressings (films and wafers) using a Hitachi SU 8030 (Hitachi High-Technologies, Germany) scanning electron microscope at low accelerating voltage (10 KV). The dressings were cut into small pieces and attached to aluminium stubs (15 mm diameter), with the help of double-sided adhesive carbon tape (Agar Scientific G3357N). After that, samples were either chromium or gold sputter coated before visualization in the microscope. The images of films and wafers were captured at working distances between 8.1 mm to 21.4 mm at a magnification of x200 and x6000 respectively using i-scan 2000 software.

2.3.6 X-ray diffraction (XRD)

XRD was used to investigate the physical form (amorphous or crystalline) of the pure drugs, polymer and the BLK and DL dressings. The films were cut into the appropriate shape to cover the round tiles of the holder and tightly attached to the sample cells with the help of transparent plastic cling film. In case of wafers, samples were compressed with a glass slide before attaching to the sample cells. The experiment was performed using a D8 Advance X-ray diffractometer (Bruker, Germany) instrument in transmission mode. The instrument was set at

a voltage and current of 40 KV and 40 mA respectively with a primary solar slit of 4º and a secondary solar slit of 2.5º whereas the exit slit was 0.6mm. Lynx Eye silicon strip position sensitive detector was set with an opening of 3º and the Lynx Iris was set at 6.5mm. The samples were scanned between 5-50º 2 theta at a rotation speed of 15 rpm. The step size was 0.02º and counting time was 0.1 s per step. The percentage crystallinity of the dressings was computed by EVA software in which a background was selected which represented air and incoherent scatter. The curvature value was adjusted without cutting into the crystalline peaks and appended to get only crystalline contribution to the scatter. After that, an area region was selected which covered all the crystalline peaks. The percent crystallinity was calculated from the ratio beween the values of intensities of amorphus and cryatalline contribution, and the value of intesities of crystalline only contribution respectively.

2.3.7 Attenuated total reflectance Fourier transform infrared spectroscopy (ATR-FTIR)

FTIR spectra of pure drugs, polymer and BLK and DL dressings were obtained by a Spectrum Two Perkin Elmer spectrophotometer (Perkin Elmer, USA) equipped with a crystal diamond universal attenuated total reflectance (UATR) sampling accessory. The ATR crystal, plate and the metal tip were carefully cleaned using tissue paper and isopropanol before each run. The background spectrum was recorded for calibration before starting the experiments. The samples were placed onto the plate to just cover the crystal, followed by turning the metal tip close to the plate. With the metal tip touching the samples, the force gauge was adjusted to reduce the noise of the peaks. The spectra were recorded at a resolution of 4 cm^{-1} with 4 scans per spectrum using a wavenumber range of 650-4000 cm^{-1}.

2.3.8 Texture analysis
2.3.8.1 Mechanical (tensile) properties of films

Tensile strength, Young's modulus and percent elongation at break of solvent cast films were measured with a TA HD Texture analyser (Stable Microsystem Ltd., Surrey, UK) fitted with a 5 kg load cell and *Texture Exponent 32* software program to plot and display data. The films ($n = 3$), free of any physical defects (cracks, tears, stickiness and patches) were cut in the shape of a dumb-bell (80 mm long, 30 mm gauge length and 3.5 mm width) and average thickness was measured prior to testing. The mechanical analysis was performed by stretching between two tensile grips at a test speed (stretching rate) of 0.10 mm/sec with a maximum trigger force 0.05 N to determine the maximum tensile strength for each matrix. The pre-test

and post-test speeds were set at 1.00 mm/sec and 10.00 mm/sec respectively. The texture analyser was run in tension mode with maximum extension of 50 mm. Initially, the test was carried out on the BLK films (non-DL) containing different percentages of plasticizer (CA-9.09% GLY, CA-20.00% GLY, CA-33.33% GLY, CA-42.86% GLY and CA-50.00% GLY) to define the optimum mechanical properties for drug loading (Boateng *et al.*, 2013a). Later, DL films were tested to determine the effect of drug loading on the films. The tensile strength, Young's modulus and elongation at break were calculated using equations 1.1, 1.2 and 1.3 (Momoh *et al.*, 2015)

$$\text{Tensile strength } (\text{N/mm}^2) = \frac{\text{Force at break (N)}}{\text{Initial cross sectional area } (\text{mm}^2)} \qquad \text{(Equation 1.1)}$$

$$\text{Young's modulus (MPa)} = \frac{\text{Slope}}{\text{Film thickness (mm) x cross−head speed (mm/s)}} \qquad \text{(Equation 1.2)}$$

$$\text{Elongation at break (\%)} = \frac{\text{Increase in length (mm) at break}}{\text{Initial film length (mm)}} \text{ x } 100 \qquad \text{(Equation 1.3)}$$

2.3.8.2 Mechanical hardness of wafers

The hardness (resistance to compressive deformation and ease of recovery) of the wafers was investigated using the same texture analyser and software program mentioned above. The average thickness (5-6 mm) of the wafers measured by a digital Vernier calliper electronic micrometre gauge (one in the middle and four edges) were entered into the software before compression. The instrument was set to compression mode and height of the 6 mm diameter (p/6) cylindrical stainless-steel probe above the stage calibrated prior to compression. Three different wafers of each formulation (*n* = 3) were compressed by the probe at three different locations, on both sides of the wafers using a trigger force of 0.001 N, to a depth of 2 mm, at a speed of 1 mm/sec, with a 10 mm return distance (Pawar *et al.*, 2014). The BLK and DL wafers were evaluated to determine the effect of increasing drug content on flexibility to select optimum drug loading.

2.3.8.3 *In-vitro* adhesion studies

In-vitro adhesion of the films and wafers were investigated using the same texture analyser and software program mentioned above. In this test, a 35 mm diameter (p/35) cylindrical stainless-steel probe was attached to the dressings using double-sided adhesive tape. To represent chronic wound surface, 500 µl of simulated wound fluid (SWF) containing either 2% (w/w) bovine serum albumin (BSA) or 5% (w/w) BSA was spread onto set gelatine (6.67% w/w) gel. The dressing fitted with the probe was lowered until it made contact with the surface of the gelatine gel. The texture analyser was set to run in tensile mode; followed by 60 s contact time with applied force of 1 N and detached at pre-test and test speeds of 0.5 mm/s and post-test speed of 1 mm/s, 0.05 N trigger force and 10 mm return distance. The maximum force required to separate dressings from the surface of gelatine gel, the area under the curve of force versus distance plot and the total distance (in mm) travelled by dressings till complete separation were recorded to represent stickiness (peak adhesive force), total work of adhesion (WOA) and cohesiveness respectively. Each formulation was tested in triplicate ($n = 3$).

2.3.9 Statistical analysis

Measurements of each mechanical property were in triplicates for tensile strength, elastic modulus, elongation and adhesion. One-way ANOVA (analysis of variance) test was carried out to detect mean differences. Results are statistically significant when P values less than 0.05.

2.4 Results and discussion

2.4.1 Preliminary formulation development of films and wafers

CA gels were prepared by the exchange of calcium ions with the monovalent sodium ions of the surrounding medium thus forming arranged structures (Shilpa *et al*., 2003). The resultant structure is referred to as an egg-box model (Lee and Mooney, 2012). In the gels, calcium carbonate was formed by reaction between CA and sodium carbonate in which positive calcium ions of CA react with negative carbonate ions of sodium carbonate. The gels were prepared by vortex hydration with heat (Boateng *et al*., 2009) which helps to quickly hydrate the undissolved polymer preventing lump formation. Heat also helps to reduce the viscosity of the gels resulting in ease of pouring into the casting surface and to remove air bubbles entrapped during stirring (Boateng *et al*., 2009). Due to gel uniformity (homogeneity), viscosity, absence of lump formation and ease of pouring, 1% w/w polymer gels were selected and further investigated to improve the transparency and flexibility of the resulting films. The films

obtained from gels at concentrations greater than 1% w/w were very hard, brittle, deformed, opaque and inflexible, whereas, films obtained from 0.5% w/w gel were too thin and weak to handle and easily torn. This shows that higher amount of polymer made the films hard and leads to compact structure (Boateng *et al*., 2010).

| CA 0.5% w/w | CA 1.0% w/w | CA 1.5% w/w |

| CA 2.0% w/w | CA 2.5% w/w |
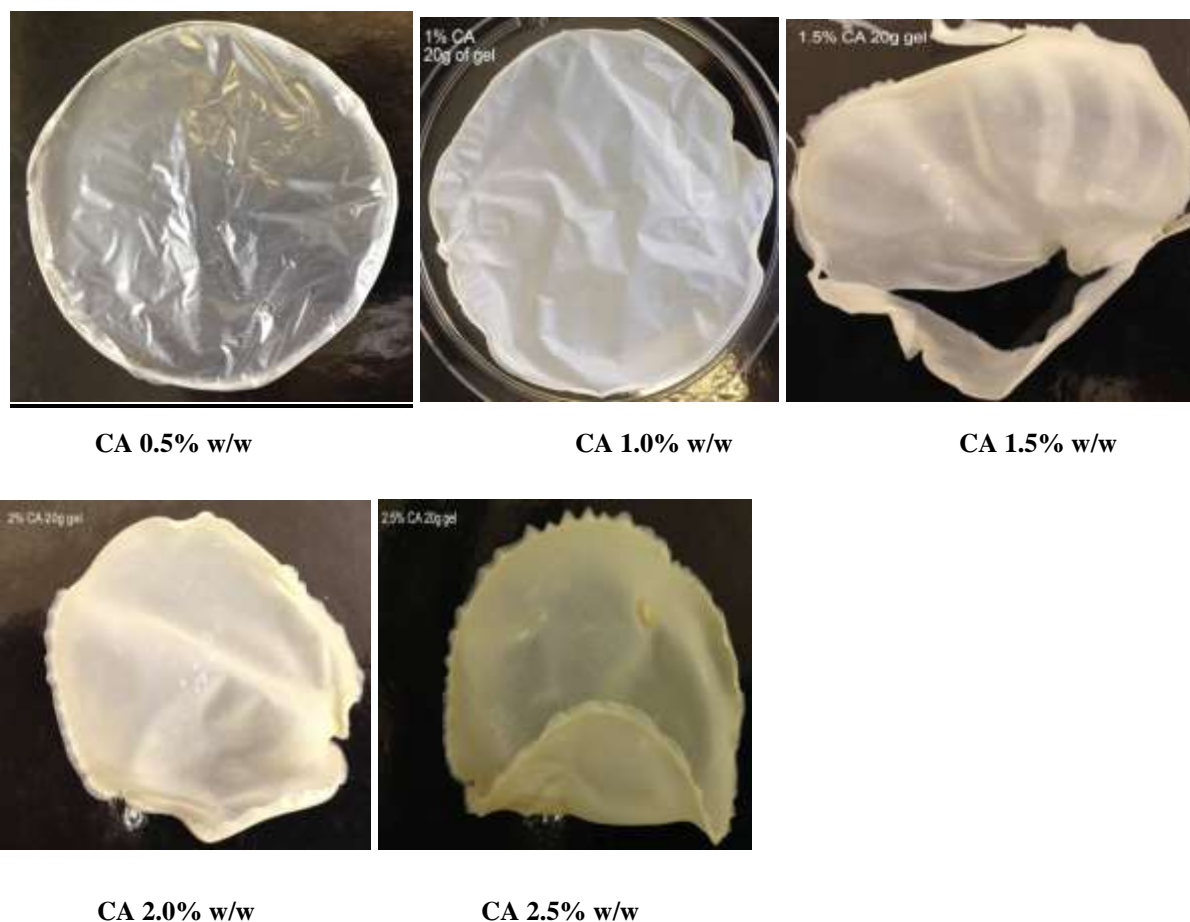
Figure 2.3   CA based films prepared from different percentage concentrations of gels based on total polymer weight.

However, films obtained from CA- 0.5% w/w gels were more transparent but with visible calcium carbonate precipitation (see XRD discussion below). This could be due to low amount of polymer resulting in a film with very low thickness and reduced density that made them more transparent. Film obtained from 1% w/w gel was less brittle and lower precipitation of calcium carbonate as compared to all other films, however, they were less transparent (translucent) as shown in **Figure 2.3.** This could be because the amount of CA and sodium carbonate was optimum for ionic cross-linking resulting in stable rigid structure and less calcium carbonate precipitation on the film's surface. Moreover, they were less transparent than the film obtained from 0.5% w/w gel due to higher thickness (Santana and Kieckbusch, 2013).

Further investigation was carried out by dissolving CA in different concentrations of sodium carbonate solution to reduce calcium carbonate precipitation on the films' surface. **Figure 2.4** shows films obtained from CA gels prepared using 0.005-0.011 M sodium carbonate solution were fragile, brittle, deformed, cracked and even CA precipitation. This could be due to the fact that there was not enough sodium ions present. Therefore, the gels were less viscous and evaporated quickly during drying. CA dissolved in 0.028 M sodium carbonate resulted in the least brittle film but precipitation of calcium carbonate was high when observed visually. CA dissolved in 0.014 M sodium carbonate gave uniform, homogenous and adequate viscous gel, permitting ease of pouring into the Petri dish and resulting in the least precipitation of calcium carbonate among all films. This could be because the ratio between CA and sodium carbonate was optimum for ionic cross-linking, leaving less calcium carbonate residues.

CA- 0.005 M sodium carbonate   **CA- 0.007 M sodium carbonate**   **CA- 0.009 M sodium carbonate**

CA- 0.011 M sodium carbonate   **CA- 0.014 M sodium carbonate CA- 0.028 M sodium carbonate**
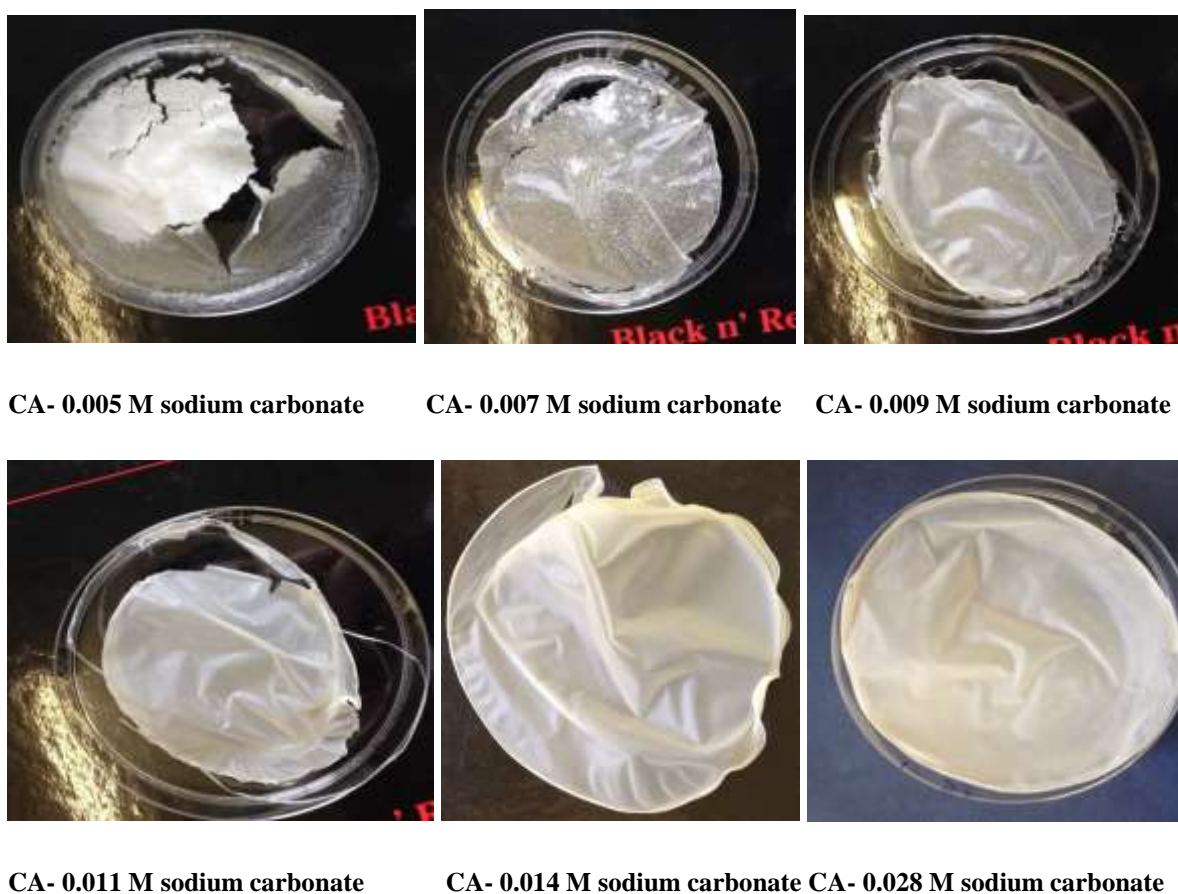
Figure 2.4   Films obtained from 1% w/w gels by dissolving CA in different concentrations of sodium carbonate solution.

All the unplasticized films did not show the ideal mechanical properties of film i.e. durable, soft, flexible, pliable and elastic (Boateng *et al*., 2013a). To achieve that, the films

obtained by dissolving CA in 0.014 M sodium carbonate, were plasticized with different amounts of GLY and digital photographic images are illustrated in **Figure 2.5**.

CA-9.09% GLY	**CA-20.00% GLY**	**CA-33.33% GLY**

CA-42.86% GLY	**CA-50.00% GLY**
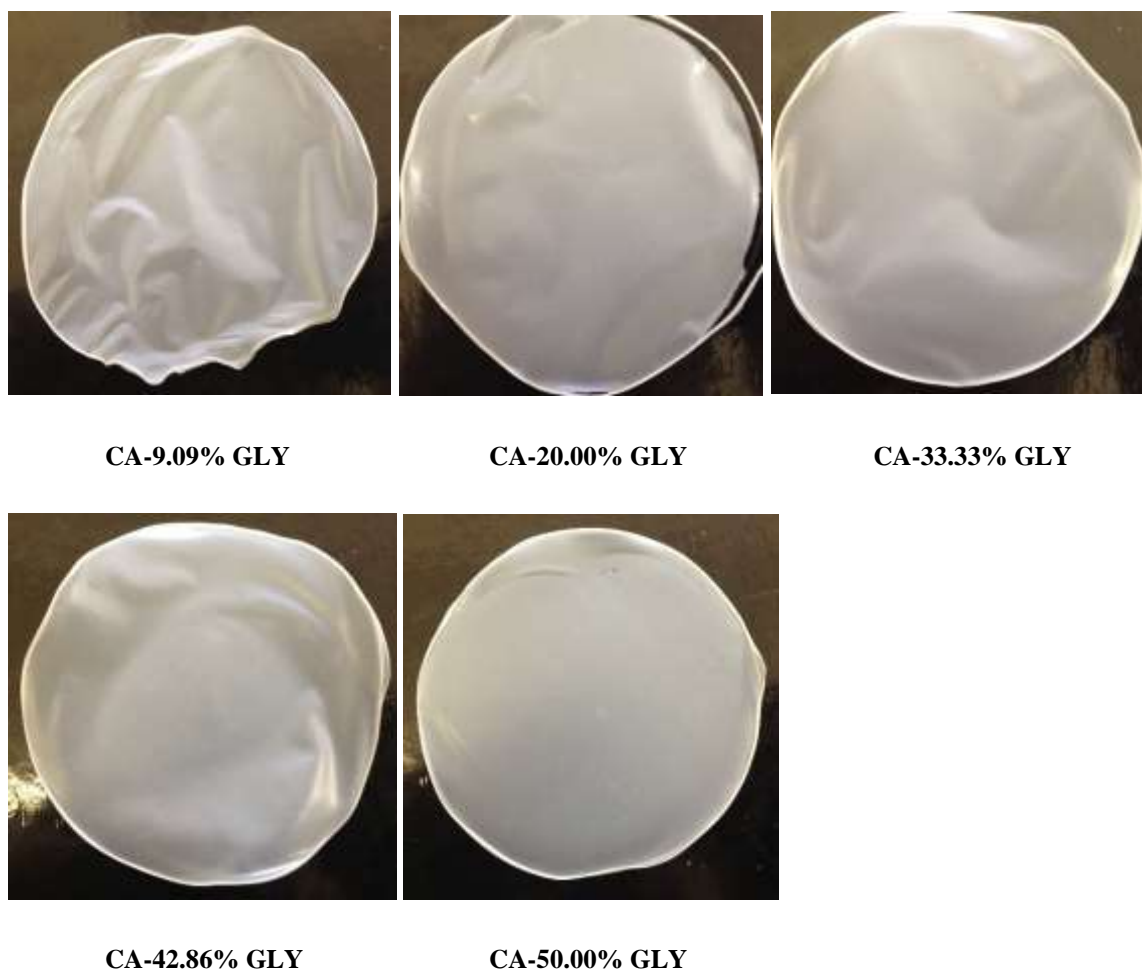
Figure 2.5   Films prepared from plasticized gels of different concentration based on total dry weight.

Addition of GLY made them more flexible and pliable. The films plasticized with GLY greater than 33.33% w/w were difficult to remove from the Petri dish owing to strong adhesion as the films became sticky due to the migration of GLY toward the surface, through a leaching phenomenon (Lin *et al*., 1991). However, all plasticized films were appeared to be transparent which will allow the inspection of wound bed without removal of the dressings. However, the tranperency of the films need to be confirmed by imaging against appropriate background such as printed block letters under the films. It was observed that films containing GLY at 33.33% w/w (based on total dry weight) were more flexible and tougher than any other plasticized films. The flexibility of the films is important to ensure ease of application to the wound area whilst toughness is important to allow handling as well as resisting the external pressure exerted during

body movements around the wound area. Therefore, the plasticized film containing 33.33% w/w GLY was selected for drug loading.

The common problem of DL films is the precipitation of drug by recrystallization during film drying process as water evaporates from the gel (Boateng *et al*., 2013b) especially at high drug loading. **Figure 2.6** illustrates the CIP loaded films with ideal optical appearance representing no drug recrystallization visible. However, visible drug precipitation was observed on the surface of FLU loaded films indicating recrystallization of drug during film formationas solvent evaporated from the gel (Boateng *et al*., 2013b).

CA-CIP 0.005%	**CA-CIP 0.010%**	**CA-CIP 0.025%**
CA-FLU 0.05%	**CA-FLU 0.10%**	**CA-FLU 0.20%**
CA-CIP:FLU (1:10)	**CA-CIP:FLU (1:20)**	
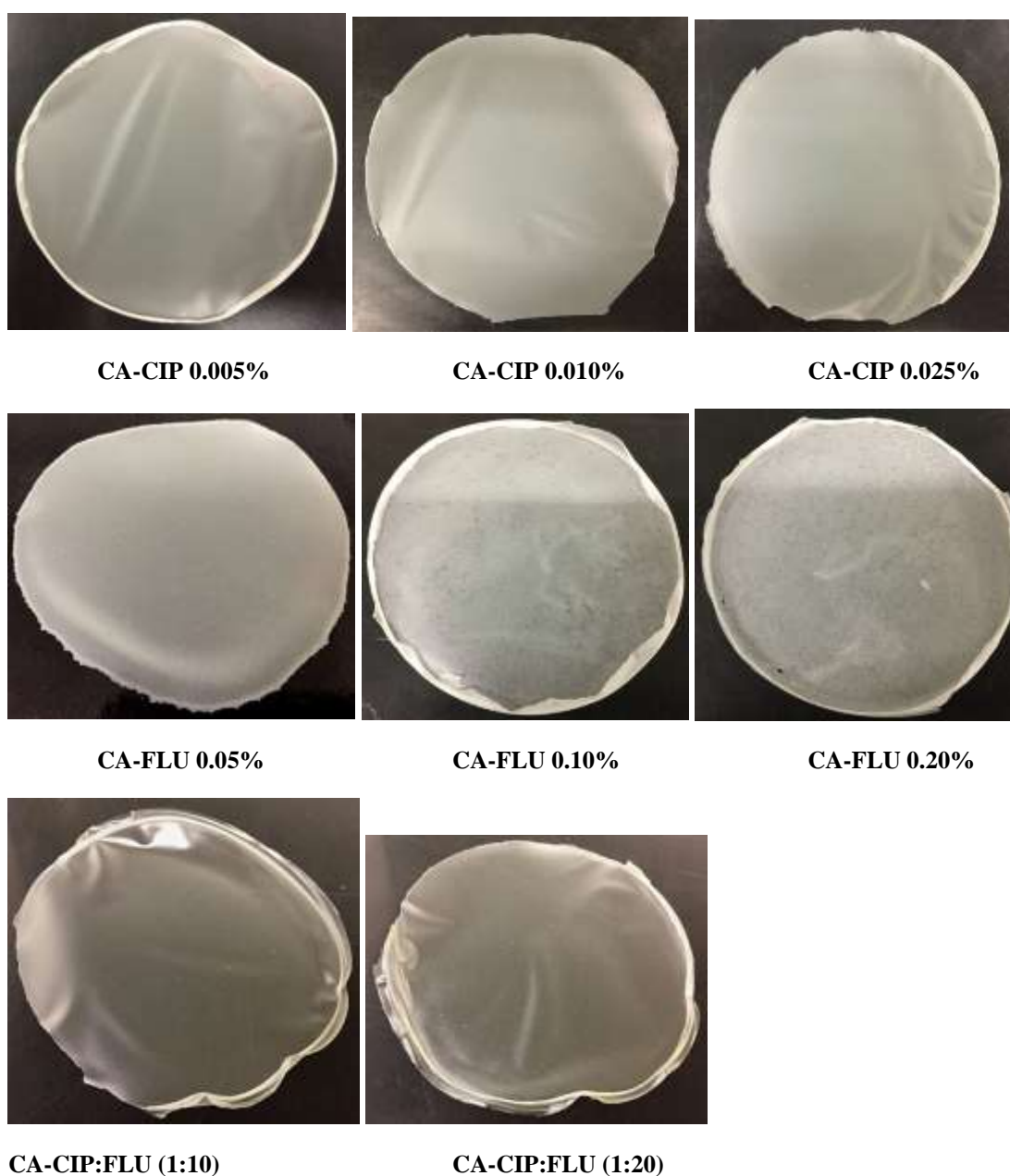
Figure 2.6   Digital images of DL films.

Incorporation of FLU resulted in high viscous gels followed by loss of plasticizing effects of GLY. Therefore, the flexibility of the formulations was restricted by increased intermolecular interactions between the polymer chains with resultant decrease in chain mobility, which reduced drug entrapment within the polymeric matrix. Moreover, high amount of FLU might be poorly soluble in highly basic CA gel, resulted in precipitation of undissolved drug particles on the film surface through recrystallization. Crystallization of the FLU loaded films was also confirmed by SEM and XRD observation. Less precipitation of the drug was observed in the film loaded with 0.05% FLU indicating low FLU loading capacity of CA film. Interestingly, films loaded with both CIP and FLU appeared more transparent than the films containing only FLU (**Figure 2.6**). Such phenomena could be due to the presence of CIP which increased the drugs-polymer miscibility resulting in uniform distribution of the drugs with no visible crystal aggregates on the film's surface. The DL plasticized films, BLK plasticized films and BLK unplasticized films were further tested by texture analyser for tensile strength, elasticity, rigidity and adhesion properties to understand the effects of drug loading and plasticizer in the polymeric matrix.

2.4.2 Formulation development of wafers

Figure 2.7 shows the digital images of CA based wafers prepared by freeze-drying different gel concentrations (% w/w). Interestingly, wafers were not transparent compared to the films, which is one of the disadvantage of wafer dressings. Transperency depends on the passing of light through the matrix and in the case of wafers, light scatters outward incoherently and does not pass through to a noticible extent due to its interconnected pores through out the matrix. However, after freeze-drying, all wafers appeared to be of uniform texture and thickness except wafer prepared from of 0.5% w/w gel. After that, hardness of all formulated wafers was tested to select optimum gel concentration for drug loading. Wafers prepared from 1% w/w gels were flexible to handle (see hardness data below) whereas wafers prepared from 1.5% and 2% w/w gels were very brittle and inflexible. On the other hand, wafers prepared from 0.5% w/w gel did not retain uniform structure because of low viscosity of the gel and subsequently low polymer network density. Subsequently, lyophilization of less viscous gel promoted premature ice crystallization during freezing and sublimation phases which resulted in flaky wafers. Therefore, the drugs were loaded into 1% w/w gels to obtain DL wafers.
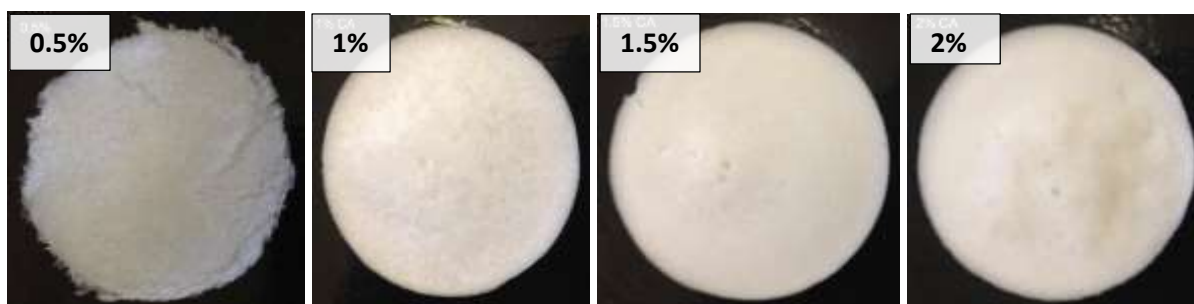
Figure 2.7 Digital images of CA wafers prepared from gels of different concentrations based on total polymer weight.

2.4.3 Scanning electron microscopy (SEM)

From **Figure 2.8,** it can be observed that the surface of the films is not smooth possibly due to crystallization from calcium carbonate precipitation in the formulations and confirmed by XRD (**Figure 2.11 b**).

CA-0.00% GLY   CA-0.09% GLY   CA-20.00% GLY

CA-33.33% GLY   CA-42.86% GLY   CA-50.00% GLY
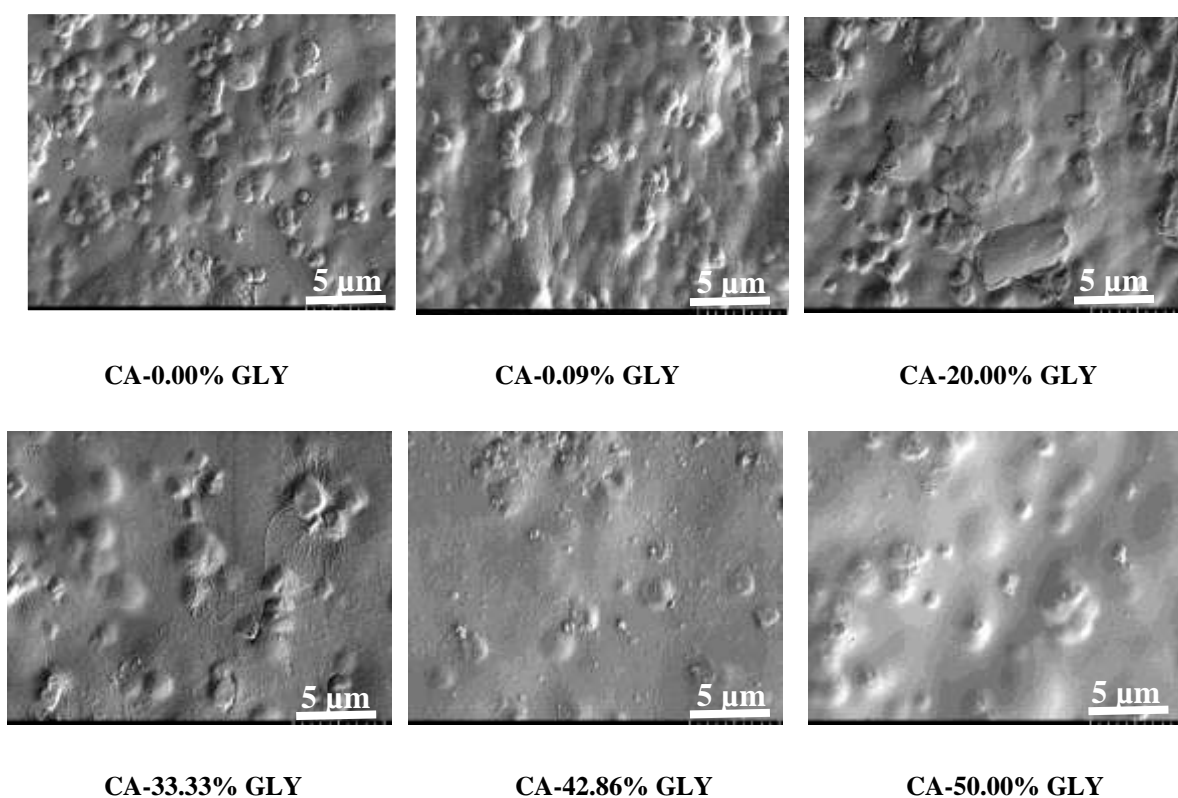
Figure 2.8 SEM images of unplasticized and plasticized (non-DL) films captured at x6000 magnification.

The plasticized films appeared less rough and were smoother than unplasticized films. This indicates that addition of GLY largely improves the homogeneity of the CA films by masking calcium carbonate precipitation. As the amount of GLY increased, the crystallinity visible on

the surface was decreased. This is because the hydroxyl groups in GLY penetrated the polymeric matrix and formed hydrogen bonds with hydroxyl groups of CA thus creating larger spaces between the polymeric chains, resulting in reduced crystallinity (Gao *et al*., 2017). However, presence of calcium carbonate did not affect the homogeneous distribution of the drug throughout the films confirmed by drug content uniformity test (**Chapter 3**).

The surface of the plasticized films (CA-33.33% GLY) became smoother after loading CIP shown in **Figure 2.9**. This could be explained by the fact that, after adding the drug, the number of hydroxyl groups increased, thus enhancing interaction between CIP molecules and CA resulted in lower precipitation of calcium carbonate on the film's surface.

CA-CIP 0.005% **CA-CIP 0.010%** **CA-CIP 0.025%**

CA-FLU 0.05% **CA-FLU 0.10%** **CA-FLU 0.20%**

CA-CIP:FLU (1:10) **CA-CIP:FLU (1:20)**
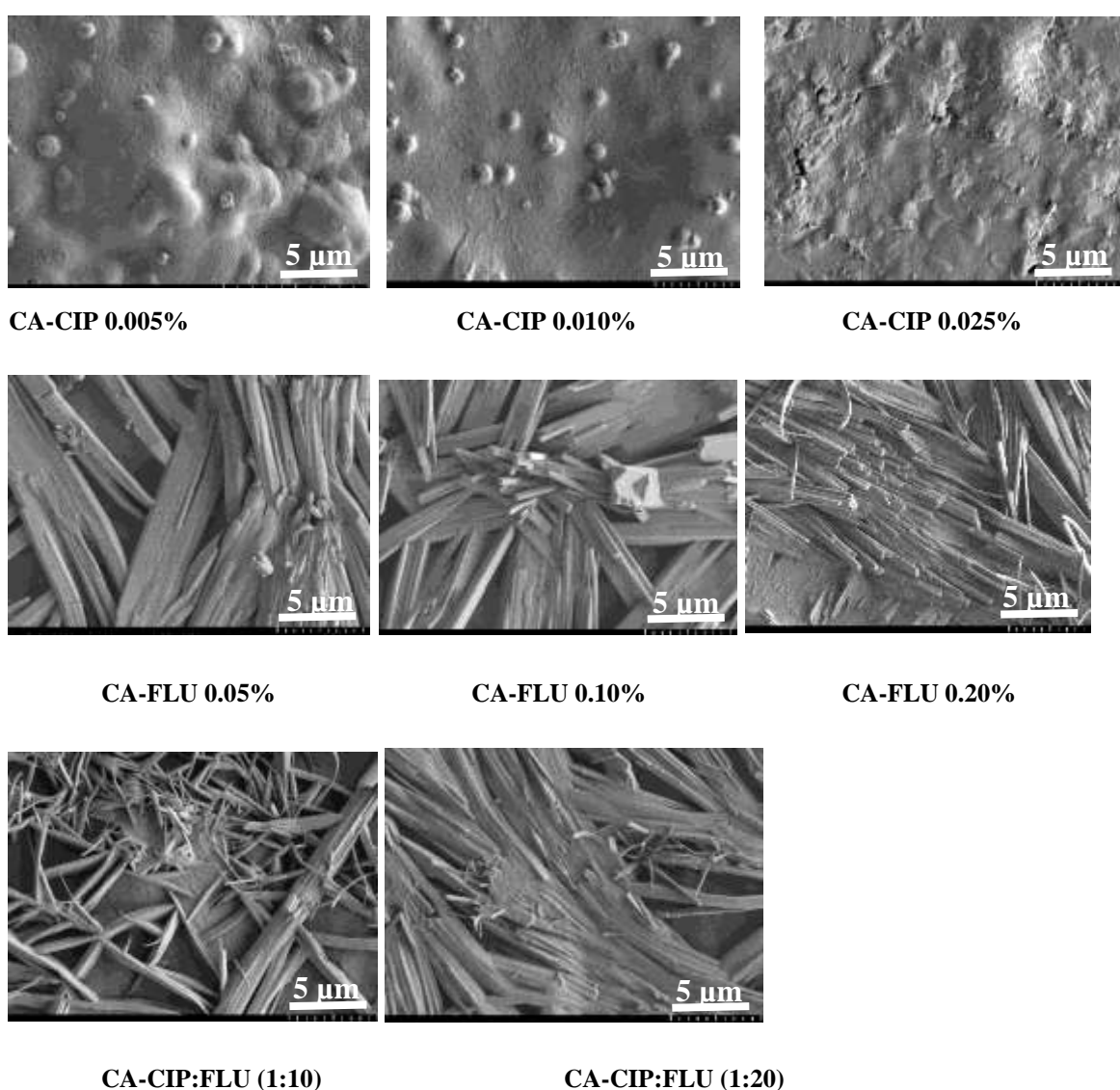
Figure 2.9   SEM images of plasticized DL films captured at x6000 magnification.

On the other hand, FLU loaded films exhibited spherulitic crystallization, which appeared as monoclinic unit cells. A very close observation revealed that the spherulitic crystallization increased with increasing concentration of FLU into the films. The crystalline nature of FLU was also confirmed by XRD (**Figure 2.11**) Moreover, the roughness of the film's surface (**Figure 2.6**) indicates recrystallization of drug on the film's surface. Such differences in distribution of the drug particles on the film surface can influence fluid handling properties and drug dissolution. Spherulitic crystallization was also observed in combined (CIP and FLU) DL films but to a lesser extent than the FLU only loaded films. In the combined DL films, CIP might have interacted with FLU via hydrogen bonding and increased miscibility between the drugs within the polymeric matrix. Therefore, the combined DL films showed comparatively smoother and more homogenous surface (**Figure 2.6**) than FLU loaded films. It also confirms that hydrogen bonding between two drugs is responsible for lowering spherulitic crystallization of combined DL films.

SEM images of wafers revealed that the BLK wafers were highly porous in morphology with large, uniform and circular shaped pores surrounded by a network of polymeric strands as shown in **Figure 2**.10 **(A).**

CA-BLK	**CA-CIP 0.0001%**	**CA-CIP 0.0005%**
CA-CIP 0.0010%	**CA-CIP 0.0025%**	**CA-CIP 0.005%**
CA-CIP 0.010%	**CA-CIP 0.025%**	**CA-CIP 0.040%**
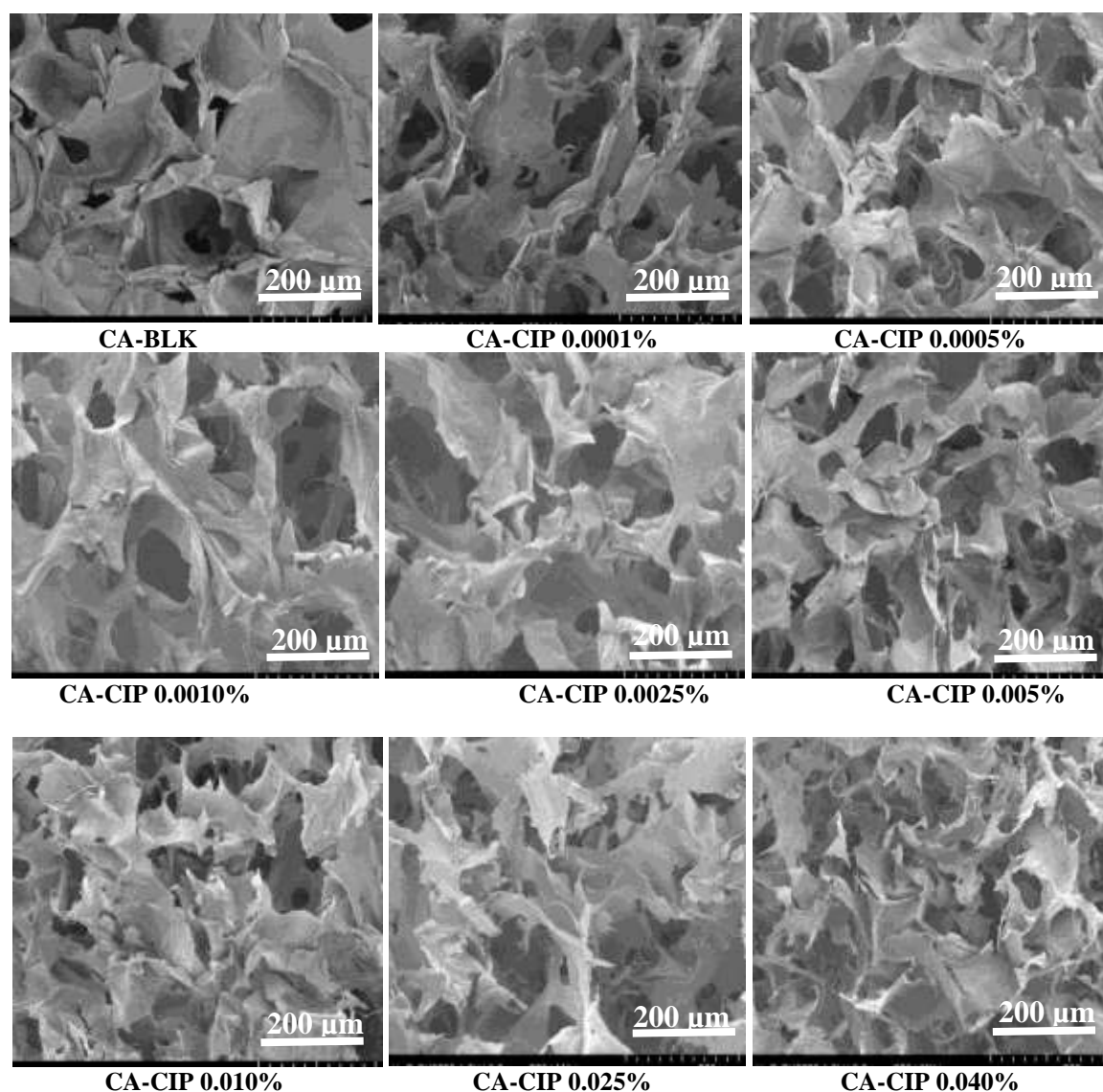
Figure 2.10 (A) SEM images of BLK and CIP loaded wafers captured at x200 magnification.

It is reported that gels made from high α-L-guluronic acid alginates exhibit the highest porosity (Gombotz and Wee, 1998). However, incorporation of CIP changed the uniformity of the pores in wafers. Increasing amount of CIP resulted in denser pores due to possible crosslinking between the drug and polymer during the freeze-drying process. The morphology of the FLU loaded wafers shown in **Figure 2.10 (B)** also revealed large and uniform pores when the wafers contained up to 0.15% w/v FLU. The uniformity of the pores was disturbed in FLU loaded wafers when the drug content exceeded 0.15% w/v in the original gel. It can also be observed that wafers containing high concentrations of FLU (0.30 and 0.40% w/v) in the

original gel possessed a rough surface texture. In addition to their roughness, visible drug particle precipitation was observed on the walls of the pores, which was deemed non-ideal. Wafers containing combined CIP and FLU in the ratios of 1:10 and 1:20 retained large circular and uniform pore size distributions as shown in **Figure 2.10 (B)**.

| **CA-FLU 0.05%** | **CA-FLU 0.10%** | **CA-FLU 0.15%** |

| **CA-FLU 0.30%** | **CA-FLU 0.40%** | **CA-CIP:FLU (1:10)** |

| **CA-CIP:FLU (1:20)** | **CA-CIP:FLU (1:30)** |
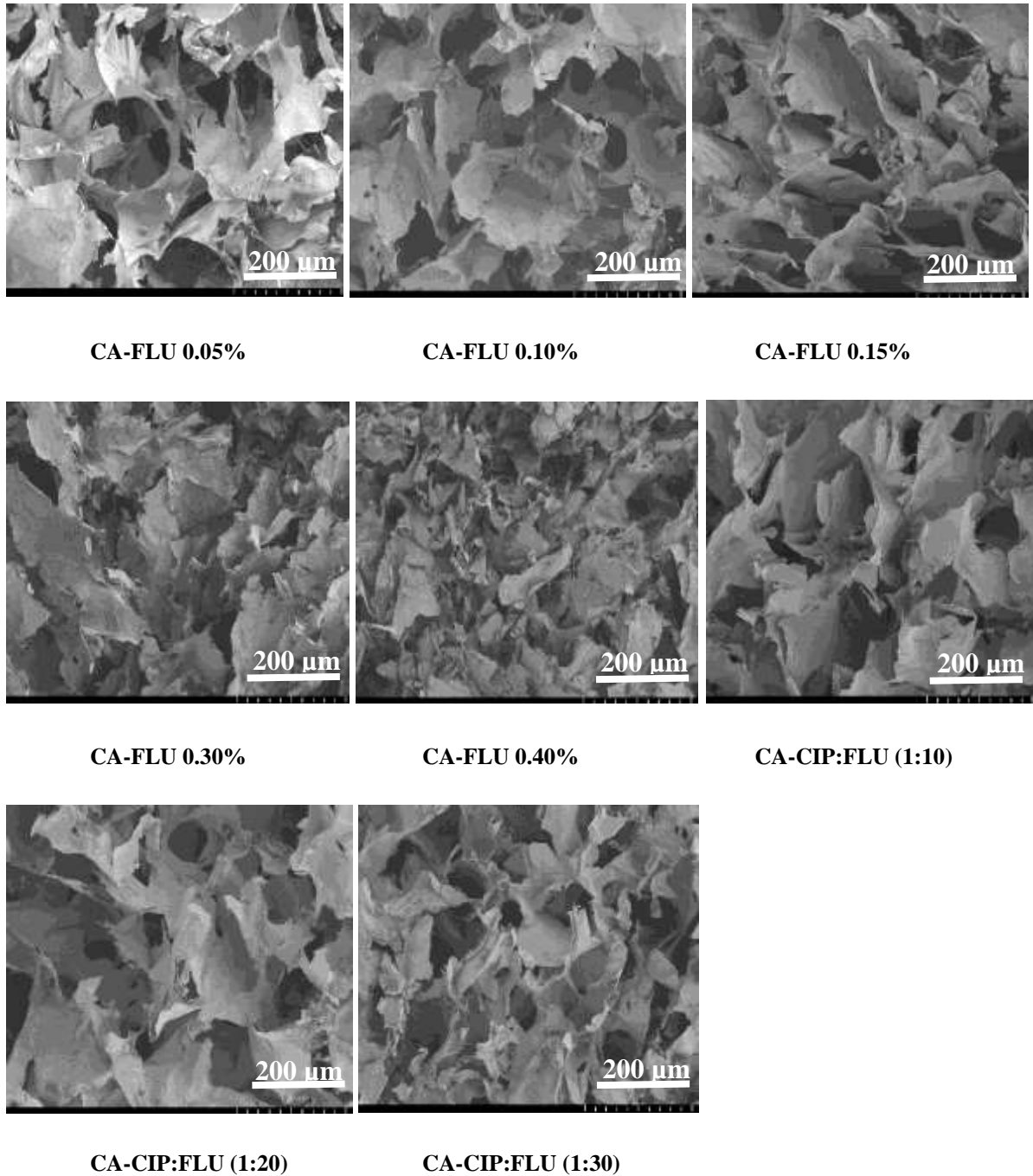
Figure 2.10 (B)   SEM images of FLU loaded and combined DL wafers captured at x200 magnification.

Wafers incorporated with both CIP and FLU in the ratio of 1: 30 showed non-uniform pores with reduced pore size. This could be attributed to the higher content of FLU in the wafer's matrix resulting in denser cores. The changes in surface characteristics have impact on other physico-chemical properties such as hardness, swelling, adhesion, EWC, water absorption and WVTR (Pawar *et al*., 2014; Kim *et al*., 2007). **Figure 2.10 (C)** shows the surface morphology of the top and bottom sides of the wafer. The bottom part of the wafer looks more porous than the top part resulting in varied hardness between the different parts.

Top   **Bottom**
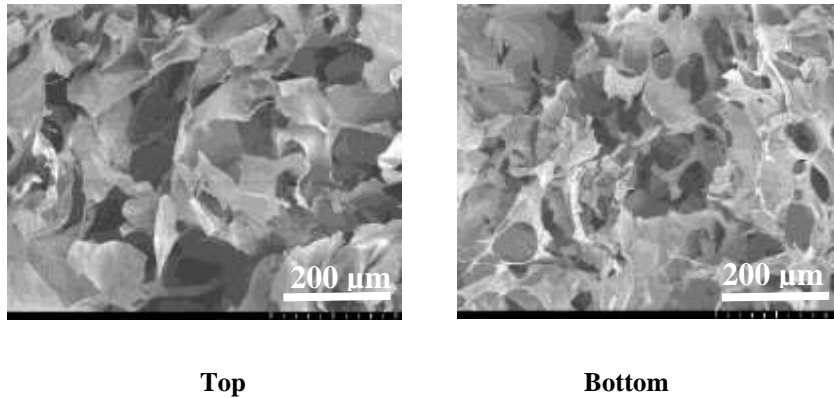
Figure 2.10 (C)   Representative SEM images of top and bottom surface of typical wafer captured at x200 magnification.

2.4.4 X-ray diffraction (XRD)

Figure 2.11 shows XRD transmission diffractograms of (a) pure CA, (b) CIP, FLU and $CaCO_3$. The diffractogram of CA showed the characteristic of an amorphous sample as no sharp peak appeared, whereas the diffractogram of CIP showed three distinct sharp peaks at around $2\theta = 14.43°$, $20.67°$ and $25.50°$ due to some crystalline character of the drug. FLU also exhibited a highly crystalline nature, with several characteristic sharp peaks at $2\theta = 9.16°$, $15.09°$, $16.14°$ and $20.03°$.
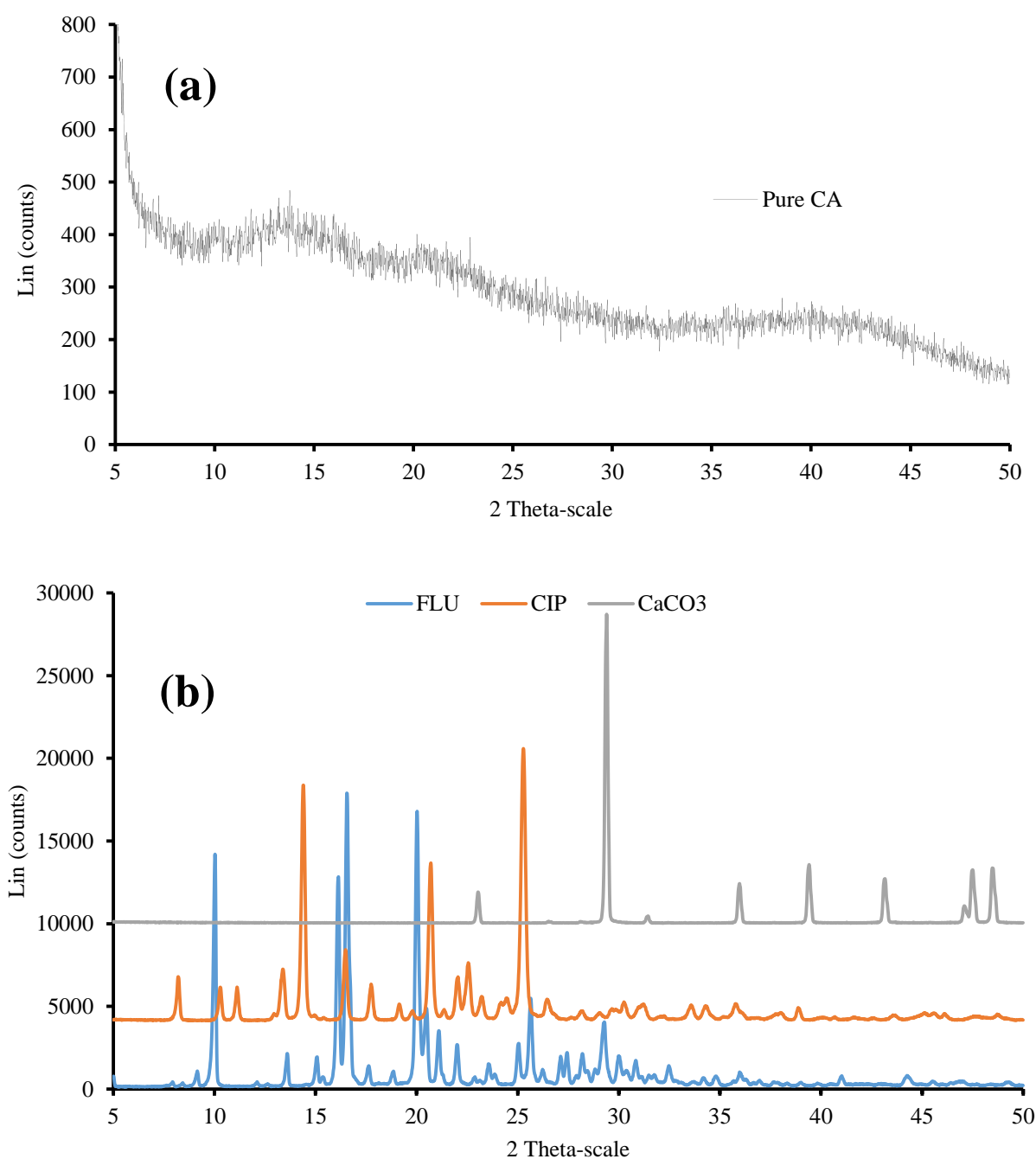
Figure 2.11   X-ray diffractograms of (a) pure CA, and (b) pure CIP, FLU and $CaCO_3$.

CA dressings showed eight common peaks at 2θ of 22.81º, 29.58º, 31.76º, 36.07º, 39.42º, 43.16º, 47.64º and 48.5º (**Figure 2.12 & Figure 2.13**) all attributed to the presence of calcium carbonate formed during gel preparation. After loading drugs in CA-33.33% GLY film, crystalline nature of the drugs was altered due to interaction and entrapment of drug molecules into the polymeric matrix. It was observed that the three distinct characteristic peaks of CIP disappeared in the diffractogram of CIP loaded film dressings indicating molecular dispersion of the drug within the polymeric matrix.
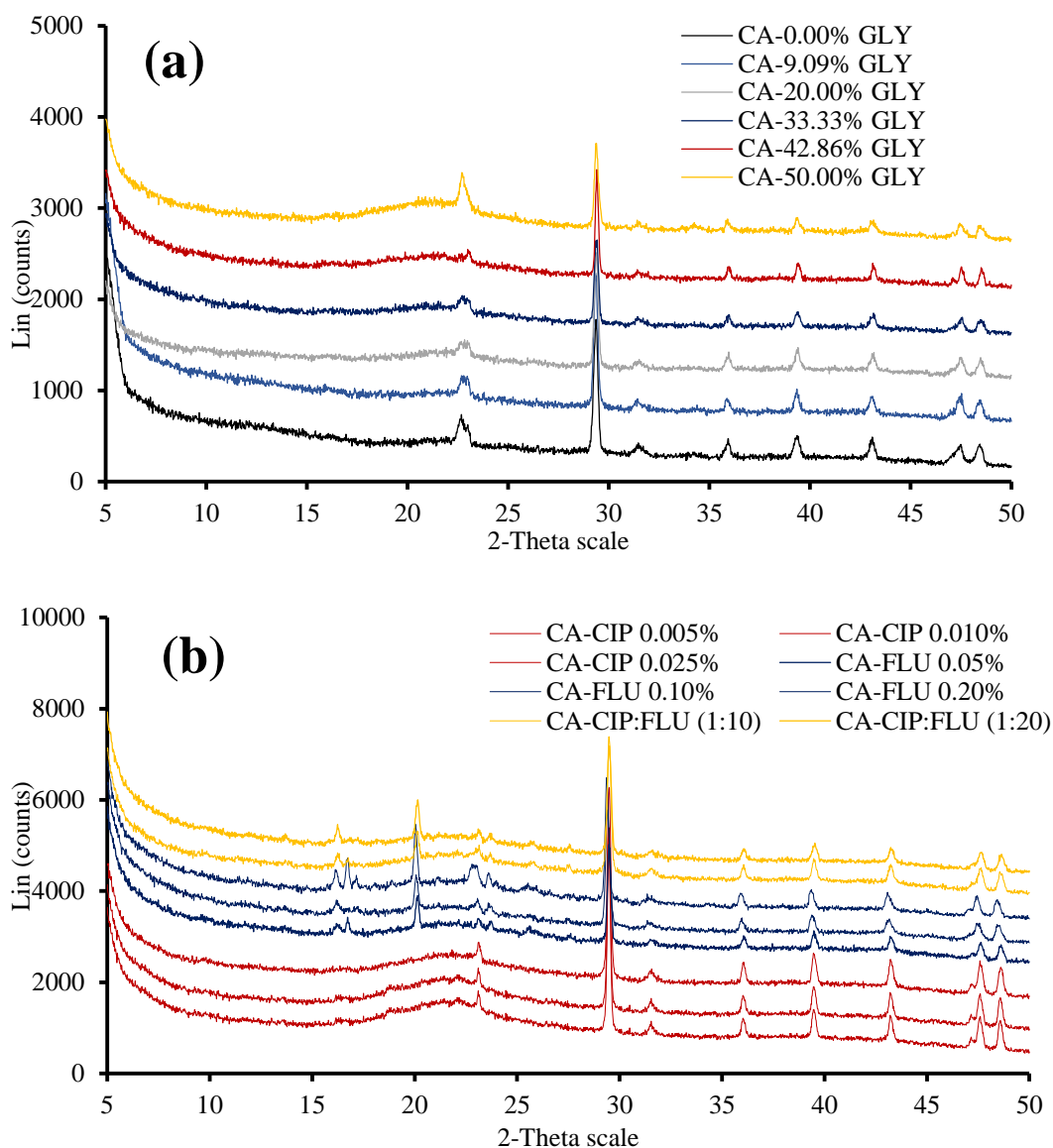
Figure 2.12   XRD patterns of (a) unplasticized BLK, plasticized-BLK and (b) plasticized-DL films.

On the other hand, the two strongest peaks of FLU (at $2\theta = 16.14º$ and 20.03º) appeared in the diffractograms of combined DL and only FLU loaded films (**Figure 2.12b**). This

indicates that FLU was partially dispersed through the polymeric matrix. That means films have low FLU loading capacity. The XRD patterns of the films (**Figure 2.12 b**) containing both CIP and FLU were all identical to the films containing only FLU. This could be attributed to the higher amount of FLU compared to CIP within the polymeric matrix. It was also noted that the peaks of all DL films were slightly shifted to higher diffraction angles indicating the interaction of drug with the polymer.

The percentage crystallinity of the films was also estimated (**Table 2.2**) with the unplascized BLK film showing 90.25% crystallinity whilst the crystallinity decreased to 51.59% after adding the maximum amount of GLY (50% w/w) (**Figure 2.12 a**). This is because, GLY decreased the spaces between the crystal lattice and made the polymeric chain flexible. The plasticized BLK (CA-BLK) film containing 33.33% GLY showed 69.02% crystallinity and the crystallinity was further decreased to 48.62% after loading 0.025% w/v CIP.

Table 2.2   The estimated percentage crystallinity of $CaCO_3$ retained in the films.

Films	Crystalinity (%)
CA-0.00% GLY	90.25
CA-9.09% GLY	86.98
CA-20.00% GLY	76.42
CA-33.33% GLY	69.02
CA-42.86% GLY	60.62
CA-50.00% GLY	51.59
CA-CIP 0.005%	68.23
CA-CIP 0.010%	56.22
CA-CIP 0.025%	48.62
CA-FLU 0.05%	56.60
CA-FLU 0.10%	63.95
CA-FLU 0.20%	68.96
CA-CIP:FLU (1:10)	52.33
CA-CIP:FLU (1:20)	62.58

FLU loaded films showed more crystalline nature (about 68.96%) than CIP loaded films. This was in agreement with the digital images (**Figure 2.6**) and SEM morphological (**Figure 2.8**) observations. The crystallinity of combined DL films was lower than FLU only films but higher

than CIP loaded films. Generally, drug concentration dependent crystallinity was also observed in the DL films. The crystallinity of CIP loading films was reduced from 67.12% to 48.62% after loading 0.005-0.025% w/v CIP but the crystallinity of FLU loaded films was increased from 56.60% to 68.96% after loading 0.05-0.20% w/v FLU. In case of combined drug loaded films, the crystallinity increased from 62.58% to 52.33% when amount of FLU was increased. Overall, the above observations revealed that generally addition of CIP decreased whilst the addition of FLU increased crystallinity of the films and confirmed the previous results from visual and SEM observations.
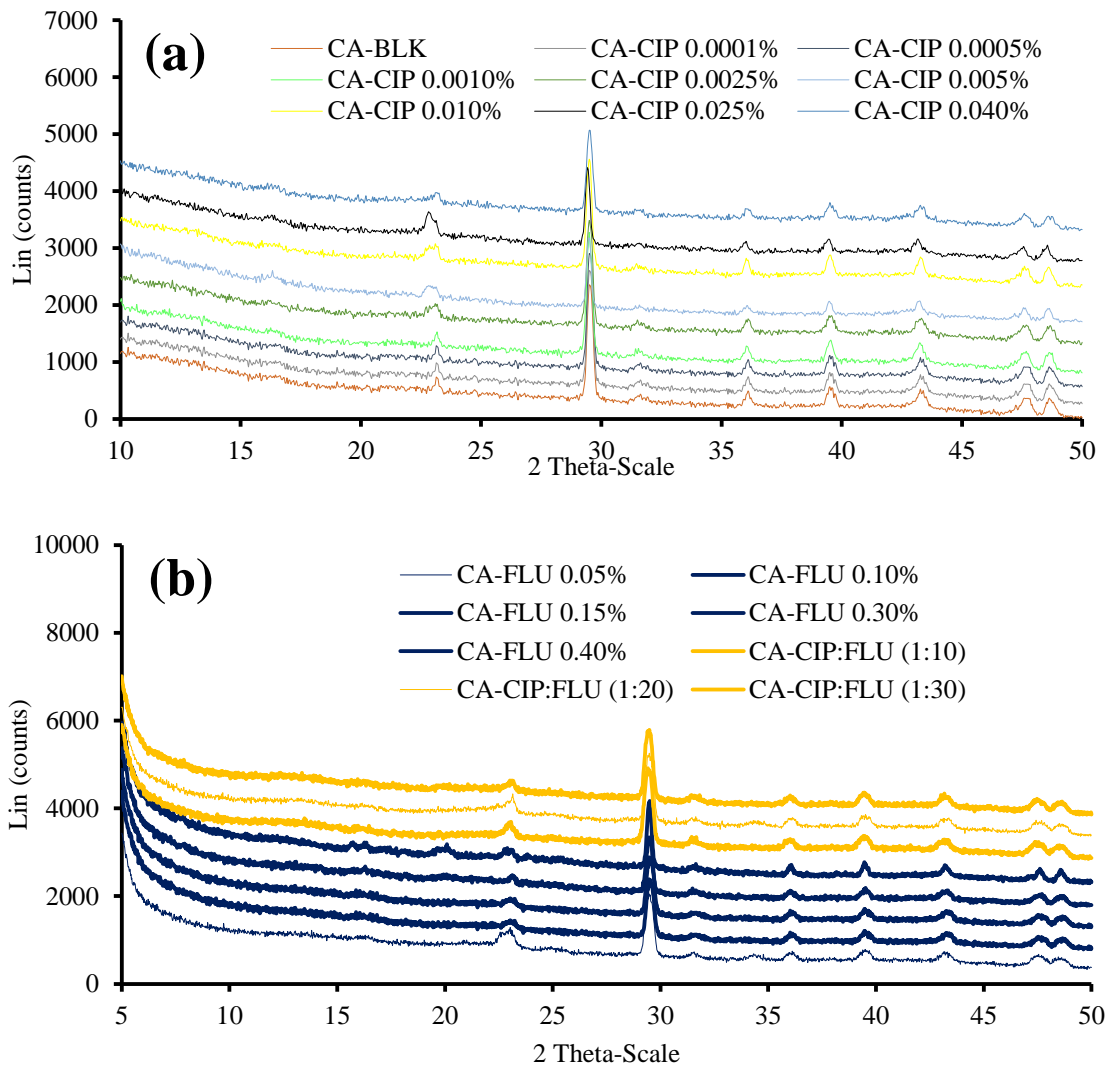
Figure 2.13   XRD transmission diffractograms of (a) CIP loaded wafers and (b) FLU loaded and combined DL wafers.

Figure 2.13 shows the XRD diffractograms of BLK and DL wafers. XRD pattern of all DL wafers also demonstrated the existence of calcium carbonate as in the film dressings.

Disappearance and / or decrease in intensity of the characteristic peaks of CIP (2θ = 14.43º, 20.67º and 25.50º) and FLU (2θ = 9.16º, 15.09º, 16.14º and 20.03º) in the wafer dressings suggests that the drugs were molecularly dispersed within the polymeric micro-matrix and this is expected to impact upon the rate of hydration and drug release. Here, it is also important to note that the characteristic peaks of the dressings were slightly shifted to higher diffraction angle that indicated the interaction of drug with the polymer. Interestingly, the wafers appeared more crystalline than the films. This could be because the presence of plasticizer in the film dressings reduced the glass transition temperature with increasing free molecular mobility by reducing order of crystal lattice (Panda *et al*., 2014). Moreover, GLY could mask the crystalline calcium carbonate precipitate in the film and hence reduced crystallinity. The lyophilization process and absence of plasticizer could have resulted in higher calcium carbonate precipitation thus making the wafers more crystalline than film dressings. Drug concentration dependent crystallinity was also observed in the DL wafers with higher amount of drugs, resulting in higher crystallinity of the dressings (**Table 2.3**).

Table 2.3   The estimated percentage crystallinity of $CaCO_3$ retained in the wafers.

Wafers	Crystalinity (%)
CA-BLK	85.61
CA-CIP 0.005%	77.55
CA-CIP 0.010%	77.63
CA-CIP 0.025%	82.29
CA-FLU 0.05%	77.21
CA-FLU 0.10%	82.10
CA-FLU 0.15%	83.24
CA-FLU 0.30%	84.41
CA-FLU 0.40%	85.00
CA-CIP:FLU (1:10)	78.50
CA-CIP:FLU (1:20)	82.88
CA-CIP:FLU (1:30)	84.17

2.4.5 Fourier transform infrared spectroscopy (FTIR)

FTIR spectra of FLU, CIP, CA, plasticized films, BLK and DL dressings were studied to analyse the nature and extent of interaction between the drugs, polymer and plasticizer (films). The FTIR spectrum (**Figure 2.14**) of pure CA showed broad peak of OH stretching at 3204 cm^{-1} and two other peaks were detected at 1591 cm^{-1} and 1411 cm^{-1} respectively representing the asymmetric and symmetric stretching of carboxylate ion. Further, another peak was observed at 1025 cm^{-1}, due to C-O-C antisymmetric stretching vibration of pyranosyl ring. An absorption band at 947 cm^{-1} was also associated with C-O stretching vibration of uronic acid and C-C-H and C-O-H deformation, whereas the absorption band at 874 cm^{-1} was attributed to β-C1-H deformation vibration. The spectrum (**Figure 2.14**) of CIP also revealed prominent characteristic band between 3600 and 3045 cm^{-1} of OH stretching and intermolecular hydrogen bonding. In addition, the band at 3000-2845 cm^{-1} represented alkene and C-H stretching. The peak between 1675 to 1660 cm^{-1}, was assigned to carbonyl C=O stretching whilst the bands from 1650-1600 cm^{-1} represented quinolones and that at 1450-1400 cm^{-1} was attributed to carbonyl group (C-O) vibration. The peak between 1300 and 1250 cm^{-1} is associated with bending vibration of O-H group and a strong characteristic peak between 1050 cm^{-1} to 1000 cm^{-1} was assigned to aryl fluoride (C-F) stretching vibration (Kataria *et al.*, 2014). In the FTIR spectra of pure FLU (**Figure 2.14**), the peak at 3650 cm^{-1} was assigned to OH stretching and another characteristic peak at 2981 cm^{-1} was related to C-H stretching of the triazole ring. The peak at 1618 cm^{-1} was related to C=C stretching of 2,4-difluorobenzyl group and the band at 1500 cm^{-1} was attributed to C-C stretching of aromatic ring. A band at 1408 cm^{-1} indicated C-H$_2$ scissor of propane backbone and the characteristic strong peak at 1270 cm^{-1} signified C-F stretch of 2,4-difluorobenzyl group. A medium sharp band at 1210 cm^{-1} was related to β-CH triazole ring. Two characteristic sharp peaks at 1135 and 1115 cm^{-1} corresponded to ring breathing of triazole group and C-C stretch of propane backbone respectively. The peaks corresponding to CH deformation of 2,4-difluorobenzyl group and C-(OH) stretching of propane backbone were observed at 1075 cm^{-1} and 1011 cm^{-1} respectively. The three strongest peaks in the spectrum of FLU appeared at 960, 845 and 673 cm^{-1} representing the ring bending of triazole group, γ-CH triazole ring and deformation of aromatic ring respectively (Caira *et al.*, 2004; Bourichi *et al.*, 2012; Alkhamis *et al.*, 2002).
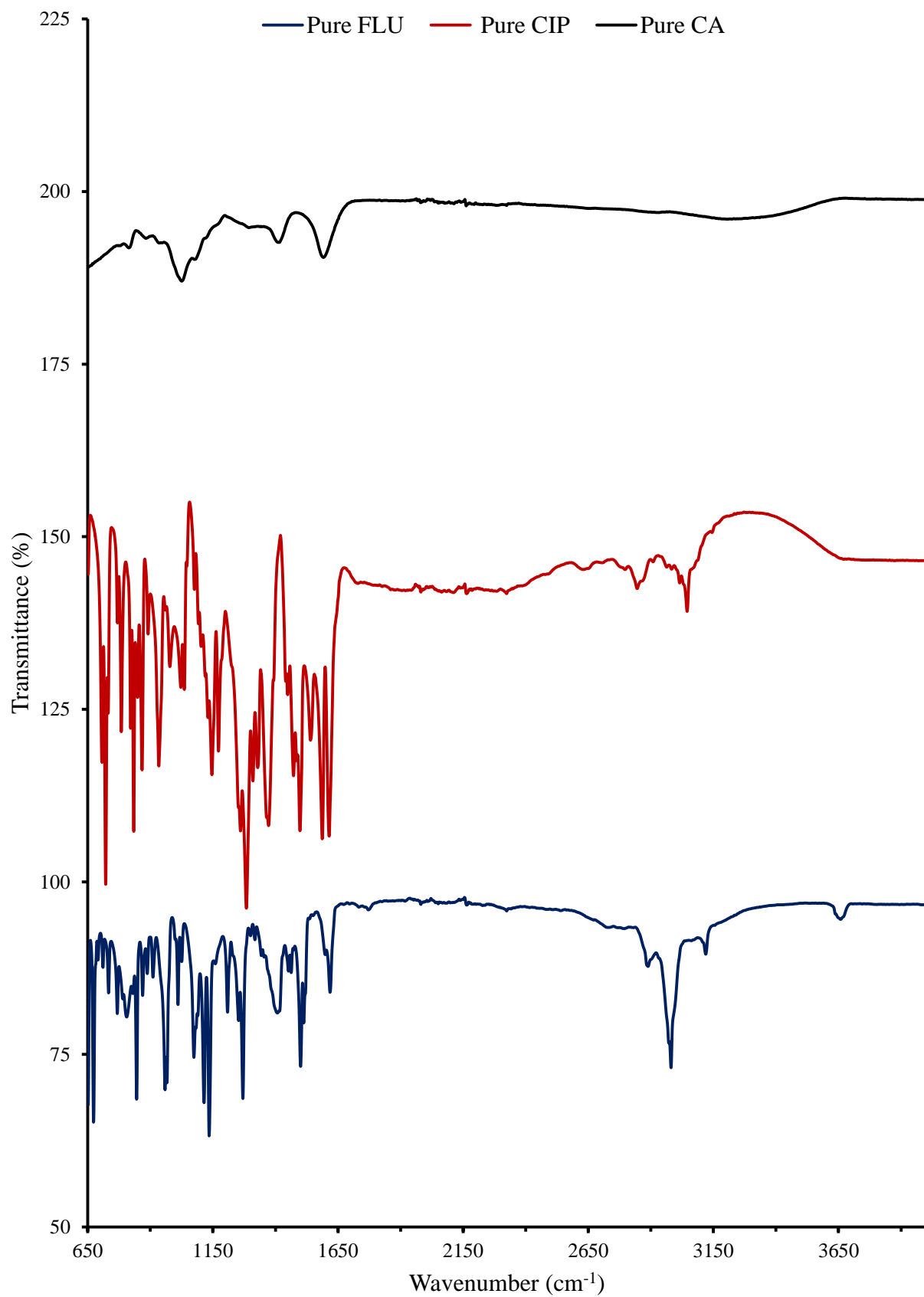
Figure 2.14 FTIR spectra of different starting components (FLU, CIP and CA).

As shown in **Figure. 2.15**, the broad peak of OH stretching at 3204 cm^{-1} of CA was shifted to higher wavenumber (3237-3272 cm^{-1}) after plasticizing the films. All other peaks were also shifted to higher wavenumber with addition of GLY. The shift of peaks towards a higher wavenumber was due to multiple –OH groups present in GLY that penetrated the polymeric matrix. Therefore, hydrogen bonding between water and CA was replaced by the hydrogen bonds between GLY and CA (Gao *et al*., 2017). The intensity of the bands also increased with GLY content because of the increasing –OH groups supplied by GLY.
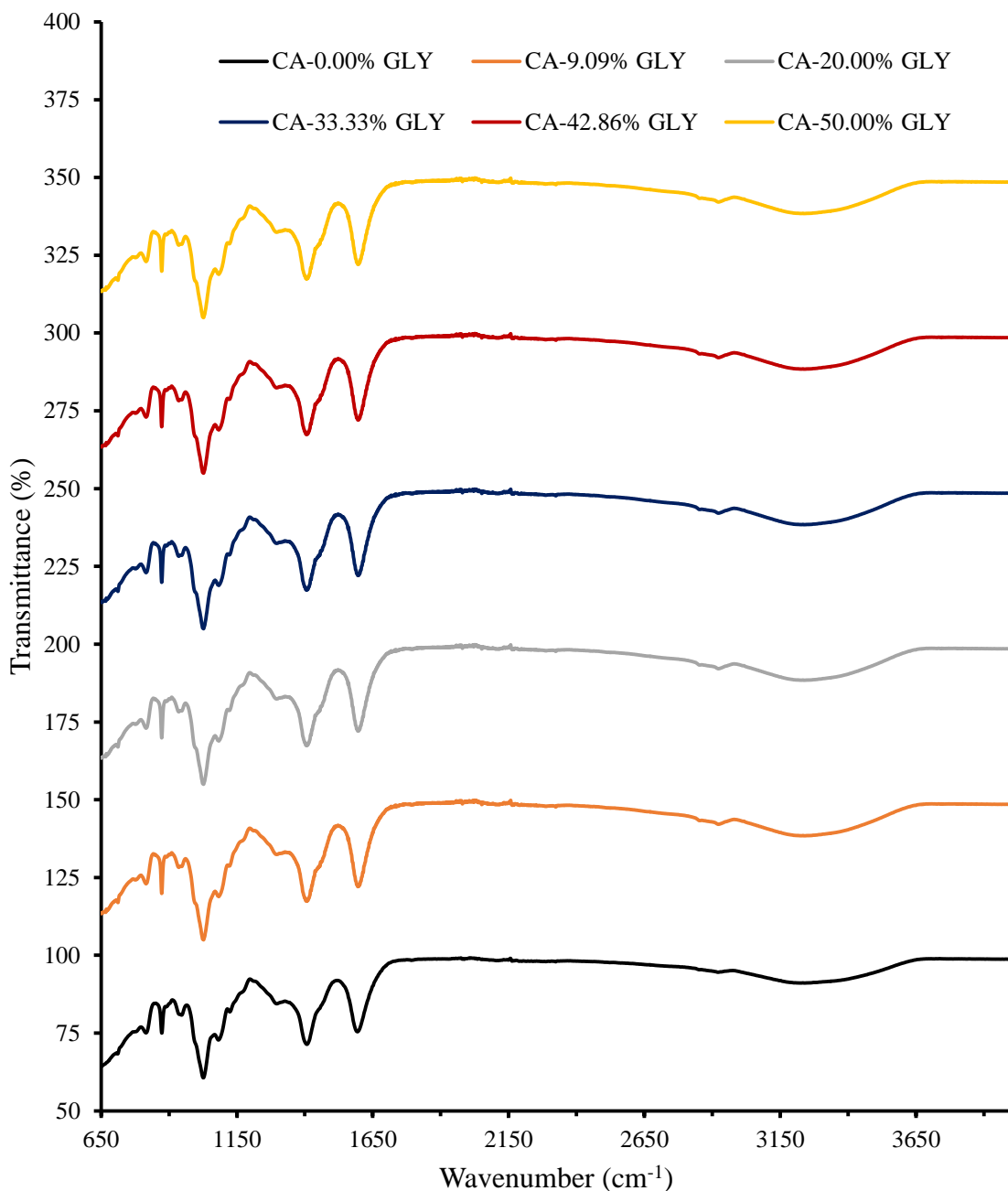
Figure 2.15   FTIR spectra of unplasticized BLK and plasticized-BLK films.

The peak of OH stretching of CIP loaded films remained within the range of plasticized films. Some of the characteristic peaks from CIP such as aryl fluoride (at 1050 cm^{-1}), carbonyl group (at 1450 cm^{-1}) and quinolones (at 1650 cm^{-1}) were invisible in the spectra of CIP loaded films (**Figure 2.16**).
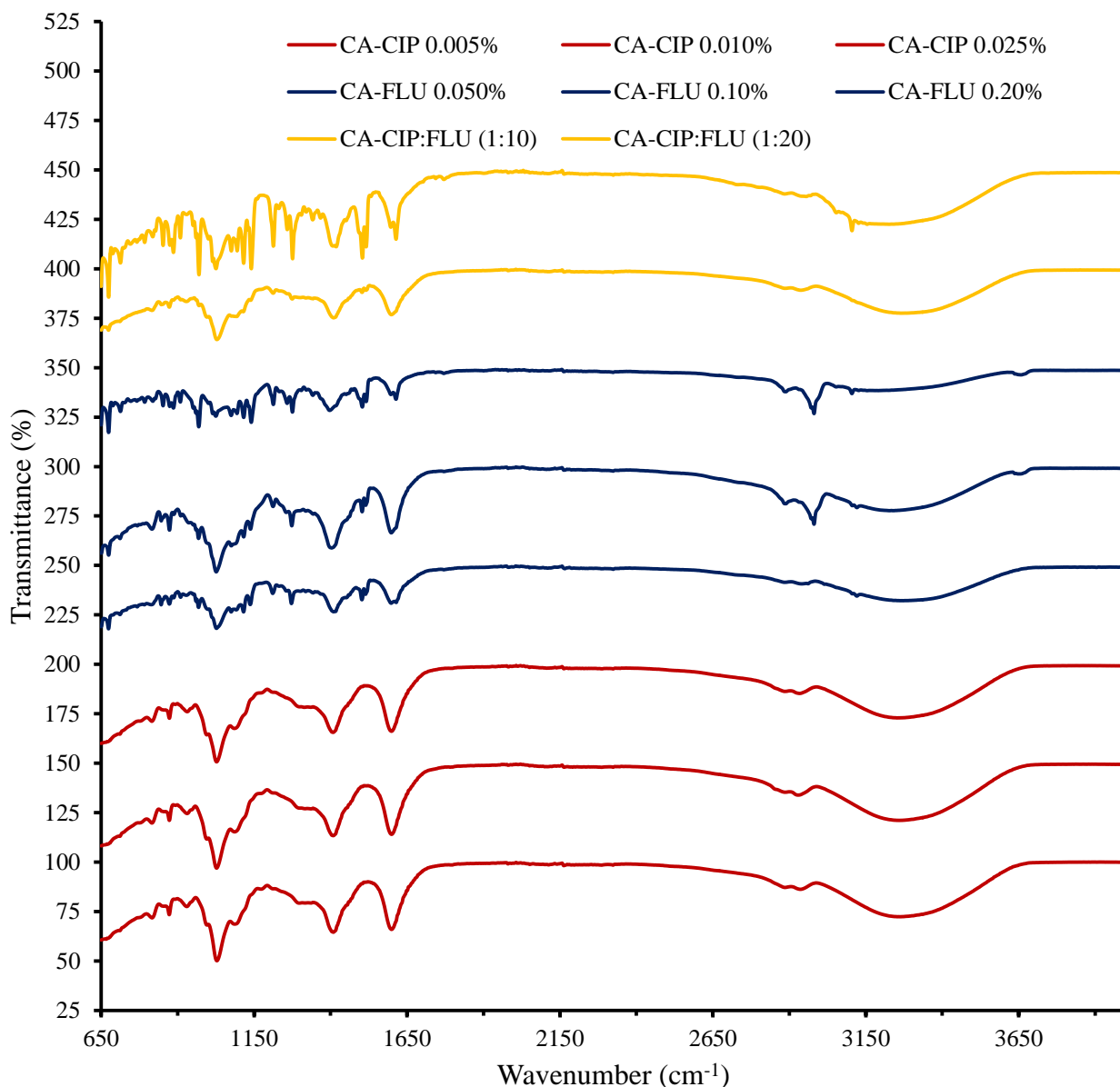
Figure 2.16   FTIR spectra of plasticized-DL films.

This might be due to the fact that the relatively low amounts of CIP incorporated were suppressed by the higher amounts of polymer and plasticizer that prevented them from being visible in the spectra. This also suggests the possible molecular dispersion of drug into the polymeric matrix. The broad peak of OH stretching at 3204 cm^{-1} of pure CA became broader (band between 3045 and 3600 cm^{-1}) after loading CIP due to intermolecular hydrogen bonding.

77

Most of the peaks of CA-BLK (CA-33.33% GLY) and CIP loaded films were similar to the pure polymer but different in intensity.It can be observed from the spectra (**Figure 2.16**) of FLU loaded films that the distinct peaks of both polymer and drug appeared with slight variations. The characteristic asymmetric and symmetric stretching of carboxylate ion (COO$^-$ (C=O) of pure CA was seen at 1598 and 1404 cm^{-1} respectively, C-O stretching of uronic acid at 968 cm^{-1}, β-C1-H deformation vibration at 873 and prominent peak corresponding to C-O-C antisymetric stretching of pyranosyl ring was observed at 1027 cm^{-1}. Strong characteristic peaks of FLU appeared as weak bands in the spectrum of the FLU loaded films. These include C-C stretching of aromatic ring at 1504 cm^{-1}, C-F stretching at 1275 cm^{-1}, ring breathing of triazole group at 1138 cm^{-1}, C-C stretching of propane backbone at 1116 cm^{-1}, ring bending of triazole group at 968 cm^{-1}, γ-CH triazole ring at 873 and 815 cm^{-1}(seen as doublet peak) and aromatic ring deformation at 674 cm^{-1}. The strong peak at 2981 cm^{-1} corresponding to C-H stretch of triazole ring were observed at same position as the pure FLU. However, some of the characteristic peaks from FLU such as C=C stretching of 2,4-difluorobenzyl group (at 1618 cm^{-1}), C-H$_2$ scissor of propane backbone (at 1408 cm^{-1}), CH deformation of 2,4-difluorobenzyl group (at 1075 cm^{-1}) and C-(OH) stretching of propane backbone (at 1011 cm^{-1}) of FLU were absent in the spectrum of the FLU loaded films. This could be due to the secondary interactions of FLU with the polymer and/or overlapped in FLU loaded films due to relative similarity and shifting. These observations suggest that FLU loading capacity of CA film was low due to its incompatibility with GLY. However, most of the peaks of FLU were seen in the spectrum of the film containing 0.20% w/v FLU and the film containing CIP and FLU in the ratio of 1:20 (**Figure 2.16**). It could be the fact that once the saturation point is reached, excess FLU crystalizes out of the polymer matrix during film drying. Therefore, it had impact on drug content uniformity and drug release. The FTIR spectrum of the film containing both CIP and FLU in the ratio of 1:10 was identical to the spectrum of pure CA and CIP loaded films indicated that low amount of FLU offered homogeneous mixture of the drugs.

In CIP loaded wafers shown in **Figure 2.17,** the OH peak became broader and less intense as the amount of drug increased. This could be explained by the fact that the higher the concentrations of the drug, the shorter the distance between CIP molecules and the hydroxyl group of CA, resulting in hydrogen bond formation by interaction of fluorine, carbonyl, and amino (-NH) groups of the CIP with hydrogen atom of CA. Moreover, after drug incorporation, a sharp peak appeared at 2981 cm^{-1} due to aromatic C-H stretching of CIP.
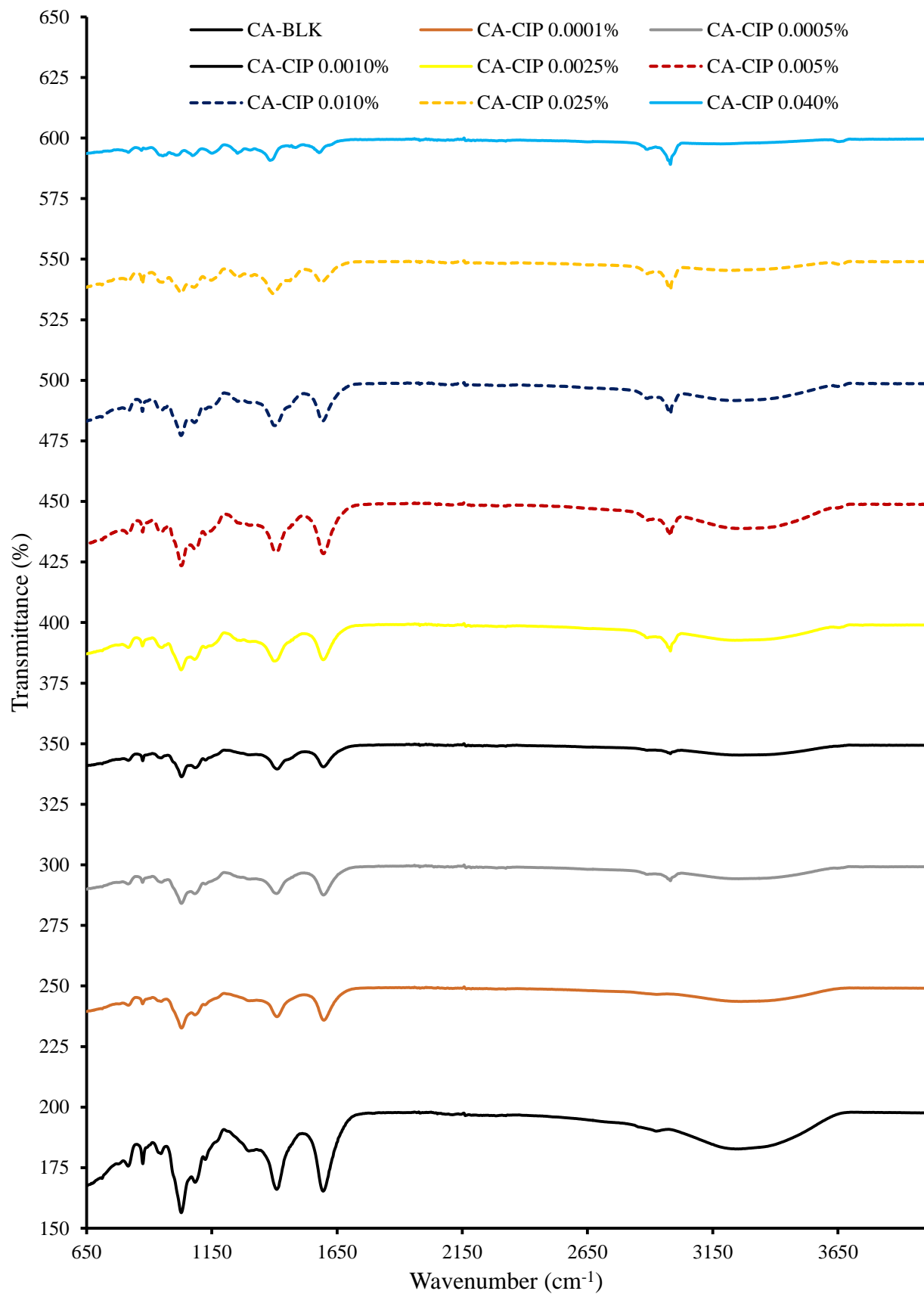
Figure 2.17   FTIR spectra of CIP loaded wafers.

The band of asymmetric carboxylate salt at 1595 cm^{-1} was the same for 0.0001-0.010% CIP loaded wafers while this band was shifted to lower wavenumbers at 1587 cm^{-1} and 1578 cm^{-1} respectively for 0.025 and 0.04% CIP loaded wafers. On the other hand, the peak for symmetric carboxylate salt at 1411 cm^{-1} for 0.025 and 0.040% CIP loaded wafers was visible at 1395 cm^{-1} and 1383 cm^{-1} respectively. It was also observed that the C-O-C antisymmetric vibration of pyranosyl ring, C-O stretching vibration of uronic acid and β-C1-H deformation vibration remained the same with their bands appearing at approximately 1025 cm^{-1}, 947 cm^{-1} and 874 cm^{-1} for all the CIP loaded wafers except the wafer with 0.040% CIP. In the case of CA-CIP 0.040% wafer, these bands were shifted to 1073 cm^{-1}, 956 cm^{-1} and 880 cm^{-1} respectively. The peaks of –NH stretching and O-H group bending vibration occurred at 3600 cm^{-1} and 1252 cm^{-1} respectively from CIP was observed in 0.040% DL wafer. It can be observed that most of the peaks of CIP were overlapped in CA-CIP wafers due to relative similarity and shifting. This indicates that CIP was homogeneously mixed and molecularly dispersed in the polymeric matrix. However, molecularly dispersed drug in the polymer network helps to achieve rapid release of drug from the dressing (Pawar *et al*., 2014). All the characteristic peaks of CA were present in the FLU only loaded wafers and combined DL wafers indicating integration of the drugs within the CA chains (**Figure 2.18**). However, the intensities of the peaks were higher in the wafers than pure CA indicating chemical interactions between the drug(s) and polymer during formulation.
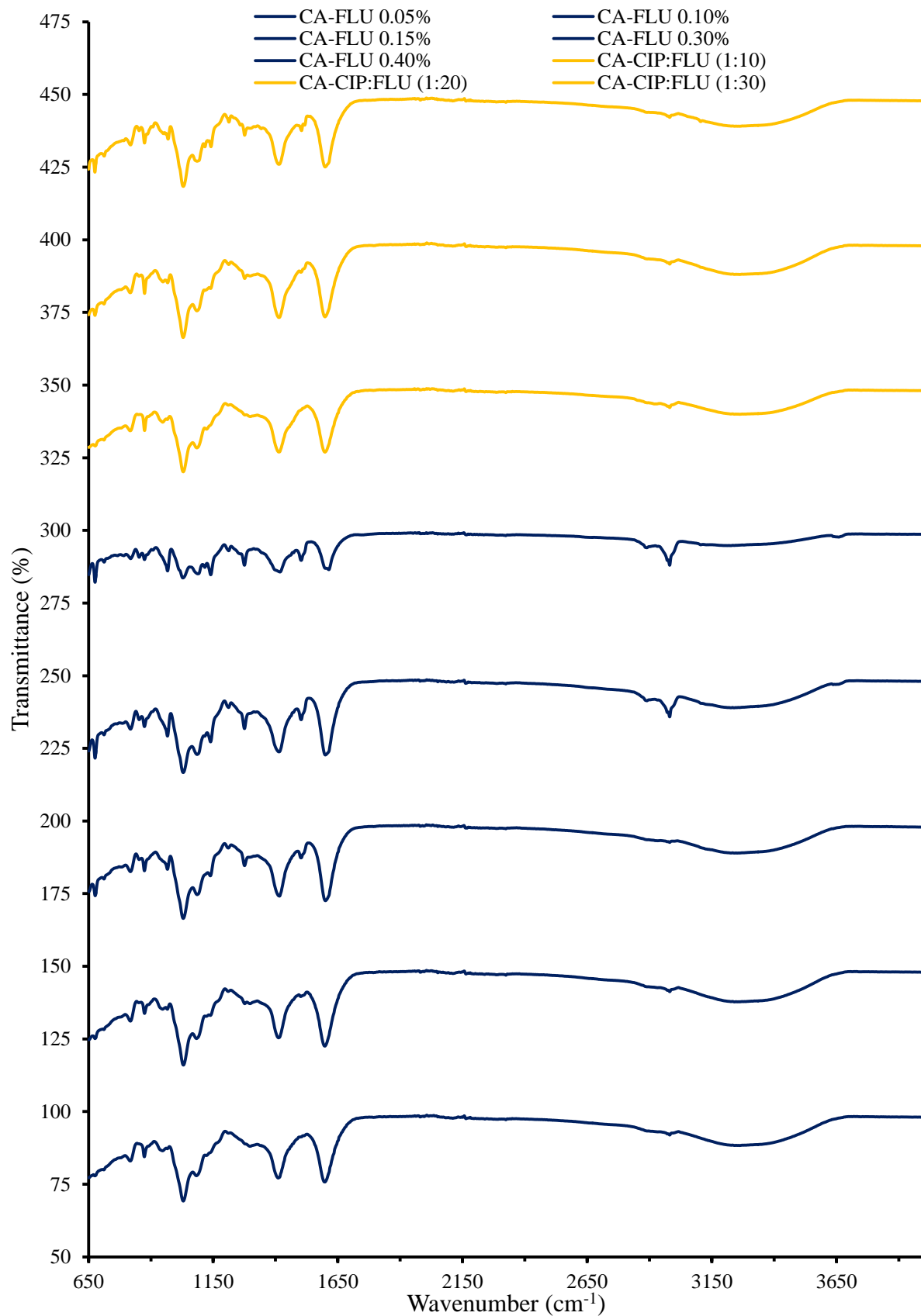
Figure 2.18   FTIR spectra of only FLU loaded and combined DL wafers. **2.4.6 Texture analysis**

2.4.6 Texture analysis

2.4.6.1 Mechanical (tensile) properties of films

The ideal film dressing should be flexible, durable, soft, elastic, pliable and stress resistant against different parts of the body during application. Texture analysis was used to investigate whether the formulated film dressings possessed these ideal mechanical properties. A clear correlation between GLY content and the tensile properties of films were observed with unplasticized films being too brittle (**Figure 2.3:** CA-1.0% w/w) and failed during texture analysis. **Figure 2.19** shows the tensile strength of the plasticized films increased with addition of GLY up to 33.33%. The values ranged from 5 ± 1 N/mm^2 to 15 ± 2 N/mm^2. However, addition of higher amounts of GLY (42.86% and 50.00 %) resulted in a lowering of tensile strength (9 ± 1 N/mm^2 and 7 ± 1 N/mm^2). The decrease in tensile strength at higher GLY content might be due to leaching phenomena with significant reduction of intermolecular and intramolecular bonding between the polymer chains and promoting hydrogen bond formation between the plasticizers and CA molecules. Such disruption of CA molecular chains reduced rigidity with increasing molecular chain mobility and subsequently decreased tensile strength of the films (Santana and Kieckbusch, 2013). Therefore, such higher amount of GLY in the films can lead to accumulation of exudate in highly exuding wounds such as DFUs because, films rich in moisture will not allow further absorption of exudales. The accumulation of exudate underneath dressings is not ideal due to the risk of skin maceration.
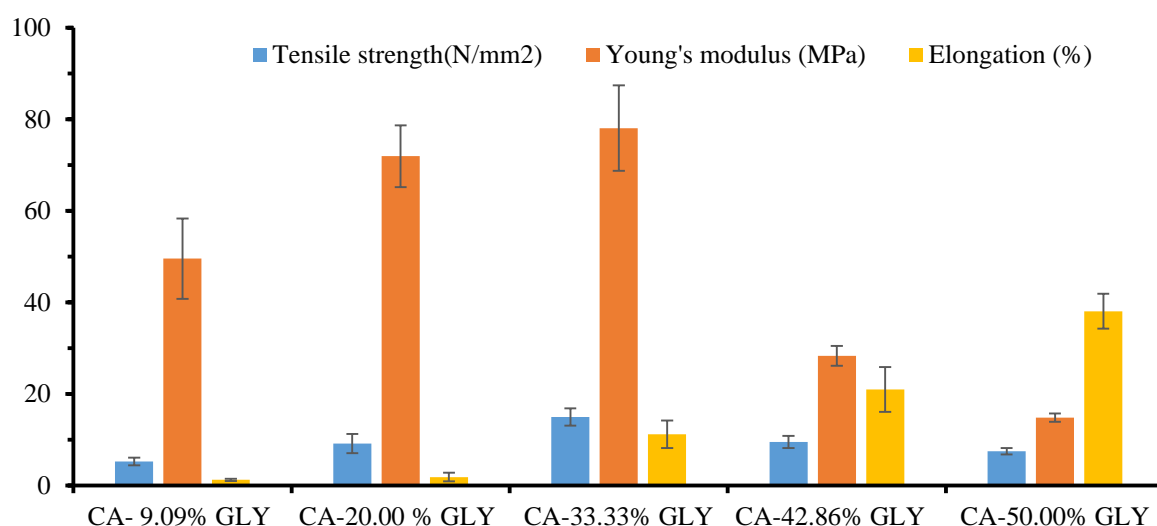
Figure 2.19   Effect of GLY on mechanical properties of films without drug represents tensile strength, Young's modulus and elongation ($n = 3 \pm$ SD).

Further, investigations were undertaken by measuring Young's (elastic) modulus and elongation at break to optimize GLY content for DL films. Young's modulus was estimated from the slope of the initial linier portion of stress-strain curve. **Figure 2.19** shows that the Young's modulus increased gradually with increasing GLY and after certain GLY content it drops as was the case with tensile strength of the films. The maximum Young's modulus (78 ± 9 MPa) was achieved at a GLY concentration of 33.33% w/w. **Figure 2.19** also illustrates the effect of GLY on the films elongation, which increased with increasing GLY content. This is because addition of GLY increased the number of –OH groups resulting in weak hydrogen bonding within CA. The intermolecular force decreased resulting in increased mobility caused by increased and enlarged spaces between polymeric chains and subsequently increased in percentage elongation at break. A sharp rise in elongation can be observed in **Figure 2.19** when the concentration of GLY was above 33.33% w/w in the gel. The significant ($p = 0.002$) increase in elongation is corresponding to a decrease in Young's modulus.

By considering the above mechanical properties, film containing 33.33% w/w of GLY was selected for drug loading. **Figure 2.20** shows the mechanical properties of BLK (CA-33.33% GLY) and DL films. It could be observed from the figure that there were no significant differences ($p = 0.26$) in tensile strength between BLK and DL films. However, incorporation of drugs had impact on Young's modulus. The result showed that Young's modulus was significantly ($p = 0.01$) decreased after loading CIP. In case of the films containing FLU alone, the Young's modulus was significantly ($p = 0.02$) increased when the films loaded with more that 0.05% w/v FLU.
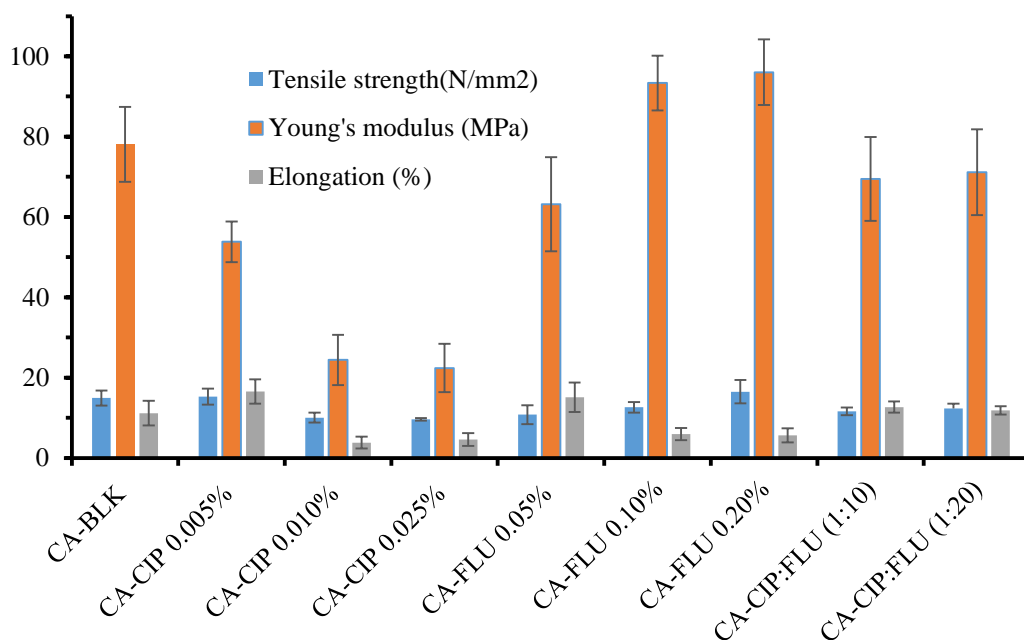
Figure 2.20   Tensile strength, Young's modulus and elongation of BLK and DL films ($n = 3$ ± SD).

There were no significant differences ($p = 0.57$) in Young's modulus of the films containing both CIP and FLU compared to BLK. This indicates that addition of CIP suppressed rigidity and addition of FLU extended rigidity of the films. CIP might have plasticizing effects as previously reported for some drugs such as ibuprofen, lidocaine HCl, ketoprofen, metoprolol tartrate and chlorpheniramine maleate have plasticizing effects (Kianfar *et al*., 2011; Wiranidchapong *et al*., 2015). The plasticizing effects of CIP might have lowered the glass transition temperature of the polymer, thereby allowing the chain segments to move or rotate freely and ultimately reduction in rigidity. On the other hand, FLU might have the opposite effect and inducing intrinsic mobility of the polymer chains, resulting in an increase in rigidity of the films (Aguirre *et al*., 2013). However, the mechanism and cause of antiplasticization have not been clearly elucidated and hypothesized and several mechanisms may involve. The film flexibility was increased, and films loaded with more than 0.005% CIP and 0.05% FLU were highly brittle and inadequate rigid as evidenced by having the lowest elongation (3.73 ± 1.64% for CIP and 5.62 ± 1.78% for FLU). Films containing both CIP and FLU showed same percent elongation (about 12.76%) just like BLK films. None of the DL films as well as BLK showed ideal values (30-50%) of elasticity (Boateng and Popescu, 2016). However, the Young's modulus and tensile strength values showed the films containing 0.005% CIP and 0.05-0.20% FLU were not too brittle, and this was confirmed during handling of the films. A close

observation at **Figure 2.20** revealed that the tensile strength and Young's modulus of the FLU loaded films increased with increasing amount of the drug, coupled with reduced elasticity. Combined DL films exhibited similar mechanical properties as like BLK. Moreover, the mechanical properties of CA films depend on the source and extraction treatment, and ratio of guluronic and mannuronic acid of the polymer (Gao *et al*., 2017). The mechanical properties of CA films can be improved by combining the polymer with either natural or synthetic polymers as reported by Boateng and co-workers (Boateng *et al*., 2009, 2013a; Pawar *et al*., 2013).

2.4.6.2 Mechanical hardness of wafers

The wafers (*n* = 3) were compressed at three different positions on the top and bottom sides to investigate the hardness (resistance to compressive deformation), and to check the brittleness and uniformity of texture. Hardness of all formulated wafers was tested to select optimum gel concentration for drug loading. Wafers prepared from 1% w/w gels showed excellent resistance to compression whereas wafers prepared from 1.5% and 2% w/w gels appeared very hard and brittle. On the other hand, wafers obtained from 0.5% w/w gel appeared to be very soft and flaky in nature, which made them very difficult to handle. Therefore, the drugs were loaded into 1% w/w gels to obtain medicated wafers.

Figure 2.21 and Figure 2.22 demonstrate the differences in hardness between the top and bottom sides of the wafers. The hardness of the top part of the wafers appeared higher than the lower part. This could be due to the higher polymer density on the upper part of the wafers than the bottom part. This is possible because in the shelf type freeze dryer used, the condenser is present in the lower part of the instrument and freezing starts from bottom of the gel upwards. The higher polymer density leads to a more compact structure on the top surface of the wafer, which causes higher resistance to probe penetration. The difference in hardness between the sides of the wafers could also be attributed to differences in porosity (Boateng *et al*., 2010). As porosity increases, there is less force required to reach the required depth of penetration. Therefore, the lower surface of the wafers will be an ideal application site for applying to the wound bed as it will quickly absorb wound fluid due to higher porosity. Further, lower hardness will reduce the likelihood of damaging sensitive newly formed skin cells on a healing wound. However, to maintain hardness consistency of the wafers from container to container on a commercial scale, the containers must be flat bottom, with a wider diameter so that the gel and final wafer height (thickness) after freezing is not too big. Further, same amount of free-flowing gel need to be poured in each well of the container. This way, the heat distribution within the frozen gel during primary drying will be more uniform between the top and bottom sides. This

will yield thinner flat sheets similar to foam dressings and help produce consistent thickness and polymer density and subsequently will give consistent hardness. The advantage of wafer dressing is that it can be produced in different sizes and shapes depending on the casting container and it can be delivered to the patients to suit the specific application area.

The BLK wafers showed significantly ($p = 0.0001$) higher hardness than the DL wafers (**Figure 2.21 and Figure 2.22**). The hardness of CIP incorporated wafers (**Figure 2.21**) decreased gradually with increasing drug content. This could be explained by the fact that after loading CIP, the availability of free polymer was reduced throughout the matrix, therefore the rigidity of polymeric matrix decreased, and these results support the SEM observation (**Figure 2.10 A**). Moreover, the plasticizing effects of CIP might cause the loss of structural integrity of the wafers, which resulted in reduced hardness. In the case of FLU loaded wafers (**Figure 2.22**), the hardness increased gradually with increasing amount of the drug. The crosslinking between FLU and CA resulted in denser pores and subsequently reduced porosity perhaps resulted in an increase in resistance to compressive deformation.
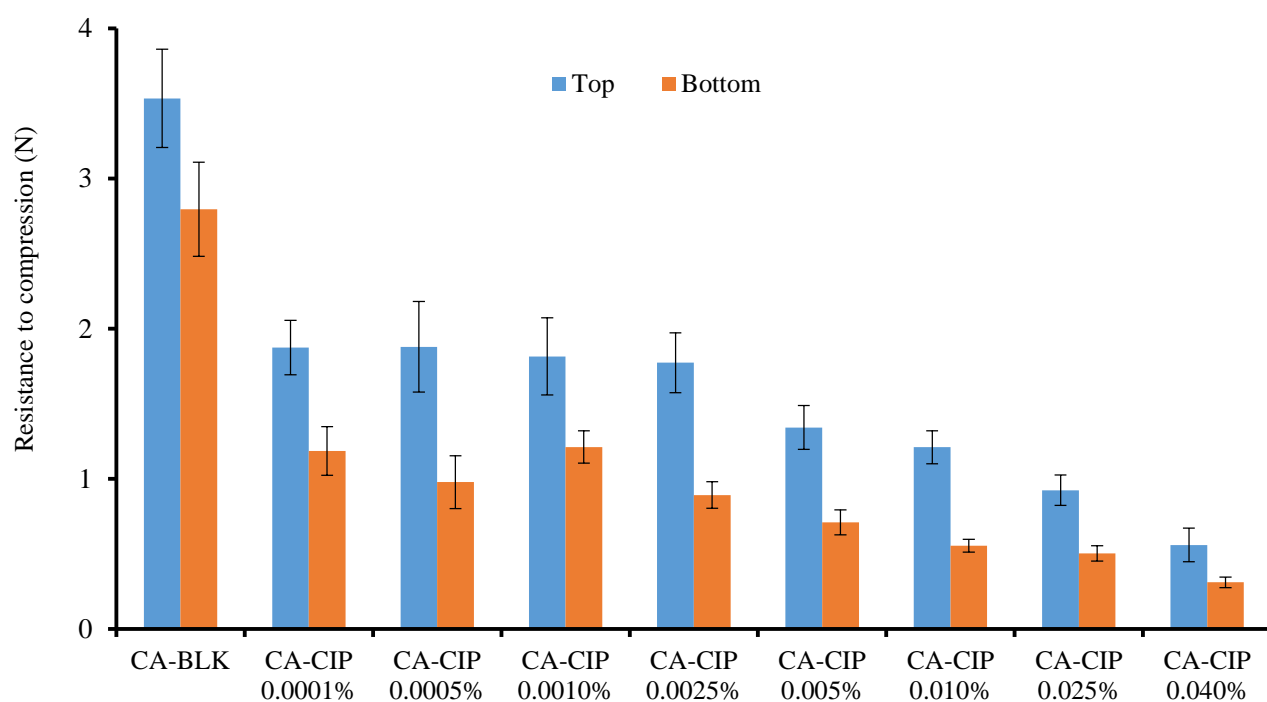
Figure 2.21 Hardness profiles of BLK and CIP loaded wafers ($n = 3 \pm SD$) prepared from 1% w/w gels, compressed at three different places on both sides of the dressing showing effect of drug loading.

Wafers containing both CIP and FLU in the ratio of 1:10 showed the highest hardness (about 2.50 ± 0.18 N) amongst all DL wafers.

This could be due to the formulation containing this CIP and FLU ratio exhibiting uniform pore size distribution (also confirmed by SEM observation, **Figure 2.10 B**) resulting in high mechanical strength. Adequate hardness of the wafers is required for physical and mechanical stability during handling as well as avoiding potential contact irritation during application (Rezvanian *et al.*, 2016). In addition, hardness has impact on physicochemical properties such as swelling, mucoadhesion, EWC, WVTR and drug release (Ahmed *et al.*, 2017; Catanzano *et al.*, 2017).
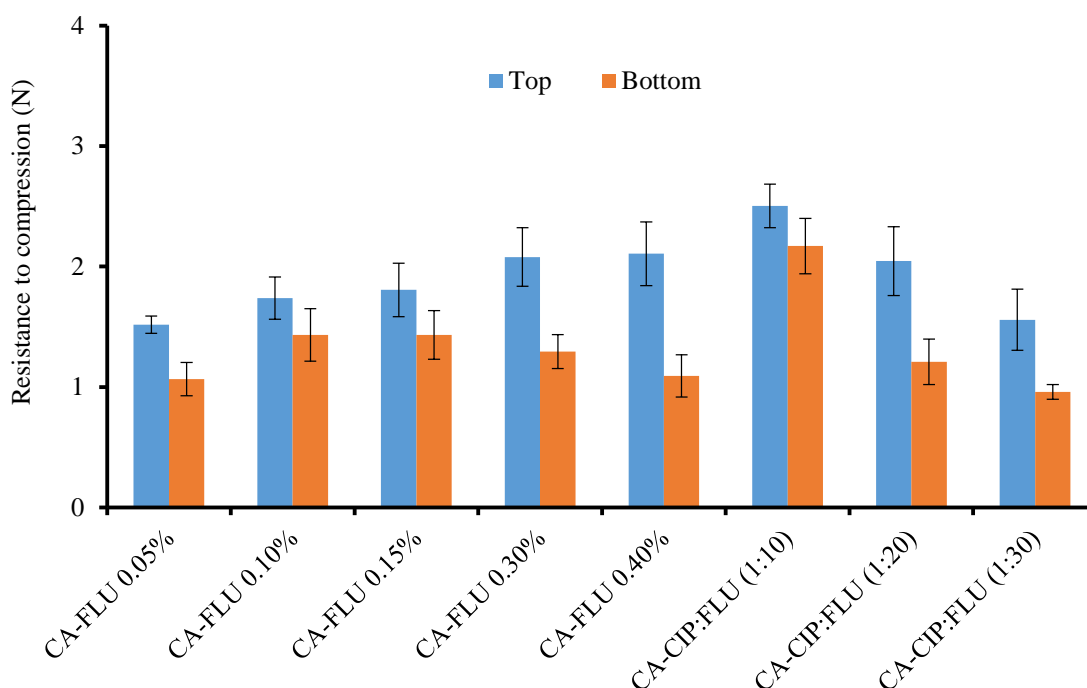
Figure 2.22 Hardness profiles of FLU and combined DL wafers ($n = 3 \pm$ SD) prepared from 1% w/w gels, compressed at three different places on both sides of the dressing showing effect of drug loading.

2.4.6.3 *In-vitro* adhesion studies

Stickiness, work of adhesion and cohesiveness are associated with the bond formation between the polymeric matrix and gelatine gel during contact time. Usually chronic wounds such as DFUs contain highly viscous exudates (Speak, 2014), therefore in this study two different concentrations of BSA (2% w/w and 5% w/w) were used to represent thin and viscous wound exudate respectively. Each formulation was cut into 35 mm diameter same as the diameter of the probe of texture analyser to minimize the inference between the probe and the

gelatine surface. The test was performed using gelatine layer, to simulate adhesion of the films to the wound surface. The composition and biological properties of gelatine are almost identical to collagen, which forms part of the natural skin matrix and its deposition is a key part of the wound healing process; therefore, it can represent a wound surface in the presence of SWF (Rattanaruengsrikul *et al*., 2009). The applied force was kept at 1 N by considering newly formed tissue which may be interrupted or damaged if high forces were applied.

2.4.6.3.1 Adhesion of films

As shown in **Figure 2.23**, the stickiness increased with increasing GLY content in the films when tested with SWF containing 2% w/w BSA (thin fluid). This could be explained by the fact that GLY enhances the hydrogen bonding between the polymeric chain and model wound surface and therefore increases adhesion properties. Furthermore, GLY acts as a humectant that promotes quick hydration in the presence of SWF, which consequently imparts higher stickiness. The stickiness of plasticized films was similar to that of unplasticized film in the presence of SWF containing 5% w/w BSA (thick/viscous fluid).
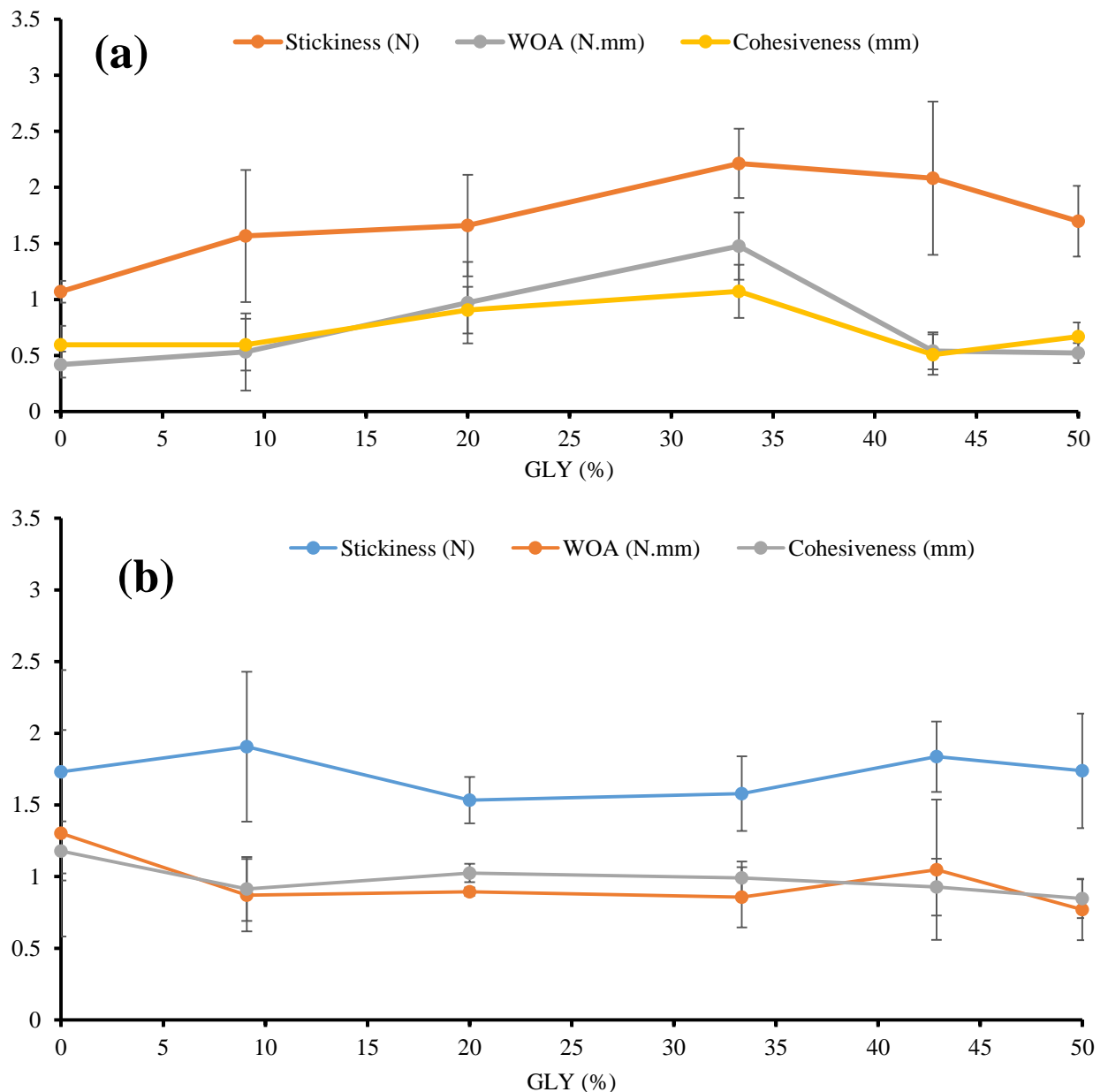
Figure 2.23 Adhesive test of unplasticized and plasticized BLK films ($n = 3 \pm \text{SD}$) with SWF containing 2% (w/w) BSA (a) and 5% (w/w) BSA (b).

Films containing 0.025% CIP showed the highest stickiness (2.61 N ± 0.41) amongst all films (**Figure 2.24 a**). This could be due the highest plasticizing effect of CIP at the highest concentration. FLU loaded and combined DL films showed significantly (*p = 0.02*) lower stickiness as compared to BLK and CIP loaded films. This could be because in the presence of thin SWF, FLU precipitated on the surface of the films resulting in reduced plasticizing effect, which ultimately decreased stickiness.
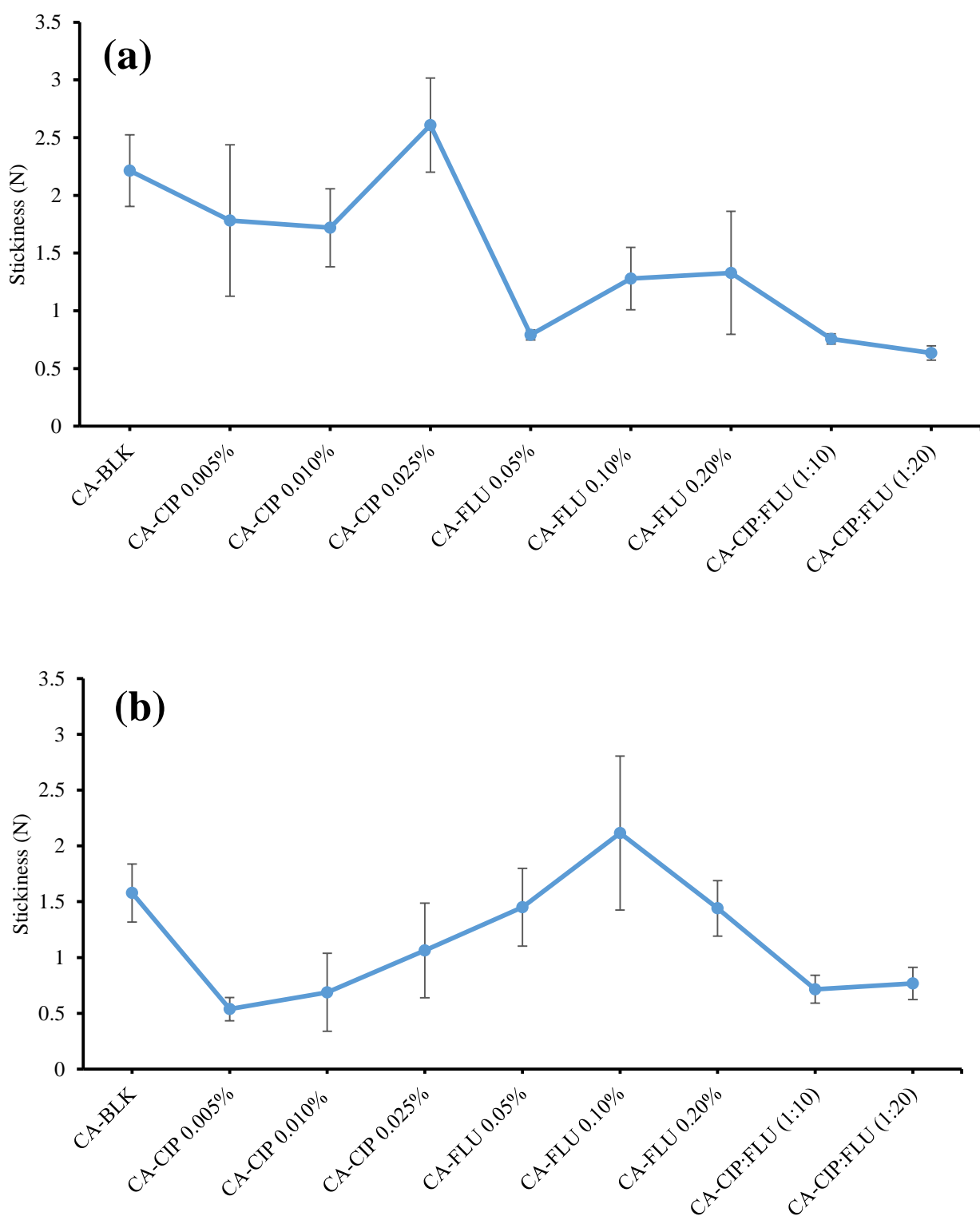
Figure 2.24 Stickiness test of BLK and DL films with SWF containing 2% (w/w) BSA (a) and 5% (w/w) BSA (b) ($n = 3 \pm$ SD).

As shown in **Figure 2.24 b**, CIP loaded films had lower stickiness ($0.54 - 1.06$ N) than CA-BLK (1.56 ± 0.26 N) in the presence of thick fluid. Combined DL films also showed low stickiness of about 0.72 ± 0.12 N. However, the stickiness of FLU loaded films in the presence

of thick fluid was similar to BLK film. This might be due the fact that the protein rich viscous wound fluid does not allow further hydration.
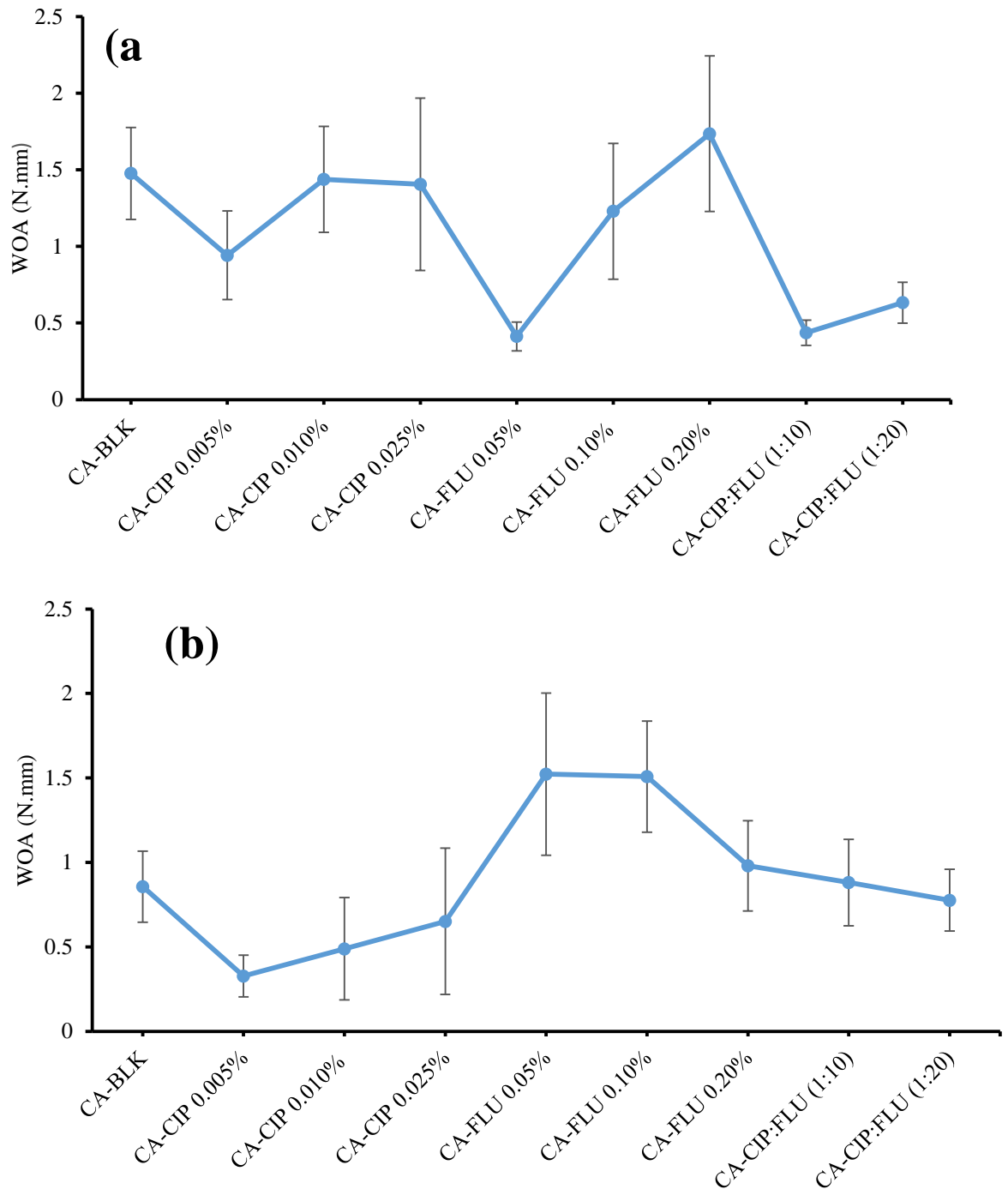
Figure 2.25 WOA of BLK and DL films with SWF containing 2% (w/w) BSA (a) and 5% (w/w) BSA (b) ($n = 3 \pm$ SD).

Figure 2.25 also shows the WOA of BLK and DL films representing the total energy required to separate the probe from the wound surface. The WOA slightly increased with increasing CIP concentration when tested with both fluids. This was because higher concentration of CIP resulted in higher stikiness, subsequently higer enery was required to separate the probe from

the model wound surface. However, the values for 0.05% and 0.10% FLU loaded films (0.41 ± 0.09 and 1.23 ± 0.44) and combined DL films (0.44 ± 0.08, and 0.63 ± 0.13) did not exceed the value (1.47 ± 0.31 N.mm) for BLK film when tested with thin fluid. Futher, there was no significant difference ($p = 0.6$) in WOA between BLK and DL films in the presence of thick fluid (**Figure 2.25 b**). Cohesiveness means ability to repel the detachment from model wound surface. All DL formulations except the film containing 0.025% CIP showed significantly ($p = 0.001$) higher cohesiveness than BLK film (**Figure 2.26**). The value increased from 1.07 ± 0.24 mm to 7.02 ± 0.24 mm and from 0.99 ± 0.11 mm to 7.44 ± 1.64 mm in thin and viscous SWF respectively. This indicates that the medicated films will adhere onto the wound surface better. Films loaded with 0.025% CIP showed low cohesiveness of about 2.05 ± 0.43 mm and 0.99 ± 0.08 mm with thin and thick SWF respectively and is due to poor mechanical properties in terms of Young's modulus, elongation and tensile strength.
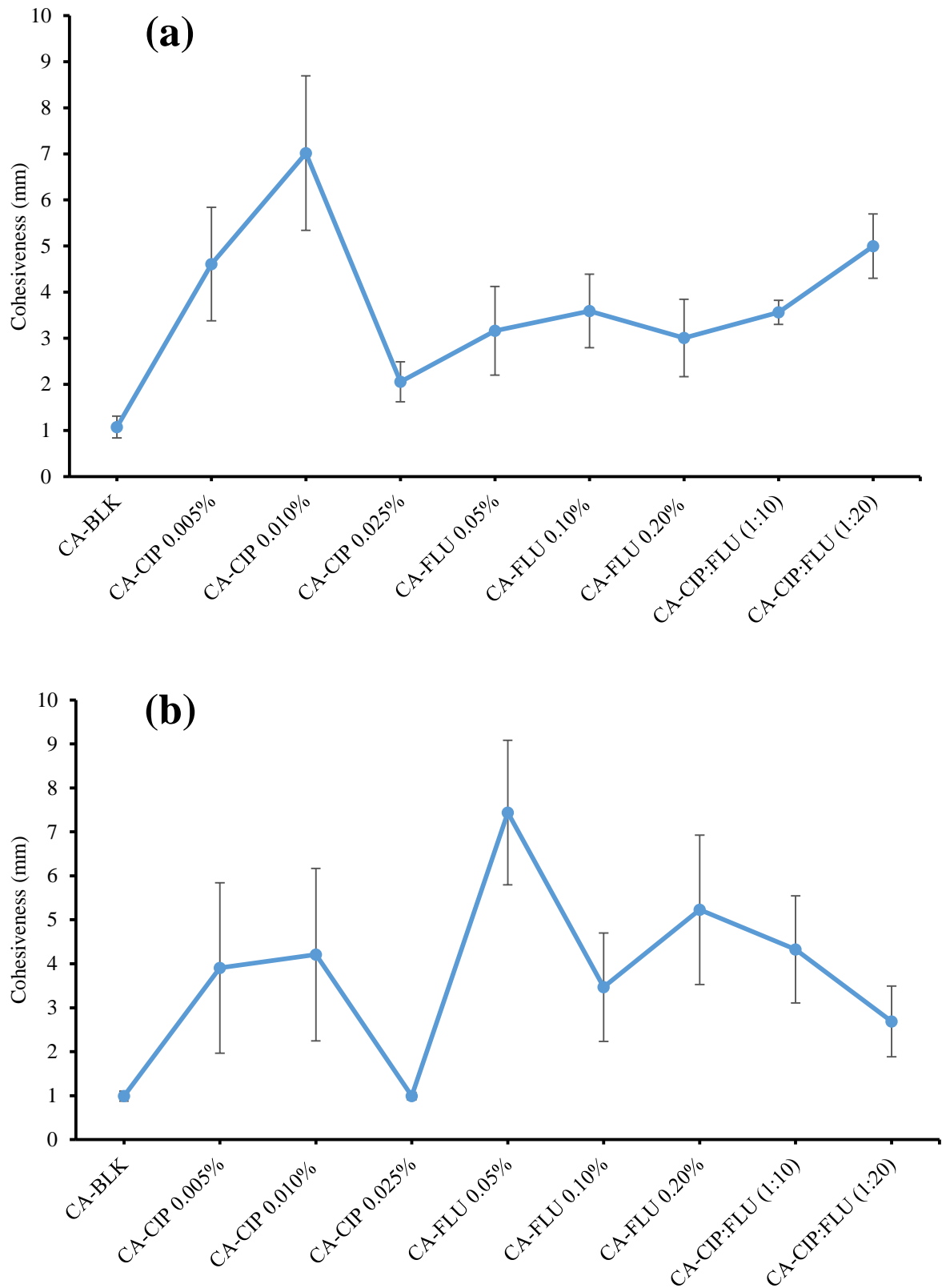
Figure 2.26 Cohesiveness test of BLK and DL films with SWF containing 2% (w/w) BSA (a) and 5% (w/w) BSA (b) ($n = 3 \pm$ SD).

2.4.6.3.2 Adhesion of wafers

CA-BLK wafers showed similar stickiness (1.82 ± 0.06 N and 1.54 ± 0.47 N) in the presence of thin SWF (2% w/w BSA) and viscous SWF (5% w/w BSA) respectively. DL wafers showed peak adhesive force values around 0.24-0.55 N in the presence of thin SWF (2% w/w BSA) and values around 0.27-0.64 N in the presence of viscous SWF (5% w/w BSA). It can be observed in **Figure 2.27 and Figure 2.28** that the CA-BLK wafer showed higher stickiness and WOA values than the DL wafers in both types of exudates. This could be because incorporation of the drug into the wafers resulted in poor contact between the polymer chains and hence reduced adhesive properties and confirmed the hardness results. Stickiness also depends on the pore size distribution of the polymeric matrix.

SEM images (**Figure 2.10**) illustrated the disturbance in pore size distribution of DL wafers and poorer hydration capacity possibly resulting in reduction in the stickiness. There was a significant difference ($p = 0.04$) in WOA of CA-BLK wafer between thin (2.24 ± 0.49 N.mm) and thick (1.06 ± 0.59 N.mm) exudate. Moreover, WOA and cohesiveness increased steadily with increasing amount of CIP up to 0.025% w/v in the presence of normal SWF (2% w/w BSA), whereas WOA and cohesiveness increased inconsistently in the presence of viscous excaudate (5% w/w BSA).
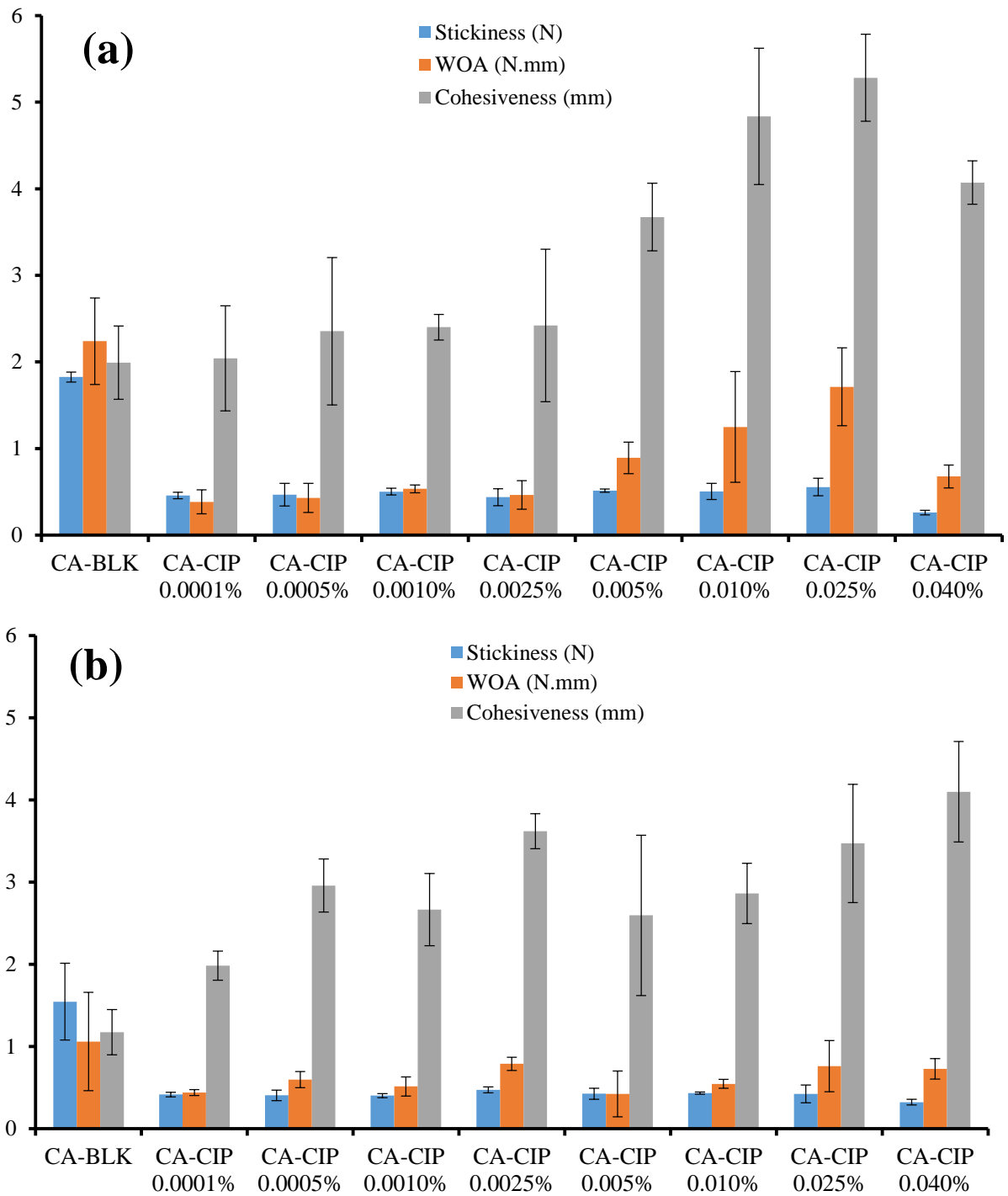
Figure 2.27 Adhesive profiles of CIP loaded wafers in the presence of (a) thin SWF containing 2% (w/w) BSA and (b) viscous SWF containing 5% (w/w) BSA ($n = 3 \pm$ SD).
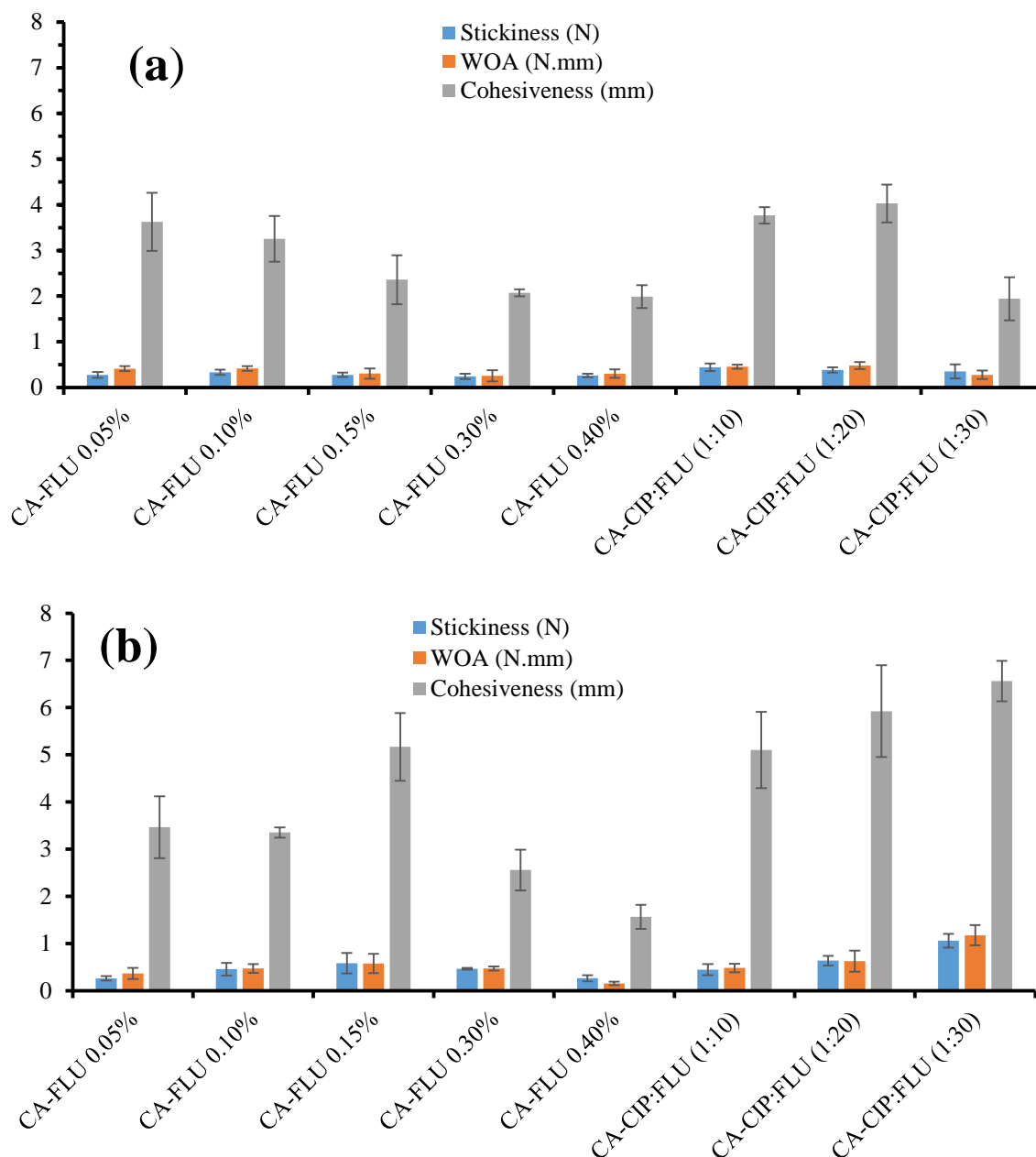
Figure 2.28 Adhesive profiles of FLU loaded only wafers and combined DL wafers in the presence of (a) thin SWF containing 2% (w/w) BSA and (b)viscous SWF containing 5% (w/w) BSA ($n = 3 \pm$ SD).

There were no significant differences ($p > 0.05$) in WOA of the combined DL and FLU only loaded wafers in the presence of both thin and viscous SWF (**Figure 2.28**). However, cohesiveness of FLU loaded wafers was decreased gradually with increasing amount of drug in the presence of thin SWF. This might be attributed to the higher content of drug which reduced the intermolecular attraction between the wafers and the wound substrate resulting in reduced cohesion. The cohesiveness of FLU loaded wafers was inconsistent in the

presence of thick SWF. In the presence of thin SWF, wafers containing both CIP and FLU at the ratios of 1:10 and 1:20 showed higher cohesiveness about 3.77 ± 0.18 and 4.03 ± 0.41 mm respectively than the wafers containing FLU alone. Moreover, in the presence of viscous SWF, the combined DL wafers revealed the highest cohesiveness amongst all formulated wafers. This may be associated with the fact that presence of both CIP and FLU in the polymeric matrix enhanced the extent of diffusion of polymer molecules and intermolecular attraction which results in increased cohesion. Overall, film dressings showed better adhesion properties in terms of stickiness and cohesiveness, but wafers showed better WOA enabling close contact with the wound surface for a longer period and hence enhancing drug concentration on the target site.

2.5 Conclusions

A medicated CA dressing to be applied as a wound drug delivery system in DFUs was formulated and characterized in terms of physico-chemical properties. The films with 33.33% w/w GLY content were deemed optimum being soft, flexible, elastic, pliable and transperant while lyophilized wafers prepared from 1% w/w gel were soft, of uniform texture and thickness, and pliable in nature and therefore these were selected for drug loading. Incorporation of optimum concentrations (0.005-0.025% for CIP, 0.05% for FLU) of drugs did not affect the transperency of the film dressings and therefore confirmed the uniform drug distribution without recrystalization and precipitation. The uniform distribution of drugs within the calcium alginate based polymeric matrix was further confirmed by SEM, XRD and FTIR. SEM revealed the precipitation of calcium carbonate on the surface of the film dressings and addition of GLY reduced the precipitation. Lyophilized wafers were porous in nature and appeared to be potentially useful for handling high exudate in DFUs. XRD and FTIR investigation revealed the overlapping/disappearance of characteristic peaks of CIP and FLU and confirmed the uniform drug distribution throughout the polymeric matrix. The bottom part of the wafers appeared soft and porous which could be an ideal application site for applying to the wound bed. Significant differences in adhesive properties of films and wafers were observed. The stickiness and cohesiveness of films were greater than wafers due to presence of GLY in films. On the other hand, wafer showed the higher work of adhesion than films due to high porosity of wafer dressings.

CHAPTER 3: FUNCTIONAL (FLUID HANDLING AND DRUG RELEASE) CHARACTERISTICS OF CALCIUM ALGINATE BASED DRESSINGS

3.1 Introduction

Modern dressings are developed based on the essential functional characteristic requirement to retain and provide a moist environment around the wound to promote wound healing (Boateng *et al*., 2008). On the other hand, advanced dressings are meant to be multi-functional for example, they must have the ability to prevent microbial infection, reduce pain as well as maintaining a moist environment. (Catanzano *et al*., 2017; Pawar *et al*., 2014). The ideal dressing should provide adequate moist environment to the wound site as well as thermal insulation, easy removal without causing trauma, remove drainage and debris, and promote tissue reconstruction process (Kim *et al*., 2007). It is reported that semipermeable dressings such as films are very effective in acute and chronic wounds by keeping the balance of wound exudate between the wound and the dressing, so that wound fluid does not build up (Okoye and Okolie, 2015). Lyophilized wafers are also reported as a potential means of delivering antimicrobials to wound surface to aid healing (Pawar *et al*., 2014).

Polymer based matrix delivery systems such as films and wafers have the advantages of delivering poorly soluble drugs (Kianfar *et al*., 2012). In matrix-based systems, the drug is entrapped into the polymeric matrix where water penetration leads to hydration and swelling. The swelling effect expands the geometrical volume of the bulk polymeric material causing opening of pores that cause leaching out of the hydrophilic or hydrophobic drug molecules and released from the matrix (Patra *et al*., 2013). The advantage of polymer-based dressings is obtaining maximum bioavailability of the drug at the target site by controlled, sustained and burst release of drugs (Karthikeyan *et al*., 2015; Fu and Kao, 2010). However, the release of drugs from the polymeric matrix depends on the several factors such as composition, structure, swelling, degradation of polymer material, pH, temperature, ionic strength of the dissolution medium and solubility, stability, charges and osmotic properties of the drugs (Fu and Kao, 2010; Wang *et al*., 2007; Patra *et al*., 2013).

In the previous chapter, the physical properties of the films and wafers were discussed in terms of mechanical characterization (hardness, tensile strength, mucoadhesion), as well as analytical characterization by scanning electron microscopy (SEM), X-ray diffraction (XRD)

and Fourier transform infrared spectroscopy (FTIR). This chapter focuses on the evaluation of functional (fluid handling and drug release) properties of CA based dressings for healing of chronic DFUs. The functional properties required for ideal wound dressing such as porosity, swelling capacity, water absorption (Aw), equilibrium water content (EWC), water vapour transmission rate (WVTR), moisture content and evaporative water loss (EWL) were tested. In addition, *in vitro* drug dissolution and release kinetics were studied to understand the bio efficacy of the formulated medicated dressings for potential wound healing. Further, the fluid (exudate) handling properties of the formulated dressings were compared with two commercial CA based dressings such as Algisite Ag® (Smith & Nephew, UK) and Actiformcool® (Activa Healthcare, UK).

3.2   Materials

Calcium alginate (mannurronic acid: guluronic (59:41), molecular weight: 398.32 g/mol) [CA, (lot number: BCBM8132V)], ciprofloxacin (lot number: LRAA6508), Fluconazole (lot number: LRAA6502) and tris(hydroxymethyl)aminomethane (lot number: SLBH9329V) were purchased from Sigma-Aldrich (Gillingham, UK). Sodium carbonate (lot number: 1546575), sodium chloride (lot number: 1560652), bovine serum albumin [BSA, (lot number: 1158022)], hydrochloric acid [HCl, (lot number: 1480980)], ethanol (batch number: 0933421), acetic acid and (lot number: 1400245), acetonitrile (lot number: 1403054) were ordered from Fisher Scientific (Loughborough, UK). Calcium chloride (lot number: S42528-427) was obtained from Riedel-de-Haen, Germany. HPLC vials (P/N VI-04-12-022) were purchased from Chromatography, UK

3.3 Methods

3.3.1   Porosity

The porosity of formulated dressings (films and wafers) and commercial products (Algisite Ag® and Actiformcool®) was determined by the solvent displacement method as previously described (Han *et al*., 2010; Catanzano *et al*., 2017; Guan *et al*., 2005; Zhang *et al*., 2001). The geometrical dimensions (thickness and diameter) of samples were measured by a digital Vernier caliper electronic micrometer gauge and total pore volume (V_0) was calculated. After that, samples were weighed (W_0) before immersing in 10 ml of ethanol for 3 h to reach saturation, with ethanol displacing the void space within the samples. Finally, the samples were carefully removed from the solvent, blotted with tissue paper to remove excess solvent and immediately

weighed (W_1) to avoid loss of ethanol because of its volatile nature. The porosity of the dressings was calculated from **Equation 3.1**.

Porosity (%) = (W_1-W_0)/($\rho_{eth}V_0$) x 100　　　　　　　　　　　　　(Equation 3.1)

ρ_{eth} : density of ethanol = 0.789 g/cm^3

3.3.2　Water absorption, equilibrium water content and swelling index

Water absorption (Aw) and equilibrium water content (EWC) tests were performed to investigate the maximum water uptake and water holding capacities respectively of the dressings. In addition, swelling studies were undertaken to investigate the rate of water uptake capacity of formulated BLK and DL dressings compared with a commercial fiber mat, Algisite Ag$^®$ and a hydrogel, Actiformcool$^®$. The Aw, EWC and swelling index of all samples were investigated in simulated wound fluid (SWF) containing 2% (w/w) bovine serum albumin (BSA), 0.02 M calcium chloride, 0.4 M sodium chloride, 0.08 M tris (hydroxymethyl) aminomethane in deionized water at a pH of 7.5. To determine the Aw, samples were weighed and kept in 10 ml of SWF over a 24 h period at a temperature of 37 ºC. After 24 h, samples were carefully wiped using tissue paper to remove excess SWF and reweighed and the Aw calculated using **Equation 3.2** below. Each measurement was performed in triplicate ($n = 3$)

$$Aw(\%) = \frac{Ws-Wi}{Wi} x\ 100$$　　　　　　　　　　　　　(Equation 3.2)

Where Ws is the swollen weight and Wi is the initial weight before immersion into SWF.

To determine the EWC, the same procedure was followed as for Aw, however, the EWC ($n = 3$) was calculated using **Equation 3.3** below.

$$EWC(\%) = \frac{Ws-Wi}{Ws} x\ 100$$　　　　　　　　　　　　　(Equation 3.3)

For swelling, the weighed samples were dipped into 10 ml of SWF (at ambient temperature) and changes in weight of swollen films recorded at 15 min intervals up to 1 h and subsequently every 60 min until 5 h. The swelling index (Is) was calculated ($n = 3$) from **Equation 3.4** below.

$$Is\ (\%) = \frac{Wst-Wi}{Wd} x\ 100$$　　　　　　　　　　　　　(Equation 3.4)

Where W_i is the dry weight of samples before hydration and W_{st} is the swollen weight of samples at different hydration times.

Further, the effect of drug concentration on Aw, EWC and *Is* was determined.

3.3.3   Water vapour transmission rate (WVTR)

With the help of epoxy glue, the dressings were mounted on the mouth of a cylindrical plastic tube (15 mm diameter) containing 4 ml water with 8 mm air gap between the samples and water surface. The whole setup was placed in an air-circulated oven at 37 °C for 24 h. The WVTR was calculated using **Equation 3.5**

$$\text{WVTR} = \frac{Wi - Wt}{A} \text{x} 10^6 \, \text{g/m}^2 \, \text{day}^{-1} \qquad \text{(Equation 3.5)}$$

Where A is the area of the mouth of the plastic tube (πr^2), Wi and Wt are the weight of the whole setup before and after placing into oven respectively.

3.3.4   Evaporative water loss (EWL)

The samples were immersed in 10 ml of SWF and kept in an oven at 37 °C for 24 h after which the samples were taken out and dried in the oven at 37 °C for 24 h and the weight of the samples was recorded at regular time intervals. Evaporative water loss was calculated according to the formula in **Equation 3.6**:

$$\text{Water loss (\%)} = W_t / W_0 \text{ x } 100 \qquad \text{(Equation 3.6)}$$

Where W_t and W_0 represent the weight after time '*t*' and initial weight after 24 h immersion time respectively.

3.3.5   Moisture content

The residual moisture content of the samples was determined by thermogravimetric analysis (TGA) using a Q5000-IR TGA instrument (TA Instruments, Crawley, UK). About 1.0 - 1.5 mg of sample was loaded and analysed with dynamic heating from room temperature (~25 °C) to 300 °C at a heating rate of 10 °C/min under inert nitrogen (N2) gas at a flow rate of 50 ml/min. The percentage water content was calculated at 100 °C using *TA Instruments Universal Analysis 2000* software program.

3.3.6   Determination of surface pH

The surface pH of the dressings were determined by dipping the dressings in 10 ml of water and allowed to hydrate for 2 h at 37 °C. After that, the surface pH was detected by touching the electrode of a pH meter (Mettler Toledo, UK) at the surface of the hydrated dressings (Okoye and Okolie, 2016).

3.3.7 *In-vitro* drug dissolution and release profiles

The total content of CIP and FLU within the DL films and wafers was determined before performing drug dissolution and release studies. This was done by hydrating the whole film in 50 ml and wafer in 10 ml of HPLC grade purified water respectively at 37 °C with stirring and left overnight to dissolve completely. The concentration of CIP and FLU in water was determined by HPLC and used to calculate the total amount of drugs present representing total drug content (assay) within the dressings. Calibration samples were prepared in triplicate in specific concentration range (1 to 100 μg/ml for CIP and 25 to 500 μg/ml for FLU) to plot standard curves (**Chapter 8: Figure A3.2**) for CIP and FLU respectively. After that, the standard curves were used to determine drug loading efficiency (%) of the selected formulations used for drug dissolution studies as well as the percent drug released at each time point. The drug loading efficiency was computed by the following equation:

$$\text{Drug loading efficiency (\%)} = \frac{\text{total actual drug content}}{\text{amount of theoretical drug loading}} \text{ x } 100 \quad \text{(Equation 3.7)}$$

In addition, drug content uniformity (DCU) of the films and wafers were performed to investigate uniform distribution of drug within the dressings' matrix. This was done by cutting the films into circular strips (6 mm diameter) and the wafers were cut into portions from three different locations and accurately weighed (~ 1-1.5 mg). The dressings were selected in triplicate from different batch of formulations. The sample portions of film and wafer were placed in 2 ml of HPLC grade purified water at 37 °C with stirring and left overnight to dissolve completely. The quantity of drugs in solution was determined by HPLC method after filtration by 0.2 μm filter.

In vitro drug dissolution studies were performed using a diffusion cell (developed in-house at the University of Greenwich) containing SWF (pH 7.5) as dissolution medium but with no BSA to avoid blocking of the HPLC column. The diffusion cell was designed with a wire mesh on which the samples were placed. The dissolution medium was poured just up to the wire mesh so that the lower surface of the samples was always just touching the dissolution medium. The film containing only CIP (0.005-0.025%), only FLU (0.05-0.20%), both drugs in different ratio (1:10 and 1:20) and the corresponding DL wafers (CA-CIP 0.005-0.025%, CA-FLU 0.05-0.40% and CA-CIP:FLU 1:10, 1:20 & 1:30) were investigated for drug release. The samples were placed on the wire mesh and the whole assembly placed in a water bath maintained at a temperature of 37 °C with constant stirring (600 rpm). At predetermined time

intervals, 1 ml aliquots of dissolution medium were withdrawn and analysed by HPLC, and also replaced with same amount of fresh warm medium (37 ℃) to keep a constant volume throughout the experiment. The dilution due to replacing fresh medium was considered while calculating the percentage drug release at each time point. The concentration of the drugs released from the dressings was determined by applying calibration curve and percentage drug release plotted against time. Triplicate determinations ($n = 3$) were undertaken for each dressing selected.

3.3.8 HPLC analysis

The HPLC analysis was carried with an Agilent 1200 series HPLC (Agilent Technologies, UK) equipped with a quaternary pump (serial number: DE62976352), degasser (serial number: 5P94177529), auto sampler (serial number: DE64779297), and Agilent Chemstation® software package for running the instrument, data acquisition and data analysis. The analyte was separated at ambient temperature using a C18 analytical column (YMC-Pack ODS-AQ AQ-303-5, 250x4.6 mm I.D, S-5 μm, 120A, NO.042512322).

Table 3.1   List of mobile phase systems and wavelength used for the drug release study of different formulations.

Sample	Mobile phase		Wavelength (nm)
	Solvent A	Solvent B	
CIP loaded dressings	2% Acetic acid (70 %)	Acetonitrile (30 %)	280
FLU loaded dressings	Water (65%)	Acetonitrile (35%)	264
Combined DL (CIP and FLU) dressings	2% Acetic acid (55 %)	Acetonitrile (45%)	264

The ultra violet (UV) detector was set at 280 and 264 nm for CIP and FLU respectively. A two-solvent isocratic elution was used in the mobile phases (**Table 3.1**) at a flow rate of 1 ml/min and injection volume at 20 μl.

3.3.9 Drug release kinetics

The kinetics of drug release from the films and wafers in SWF (without BSA) were determined by finding the best fit of the % release against time data to Higuchi (**Equation 3.8**), Korsmeyer-Peppas (**Equation 3.9**), zero order (**Equation 3.10**) and first order equations (**Equation 3.11**).

$$Q_t = k_H t^{1/2} \qquad \text{(Equation 3.8)}$$

where, Q_t is the amount of drug released at time (t), k_H is the Higuchian release rate constant.

$$\ln\left(\frac{Q_t}{Q_\infty}\right) = \ln k + n \ln t \qquad \text{(Equation 3.9)}$$

Q_t and Q_∞ are the absolute cumulative amounts of drug release at time (t) and infinitive time respectively, k is the constant of structural and geometrical characteristic of the films and wafers and n is the exponent release constant.

$$Q_t - Q_0 = k_0 t \qquad \text{(Equation 3.10)}$$

Q_t is the amount of drug released in time (t), Q_0 is the amount of drug dissolved at time zero, K_0 is the zero-order release constant.

$$\ln\left(\frac{Q_\infty}{Q_t}\right) = k_1 t \qquad \text{(Equation 3.11)}$$

Q_t and Q_∞ are the absolute cumulative amounts of drug release at time (t) and infinitive time respectively, k_1 is the first order release rate constant.

The following profiles were plotted: % of cumulative drug release against square root of time (Higuchi model); log of cumulative drug release % against log time (Korsmeyer model); cumulative % drug release against time (zero-order kinetic model) and log of % cumulative drug remaining against time (first order kinetic model).

3.3.10 Statistical analysis

Statistical methods such as *t-test* and *ANOVA test* were performed using Excel to compare experimental values between BLK, DL dressings and commercial products, and *p* values lower than 0.05 were considered significant.

3.4 Results and discussion

3.4.1 Porosity of film dressings

Films are semipermeable in nature and generally appear as continuous sheets of polymer with limited porosity. As shown in **Figure 3.1,** the unplasticized blank film showed the highest porosity of $55.62 \pm 1.25\%$ amongst all the formulated films. Addition of GLY decreased porosity because it coated the surface of the films and therefore reduced pore size. The porosity was significantly ($p = 0.0002$) reduced when the films were plasticized with 33.33% GLY or above because higher concentrations of GLY increased the viscosity of the gels and subsequently yielded non-porous (denser) sheets of polymer. However, incorporation of CIP into polymeric matrix (CA film) increased the porosity significantly ($p = 0.009$) when compared to the CA-BLK film (CA-33.33% GLY). CIP reduced the intermolecular polymer chain interaction and increased void spaces between the polymer chains resulting in higher porosity than the BLK films. Moreover, the porosity was slightly increased with increasing amount of CIP into the films.
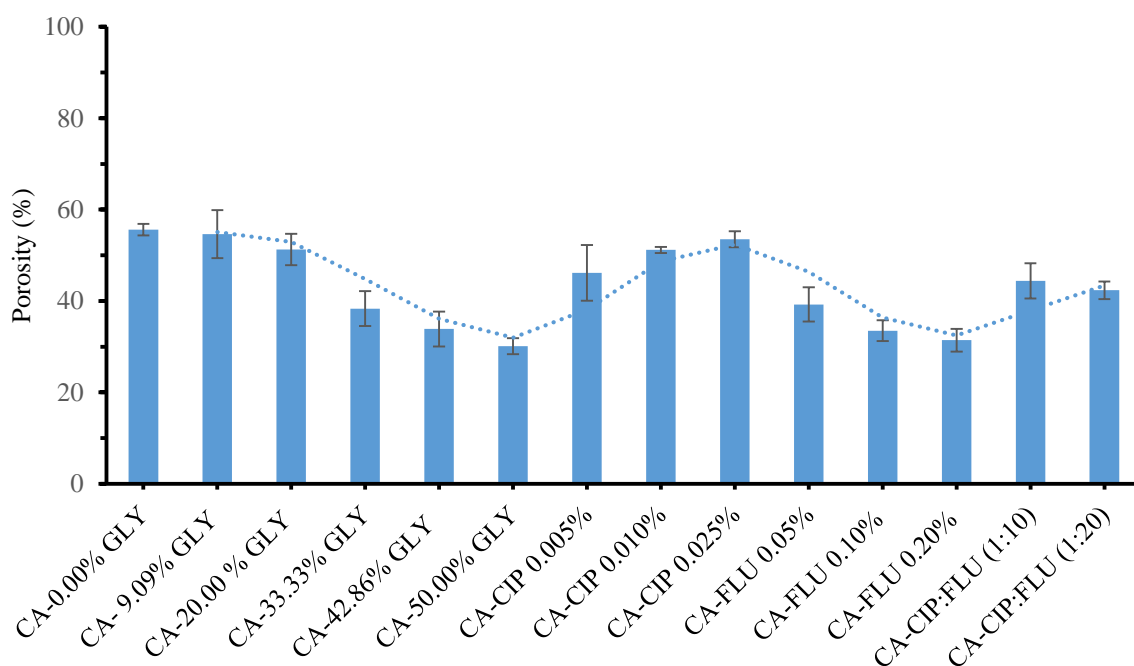
Figure 3.1   Porosity of different film formulations ($n = 3 \pm$ SD).

FLU loaded films with drug content in gel above 0.05% w/v showed lower porosity (33.50-31.43%) than the BLK films. The decrease in porosity of the FLU loaded films is attributed to the increased crystallinity (confirmed by XRD) of these films after loading FLU which made the films more rigid. It was also confirmed by testing Young's modulus (**Chapter**

2: Figure 2.17) that higher concentration of FLU into the films increased rigidity. Therefore, the void space in the microstructure of the films was condensed with FLU loading and subsequently reduced porosity. It was also observed that (**Figure 3.1**) the higher the concentration of FLU, the lower the porosity of the films because of gradually increasing rigidity. Films containing both CIP and FLU showed higher porosity (42.34 − 44.43%) than FLU loaded films but lower porosity than CIP loaded films. This could be explained by the fact that CIP had the tendency to reduce the intermolecular polymer chain interaction that enhanced void space in the polymeric matrix followed by decreasing rigidity resulting in higher porosity than the films containing only FLU. On the other hand, FLU had the tendency to increase intermolecular forces resulting in decreased mobility and therefore, tighter spaces between polymeric chains and subsequently decrease in porosity when compared to the films containing only CIP.

3.4.2   Porosity of wafer and commercial dressings

The highly porous structure of the wafers was obtained by freeze drying where, the gels were initially cooled (freezing) until pure ice crystals form and then sublimated (primary drying) from its frozen state under vacuum at low temperature (-25 ℃), leaving a highly porous microstructure (Nireesha *et al*., 2013). Their highly porous structure permits transportation of gases, nutrients and regulatory factors to allow cell survival, proliferation and differentiation (Dhandayuthapani *et al*., 2011). The porosity of BLK and DL dressings was determined by the solvent (ethanol) displacement method to avoid hydration of the polymer matrix and collapse of the pores. As shown in **Figure 3.2** wafers containing more than 0.0001% CIP showed a high percentage porosity between $98.20 \pm 0.56\%$ to $88.42 \pm 4.03\%$. This could be because the solvent penetrated well into the capillaries of wafers due to the roughness of the pore walls as shown in SEM images (**Chapter 8: Figure 2.10 A**). All FLU loaded wafers showed lower porosity than CIP loaded wafers. This can be explained by the strong interaction between FLU and CA, which enhanced the close packing of polymeric chains and resulted in reduced void space in the microstructure of wafers and therefore, lower porosity. However, the porosity of FLU loaded wafers (87.14-84.07%) was higher than BLK ($80.28 \pm 1.45\%$) when the wafers contained up to 0.15% FLU.
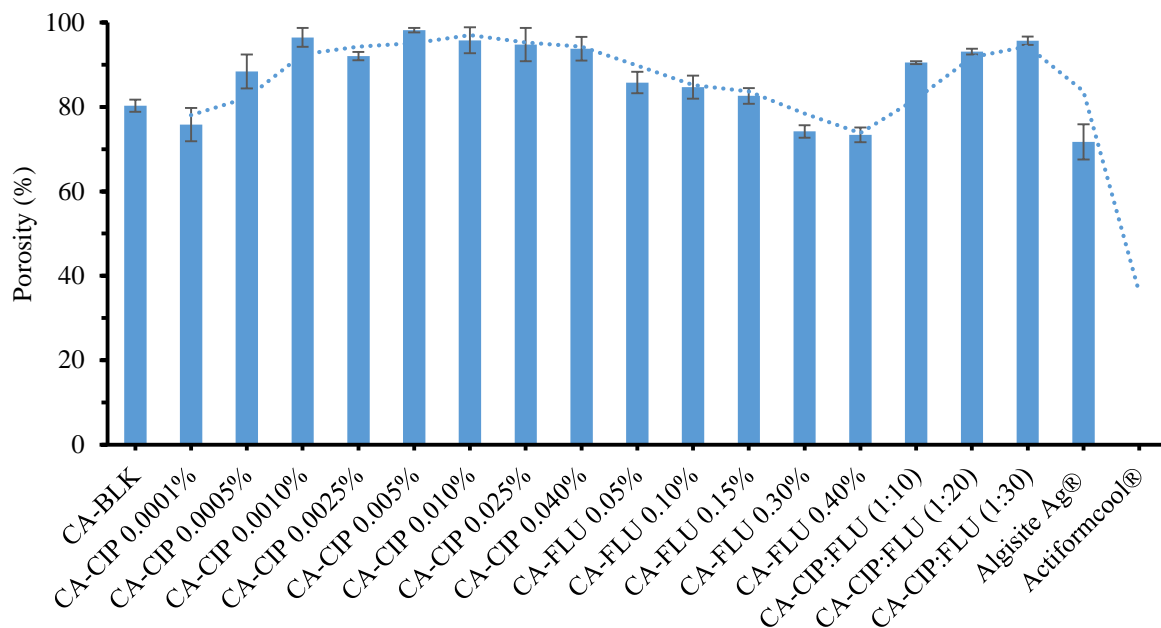
Figure 3.2 Porosity of different wafer formulations and the commercial dressings ($n = 3 \pm$ SD).

Wafers containing more than 0.15% FLU showed significantly ($p = 0.02$) reduced porosity at about 74.19-73.38%. The lower porosity might be attributed to the higher amount of FLU produced denser pores. Wafers containing both CIP and FLU showed higher porosity between $90.50 \pm 0.33\%$ and $95.70 \pm 0.98\%$ than the FLU loaded wafers. The fact could be due to the loading of both drugs together into the wafer matrix, which increased degree of bond rotations within the polymer structure. Therefore, the polymeric chain flexibility was increased and hence, enhanced porosity compared to FLU loaded wafers. The highly porous wafer dressings would play a vital role in carrying oxygen into the blood thus preventing ischemia in diabetic foot.

The commercial dressing Algisite Ag® showed porosity about $71.72 \pm 4.17\%$ whereas Actiformcool® did not show any porosity because of its hydrogel nature. Due to nonporous and high water content (about 96%), hydrogel dressings cannot absorb sufficient exudates thus creating maceration in highly exudative wounds (Yazdanpanah *et al.*, 2015; Boateng *et al.*, 2008; Hilton *et al.*, 2004). All formulations showed higher porosity than the tested commercial dressings, therefore, the formulated medicated dressings will be expected to absorb more exudates than the commercial products. This is because high porosity has an effect on swelling, Aw, EWC, WVTR and drug release as described below.

3.4.3 Swelling studies

The fluid handling ability of dressings has a vital role in healing wound as it prevents collection of excess exudate and maceration of healthy skin tissue in highly exuding DFUs. The swelling capacity (index) of the dressings is closely related to pore size distribution and porosity, crystallinity, residual moisture content and surface pH (Vishal and Shivakumar, 2012; Gabriel *et al*., 2007, Negoro *et al*., 2016). Normally, the greater number of pores allow rapid ingress of water that accelerates higher swelling ability. However, it also depends on the shape, size and uniformity of the pores in the polymeric matrix as well as chemical interaction of polymer and drug with the swelling medium (Pawar *et al*., 2014). Calcium alginate, CIP and FLU all contain hydrophilic and hydrophobic functional groups, which have effect on the swelling properties. Hydrophilic groups present in the polymer and drug such as hydroxyls, carboxyls, amines and carbonyls increase the number of hydrogen bonding sites thus resulting in higher hydration and subsequently improve swelling capacity. The initial phase of fluid uptake of CA dressings can be explained as follows; the Ca^{2+} ions present in the mannuronate units of alginate are exchanged with Na^+ ions in SWF thus allowing faster ingress of fluid into the polymeric matrix.

The swelling behaviour of the films was evaluated in SWF (pH 7.4) and the effect of GLY and drug was also investigated (**Figure 3.3 & Figure 3.4**). The unplasticized film (CA-0.00% GLY) showed the highest swelling capacity ranging from $453.11 \pm 35.43\%$ to $434.45 \pm 22.28\%$ over 60 min, while film plasticized with 50% GLY showed the lowest swelling index ranging between $206.24 \pm 2.29\%$ and $197.29 \pm 3.52\%$. The addition of GLY reduced swelling capacity because of the reduction in porosity as well as its humectant properties (Stout and McKessor, 2012). As porosity decreases, water ingress into the matrix also decreases resulting in reduced initial hydration and subsequent swelling. Moreover, GLY is already rich in moisture, so it does not allow absorption of high amounts of moisture, however, the plasticized film dressings can provide moisture in dry wounds to avoid wound desiccation.
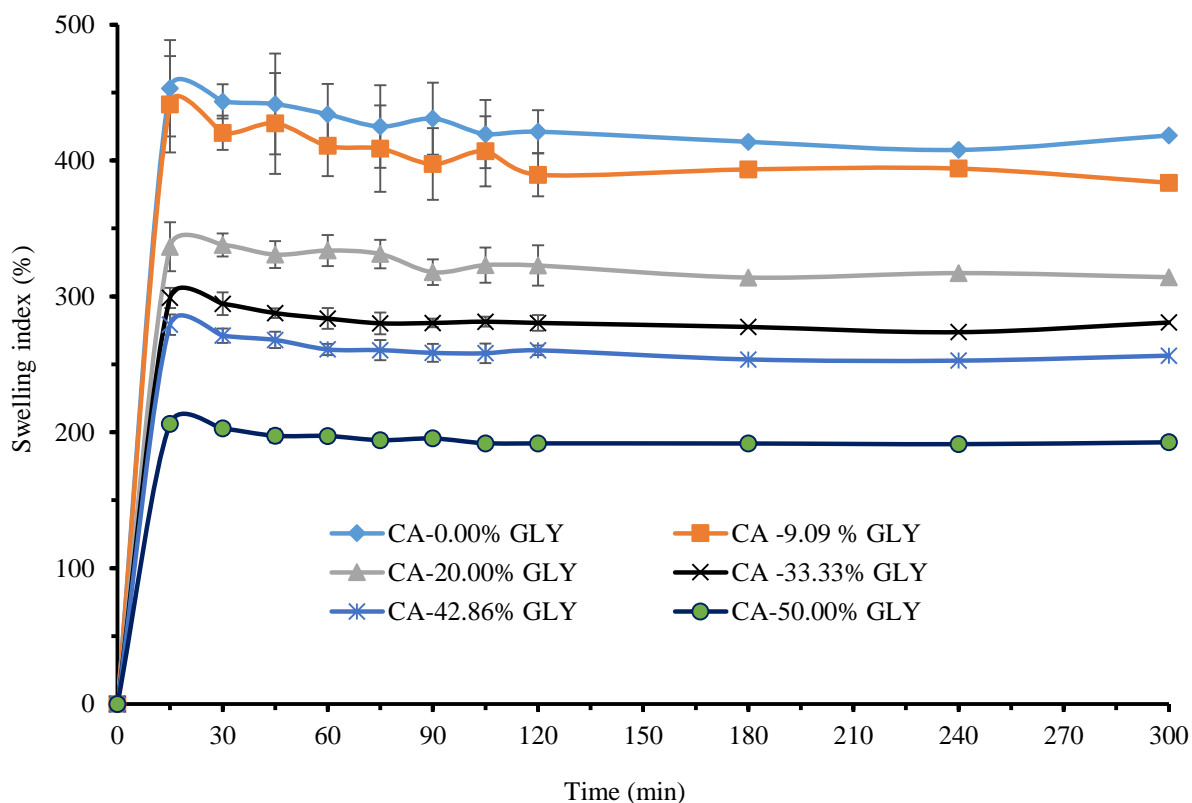
Figure 3.3 Swelling profile of unplasticized and plasticized films ($n = 3 \pm SD$).

The film containing 33.33% GLY (CA-BLK) showed swelling capacity value ranging from $298.92 \pm 7.38\%$ to $283.69 \pm 7.67\%$ over 60 min. After loading CIP into this film, the swelling capacity did not change in a significant way. However, the plasticized (CA-33.33% GLY) film containing 0.005% CIP showed the lowest swelling capacity amongst the CIP loaded films, with values ranging from $231.18 \pm 17.42\%$ to $229.14 \pm 6.96\%$ over 60 min. This could be because the film containing 0.005% CIP was more rigid (also confirmed by texture analysis, **Chapter 2: Figure 2.17**) than other DL films which resulted in lower porosity (**Figure 3.1**) and therefore lower rate of water intake. It can also be observed that all CIP loaded films maintained steady swelling after 15-45 min. It can be observed from **Figure 3.4** that FLU loaded films containing 0.05% FLU reached steady swelling after 60 min whilst those containing 0.10 and 0.20 % drug attained equilibrium after 90 min. The slower water ingress of FLU loaded films compared to CIP loaded films was due to higher rigidity. Therefore, the higher rigidity followed by denser sheet resulted in lower water intake. Film containing 0.20% FLU showed the highest swelling property amongst all DL films, with value range from $289.69 \pm 17.19\%$ to $447.22 \pm 22.27\%$ over 300 min (**Figure 3.4**). Incorporation of higher amounts of FLU enhanced the hydrophilic nature of the films by hydrogen bonding that influenced more water ingress.

Moreover, it was evident by visual observation that the FLU mostly appeared on the film's surface when film loaded with high amount of the drug. The excess FLU quickly leached out from the film's surface upon hydration that increased the surface area allowing high swelling. However, addition of both CIP and FLU together into the polymeric matrix did not affect swelling properties of CA films in a significant way.
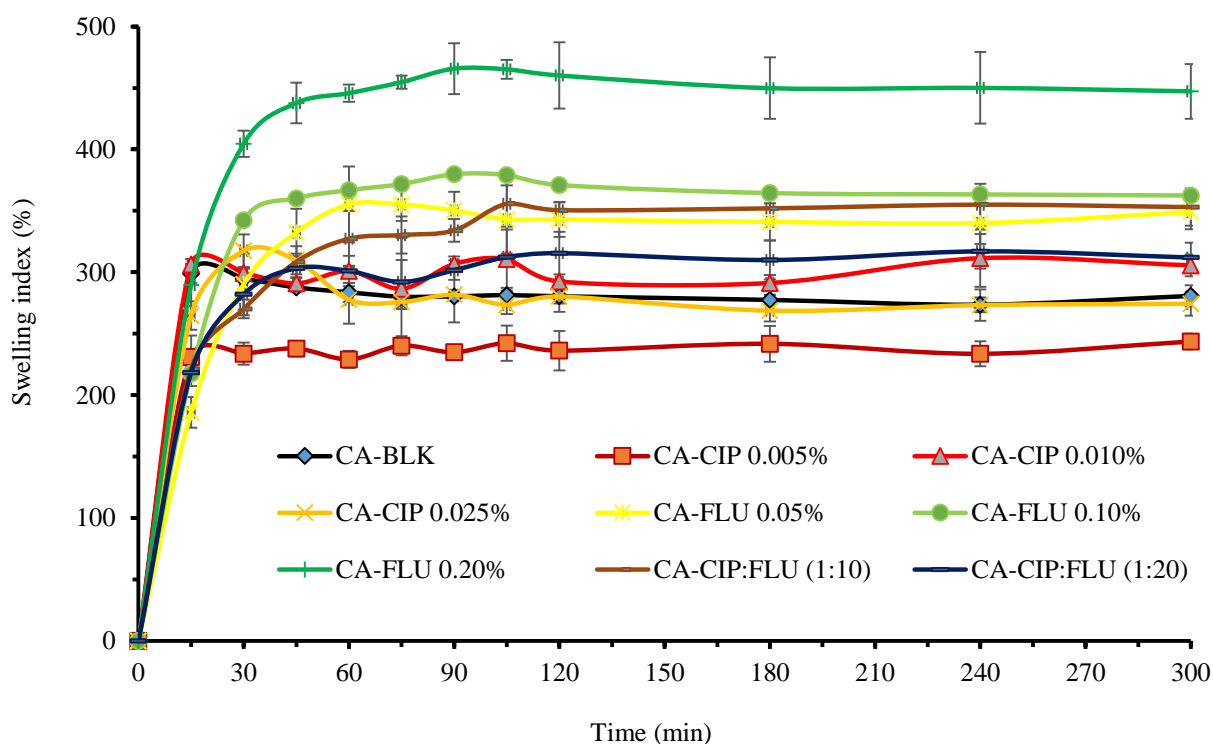
Figure 3.4   Swelling profile of BLK and DL films ($n = 3 \pm$ SD).

Figure 3.5 shows the swelling profiles of BLK and CIP loaded wafers in SWF. The initial swelling ability of CIP loaded wafers (0.0001-0.005% CIP) was higher compared to BLK wafer with values ranging from 2055.30 ± 192.65% to 1476.90 ± 95.69% for the first 15 min. After that, the swelling capacities of all CIP loaded wafers gradually decreased up to 120 min, and then remained steady for the rest of the study. Wafers containing more than 0.005% CIP exhibited lower swelling capacity possibly due to losing their structural integrity resulting in easier polymer erosion in SWF during handling and blotting with the tissue paper. The steady water retention capability of the wafers occurred over an extended period thus indicating that the dressings can be used in highly exuding DFUs to prevent maceration whilst maintaining a moist wound environment.

110
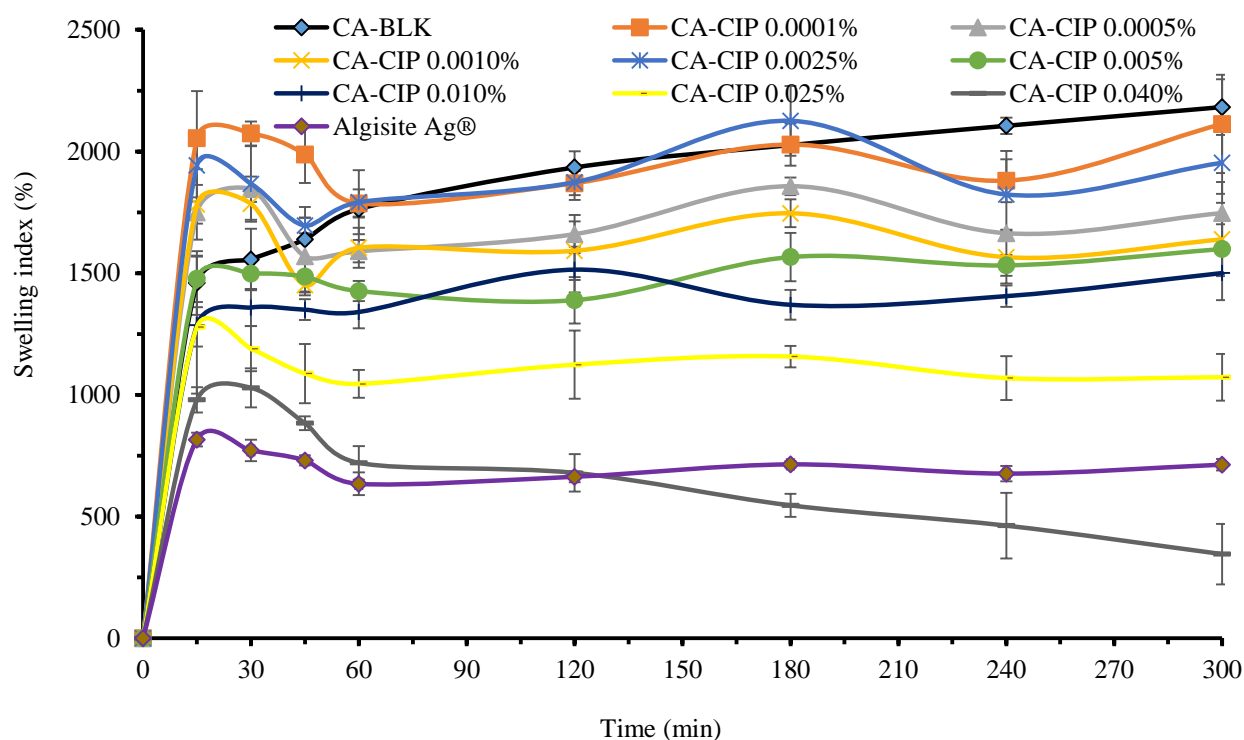
Figure 3.5   Swelling behavior of BLK, CIP loaded wafers and Algisite Ag® ($n = 3 \pm SD$).

The swelling capacities of formulated wafers were compared with a commercial dressing, Algisite Ag® (Smith & Nephew, UK). It was observed that the maximum swelling of Algisite Ag® was about $816.16 \pm 28.58\%$ within 15 min ($p = 0.0008$), which was less than any CIP loaded wafers but more than any CIP loaded films. It could be because the Algisite Ag® fiber mats appeared be less porous (**figure 3.2 & Figure A.3.1**) in nature than wafers but higher in porosity than the films. When comparing the swelling capacity of CIP loaded films with the wafers, it was observed that wafers containing 0.0001-0.025% CIP exhibited 5 - 7 times more swelling capacity (1072.58-2112.97 %) than the CIP loaded films (243.68-305-63 %) which was due to the higher porosity of wafers, which permitted enhanced rate of water ingress than the films.

Figure 3.6 shows swelling characteristics of BLK, FLU loaded and combined (CIP and FLU) DL wafers. In addition, the swelling profiles of the formulated wafers were compared with the commercial hydrogel dressing (Actiformcool®). The initial (15 min) swelling capacity of the wafers containing 0.05-0.15% FLU was about $2056.52 \pm 131.46\%$ to $1775.07 \pm 25.76\%$ which was higher than CA-BLK wafer ($1459.58 \pm 130.83\%$) and similar to the wafers containing 0.0001- 0.0025% CIP (**Figure 3.5**). This is because addition of FLU up to 0.15% showed higher porosity (**Figure 3.2**) than BLK wafer. In contrast, the wafers containing lower amounts of CIP and FLU might have same hydration effect for swelling.

111
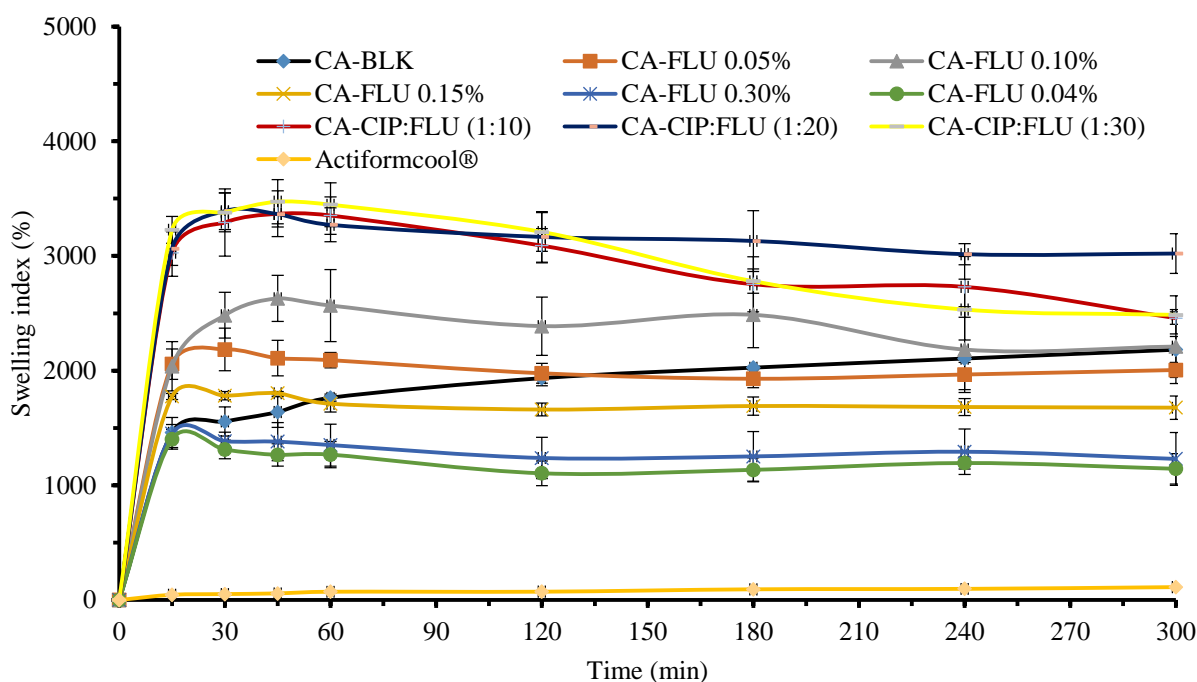
Figure 3.6 Swelling behavior of BLK, FLU loaded, combined DL wafers and Actiformcool® ($n = 3 \pm SD$).

However, incorporation of higher amounts of FLU (> 0.15%) into the wafers resulted in significantly ($p = 0.01$) lower initial and overall swelling ability (values ranging from $1401.78 \pm 77.65\%$ to $1144.09 \pm 230.09\%$) which was similar to the wafers containing 0.005-0.025% CIP. The fact was that high amount of FLU into the wafer's matrix condensed micro pores followed by decreasing porosity (**Figure 3.2**), which resulted in lower water ingress. In case of CIP loaded wafers, higher amount of CIP caused polymer erosion during handling and blotting with the tissue paper, which resulted in lower swelling values. Wafers containing both CIP and FLU exhibited the highest initial swelling ability (about $3228.39 \pm 116.83\%$) amongst all formulated dressings. The highest swelling property of the combined DL wafers was due to hydrophilic nature of the drugs that boosted hydrogen bonding and hence enhanced hydration resulting in quick absorption of SWF. Moreover, high porosity (**Figure 3.2**) of the combined DL wafers enhanced water uptake during swelling. The rapid initial absorption of exudates will play a vital role in reducing heavy exudates present in DFUs and therefore, it will promote wound healing. It can also be observed from **Figure 3.5** and **Figure 3.6** that wafers containing CIP or FLU alone and combined drugs attained equilibrium state after 60 min. After that, the swollen wafers slightly began to lose mass probably due to dissolution or erosion. Actiformcool® showed the lowest swelling capacity (about 45.28-112.27% over 300 min) amongst all formulated dressings as because high moisture content allowed low water ingress to the swollen hydrogel matrix.

112

3.4.4 Water absorption (Aw) and Equilibrium water content (EWC)

The Aw and EWC capacity are the two important factors affecting the rapid absorption of exudates. EWC and Aw of the films gradually decreased with increasing GLY content as shown in **Figure 3.7**. The unplasticized films showed the highest EWC and Aw of 79.16 $\pm$ 0.50% and 380.10 $\pm$ 11.66% respectively whereas films plasticized with 50% w/w GLY showed the lowest EWC and Aw of 65.81 $\pm$ 0.54% and 192.53 $\pm$ 4.62% respectively. The possible reason can be attributed to the porosity of the dressings where addition of GLY into the films decreased porosity (see **Figure 3.1**) and therefore, decreased the EWC and Aw.
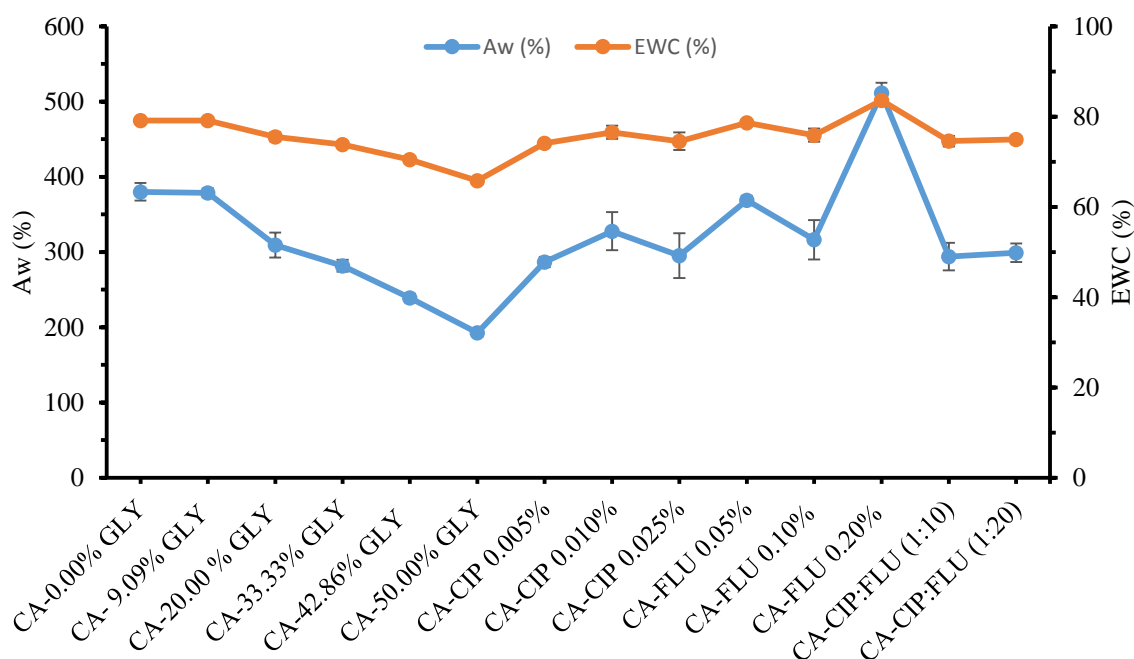
Figure 3.7 Aw and EWC of different film formulations ($n = 3 \pm$ SD).

The CIP loaded films showed a higher EWC and Aw compared to CA-BLK film. The values of EWC and Aw of CA-BLK film increased from 73.80 $\pm$ 0.55% and 76.53 $\pm$ 1.45% to 281.85 $\pm$ 7.85% and 327.68 $\pm$ 25.35 respectively; after loading 0.010% w/v CIP. This is also due to increase in porosity of the CIP loaded films which allowed the ingress of more fluid and be able to hold on to more of this fluid within the swollen film matrix. Films containing 0.05-0.20% FLU showed water absorption with values ranging from 368.80 $\pm$ 6.04% to 511.35 $\pm$ 13.83%, which were higher than CA-BLK films. The higher Aw of the FLU loaded films was due to increase in hydrophilicity. The hydrophilicity enhanced the water uptake affinity and hence showed higher water absorption. Moreover, water absorption of the DL films also

depends on the osmotic properties of the drug (Panomsuk *et al.*, 1996). Once the dressing is hydrated, the polymeric chains start losing their structural integrity and ability to maintain its strong network structure, which allows further water penetration. Further, when the drug is dissolved inside the matrix, it generates an osmotic pressure that promotes high water penetration into the matrix. It was also reported that the polymeric matrix exhibits high swelling at pH between 6.2 and 7.4 (Vishal and Shivakumar, 2012; Gabriel *et al.*, 2007). Therefore, the surface pH of the prepared dressings was investigated and found that the pH of all DL films lied between 6.61 ± 0.05 and 7.35 ± 0.04 whilst CA-BLK had the surface pH of 9.53 ± 0.18 (**Chapter 8: Table A3.1**).

Films containing both CIP and FLU showed water absorption between $294.11 \pm 18.21\%$ and $299.28 \pm 12.35\%$, which was less than the films containing only FLU. That means addition of CIP, decreased hydrophilicity of the films resulting in lower water absorption. There was no significant ($p = 0.96$) differences in EWC among BLK, CIP, FLU and combined DL films. However, films containing 0.20% FLU showed slightly higher EWC capacity (83.63 ± 0.37) than any other films. The phenomena could be due to high amount of FLU into film matrix may exist in between the polymeric chains allowing each chain to hydrate freely and enabled to maintain the structural resistance of swollen matrices that allowed to hold more water. Moreover, the high crystallinity followed by enhanced rigidity (**Figure 2.17**) could resist the erosion of the film in water that permitted high water holding capacity of the CA-FLU 0.20% film.

As shown in **Figure 3.8**, the BLK wafers exhibited the highest Aw ($3373.54 \pm 169.85\%$) and EWC ($97.11 \pm 0.14\%$). After CIP loading into the wafer matrix, the Aw and EWC gradually decreased with increasing drug content due to the increased cross-linking density of CIP within the polymer. The crosslinking between CIP and CA was evident by XRD and FTIR. In XRD observation, it was found that the peaks of CIP loaded wafers were slightly shifted to higher diffraction angle when compared to BLK wafer indicating the interaction of CIP with the polymer. Moreover, the crystallinity of the wafers was decreased (**Chapter 2: Table 2.3**) after loading CIP indicating drug-polymer interaction. It could also be observed in the FTIR data (**Chapter 2: Figure 2.17**) that the characteristic peaks of the CIP loaded wafers were shifted to higher wavelength when compared to BLK wafer indicating the impact of crosslinking between the drug and polymer. The reduction in capacity of Aw and EWC of CIP loaded wafers also could be due to the disturbance in pore size distribution as illustrated in SEM images (**Chapter 2: Figure 2.10 A)** after drug incorporation.
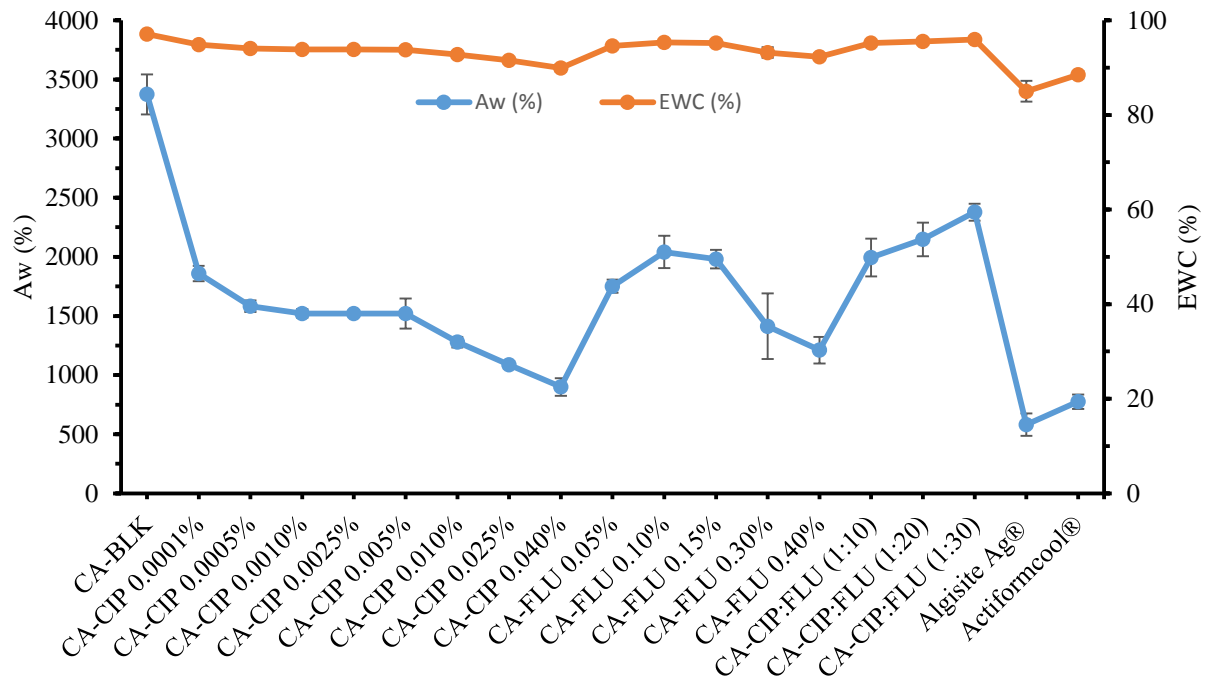
Figure 3.8 Aw and EWC of different wafer formulations and the commercial dressings ($n = 3 \pm SD$).

The irregular pores within polymeric microstructure retards water ingress, which resulted in decreasing water holding capacity into the matrix with increasing CIP loading. Wafers containing 0.0001% CIP showed maximum water uptake at about 1858.27 ± 6538 % whilst the Aw of wafers containing 0.0005-0.005% CIP were insignificant ($p = 0.77$) ranging from 1583.21 ± 49.11% to 1519.85 ± 127.61%. The water uptake capacities were dramatically decreased after loading more than 0.005% CIP. This could be attributed to the dense pore network resulting in reduced void space to absorb water. The wafers containing 0.05-0.15% FLU showed significantly ($p = 0.04$) higher water absorption about 1751.90 ± 54.56% to 2041.21 ± 135.87% than the wafers containing more than 0.15% FLU (values ranging from 1211.01 ± 112.90% to 1323.97 ± 151.53%). The fact that high amount of FLU into the matrix produced dense pores resulting in low water uptake. However, the Aw of FLU loaded wafers was significantly ($p = 0.001$) lower than CA-BLK wafer. Incorporation of FLU into the wafer matrix increased the cross-linking effect that caused the polymeric matrix to lose flexibility resulting in lower water absorption capacity than BLK wafer. Moreover, disturbance in pore size distribution as in the CIP loaded wafers might result in reduced Aw. Wafers containing both CIP and FLU at the ratio of 1: 20 and 1:30 exhibited slightly higher Aw (2147.59 ± 141.45% and 2377.52 ± 70.77% respectively) than all other formulated DL wafers. There was no statistical difference ($p < 0.05$) in EWC of all formulated wafers.

The commercial products Algisite Ag® and Actiformcool® exhibited a lower Aw (580.61 ± 95.30% and 774.82 ± 61.09%) and EWC (85.00 ± 2.21% and 88.51 ± 0.83%) than all formulations. This could be because Algisite Ag® is less porous in nature and Actiformcool® is highly rich in moisture that did not permit further water uptake. Therefore, it suggests that the proposed CA wafer developed in this study has great potential as an absorptive dressing for highly exuding DFUs.

3.4.5   Water vapour transmission rate (WVTR)

WVTR indicates the ability of dressings to absorb fluid and draw it out from the wound bed across the materials into the atmosphere. WVTR is interrelated to porosity and thickness of the dressings as well as the chemical properties of the dressing materials (Elsner *et al*., 2010). Wound dressings require an adequate level of moisture transmission to keep the wound area comfortable and promote the healing process. Dry wounds exhibit the most water loss thus decrease body temperature and rate of metabolism. Therefore, the wound dressing should not reduce the body fluid significantly but should provide adequate moisture by maintaining a balance between water absorption and transmission as well as humidity at the affected site (Kim *et al*., 2007). Higher WVTR promotes epithelization process of wound healing whilst lower WVTR delays the healing process by accumulating excess wound exudates, which leads to maceration of surrounding healthy skin, excoriation and microbial growth (Xu *et al*., 2016).

CIP loaded films exhibited higher WVTR values (**Figure 3.9**) ranging from 3257.22 ± 172.29 to 3876.53 ± 195.50 g/m^{2}day^{-1} than the BLK films ($2687.10 \pm 226.22 - 3682.32 \pm 214.99$ g/m^{2}day^{-1}). This is because; addition of CIP increases the intermolecular chain mobility, resulting in a reduction of rigidity (**Chapter 2: Figure 2.17**) that allows higher diffusion of water molecules through the films matrix. The WVTR values of CIP loaded films are ideal considering the amount of exudate produced by patients with chronic leg ulcers per day (5 g/10 cm^2 ∼ 5000 g/ m^2) (Thomas, 2007). Therefore, the CIP loaded films will absorb and take out about 65-77% fluid from full-thickness chronic wound bed whilst also maintaining a moist environment to facilitate wound healing, however, this needs to be confirmed in an in vivo study. The WVTR values of FLU loaded films were about $2291.12 \pm 172.73 - 1467.73 \pm 137.54$ g/m^{2}day^{-1}, which were lower than BLK and CIP loaded films. This was because of incorporation of FLU into the film made the rigid continues sheet resulting decreased in porosity that reduced the diffusion of water molecules through the semipermeable membrane.

The WVTR of films with both CIP and FLU was $1647.18 \pm 222.72 - 1675.44 \pm 104.93$ g/m^{2}day^{-1}, which was lower than all other prepared films indicating poorer ability to take out fluid from the wound bed.
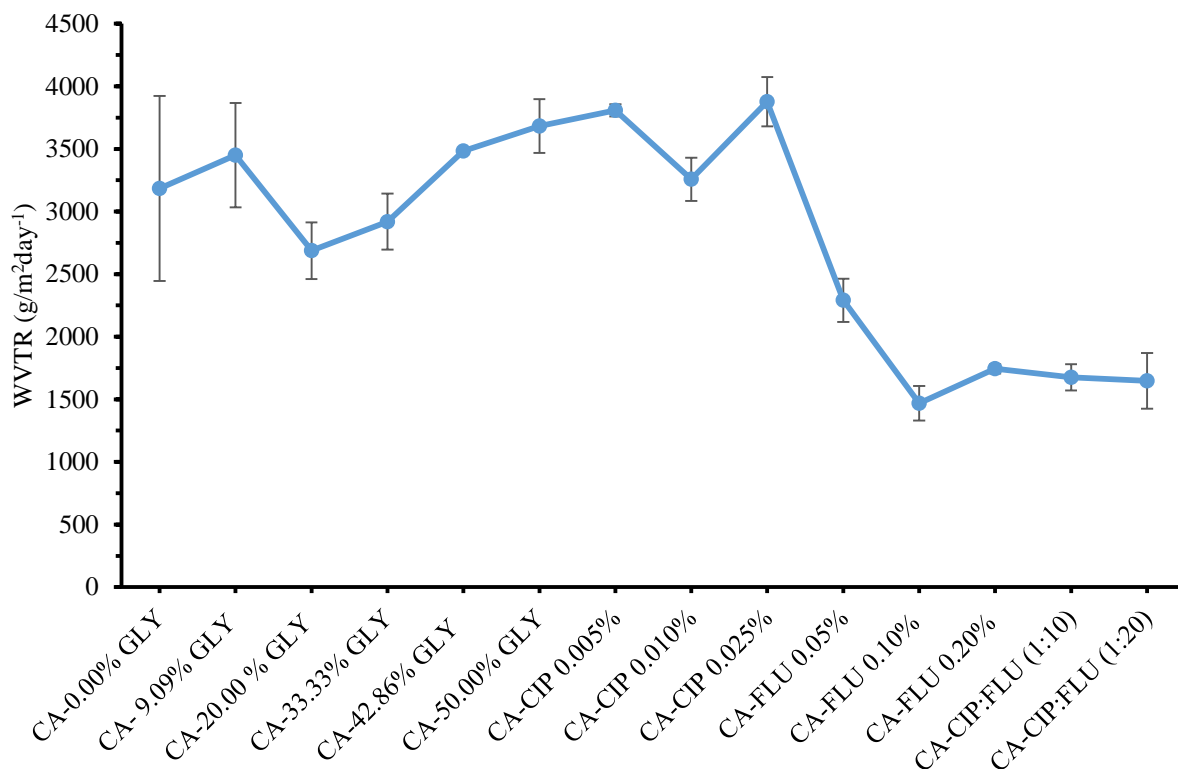
Figure 3.9 WVTR of different film formulations ($n = 3 \pm$ SD).

The CIP loaded wafers showed high WVTR values (**Figure 3.10**) ranging from $3111.79 \pm 16.79 - 3499.23 \pm 71.76$ g/m^{2}day^{-1} that will be expected absorb and transmit exudates quickly. The high WVTR is attributed to the porosity of the dressings, resulting in the increase of voids with capillary adsorbed water. Wafers containing 0.05-0.15% FLU showed WVTR around $1929.67 \pm 64.69 - 2335.78 \pm 184.38$ g/m^{2}day^{-1} whilst wafers containing more than 0.15% FLU showed slightly higher WVTR ($2720.20 - 3026.91$ g/m^{2}day^{-1}). The phenomena might be due to disturbance in porosity (**Chapter 2: Figure 2.10 B**) of the wafers containing high amount of FLU (0.30% and 0.40% w/v) that facilitated easy diffusion of water throughout the matrix.

The WVTR of the combined DL wafers was $1912.68 \pm 36.96 - 2003.23 \pm 56.21$ g/m^{2}day^{-1}, similar to the values of FLU loaded (0.05-0.15%) wafers which might be due to similar morphology (**Chapter 2: Figure 2.10 B).** According to Queen and co-workers, a WVTR of 2000-2500 g/m^{2}day^{-1}, would provide an adequate moisture level for wound healing without dehydration (Queen *et al*., 1987). Therefore, it seemed that the formulated combined (CIP/FLU) DL wafers and FLU loaded wafers would have the ability to maintain a moist wound environment. The commercial products Algisite Ag® and Actiformcool® exhibited WVTR of 2995.97 ± 115.4 and 972.97 ± 172.30 g/m^{2}day^{-1} respectively.
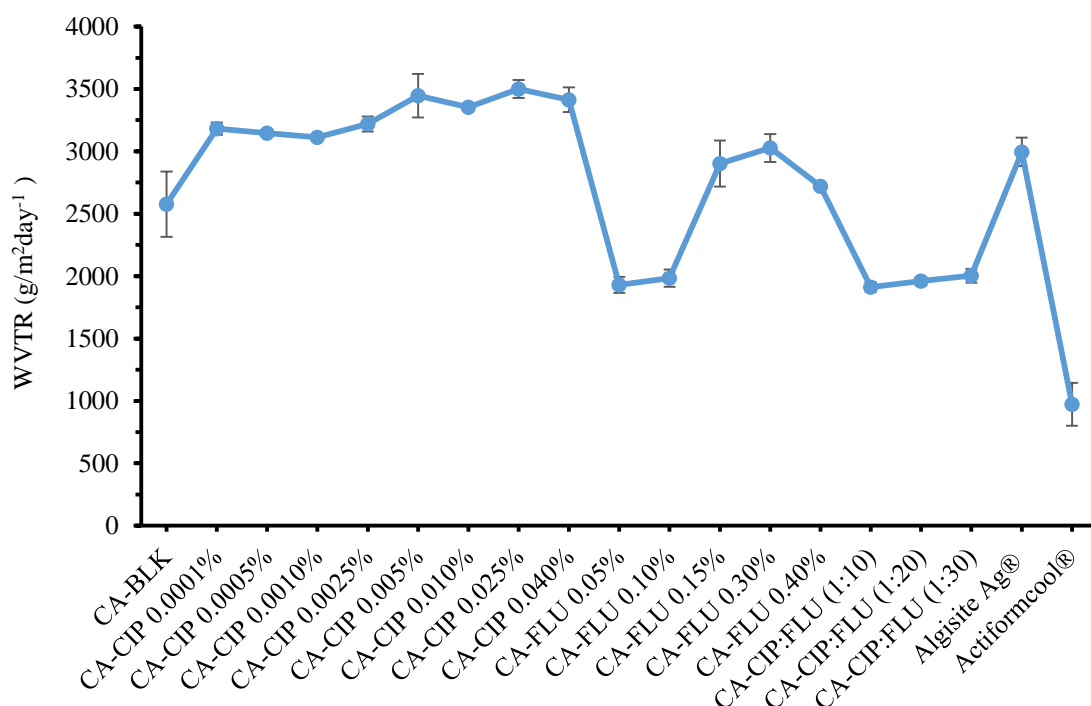
Figure 3.10   WVTR of different wafer formulations and the commercial dressings ($n = 3 \pm$ SD).

Actiformcool® hydrogel showed the lowest value of WVTR due to its hydrophilic and dense non-porous nature resulting in low water escape. Therefore, hydrogel dressing has limitations when used in highly granulating wounds.

3.4.6   Evaporative water loss

The evaporative water loss (EWL) of the films and wafers was recorded to determine the behaviour of the dressings when exposed to air. It is an important functional property of the dressings to maintain moist wound environment. It indicates the moisture loss from the swollen dressings when applied on wound bed. The unplasticized BLK film (CA-0.00% GLY) showed

66% water loss whilst the plasticized BLK exhibited water loss of about 40 - 50% within 30 min (**Figure 3.11a**). After 1.5 h the water loss from the unplasticized and plasticized BLK films was insignificant ($p = 0.54$) and retained $16 - 18\%$ of water after 6 h.
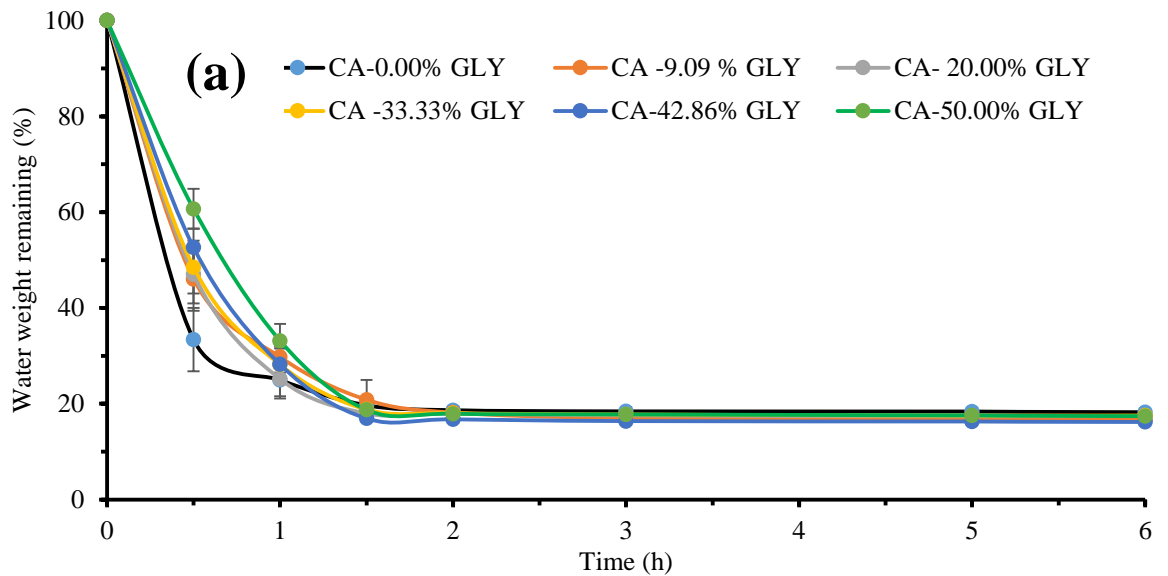
Figure 3.11a EWL from unplasticized and plasticized BLK films ($n = 3 \pm SD$).

CIP loaded films exhibited water loss of about 50% within 30 min, indicating that the dressings will lose water quickly when exposed to air and therefore, it will be effective in the early stage of highly exuding wounds such as DFUs. After 1.5 h the water loss from CIP loaded films was insignificant ($p = 0.78$) and retained 11-16% of water after 6 h (**Figure 3.11b**).
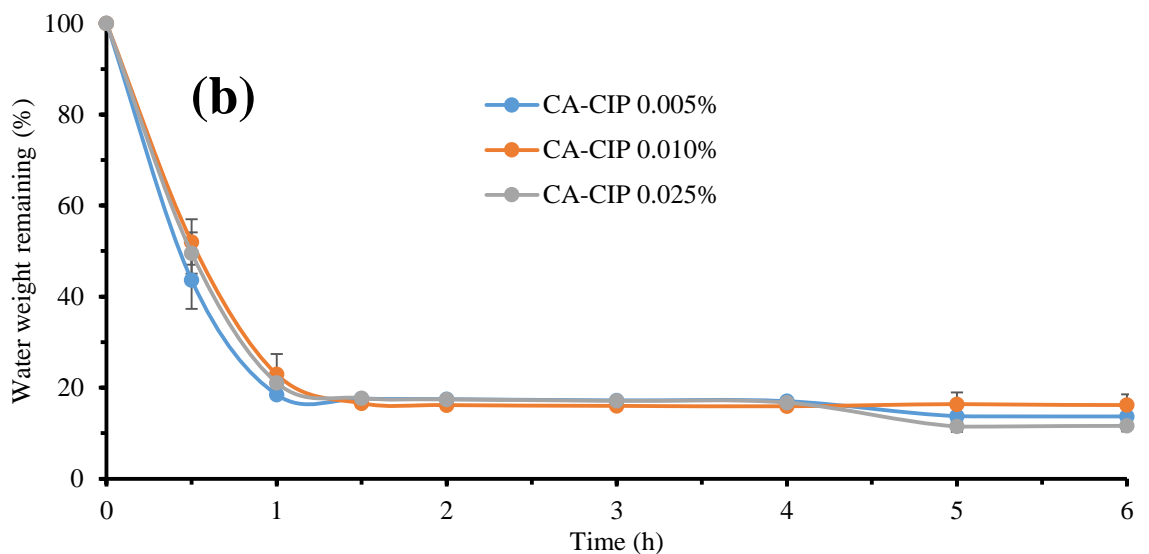
Figure 3.11b EWL from CIP loaded films ($n = 3 \pm SD$).

FLU loaded films showed about 20-40% water loss (**Figure 3.12**) within half an hour which was lower than CIP loaded films (**Figure 3.11b**) and CA-BLK films (**Figure 3.11a**). This might be due to the formation of hydrogen bonding between the FLU and CA molecules resulting in enhanced hydrophilicity that facilitated to low water evaporation. Hydrophilicity may enhance the surface wettability of the films, which resulted in reducing the evaporation flux by increasing the escape energy barrier of surficial molecules (Wang *et al*., 2012). Combined DL films exhibited 30% water loss within 0.5 h and then gradually lost water up to 2 h and retained 17% water after 6 h (**Figure 3.12**). The water loss from the films containing 0.10 and 0.20% FLU equilibrated after 1.5 h and 2 h respectively while the water loss from 0.05% FLU loaded film equilibrated after 4 h. Film containing 0.05% FLU showed slower water loss from its surface than the films containing 0.10% and 0.20% FLU. The could be due to low amount of FLU into the film (CA-33.33% GLY) did not interfere plasticizing effect as evident by similar tensile properties (**Figure 2.17**) and porosity (**Figure 3.1**) as CA-BLK film. All FLU loaded films retained 12-16% water after 6 h.
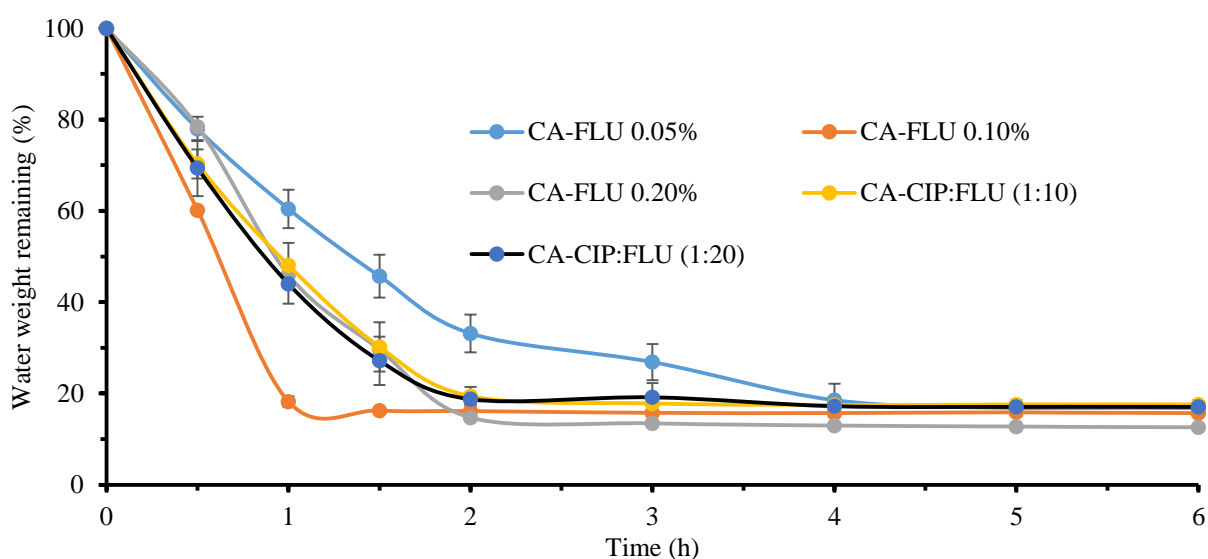
Figure 3.12   EWL from only FLU and combined DL films ($n = 3 \pm$ SD).

As shown in **Figure 3.13**, approximately 20% of water loss was observed in CA-BLK and the DL wafers containing 0.0001-0.025% of CIP within 1 h whereas 0.040% CIP loaded wafer and Algisite Ag® showed 30% and 40% water loss respectively. However, the water loss of CIP loaded wafer increased to approximately 87% within 8 h whereas Algisite Ag® had lost this amount within 3 h. After 8 h the loss of water was insignificant ($p = 0.76$) and all the CIP loaded wafers retained 10-13% of water after 8 h. It indicates that the dressings will lose water when exposed to air. Thus, the wafer dressings will be effective in the early stage of highly

exuding wounds such DFUs, as it enables the dressings to take up more exudates and edema fluid quickly from the wound bed into its matrix by an active upward-directed process to avoid excess accumulation of exudate underneath the dressing (Balakrishnan *et al.*, 2005).
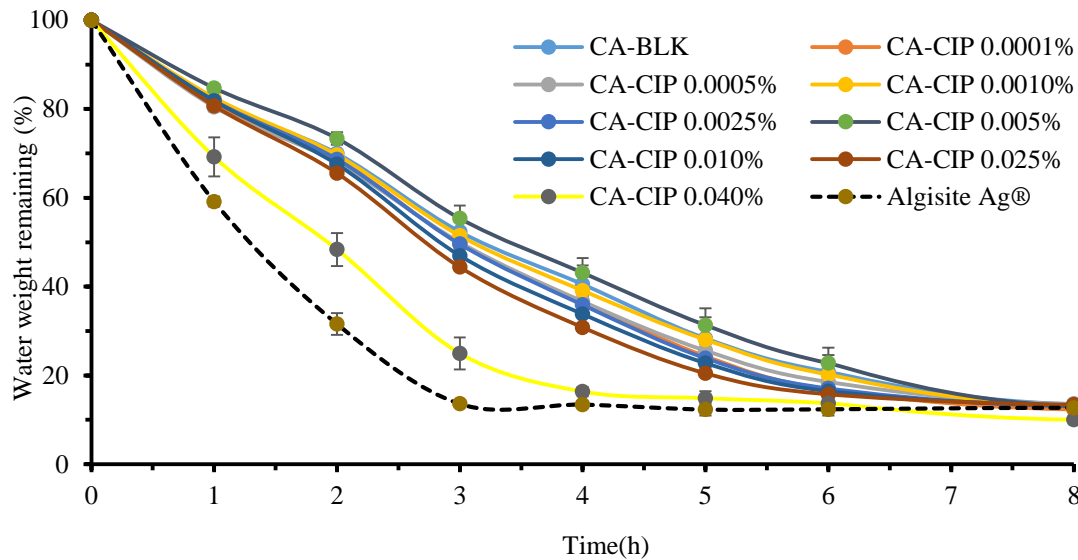
Figure 3.13   Evaporative water loss from Algisite Ag®, BLK and CIP loaded wafers ($n = 3 \pm$ SD).

Figure 3.14 shows the evaporative water loss from the wafers containing only FLU, combined drug (both CIP and FLU) and Actiformcool® hydrogel.
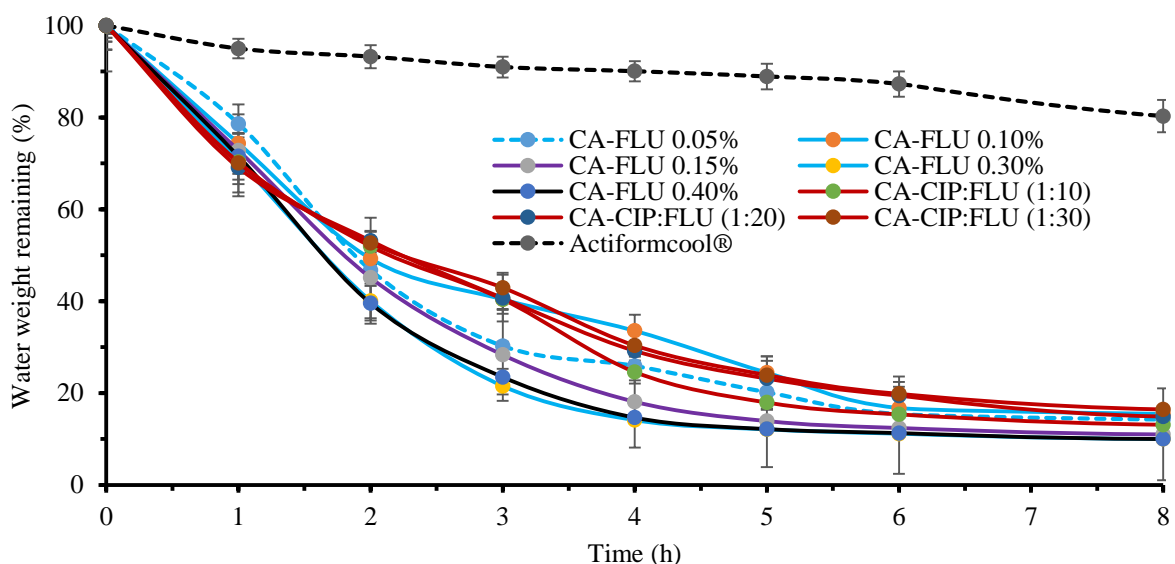
Figure 3.14   Evaporative water loss from Actiformcool®, FLU only loaded wafers and combined DL wafers ($n = 3 \pm$ SD).

Wafers containing only FLU showed water loss about 40-50% within 2 h and after that water loss was slow and weight of the wafers indicating remaining water weight equilibrated after 6 h. In the case of the wafers containing both CIP and FLU, the water loss from the dressings was similar to the wafers containing only FLU.

All FLU loaded and combined DL wafers retained 10 - 16% water after 8 h indicating that large amount of exudates will be evaporated from the swollen matrix and at the same time some moisture retained which will help to prevent excess dehydration and subsequently will provide a moist wound environment. Actiformcool® exhibited very low water loss of about 20% after 8 h, which was lower than all the other formulated dressings. The high water retaining of Actiformcool® was due to its three-dimensional structure, which possess hydrophilic properties resulting in higher affinity to retain water.

Overall, film dressings exhibited higher evaporative water loss than wafers. About 50% water loss was recorded from the films within half an hour, whereas this amount evaporated from wafers in 2-3 h. The higher water evaporation from the film surface was due its thin, semipermeable, continuous sheet that enabled them to retain less water.

3.4.7 Moisture content

Thermogravimetric analysis was used to determine the residual water content of the formulated dressings. The uplasticized films showed residual moisture content of $4.95 \pm 0.88\%$, which increased up to 8.37 ± 0.11 after addition of GLY. The increase is due to the hydrophilicity and strong humectant properties of GLY. Since GLY is highly hydrophilic, the presence of GLY in the films resulted in higher bound water and hence, enhancing residual moisture content (Rhim *et al*., 2002).
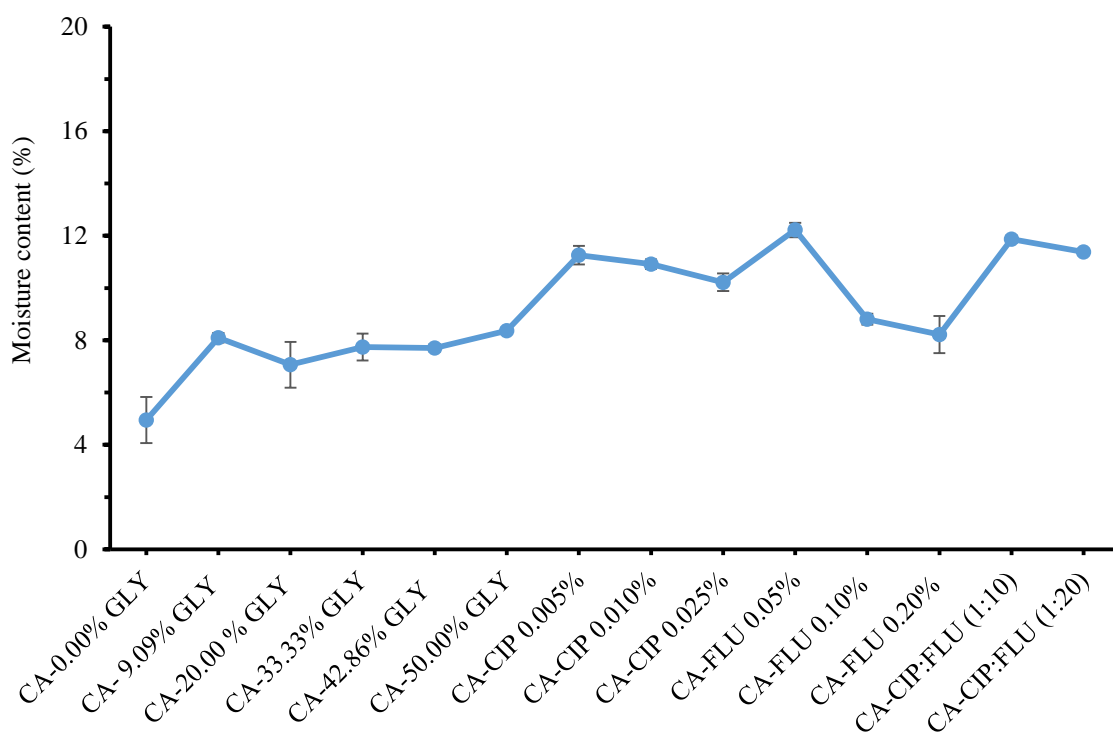
Figure 3.15 Moisture content of different film formulations ($n = 3 \pm$ SD).

After loading drug, the residual moisture content was further increased from about 8.22 ± 0.271 to 12.22 ± 0.28 because of increase in porosity, which enabled it to absorb more moisture. It could also be observed that the incorporation of drug increased hydrophilicity of the polymeric matrix resulting in higher amounts of bound water and therefore increased residual moisture content.

The wafer dressings exhibited higher residual moisture content than films. This was because in the final cycle of lyophilization, the wafers were dried at 20 °C whereas, in the solvent casting technique the films were dried at 30 °C resulting higher residual moisture in wafers than the films. Moreover, higher porosity of wafers facilitated the retention of more bound water than film dressings. The moisture content of BLK wafer was about 13.28 ± 0.86 % whereas incorporation of CIP into the polymeric wafers resulted in significantly ($p = 0.004$) higher moisture content about $16.56 \pm 0.08\%$ to $17.30 \pm 0.04\%$ respectively (**Figure 3.16**). This seems to indicate that addition of CIP resulted in higher sorption characteristics. On the other hand, the moisture content were slightly lower in FLU loaded wafers ($15.25 \pm 0.30\% - 9.78 \pm 0.76\%$) that could be attributed to the differences in hygroscopicities of the drugs. Wafers containing both CIP and FLU showed residual moisture content between $14.11 \pm 0.09\% - 13.74 \pm 0.85\%$ which were very close to BLK wafers.
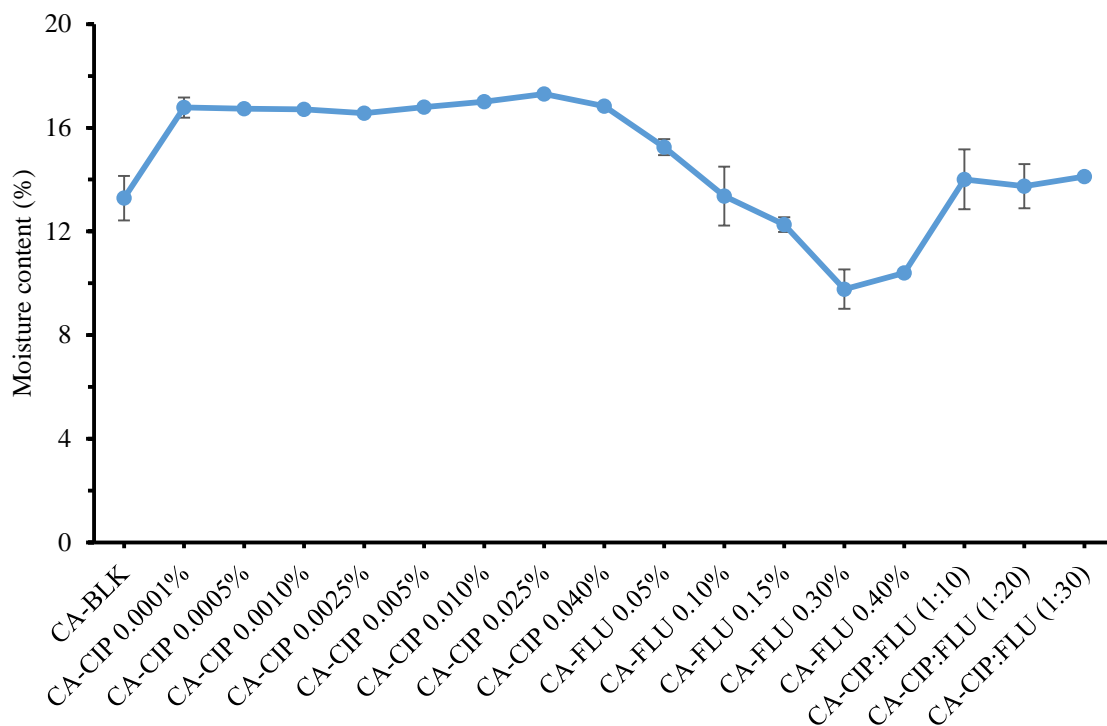
Figure 3.16   Moisture content of different wafer formulations ($n = 3 \pm SD$).

The residual water content within the wafers depends on either annealing or non-annealing process in the primary drying stage. Usually non-annealing process in the freeze cycle retains higher residual moisture content compared to annealing process (Kianfar *et al*., 2013b). In this study non-annealing process was used therefore, the dressings seemed to have a relatively higher moisture content. Though, high residual water content into wafers is susceptible to microbial growth and retards stability by accelerating crystallization of the drug upon storage (Kianfar *et al*., 2013), the levels are comparable to other reported studies (Momoh *et al*., 2015; Kianfar, *et al*., 2011). Moreover, the low residual moisture content of the films may facilitate more stability upon storage than wafers; however, this could be confirmed by long term stability studies under controlled conditions. Further, high moisture content of the wafers can maintain the wound and surrounding skin in an optimum state of hydration thus implies the dressings will function efficiently under compression (Thomas, 2008).

3.4.8 *In-vitro* drug dissolution and release studies

3.4.8.1 Drug loading efficiency and content uniformity

The drug loading efficiency of films containing 0.005%, 0.010% and 0.025% CIP recorded was $65.81 \pm 3.98\%$, $60.99 \pm 2.01\%$ and $55.01 \pm 4.27\%$ respectively (**Figure 3.17**). Further, films containing 0.05, 0.10 and 0.20% FLU showed drug loading efficiency about $90.68 \pm 0.42\%$, $60.32 \pm 0.17\%$ and $52.23 \pm 4.71\%$ respectively (**Figure 3.17**). The drug loading capacity of the films appeared relatively low except the film containing 0.05% FLU. This could be explained by the fact that the drying process during film formation results in a dense and very thin product resulting in precipitation of excess drug on the surface of the films some of which can be lost through scraping and contact during handling (Boateng *et al*., 2011). Low amount of FLU (0.05%) was entrapped within the film matrix.
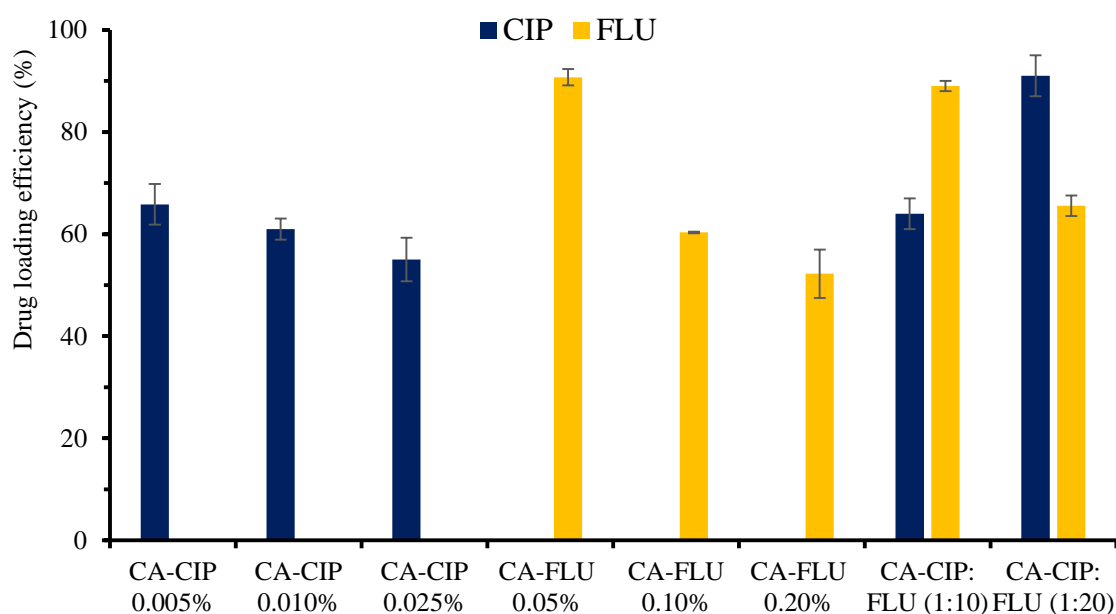
Figure 3.17 Drug loading efficiency of DL films ($n = 3 \pm$ SD).

There was no significant difference ($p > 0.05$) between loading capacity of the film containing both CIP and FLU at the ratio of 1:10 when compared to the films containing CIP or FLU alone. However, film containing both CIP and FLU at the ratio of 1:20 exhibited significantly higher ($p < 0.05$) drug loading CIP ($91.01 \pm 4.2\%$) than the film containing only CIP or FLU. This could be explained by the fact that the addition of high amount of FLU (0.10%) with CIP resulted in increasing hydrogen bonding that enhanced the miscibility between the drugs within the film matrix.

The drug loading capacity recorded for wafers containing 0.005, 0.010 and 0.025% CIP was $88.08 \pm 1.45\%$, $84.77 \pm 1.59\%$ and $83.26 \pm 3.06\%$ respectively (**Figure 3.18)** whereas, wafers containing 0.05-0.40% FLU showed $60.89 \pm 2.95\%$ − $71.41 \pm 3.88\%$ drug loading efficiency. The lower drug loading capacity of FLU loaded wafers was attributed to their lower porosity (**Figure 3.2)**. In the case of combined DL wafers, FLU showed high drug loading recovery ($70.53 \pm 1.31\%$ - $85.02 \pm 1.02\%$) during the formulation process when compared with the wafers containing same amount of FLU alone. This fact was also attributed to porosity as previously observed (**Figure 3.2**). Furthermore, it can be observed (**Figure 3.18**) that the wafers have the higher drug loading capacity than films as was previously documented by Boateng and co-workers (Boateng *et al*., 2009, 2011; Ayensu *et al*., 2012). The drug loading capacity depends on the porous network of lyophilized wafers (Ayensu *et al*., 2012). The wafers can maintain the volume, size and shape of the original gel poured due to the freezing stage of free-drying, while films shrink due to evaporation during solvent casting.
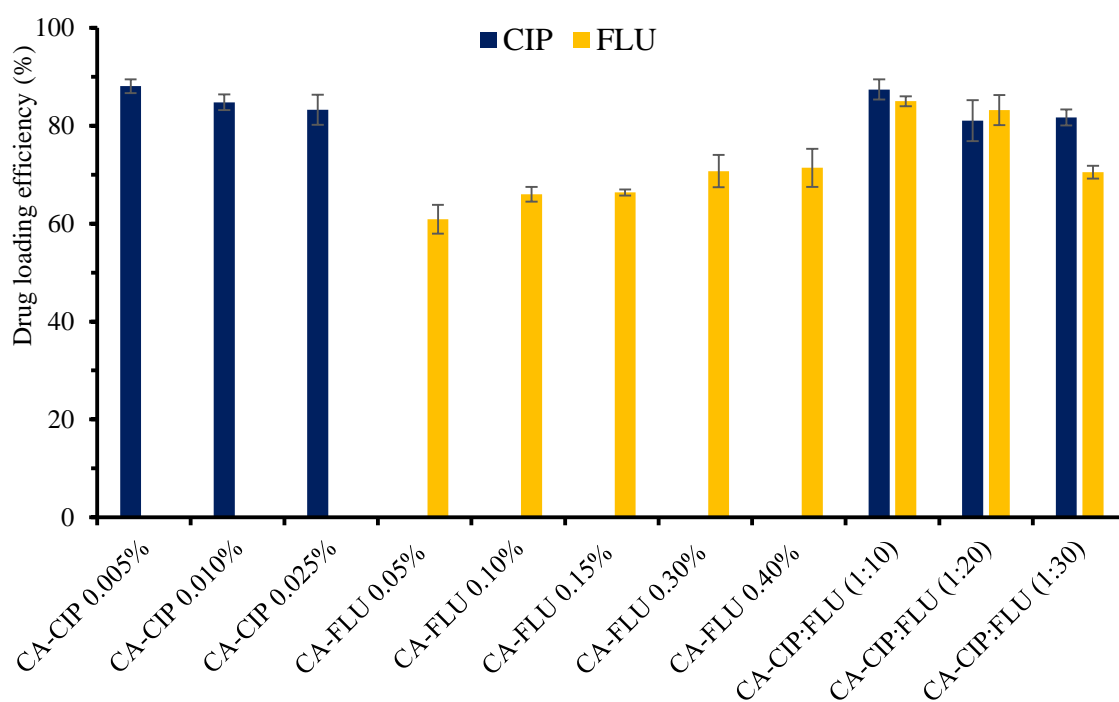
Figure 3.18   Drug loading efficiency of DL wafers ($n = 3 \pm SD$).

The lyophilization process yields porous wafers in which drug molecules can be entrapped whereas, oven drying process makes the films a continuous dense sheet resulting in less

entrapment within the matrix and precipitation of excess drug on the surface of the films some of which can be lost through scraping and contact during handling (Boateng *et al*., 2012).

Table 3.2   Observation of statistical differences in DCU of different CIP and FLU loaded dressings ($n = 3 \pm$ SD). P indicates part (6 mm) of the films.

Film	Drug content (µg)			*p* value
	P1	**P2**	**P3**	
CA-CIP 0.005%	5.03 ± 0.02	5.15 ± 0.02	5.25 ± 0.02	> 0.05
CA-CIP 0.010%	10.87 ± 0.02	10.80 ± 0.02	10.72 ± 0.01	> 0.05
CA-CIP 0.025%	22.32 ± 0.01	22.15 ± 0.06	22.15 ± 0.01	> 0.05
CA-FLU 0.05%	64.21 ± 0.03	62.54 ± 1.23	60.78 ± 0.36	> 0.05
CA-FLU 0.10%	90.03 ± 1.05	80.42 ± 1.15	96.20 ± 0.09	< 0.05
CA-FLU 0.20%	163.50 ± 0.51	185.28 ± 0.72	179.94 ± 0.80	< 0.05
Wafer				
CA-CIP 0.005%	3.63 ± 0.04	3.59 ± 0.02	3.75 ± 0.01	> 0.05
CA-CIP 0.010%	6.53 ± 0.01	6.86 ± 0.12	6.44 ± 0.62	> 0.05
CA-CIP 0.025%	15.50 ± 0.02	15.69 ± 0.07	15.51 ± 0.04	> 0.05
CA-FLU 0.05%	28.60 ± 1.59	29.88 ± 0.26	29.66 ± 0.85	> 0.05
CA-FLU 0.10%	55.75 ± 0.14	53.03 ± 0.24	55.57 ± 0.10	> 0.05
CA-FLU 0.15%	112.78 ± 0.19	109.76 ± 0.06	115.57 ± 0.09	> 0.05
CA-FLU 0.30%	252.89 ± 2.63	172.52 ± 2.24	207.60 ± 0.04	< 0.05
CA-FLU 0.40%	288.12 ± 0.05	273.79 ± 0.21	256.61 ± 0.29	< 0.05

Table 3.3   Observation of statistical differences in DCU of the dressings containing both CIP and FLU ($n = 3 \pm$ SD).

Film	Drug content (µg)						*P* value	
	P1		**P2**		**P3**			
	CIP	**FLU**	**CIP**	**FLU**	**CIP**	**FLU**	**CIP**	**FLU**
CA-CIP:FLU (1:10)	4.7 ± 0.1	63.6 ± 0.3	4.8 ± 0.0	61.5 ± 0.2	4.6 ± 0.0	63.6 ± 0.0	> 0.05	> 0.05
CA-CIP:FLU (1:20)	6.7 ± 0.0	92.9 ± 0.7	6.6 ± 0.0	92.1 ± 0.1	6.7 ± 0.0	94.2 ± 0.5	> 0.05	> 0.05
Wafer								
CA-CIP:FLU (1:10)	3.1± 0.1	40.8 ± 0.1	3.1 ± 0.0	35.2 ± 0.1	3.0 ± 0.0	38.6 ± 0.1	> 0.05	> 0.05
CA-CIP:FLU (1:20)	2.6 ± 0.0	77.9 ± 0.1	2.6 ± 0.0	75.3 ± 0.1	2.5 ± 0.0	78.2 ± 0.2	> 0.05	> 0.05
CA-CIP:FLU (1:30)	2.1 ± 0.0	107.9 ± 0.1	2.5 ± 0.0	109 ± 0.2	2.3 ± 0.0	106.4 ± 0.1	> 0.05	> 0.05

The drug content uniformity (DCU) was also investigated to check the homogeneous distribution of the drug all over dressings. All formulations retained uniform distribution of drugs except the films and wafers containing more than 0.05 and 0.15% FLU respectively. Statistical analysis revealed that there was significant differences (**Table 3.2**) in drug content on different locations of those dressings. In addition, the distribution of drugs was also confirmed by zone of inhibition (ZOI) antibacterial study (**Chapter 4: Figure 4.15 & Figure 4.16). Table 3.3** shows the statistical evaluation of DCU of the combined DL dressings. It was found that there was no significant differences ($p > 0.05$) in content of CIP and FLU on different part of the dressings, which confirmed the biocompatibility between two drugs.

3.4.8.2 *In-vitro* drug release studies

The percentage cumulative release profiles of CIP and FLU from the CA based dressings with different amounts of drugs are shown in **Figures 3.19 – Figure 3.24**. The release of drugs closely matched the swelling profiles of the dressings as shown in **Figure 3.4, Figure 3.5 and Figure 3.6**. A quick hydration of the films was observed within 15 min and within this time more than 50% drug was released. This means films containing 0.005% and 0.010% CIP can reach minimum bactericidal concentration (MBC) (99.9% inhibition) for killing *E. coli and P. aeruginosa* within that time. However, film containing 0.025% CIP can reach MBC for killing all three organisms (*E. coli*, *P. aeruginosa* and *S. aureus*) within 5 min.
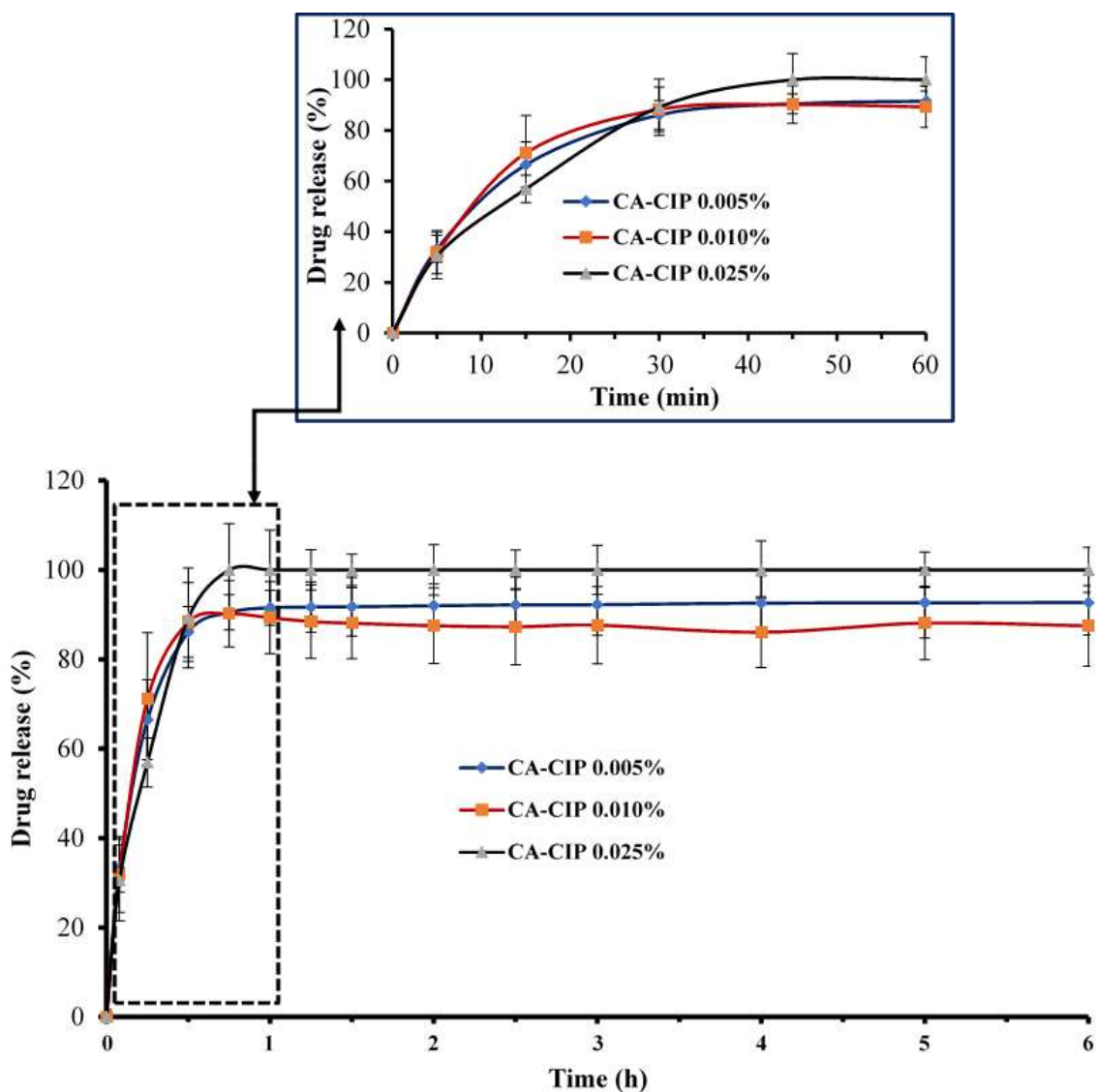
Figure 3.19 Cumulative percentage drug release profiles of CIP loaded films ($n = 3 \pm$ SD).

The films exhibited the maximum CIP release within 45 min with values of $90.50 \pm 3.93\%$, $91.18 \pm 7.44\%$ and $100.41 \pm 11.15\%$ respectively (**Figure 3.19**). This indicates that the release of CIP from the film dressings could potentially reduce microbial load very quickly, which is important in highly infected chronic wounds such as DFUs where the bacteria load needs to be significantly reduced to allow wound healing to progress beyond the inflammatory phase.

FLU loaded films appeared to have a burst release which can reach minimum inhibitory concentration (MIC) for inhibiting the growth of *C. albicans* within a short time. Films containing 0.05% FLU released 65.32 ± 3.47 % of drug within 5 min whereas, $90.03 \pm 7.12\%$ and $80.63 \pm 3.59\%$ of drug was released from the films containing 0.10 and 0.20% FLU at that time (**Figure 3.20**).
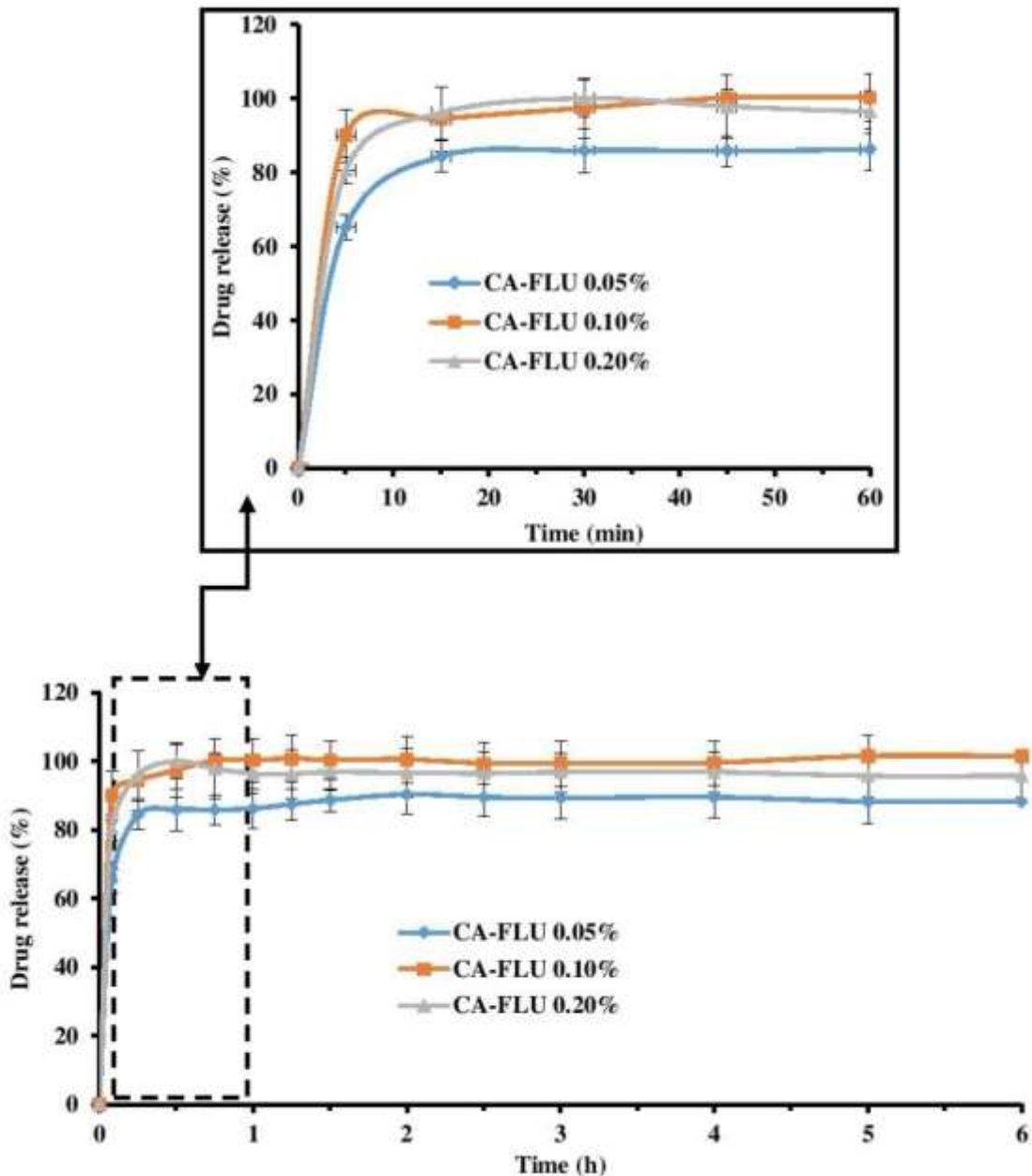
Figure 3.20 Percentage cumulative drug release profiles of FLU loaded films ($n = 3 \pm SD$).

Several factors are associated with the burst release of drug from the dressings such as geometrical shape of the dressings, heterogeneity of matrices (pore density), surface characteristic of the polymer, and heterogeneous drug distribution within the polymeric matrix (Fu and Kao, 2010). Films released drug rapid possibly due to its one-dimensional geometrical shape that allowed rapid hydration and dissolution with short swelling phase. Moreover, FLU might has high solubility in the dissolution medium resulting in burst release. The high amount of drug release within a very short time also indicated that FLU was mainly released from the surface of the film, which further confirmed the precipitation of the drug on the surface as

observed in **Figure 2.6 (Chapter 2)**. Furthermore, as previously discussed, the films containing more than 0.05% FLU had non-uniforme distribution of the drug. All these data suggest that CA film has the limitation of loading high amount of FLU. However, burst release of FLU from the films may have advantages in chronic wounds like DFUs. In DFUs, the patients require frequent dressing change to prevent accumulation of excessive exudates underneath the dressing. Thus, this sort of burst release of FLU may help to provide enough drug concentration to reduce fungal load before the next change of the dressing.

It can be observed from **Figure 3.21** that the release of CIP from the combined DL films was more controlled than FLU with maximum release occurring immediately after hydration. It was noted that, only 44.73- 67.81% CIP was released from the CA-CIP:FLU (1:10) film over 360 min and the remaining CIP might be present within the swollen matrix due to physical interactions with the polymer chains. The CIP release was higher (90.48 %) in the CA-CIP:FLU (1:20) film than the film with CIP and FLU at the ratio of 1:10. This could be attributed to the higher amount of FLU which might decrease the physical interaction of CIP with the polymer chains resulting in higher release of CIP. On the other hand, higher release of FLU was observed in CA-CIP:FLU (1:10) film (82.71 ± 0.45%) than the film with CIP and FLU at the ratio of 1:20 (66.37 ± 1.46%). This could be because the lower amount of FLU was easily leached out from the film matrix due to relatively more solubility in dissolution medium (SWF without BSA) than the formulations containing higher amount of FLU.
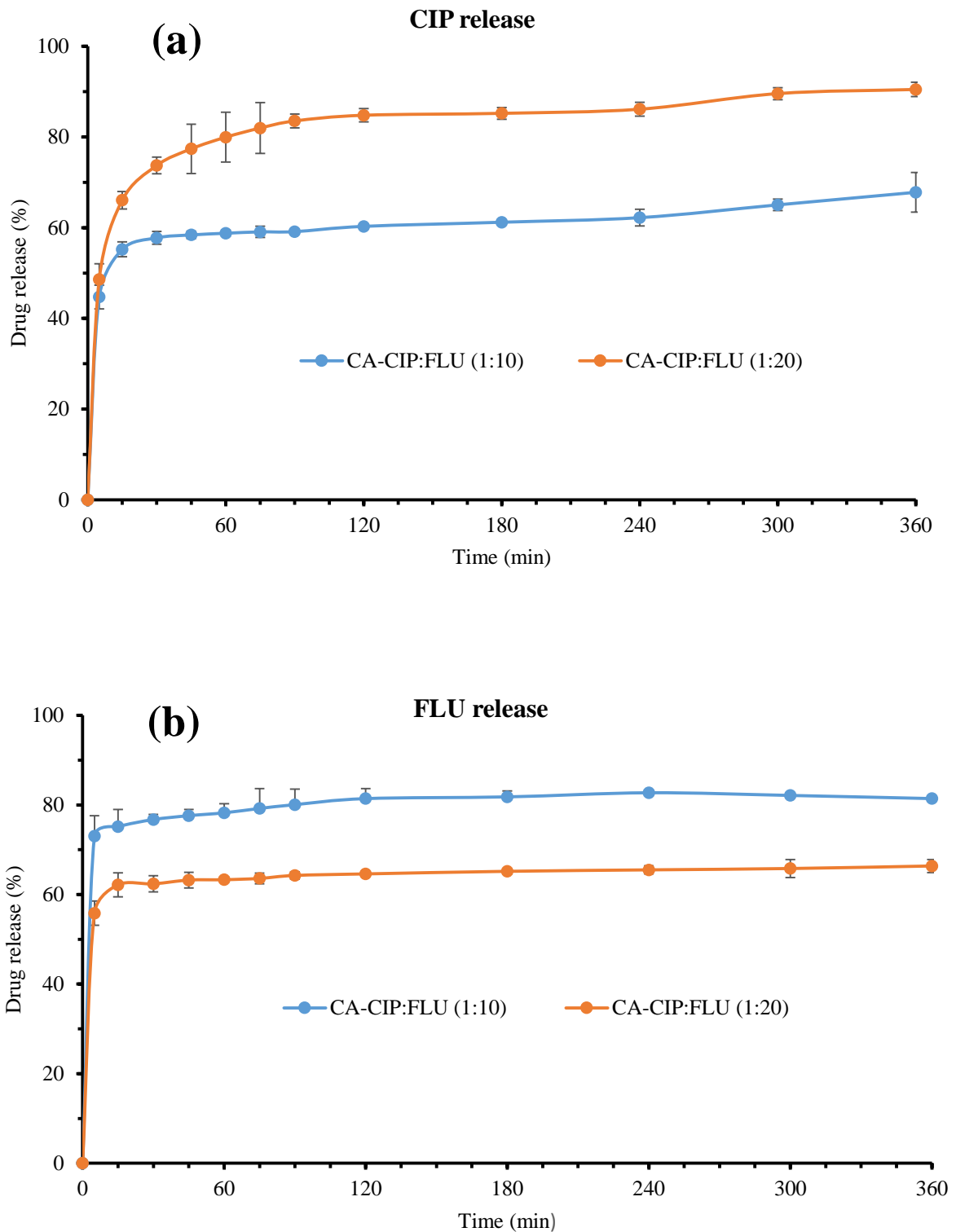
Figure 3.21 *In vitro* drug release profiles of (a) CIP and (b) FLU from films containing both drugs in different ratios, showing mean percentage cumulative release (mean ± SD, *n* = 3) against time in the presence of SWF at pH 7.5.

The percentage cumulative release profiles of CIP from the CA based wafers with different amounts of drug are shown in **Figure 3.22**. Wafers loaded with 0.025% CIP appeared to produce the fastest release rate, releasing about $68.36 \pm 3.68\%$ of the total drug content within 5 min of dissolution. This means the burst release of the dressings can reach MBC for killing *E. coli, P. aeruginosa and S. aureus* within 5 min. However, wafers containing 0.005 and 0.010% CIP showed total release around $41.89 \pm 6.74\%$ and $20.91 \pm 6.32\%$ respectively in 5 min, which is also high enough for killing *E. coli* and *P. aeruginosa.* The highest cumulative percent of CIP released in 6 h was $59.40 \pm 0.64\%$, $74.39 \pm 3.59\%$ and $91.43 \pm 1.21\%$ from the wafers loaded with 0.005, 0.010 and 0.025% drug respectively.
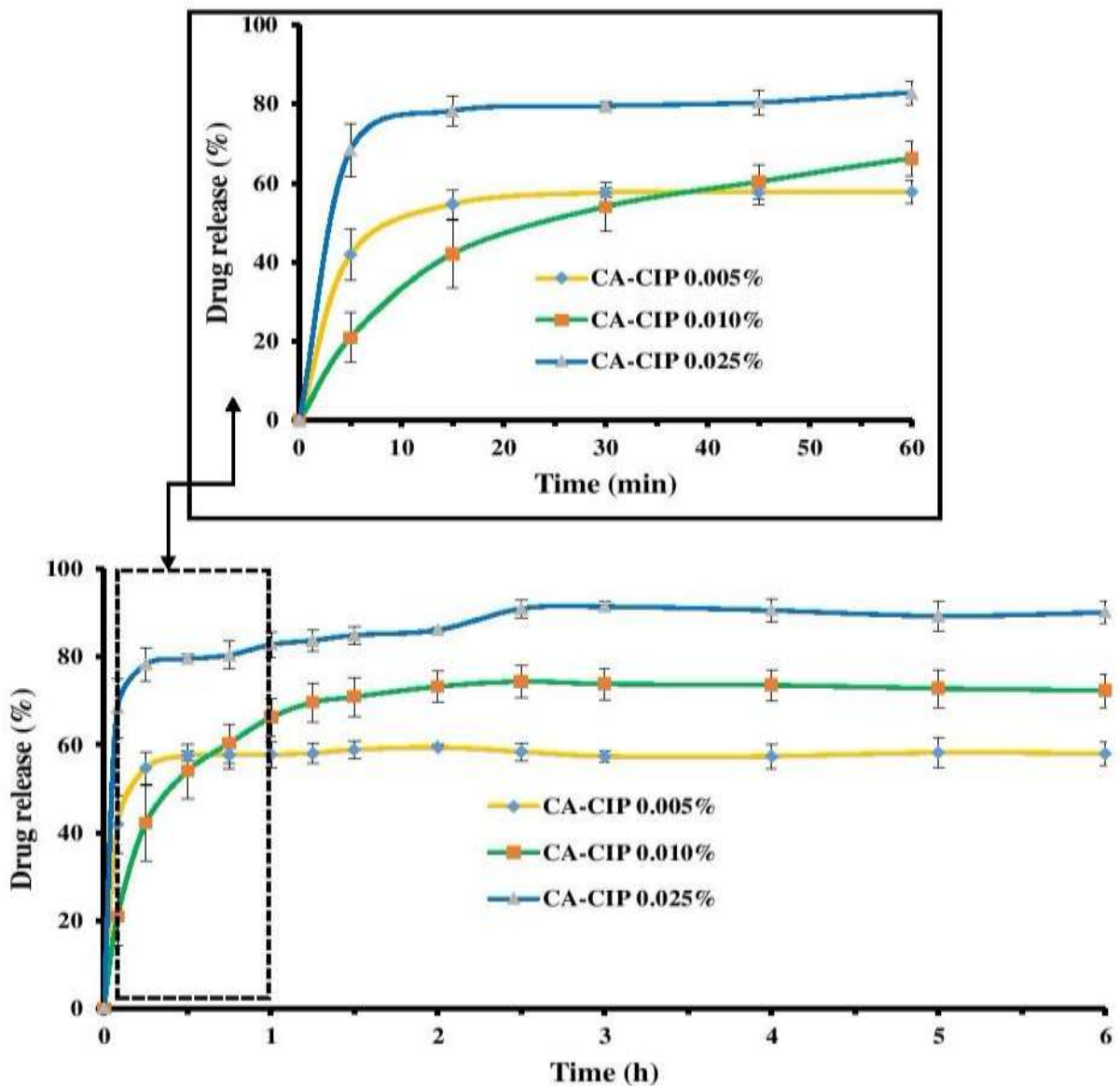
Figure 3.22 Cumulative percentage drug release profiles of optimized CIP loaded wafers ($n = 3 \pm SD$).

The dressings containing higher amounts of CIP appeared to release the drug more rapidly. This could be due to disturbance in pore distribution within the wafers at higher drug loading. The irregular pore size allows quick hydration and therefore faster rate of drug release (Ayensu *et al.*, 2012b). Though the initial fast release is over between 1 and 3 hours, the sustained amounts of CIP released from the dressings up to 6 h can prevent re-infection as well as the need for frequent dressing change. The rapid initial (5 min) release of drug (44.74 ± 2.56% − 48.27 ± 6.16%) was observed (**Figure 3.23**) in wafer containing 0.30 and 0.40% FLU. Wafers containing 0.05-0.15 % FLU showed cumulative drug release of about 21.05 ± 0.09% −26.69 ± 0.17 % within 5 min
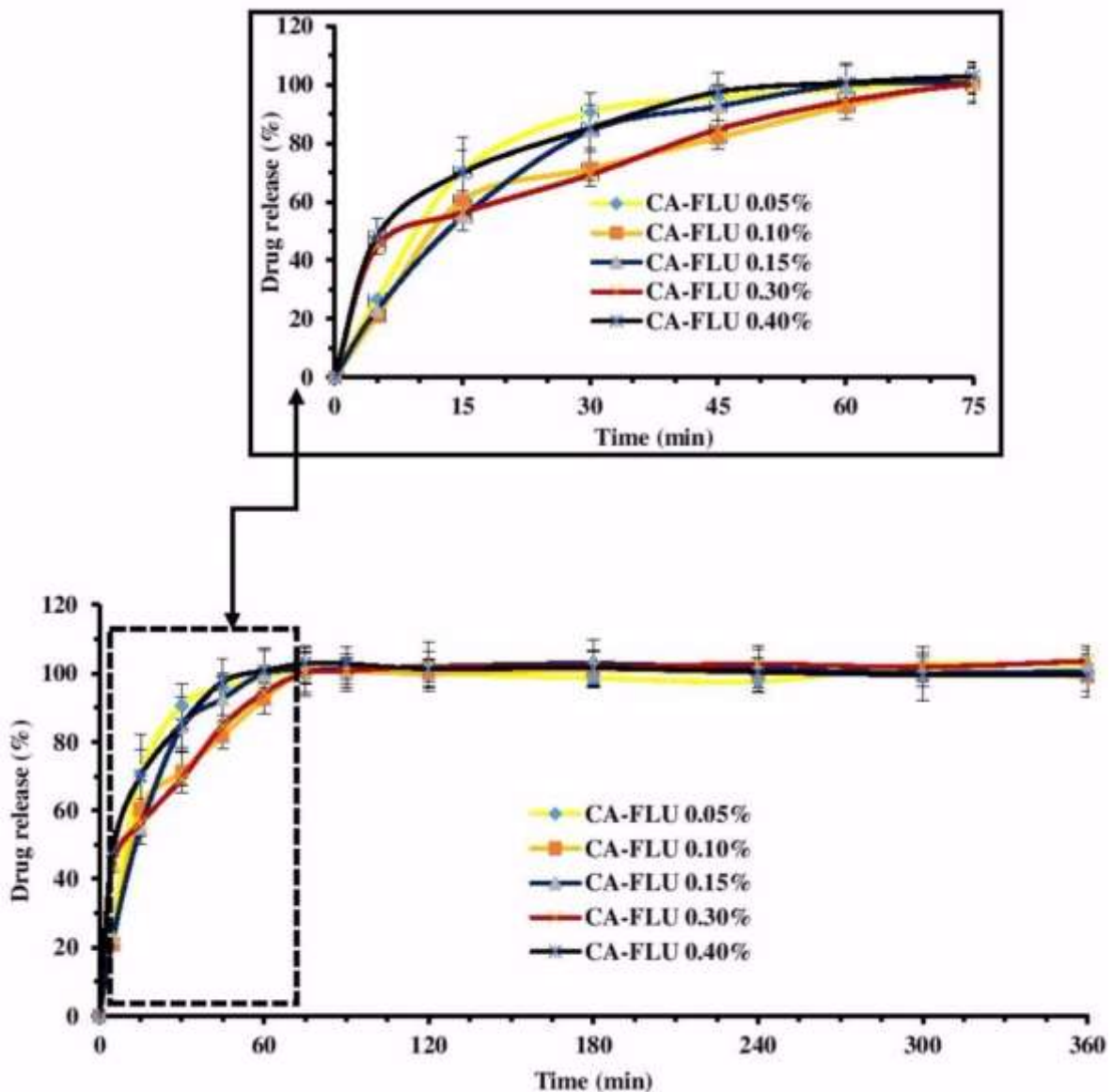
Figure 3.23 Percentage cumulative drug release profiles of FLU loaded wafers ($n = 3 \pm$ SD).

The rapid initial release could be attributed to the release of drug from pore surfaces of the dressings rather than to the drug incorporated in the wafer matrix. DCU test on the FLU loaded wafers also revealed that drug loading greater than 0.15% FLU did not show uniform distribution. More than 50% of the drug (FLU) was released within 15 min of hydration whilst 100% of the drug was released within 75 min. The rapid drug release was due to rapid hydration of wafers followed by increasing molecular mobility of polymer and the drug and therefore, it promoted easy diffusion of drug through the swollen polymeric matrix.
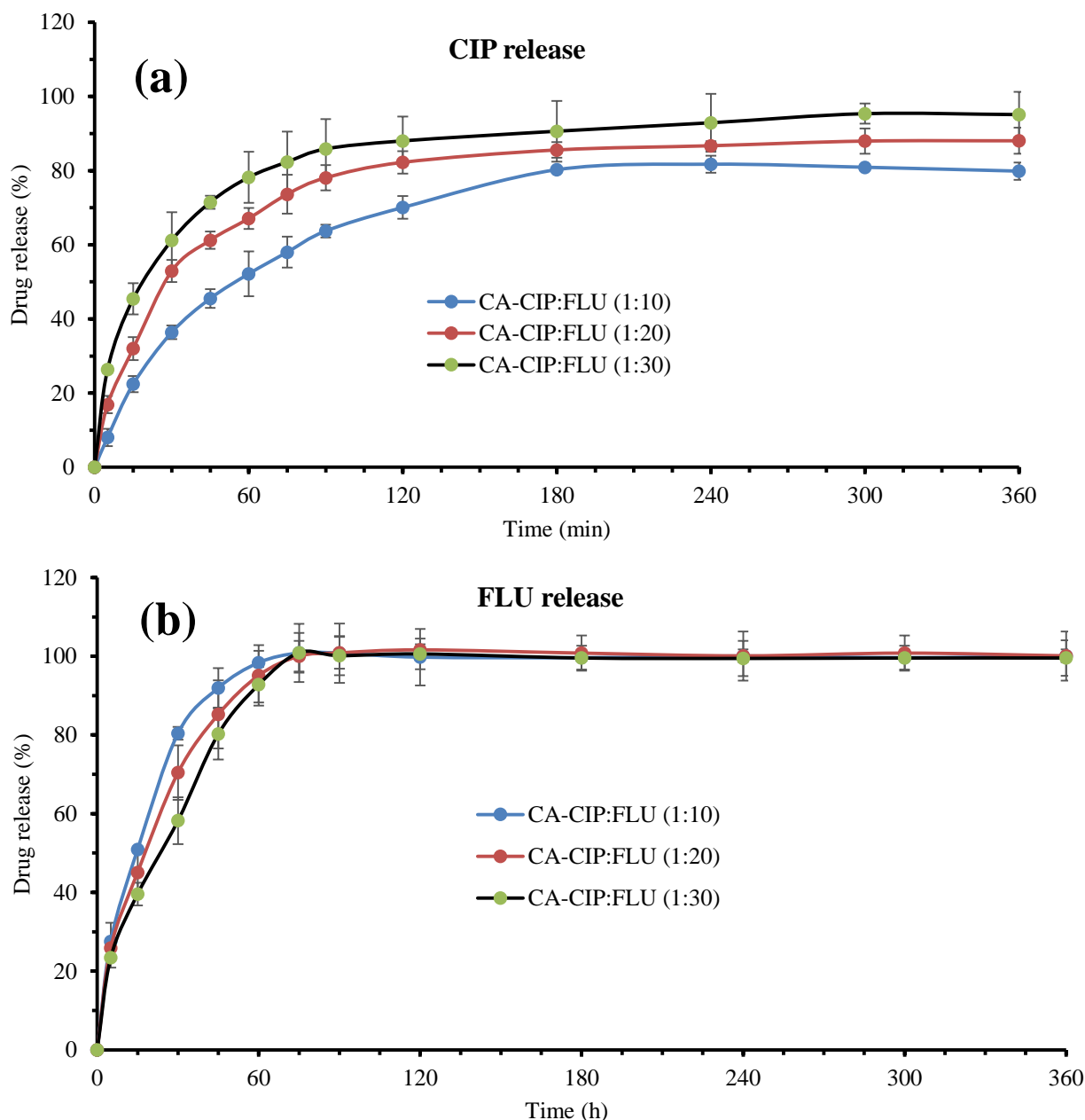
Figure 3.24 *In vitro* drug release profiles of (a) CIP and (b) FLU from wafers showing mean percentage cumulative release (mean ± SD, *n* = 3) against time in presence of SWF pH 7.5.

Figure 3.24 illustrates the release profiles of (a) CIP and (b) FLU from the lyophilized wafers. It can be observed that FLU was released faster than CIP from the wafer matrix. This could be due to difference in ionic properties of the drugs. FLU might have high affinity to the ions present in dissolution medium (SWF) that triggers leaching out of FLU molecules quickly from the swollen matrix. Moreover, it was previously reported that drugs having lower molecular weight diffused faster from microspheres than the drugs of higher molecular weight (Feng *et al*., 2015).

This could happen in this study, as FLU of lower molecular weight (306.28 g/mol) diffused faster than CIP of higher molecular weight (331.35 g/mol). It could probably due to its smaller molecular volume (205 cm) than CIP (226 cm) which promoted faster transport through the polymer phase and the small water filled pores. Furthermore, solubility of FLU into SWF could be another reason for its burst release. It is reported that FLU has higher solubility in phosphate buffer saline (PBS) (pH 7.4) than water (pH 7.0) (Sakharam *et al*., 2012). It is also reported that CIP has slow drug release due its much lower solubility at pH 7.4 in PBS (Bajgrowicz *et al*., 2015). The pH of SWF was similar to the pH of PBS. Therefore, FLU exhibited higher solubility in SWF than CIP, which resulted in rapid initial and maximum (100%) release (within 75 min). Moreover, a close observation of **Figure 3.24 b** revealed that the film containing lower amount of FLU had the higher initial release. It could be due to solubility of FLU in SWF with the lower amount of FLU dissolving quickly and resulting in faster diffusion through the swollen matrix.

However, CIP was released in a controlled manner from the combined DL wafers. Wafers containing CIP and FLU at the ratio of 1:10, 1:20 and 1:30 exhibited CIP total cumulative release of 81.73 ± 2.29%, 88.06 ± 3.52% and 95.36 ± 2.72% respectively (**Figure 3.24 a**). That means higher concentration of FLU resulted in higher CIP release. This also happened for combined DL films. The higher amount of FLU reduced the physical interaction of CIP with the polymer molecules, followed by increasing entanglement of the polymer chains, resulting in higher CIP release. This interesting fact could also depend on porosity of the polymeric matrix (Varma *et al*., 2004) as well as the solubility, ionic strength, and osmotic properties of the drugs (Patra *et al*., 2013; Wang *et al*., 2007). It can be seen (**Figure 3.2**) that higher amounts of FLU in combined DL wafers resulted in greater porosity, subsequently improved swelling and higher CIP release. In addition, the pore size of swollen matrix might exceed the size of CIP molecules in the presence of higher amount of FLU that enabled higher CIP release. Another factor could be the solubility of CIP in dissolution medium might be increased with increasing concentration of FLU into the wafer matrix that enhanced the CIP

release. In this case, pH dependent solubility of CIP occurring at higher pH led to better solubility (Roca *et al*., 2015), evident by observing surface pH of the DL wafers (**Chapter 8: Table A3.1**). Moreover, increase in drug content at a constant polymer content enhanced rate of drug release, which may be ascribed to the higher concentrations of drug leading to higher chemical gradient at the diffusion front, promoting drug escape to the outer environment (dissolution medium) efficiently (Varma *et al*., 2004).

3.4.9 Drug release kinetics

The formulated medicated films and wafers showed varied drug release profiles, evaluated by model dependant methods such as Higuchi, Korsmeyer-Peppas, zero order and first order (Boateng *et al*., 2009). All data obtained from those mathematical equations are summarised in **Table 3.4 & Table 3.5.** Amongst all the models, Korsmeyer-Peppas equation is considered as the best drug release kinetic model for swellable polymeric drug carriers formulated in cylindrical shapes (Lao *et al*., 2011). The slope (n) values from the Korsmeyer-Peppas equation also gives information about the mechanism of drug release. The n value less than or equal to 0.45 indicates Fickian diffusion, whereas n value greater than 0.45 but less than 0.89 represents anomalous (non-Fickian) transport. Further, n values of 0.89 and greater than 0.89 indicate case-II and super case-II transport respectively (Lao *et al*., 2011). It can be observed from **Table 3.4** that release of CIP from films followed first order release mechanism in which release rate depended on the concentration of drug. **Figure 3.19** also supports this kinetic mechanism of drug release where the highest amount of drug (0.025% w/v) loaded film released maximum drug within 45 min. The CIP release from wafers was the best fitted (R^2= 0.86-0.95) to Korsmeyer-Peppas mechanism compared to other equations (**Table 3.4**) as noted previously (Boateng *et al*., 2009, 2011; Momoh *et al*., 2015).

Table 3.4 Release parameters obtained by fitting experimental drug release data to different models for medicated films and wafers.

Film	Higuchi		Korsmeyer-Peppas			Zero order		First order	
	K_H	R^2	K_p	n	R^2	K_o	R^2	K_1	R^2
CA-CIP 0.005%	16.07	0.9933	2.67	0.54	0.9837	3.26	0.8301	0.06	0.9963
CA-CIP 0.010%	16.61	0.9829	2.57	0.58	0.9641	3.37	0.8279	0.07	0.9929
CA-CIP 0.025%	15.56	0.9897	2.46	0.59	0.9985	3.20	0.9215	0.07	0.9811
CA-FLU 0.05%	18.88	0.8026	3.94	0.16	0.8920	3.63	0.2543	0.06	0.7424
CA-FLU 0.10%	22.01	0.6565	4.43	0.04	0.9997	4.16	0.0126	0.10	0.7463
CA-FLU 0.20%	22.01	0.7687	4.20	0.12	0.9538	4.21	0.1925	0.21	0.9612
Wafer									
CA-CIP 0.005%	12.46	0.8390	3.45	0.19	0.9508	4.12	0.69	0.02	0.7062
CA-CIP 0.010%	10.12	0.9921	2.2	0.54	0.981	2.05	0.8248	0.02	0.9474
CA-CIP 0.025%	17.72	0.7055	4.11	0.08	0.86	2.01	0.4956	0.04	0.5887
CA-FLU 0.05%	16.57	0.9713	2.21	0.70	0.9620	3.39	0.8822	0.08	0.9981
CA-FLU 0.10%	13.42	0.9530	1.99	0.71	0.9294	2.74	0.8359	0.04	0.9360
CA-FLU 0.15%	14.51	0.9722	1.98	0.73	0.9965	3.01	0.9529	0.06	0.9940
CA-FLU 0.30%	13.94	0.9116	3.40	0.24	0.9897	2.73	0.4985	0.03	0.8609
CA-FLU 0.40%	16.92	0.9554	3.37	0.32	0.9979	3.35	0.6094	0.06	0.9576

Therefore, drug released through the polymeric matrix is either by Fickian or non-Fickian diffusion, which is the combination of both diffusion and erosion-controlled release. For a better understanding of drug release mechanism, the diffusion exponent (n) values were calculated as 0.54-0.59 and 0.08-0.54 for CIP in the films and wafers respectively. This suggested CIP was

released from the films by non-Fickian diffusion. Wafers containing 0.005 and 0.025 % CIP showed drug release by Fickian diffusion as their n values were less than 0.45.

Table 3.5   Release parameters obtained by fitting experimental drug release data to different models for films and wafers containing CIP and FLU.

	Higuchi		Korsmeyer-Peppas			Zero order		First order	
	K_H	R^2	K_p	n	R^2	K_o	R^2	K_1	R^2
CIP									
CA-CIP:FLU (1:10) Film	12.61	0.7961	3.58	0.15	0.9487	2.42	0.2421	0.02	0.6548
CA-CIP:FLU (1:20) Film	15.37	0.8920	3.52	0.24	0.9814	2.99	0.4410	0.04	0.8301
CA-CIP:FLU (1:10) Wafer	6.09	0.9465	0.74	0.85	0.9945	1.28	0.9777	0.02	0.9957
CA-CIP:FLU (1:20) Wafer	9.04	0.9791	1.79	0.63	0.9962	1.87	0.9455	0.02	0.9932
CA-CIP:FLU (1:30) Wafer	11.40	0.9981	2.52	0.47	0.9986	2.30	0.8071	0.03	0.9621
FLU									
CA-CIP:FLU (1:10) Film	17.49	0.6285	4.25	0.03	0.9982	3.29	-0.03	0.04	0.4816
CA-CIP:FLU (1:20) Film	14.15	0.6831	3.93	0.07	0.8727	2.68	0.0481	0.03	0.5235
CA-CIP:FLU (1:10) Wafer	13.98	0.9888	2.35	0.59	0.9980	2.88	0.9237	0.05	0.9921
CA-CIP:FLU (1:20) Wafer	12.36	0.9931	2.35	0.55	0.9955	2.54	0.9039	0.04	0.9921
CA-CIP:FLU (1:30) Wafer	10.49	0.9991	2.33	0.51	0.9983	2.14	0.8624	0.03	0.9776

The wafer containing 0.010% CIP showed non- Fickian diffusion (anomalous transport). The anomalous transport suggested that the diffusion of CIP through the hydrated polymer combined gel erosion and controlled diffusion of the drug.

The release data of FLU from the films and wafers showed best fit to Korsmeyer-Peppas model based on the coefficient of linear correlation (R^2). All FLU loaded films exhibited drug release by Fickian diffusion as their exponent n values were calculated to be 0.04-0.16. However, wafers containing 0.05-0.15% FLU showed drug release by non-Fickian diffusion (n value, 0.70-0.73). That indicates controlled release of FLU by diffusion due to uniform porosity confirmed by SEM. The n values for the wafers containing 0.30 and 0.40% FLU were calculated as 0.24 and 0.32 respectively, suggesting the release mechanism to be Fickian diffusion.

In the case of combined DL films, the release of both CIP and FLU followed Korsmeyer-Peppas model (**Table 3.5**). The n values ranged from 0.03−0.24 for all combined DL films indicating that the release of CIP and FLU from the polymeric films followed the Fickian diffusion. That means drugs released that were diffusion controlled as in the Higuchi model. Therefore, the both drugs were dispersed uniformly (also confirmed by **Figure 3.21**) throughout the non-degradable matrix. The best fit model for the combined DL wafers was also Korsmeyer-Peppas model. The n values (0.85−0.47) of the Korsmeyer-Peppas model suggested that the mechanism of diffusion of both CIP and FLU was non-Fickian. It indicates that both diffusion of CIP and FLU through the hydrated polymer combined with gel erosion control the release of the drugs.

3.5 Conclusions

Lyophilized wafers were highly porous in nature resulting in higher swelling capacity than films. DL wafers also showed higher water uptake (1085-2377 %) and holding capacity (EWC, 91−95 %) than the DL films. Therefore it indicates, the wafer dressings will absorb more exudates from DFUs. However, films showed higher WVTR (maximum 3876.53 ± 195.50 g/m^2day^{-1}) than wafers (maximum 3499.23 ± 71.76). This indicates films have the higher ability to absorb fluid and draw it out from the wound bed across the materials into the atmosphere than wafers. Combined DL (CIP and FLU) wafers exhibited ideal WVTR values which will be able to maintain moist wound environment. The EWL study of films and wafers reflected optimal conditions for maintaining moist environment, which is necessary for wound healing. In addition, the lower residual moisture content in the DL films (8−12 %) than DL wafers (9−17 %) will ensure higher stability upon storage and less chance of drug precipitation.

The films showed initial burst drug release whilst wafers exhibited controlled release over sustained period which will be expected inhibit microbial growth rapidly as well as prevent reinfection due to sustained drug release, especially in the wafers. The DL loaded wafers showed better functional properties than DL films in terms of fluid handling properties and drug loading capacity. Therefore, the wafers can be used as a primary dressing and films as a secondary dressing in DFUs. Moreover, the formulated wafers performed better than the Algisite Ag® and Actiformcool® in terms of all fluid handling characteristics. Films also showed better WVTR than Actiformcool®. Based on the obtained results, the formulated DL wafers will be potentially a better dressing than the tested commercial products for healing of chronic DFUs.

CHAPTER 4:   ANTIMICROBIAL PROPERTIES OF DRUG LOADED CALCIUM ALGINATE DRESSINGS TARGETTING BACTERIAL, FUNGAL AND MIXED INFECTIONS IN CHRONIC DIABETIC FOOT ULCERS

4.1   Introduction

Chronic infection is one of the major risk factors in impaired healing of diabetic foot ulcers (DFUs). Such chronic infections are the most common precursors to diabetic related amputation and 85% of lower-limb amputations is preceded by infected foot ulcerations (Nithyalakshmi *et al*., 2014; Chellan *et al*., 2012; Dowd *et al*., 2008). Around 7400 legs, toes or feet are amputated each year in England alone (Diabetes UK, 2016). Several microbial flora such as bacteria, fungi, yeast and virus are associated with infected DFUs (Peters *et al*., 2012). Therefore, it is very important to understand the ecology of such infections, how to control these and ultimately eliminate them completely. Several interdisciplinary fields such as microbiology, polymer chemistry, and molecular biology are required to understand the pathophysiology and diversity of microorganisms, interaction between the microorganisms and interaction of microorganisms with the polymer dressings for developing effective antimicrobial dressings.

Several clinical studies have reported that the most predominant bacterial species in DFUs are *Staphylococcus aureus* (*S. aureus*), *Pseudomonas aeruginosa* (*P. aeruginosa*) *and Escherichia coli* (*E. coli*) (Kavitha *et al*., 2014; Abdulrazak *et al*., 2005; Tiwari *et al*., 2012; Shanmugam and Susan, 2013). A clinical study reported that *S. aureus* and *P. aeruginosa* were isolated from diabetic foot infections in about 38.4% and 17.5% of cases respectively (Abdulrazak *et al*., 2005), whilst isolates of *E. coli* were in about 14.6% of cases (Shanmugam and Susan, 2013). In another study, 84 of patients with infected DFUs were investigated and it was found that the prevalence of *S. aureus* was the most common in diabetic foot ulcers (DFUs) and about 50% of these isolates were methicillin-resistant (Chita *et al*., 2013). Furthermore, most other studies have also suggested that *S. aureus* is most prevalent isolates in DFUs (Mendes *et al*., 2012; Mauriello *et al*., 2014; Sarheed *et al*., 2016).

Fungal infections have been reported in patients with DFUs and the most predominant fungi in DFUs is *Candida albicans* (*C. albicans*) (Abilash *et al*., 2015; Nair *et al*., 2006; Varsha *et al*., 2016; Nithyalakshmi *et al*., 2014). Abilash and colleagues reported that amongst 100 patients with DFUs, 18 patients were fungal infected and *C. albicans* strains were isolated from

16 of these fungal infected patients (Abilash *et al*., 2015). Another study reported that *C. albicans* (49%) was the most common among the *Candida* species, followed by *C. tropicalis* (23%), *C. parapsilosis* (18%), *C. guillermondi* (5%) and *C. krusei* (5%) (Nair *et al*., 2006). However, opportunistic fungal infections are often ignored due to lack of clinical studies. Fungal infection is hard to diagnose because the loss of sensation in diabetic foot often make patients unconscious about anyfungal growth and consequently leads to fatal complications such as foot amputation. Moreover, hyperglycaemia and suppressed immunity in diabetes are very prone to fungal infections. Hyperglycaemia hinders granulocyte formation in the host and hence, enhancing the growth of various fungi species, especially *Candida* spp (Heald *et al*., 2001). This can become a serious cause of morbidity or mortality in diabetic patients (Clayton and Elasy, 2009).

Mixed bacterial-fungal infections are more complicated than single microbe infections with enhanced severity of DFUs. The risk of amputations and mortality may increase significantly with the onset of mixed bacterial and fungal infections (Morales and Hogan, 2010). A study reported that amongst 160 patients with DFUs, mixed infection caused by *S. aureus* and *C. albicans* was identified in about 20% of the patients followed by the mixed infection of *P. aeruginosa* and *C. albicans* (10%). The interactions between the bacteria and fungi in wounds is still ambiguous, but such interactions may influence the growth and pathophysiology of the organisms. It has been reported that bacteria may accelerate fungal growth and vice versa (Peleg *et al*., 2010). Bacteria may also reduce fungal growth by releasing bacterial toxins that directly act on the fungal cell wall or by nutrient depletion (Peleg *et al*., 2010). Moreover, presence of bacteria with fungi may alter the environment in terms of temperature and pH, which can hinder hyphae formation in fungi (Fitzsimmons and Berry, 1994; Buffo *et al*., 1984). It is reported that *E. coli* and *P. aeruginosa* can suppress *C. albicans* growth in oral infections (Thein *et al*., 2006). In some cases, *E. coli* and *C. albicans* have mutual modulatory effects (Bandara *et al*., 2009). Moreover, antagonistic relationship between *P. aeruginosa* and *C. albicans* has been documented where *C. albicans* inhibit the growth of *P. aeruginosa* by secreting proteins (Medina *et al*., 2015). The mixed infection of *S. aureus* and *C. albicans* may enhance disease chronicity in various way (Peters and Noverra, 2013). In this type of mixed infection, *Candida* activity initially compromise the tissue and cell walls, which facilitate the penetration of *S. aureus* into internal tissues. S. aureus secretes protease in the presence of *C. albicans*, which gives synergistic effect of yeast growth (El-Azizi *et al*., 2004; Carlson, 1983). Untreated mixed infections in DFUs may lead to complex biofilm formation,

which is associated with polymicrobial infections (Fourie *et al*., 2016). Several studies reported biofilm formation between *C. albicans* and *E. coli*, *C. albicans* and *P. aeruginosa*, and, *C. albicans* and *S. aureus* (Bandara *et al*., 2009; Mear *et al*., 2013; Fourie *et al*., 2016; Kean *et al*., 2017; Nair *et al*., 2014; Harriott and Noverr, 2009).

Ciprofloxacin (CIP) and fluconazole (FLU) are broad spectrum antimicrobial drugs. CIP and FLU have been reported as the prescribed treatment of DFUs due to their low minimum inhibitory concentrations (MIC) against causative microorganisms present in diabetic ulcers (Leese *et al*., 2009; Sanniyasi *et al*., 2015). To prevent and control diabetic foot infection, orally administered antibiotics are currently being administered to hospitalized patients. It is reported that 500-750 mg CIP is given twice a day for bacterial infection and 150 mg FLU is given daily for fungal infection (Leese *et al*., 2009; Sanniyasi *et al*., 2015). However, the systemic administration of antibiotics requires high dose to achieve adequate blood serum concentration and associated with several side effects (Sarheed *et al*., 2016). In case of DFU, the systemic administration of antibiotics is sometimes ineffective due to poor blood circulation in the foot region. Therefore, it is advantageous to deliver therapeutically relevant doses of broad-spectrum antibiotics (CIP) directly to the wound site of infected DFUs. Dressings impregnated with antimicrobial agents have become one of the best choices of wound management. The ideal dressings should prevent infection in chronic wounds, as wound infection is a major risk factor for impaired healing of chronic wounds such as DFUs. Polymeric films and lyophilized wafers are also reported as a potential means of delivering antimicrobials to wound surface to aid healing (Okoye and Okolie, 2015; Pawar *et al*., 2014).

This chapter reports on the antibacterial and antifungal characteristics of CIP and FLU loaded dressings. The investigations initially determined the MIC and minimum bactericidal/fungicidal concentration (MBC/MFC) of CIP and FLU respectively. The dressings containing single drug (CIP or FLU) and combined drug (CIP and FLU together) were evaluated by turbidimetric and disk diffusion methods for antibacterial, antifungal and mixed infections performance. The rate of killing microorganisms were evaluated by time-kill assay. Along with the formulated dressings, two commercial antimicrobial dressings Algisite Ag[®] (Smith & Nephew, UK) and Actiformcool[®] (Activa Healthcare, UK) as representative standard samples were also tested for antimicrobial activity.

4.2   Materials

Calcium alginate (mannurronic acid:guluronic (59:41), molecular weight: 398.32 g/mol) [CA, (lot number: BCBM8132V)], ciprofloxacin (lot number: LRAA6508), Fluconazole (lot number: LRAA6502), Mueller hinton broth [MH, (lot number: BCBR1543V)], Brain heart infusion broth [BHI, (lot number: BCBS2394V)], Sabouraud dextrose broth (lot number: 1337899), were purchased from Sigma-Aldrich (Gillingham, UK). Luria Bertani Broth (batch number: G25418), Streptomycin [STP, (batch number: BP910-50)], Agar [agar no. 3, technical, (lot number: 1334018)], sodium chloride (lot number: 1560652), potassium chloride, sodium carbonate (lot number: 1546575), hydrochloric acid [HCl, (lot number: 1480980)], ethanol (batch number: 0933421) and were ordered from Fisher Scientific (Loughborough, UK). Calcium chloride (lot number: S42528-427) was obtained from Riedel-de-Haen, Germany. Amphotericin B (Amp B), a European pharmacopoeia reference standard obtained from EDQM, council of Europe. *Escherichia coli* (ATCC 25922), *Staphylococcus aureus* (ATCC 29213), *Pseudomonas aeruginosa* (ATCC 27853) and *Candida albicans* (ATCC 90028) were obtained from the microbiology lab of University of Greenwich, UK.

4.3   Methods

4.3.1   Preparation and storage of tested organisms

Bacterial cultures were freshly prepared by tranferring a single bead unit to 10 ml of Muller-Hinton (MH) broth and incubating at 37 ℃ for 24 h. A loop of bacterial cultures was inoculated onto a MH agar plate and incubated at 37 ℃ for 24 h to yield separate colonies. For fungal culture, a single bead unit was transferred to 10 ml of Sabouraud dextrose (SB) broth and incubated overnight at 30 ℃ . After overnight incubation, a loop of fungal culture was inoculated onto a SB agar plate and incubated at 30 ℃ for 48h to obtain separate colonies. The plates of bacterial and fungal culture were stored at 4 ℃ in a refrigerator and the microbial strains were sub-cultured in the specific agar plates weekly using a representative single colony.

4.3.2   Preparations of inocula

Bacterial inocula were prepared by inoculating 3 − 4 separate colonies of the tested organisms in 3 ml of MH growth medium. After overnight incubation at 37 ℃, the turbidity of the bacterial suspension was adjusted to a 0.5 McFarland standard (~10^8 CFU/ml) with the medium. The suspensions were further diluted (1: 100 dilutions) in medium to obtain 10^6

CFU/ml, representing a high microbial load in infected DFUs (Anisha *et al*., 2013; Unnithan *et al*., 2012).

Inoculum of *C. albicans* was prepared from 48 h fresh culture grown on SB agar at 30 ℃. A single colony from the cultured SB agar plate was introduced in 5 ml of SB broth medium and incubated in a shaking incubator at 30 ℃. After overnight incubation, the number of cells was counted by a hamocytometer. Afterwards, the inculum was adjusted to a working concentration of 10^6 CFU/ml. The fungal suspension was further diluted in SB broth medium to obtain a final inoculum concentration of 10^5 CFU/ml representing a chronic fungal infection in DFUs. Though no data has been found about the fungal load in DFUs, a study reported 10^5 cells/ml concentration of *C. albicans* for biofilm formation (Wibawa *et al*., 2015) and was used to represent chronic DFU for purposes of this study.

4.3.3 Determining minimum inhibitory concentration (MIC) and minimum bactericidal/fungicidal concentration (MBC/MFC) by broth dilution method

MIC and MBC of pure CIP were determined in MH broth by broth dilution method. MIC is defined as the lowest concentration of antimicrobial that will inhibit the visible growth of a microorganism after 24 h incubation whereas; MBC is defined as the lowest concentration of antimicrobial that will inhibit the growth of a microorganism by about 99.9% in CFU/ml when compared with the control (Andrews, 2001; Sgariglia *et al*., 2006).

Serial dilutions ranging from 0.001 to 128 µg/ml of CIP were prepared in sterile nutrient broth (MH broth) and inoculated with a final concentration of 10^6 CFU/ml bacteria (either *E. coli, S. aureus and P. aeruginosa*) in triplicate. Following 24 h of treatment, samples from each treatment and appropriate dilutions were plated in MH agar plates. Colony forming units (CFUs) were then counted after a further 24 h of incubation at 37 ℃ and used to determine MBC. The number of viable cells was plotted against antibiotic concentration. The number of cells was calculated by **Equation 4.1**:

Number of cell (CFU/ml) = (colonies counted x dilution factor)/ volume plated   (4.1)

Furthermore, MIC of pure FLU against *C. albicans* was also determined by broth dilution method in SB broth. The antifungal agent FLU was dissolved in ethanol at a final concentration of 1 mg/ml. Eleven 2-fold serial dilutions were prepared in SB broth medium, with final drug

concentrations ranging from 0.06 to 64 µg/ml of FLU. Each concentration was tested in triplicate for the inoculum of 10^5 CFU/ml *C. albicans*. One of the tubes containing only fungal suspension without drug was used as a growth control. The tubes were incubated in a shaking incubator at 30 ºC for 24 h. After the incubation period, the tubes were observed visually to see the visible inhibition of the growth in order to determine MIC of FLU. Afterwards, to determine MFC, 100 µl of the treated fungal suspension was transferred from all clear tubes onto SB agar plates. The plates were then incubated at 30 ºC for 24 h. After 24 h, CFUs were counted and the number of viable cells was calculated by **Equation 4.1**. The MFC was considered as the lowest drug concentration that kill ≥ 99.9% of fungal cells (De Aquino Lemos *et al*., 2009).

Antimicrobial activity of DL films (6 mm diameter), wafers (15 mm diameter) and two commercial dressings (Algisite Ag® and Actiformcool®) was evaluated against *E. coli, S. aureus, P. aeruginosa* and *C. albicans* by turbidimetric and Kirby-Bauer disc diffusion methods as described below.

4.3.4   Turbidimetric method

In this method, 10 ml of prepared bacterial (*E. coli*, *S. aureus* and *P. aeruginosa*) suspension (10^6 CFU/ml) was transferred to sterile test tubes each containing dressings with different amounts of CIP. The tubes containing only bacteria and pure CIP were used as negative and positive controls respectively. The tubes were incubated at 37 ºC, 180 rpm and aliquots taken at 1.5, 3, 6, 12 and 24 h and absorbance recorded at 625 nm. In addition, 0.1 ml aliquots were plated directly or after serial dilution to count the number of viable bacterial colonies with only plates having 30 to 300 colonies accepted for determining number of colony forming units/ml (Ong *et al*., 2008). The experiment was carried out in triplicate ($n = 3$) against each organism (*E. coli, S. aureus and P. aeruginosa*).

FLU loaded dressings were evaluated by turbidimetric assay in which 10 ml of fungal suspension (10^5 CFU/ml) was transferred to test tubes containing dressings with different amounts of FLU. The tube containing only *C. albicans* and pure FLU were considered as negative and positive controls respectively. The tubes were placed on a shaker (180 rpm) and incubated at 30 ºC. After incubation absorbance recorded at 405 nm at predetermined time points (1.5, 3, 6, 12, 24, 48 and 72 h), At the same time 0.1 ml aliquots were removed from each test suspension, serially diluted in Ringer's solution (0.72% sodium chloride, 0.017% calcium chloride and 0.037% potassium chloride) and plated on SB agar plate (0.1 ml) for

colony counting to determine time-kill curve. All time-kill curve assays were conducted in triplicate and average colony counts ($\log_{10}$ CFU/ml) versus time was constructed.

Mixed infection (bacteria and fungi together) study of combined DL (CIP and FLU) dressings was carried out by turbidimetric assay. In this study, *C. albicans* was cultured with either *E. coli* (*i.e. C. albicans* + *E. coli*), or *P. aeruginosa* (i.e. *C. albicans* + *P. aeruginosa*) or *S. aureus* (i.e. *C. albicans* + *S. aureus*) in BHI broth medium at 37 ℃ to represent mixed infections. BHI broth was chosen as a culture medium for mixed infection study because both fungi and bacteria can grow in this medium. Combined DL dressings were placed into 10 ml BHI broth containing both bacteria (10^6 CFU/ml) and fungi (10^5 CFU/ml). Control tubes contained either *C. albicans* alone, bacteria alone or medium alone. The absorbance was taken by a micro-plate reader at 540 nm at different time intervals (3, 6, 24, 48, and 72 h). CFU assay was also performed in which 0.1 ml aliquots were taken, serially diluted with Ringer's solution and plated on Luria Bertani (LB) agar supplemented with Amp B and on SB agar supplemented with streptomycin (STP). LB agar was supplemented with amphotericin B (Amp B) at the concentration of 25 µg/ml to prevent non-targeted fungal growth and SB agar was supplemented with STP at the concentration of 40 µg/ml to prevent non-targeted bacterial growth. These concentrations of the antimicrobials (Amp B and STP) were tested to evaluate the efficacy of preventing growth of the non-targeted organisms. The SB and LB agar plates were incubated at 30 ℃ and 37 ℃ respectively. The bacterial and fungal cells were counted after 24 h of incubation.

Mixed infection study of Actiformcool® was also carried out by turbidimetric assay and the data was compared to the formulated combined DL dressings. Actiformcool® was chosen in this study, because it has been reported to have both antibacterial and fungal activity (Moore K, 2006). However, it was not possible to undertake turbidimetric assay on Algisite Ag® due to its heavy colour change in liquid broth medium.

4.3.5 Kirby-Bauer disk diffusion method

MH agar plates were prepared according to the reported protocol (Hudzicki, 2009), where MH agar was autoclaved at 121 ℃ for 45 min, cooled to room temperature before pouring into Petri dishes. 25 ml of MH agar solution was poured into each Petri dish to obtain a 5 mm layer of solid agar slant. A sterile swab was immersed into the tube containing bacterial suspension (10^6 CFU/ml) and streaked on the surface of the entire MH agar plate three times with clockwise rotation. The circular dressings (diameter of 6 mm for films, and 15 mm for

wafers and Algisite Ag® respectively) were placed in the centre of colonised agar plates and incubated at 37 ºC for 24 h, after which zone of inhibition (ZOI) in mm were measured using a Vernier calliper. In this study, a filter disk (6 mm) containing 5 µg of pure CIP and CA-BLK were used as a positive control and negative controls respectively.

In the case of antifungal study, a sterile swab was immersed into the tube containing fungal suspension (10^5 CFU/ml) and streaked over the SB agar plates to obtain uniform growth. The FLU loaded dressings were placed onto inoculated media plates and a6 mm filter disk containing 25 µg pure FLU was used as a positive control and placed on inoculated SB agar plates. The plates were incubated at 30 ºC for 24 h and the ZOI was determined using a Vernier calliper.

Mixed infections were formed by taking 0.1 ml of bacterial suspension (10^8 CFU/ml) and 1 ml of fungal suspension (10^6 CFU/ml) from the prepared inocula (**Section 4.3.2**) and mixed in 8.9 ml of BHI broth. This resulted in final organism concentrations of 10^6 CFU/ml for bacteria (*E. coli*, *P. aeruginosa* and *S. aureus*) and 10^5 CFU/ml for *C. albicans*. Afterwards, the mixed suspensions were streaked onto the BHI agar plates with the help of a sterile swab. The combined DL dressings were placed onto the mixed colonized agar surface and incubated at 37 ºC for 24 h. The colonized plates without sample was used as a control. The growth inhibition zones were measured using a Vernier calliper. Three samples and three repeats each were tested in parallel for each experiment aseptically. The images of ZOI were taken as supplementary information. ZOI assay of Actiformcool® was not performed because it was very difficult to place on the agar plate due to its highly sticky nature.

4.3.6 Statistical analysis

The statistical differences between treated and control groups and the statistical differences between two experimental groups were evaluated by Student *t-test* and *ANOVA test.* Data with a *p* value of 0.05 was considered significant.

4.4   Results and discussion

4.4.1 Minimum inhibitory concentration (MIC) and minimum bactericidal/fungicidal concentration (MBC/MFC) of pure drugs

The MIC for CIP is reported in the literature for *E. coli*, *S. aureus* and *P. aeruginosa* as 0.015 µg/ml, 0.5 µg/ml and 0.25 µg/ml respectively (Andrews, 2001). In this study, the MIC of CIP was evaluated for the known microbial load of 10^6 CFU/ml for all three bacteria. From **Figure 4.1 (A-C),** the cloudiness of bacterial suspension became clear from the tubes containing 0.06, 0.5 and 0.125 µg/ml drug representing MIC of CIP for *E. coli*, *S. aureus* and *P.   aeruginosa*   respectively.
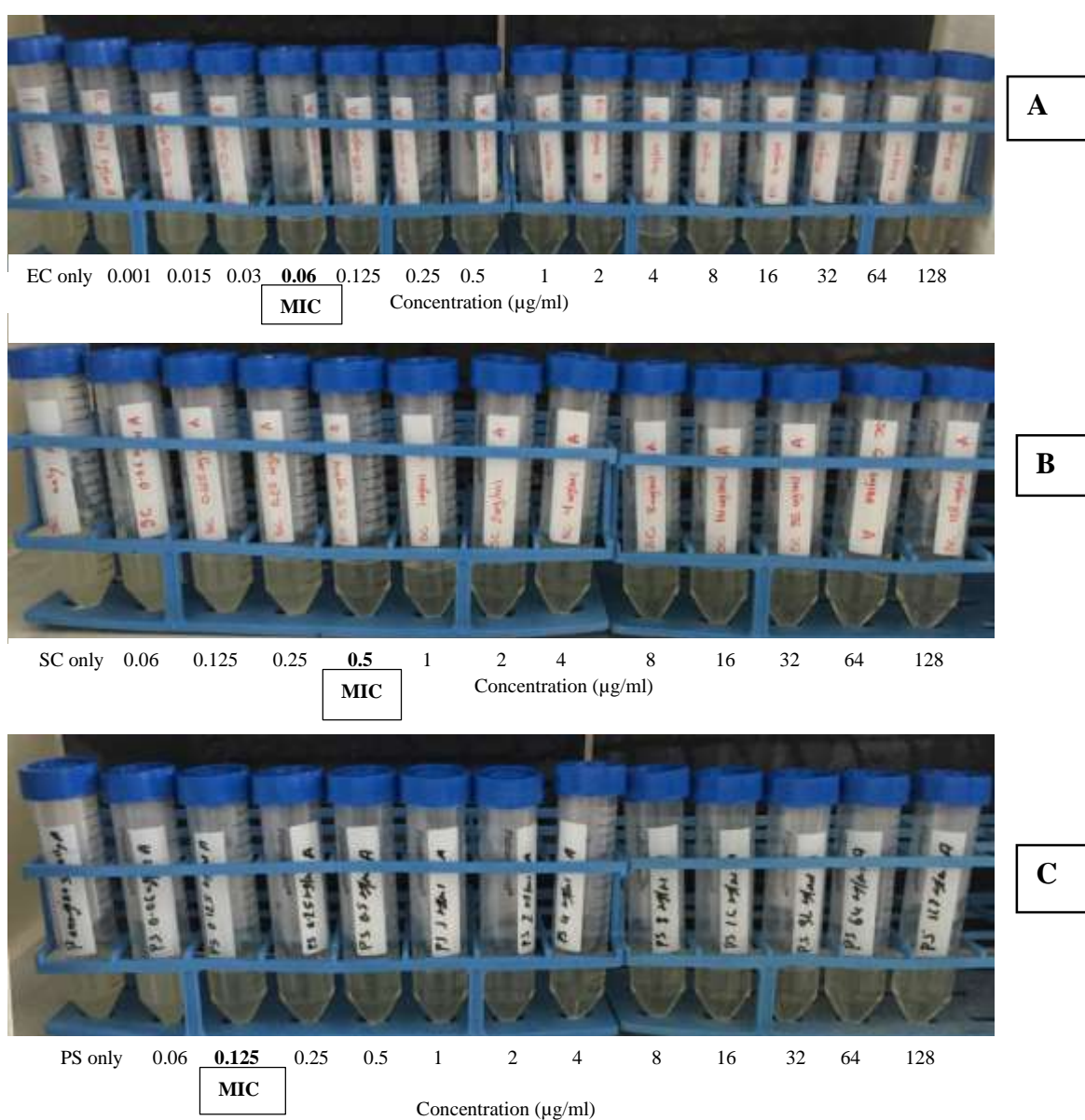
Figure 4.1   MIC determination of pure CIP by broth dilution assay *E. coli* (A), *S. aureus* (B) and *P. aeruginosa* (C). The photographs were captured after 24 h incubation at 37 °C.

Furthermore, the MBC of pure CIP was determined by counting the number of viable cells after 24 h treatment. The number of cells decreased to 10^3 CFU/ml (99.9% inhibition) at concentration of 0.25, 0.5 and 4.0 µg/ml CIP for *E. coli*, *P. aeruginosa* and *S. aureus* respectively (**Figure 4.2**). Moreover, the complete eradication of *E. coli*, *P. aeruginosa* and *S. aureus* was observed at the concentration of 4, 1 and 32 µg/ml CIP.
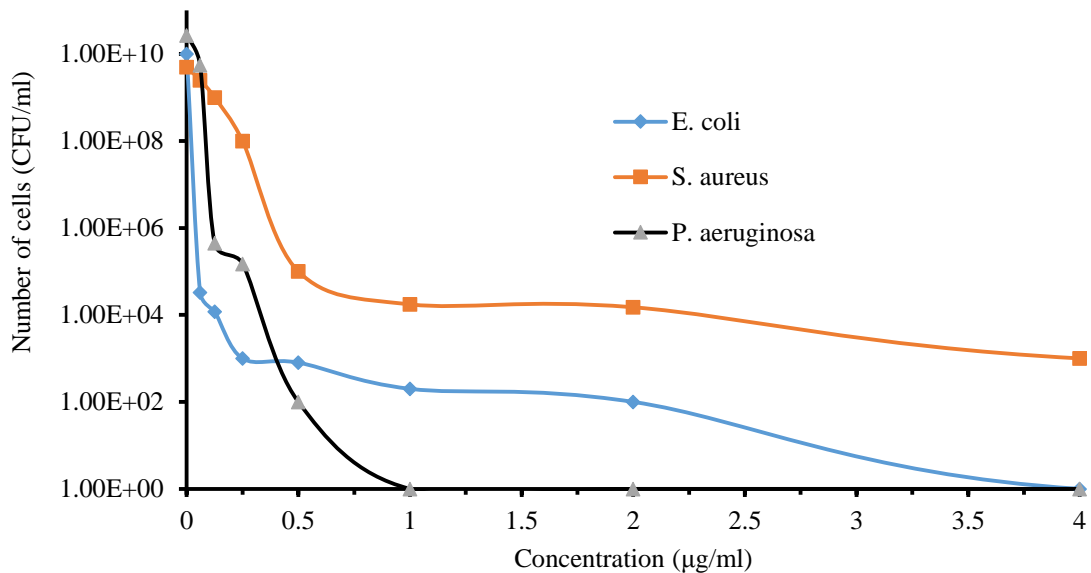
Figure 4.2 Killing curve for *E. coli, S. aureus* and *P. aeruginosa* at different concentration of CIP to determine MBC (99.9% cell reduction).

The MIC of FLU against *C. albicans* was reported between 0.25−0.5 µg/ml with initial inoculum of 10^3 CFU/ml (Kaya *et al*., 2012; Fothergill, 2012; Girmenia *et al*., 2000). It can be seen from **Figure 4.3**, the MIC value of FLU was determined as 2 µg/ml for *C. albicans* when tested with the initial inoculum of 10^5 CFU/ml.
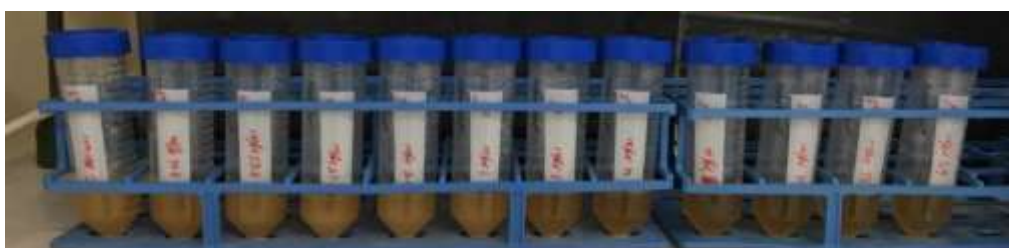
C. albicans	0.06	0.125	0.25	0.5	1	**2**	4	8	16	32	64
						MIC					

Concentration (µg/ml)

Figure 4.3   MIC determination of pure FLU *C. albicans* by broth dilution assay. The photographs were captured after 24 h incubation at 30 ºC.

The MFC range (2-512 µg/ml) of FLU was further evaluated to determine the MFC value. It was found that FLU killed 99.9% cells (1 x 10^4 CFU/ml) at a concentration of 128 µg/ml while comparing with the control (drug free culture) (2 x 10^8 CFU/ml) (**Figure 4.4**). The comparative analysis of MIC and MFC indicated that MFC of FLU was six times greater than MIC for *C. albicans*. In this study, the MFC value of FLU was comparatively higher than a previously reported study (De Aquino Lemos *et al.*, 2009) due to higher initial inoculum cell concentration (10^5 CFU/ml) employed in the current study.
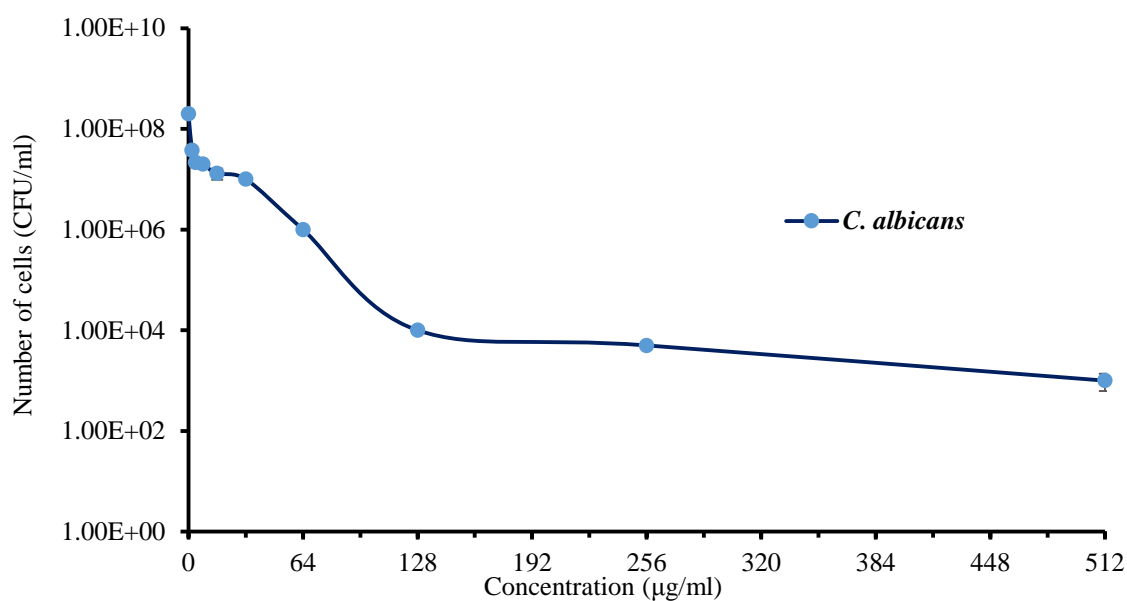
Figure 4.4 Killing curve for *C. albicans* at different concentration of FLU to determine MFC (99.9% cell reduction) ($n = 3 \pm$ SD).

4.4.2 Antibacterial activity of CIP loaded dressings

Antibacterial activity of CIP loaded dressings and Algisite Ag® were assayed by turbidimetric and Kirby-Bauer disk diffusion method. In turbidity assay, optical densities (OD) of the samples were measured at 625 nm at different time intervals and the turbidity was also analyzed visually as shown in **Figure 4.5 & Figure 4.6**. The clear solutions of bacterial suspension confirmed the effectiveness of the released antibiotic in eradicating the bacterial load.
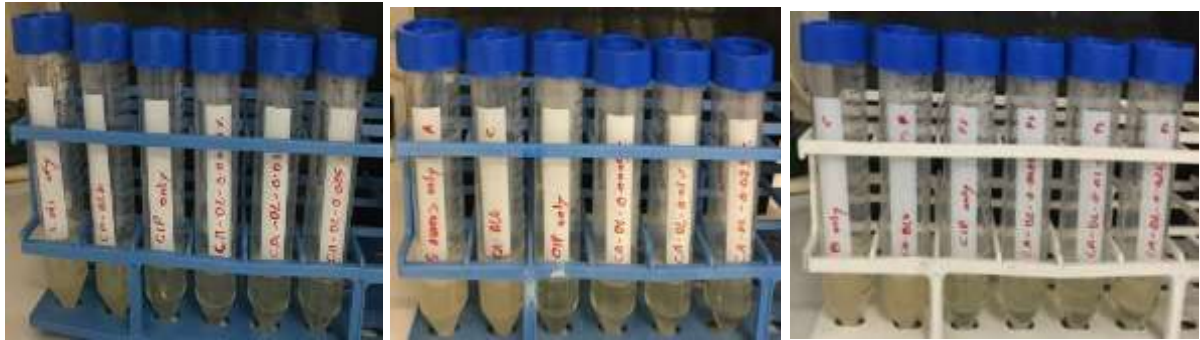
Figure 4.5 Images of turbidity assay of CIP loaded films tested against (A) *E. coli*, (B) *S. aureus*, (C) *P. aeruginosa*. The photographs were taken after incubation for 24 h at 37˚C.
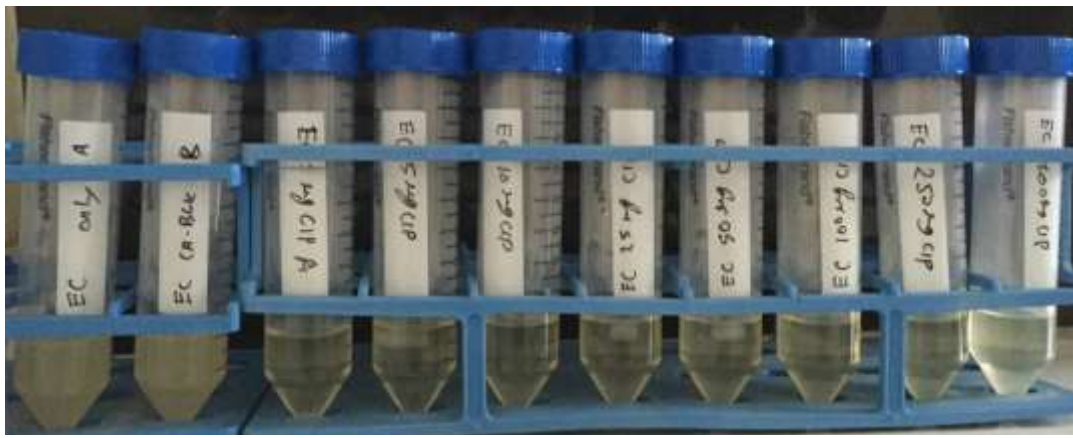
| EC only | 0.00 | **0.0001** | 0.0005 | 0.001 | 0.0025 | 0.005 | 0.010 | 0.025 | 0.40 |

CA-CIP (%) w/v

| SA only | 0.00 | 0.0001 | **0.0005** | 0.001 | 0.0025 | 0.005 | 0.010 | 0.025 | 0.40 |
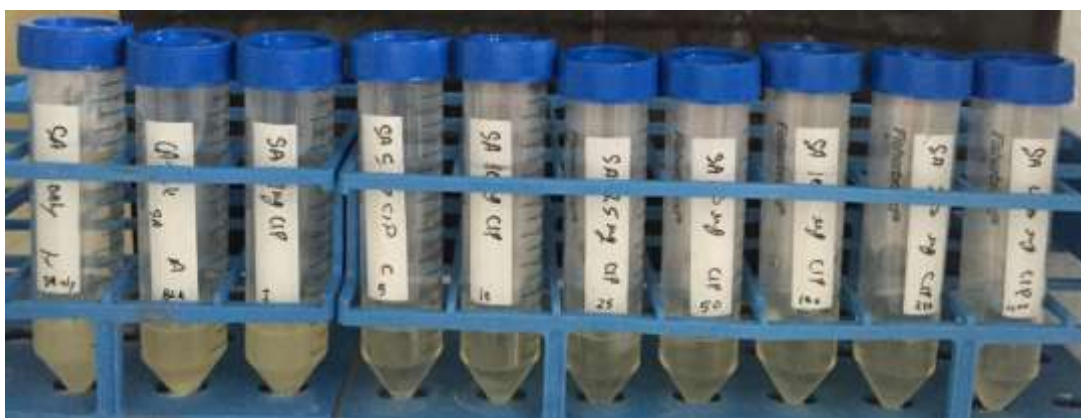
CA-CIP (%) w/v

PS only   0.00   0.0001   **0.0005**   0.001   0.0025   0.005   0.010   0.025   0.40

CA-CIP (%) w/v
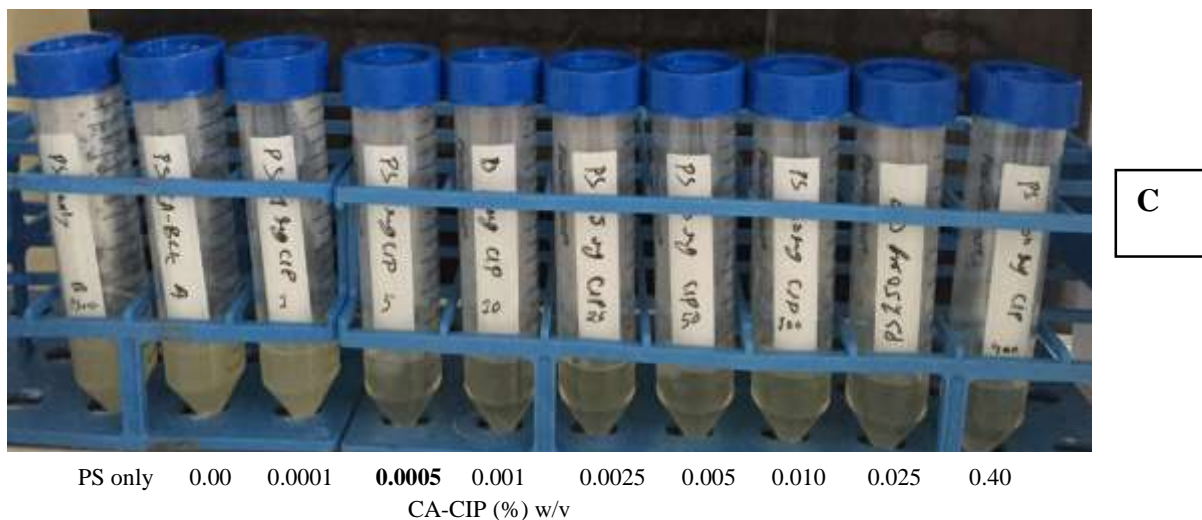
Figure 4.6   Images of turbidity assay of CIP loaded wafers tested against (A) *E. coli*, (B) *S. aureus* and (C) *P. aeruginosa*. The photographs were taken after incubation for 24 h at 37˚C.

Significant difference ($p = 0.001$) in absorbance values was detected between *E. coli*, *S. aureus* and *P. aeruginosa* incubated with BLK and CIP loaded films (**Figure 4.7, a-c)** and wafers (**Figure 4.8, a-c**).
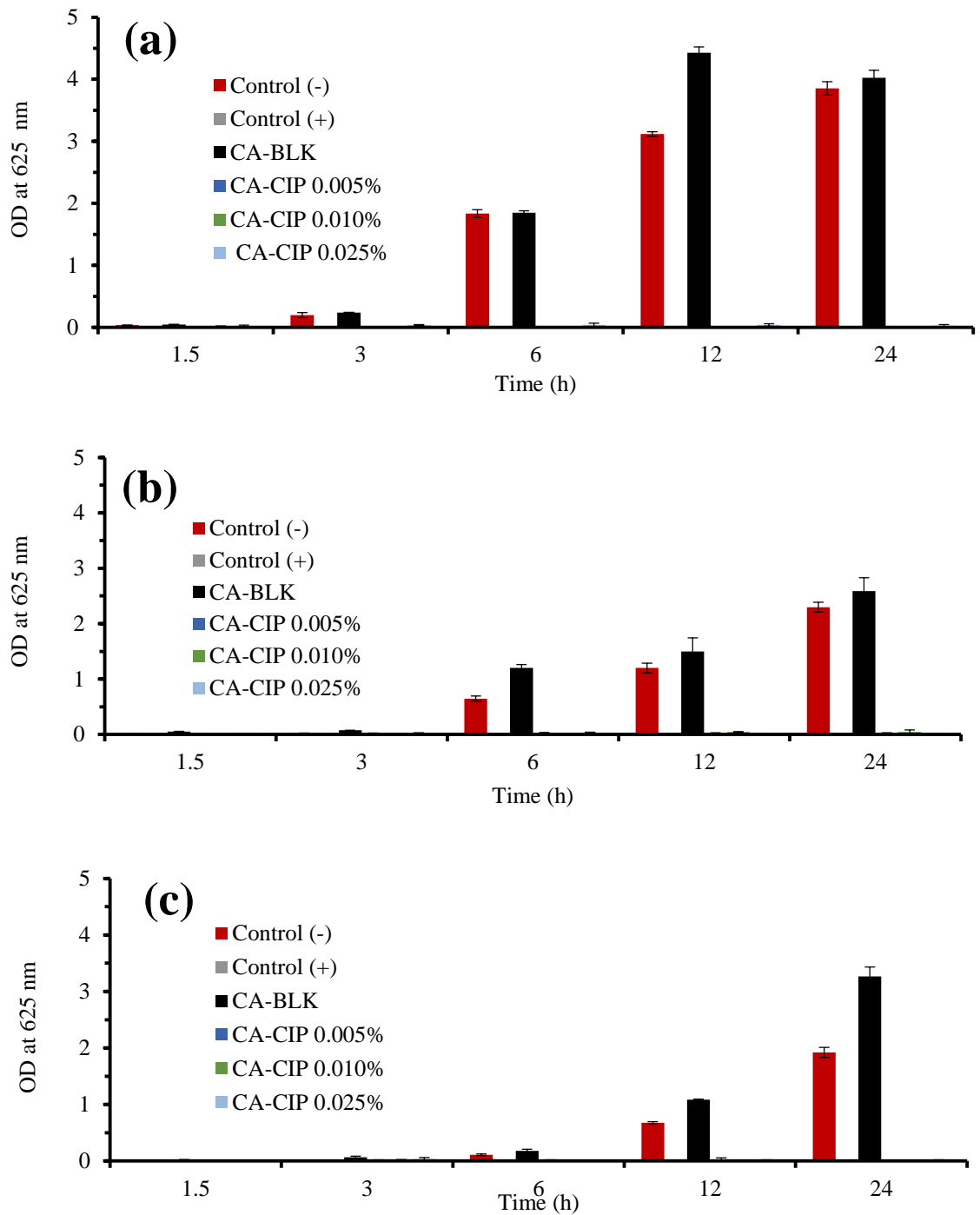
Figure 4.7 Bacterial growth evaluations of CIP loaded films by density measurement. Optical density at 625 nm measured after 1.5, 3, 6, 12 and 24 h incubating with CIP loaded films: (a) *E. coli*, (b) *S. aureus* and (c) *P. aeruginosa*. Tube containing only bacteria and pure CIP were used as control (-) and control (+) respectively ($n = 3 \pm$ SD).
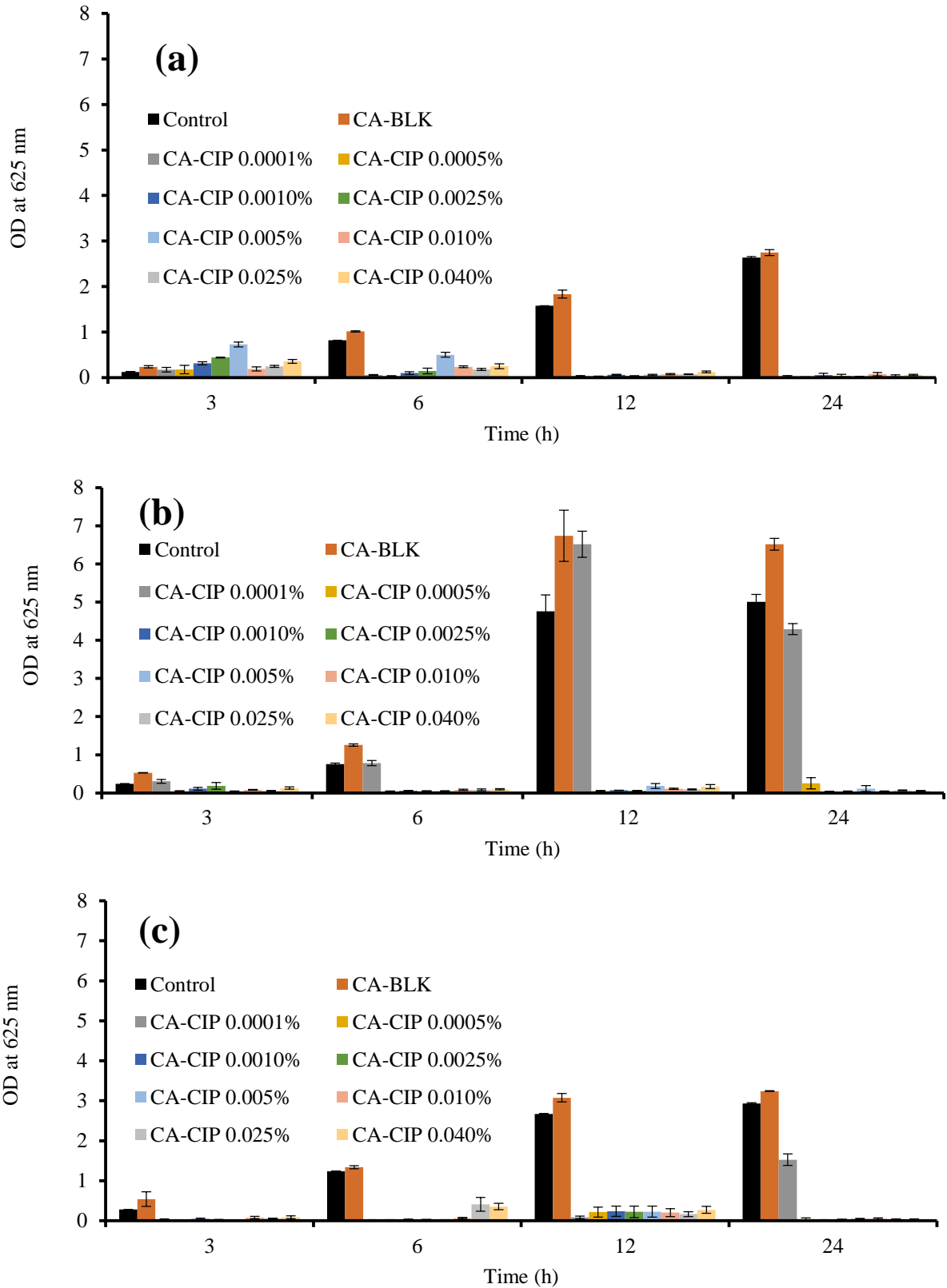
Figure 4.8 Bacterial growth evaluation of CIP loaded wafers by density measurement. Optical density at 625 nm measured after 3, 6, 12 and 24 h incubating with CIP loaded wafers: (a) *E. coli*, (b) *S. aureus* and (c) *P. aeruginosa*. Tube containing only bacteria was used as control ($n = 3 \pm$ SD).

BLK films and BLK wafers did not show any antibacterial effects, which were also confirmed by the ZOI assay (**Figure 4.11 & Figure 4.12**). However, the effectiveness of the antibiotic indicated quick release of the drug from the polymeric matrix. The OD values of the negative control (bacteria only) and CA-BLK dressings gradually increased with time, whereas the values remained below 0.25 and 0.5 in the case of CIP loaded films and wafers respectively during the incubation period. The results suggest that films had a higher bacterial inhibition ability than wafers possibly because the films showed a greater maximum drug releasing capacity (90 −100%) than wafers (59 − 91%). The low OD values of CIP loaded dressings was due to decreased turbidity because of bacterial eradication and was confirmed by the time kill assay shown in **Figure 4.9 and Figure 4.10.**

Figure 4.9 illustrates the rate of bacterial (10^6 CFU/ml representing chronic wounds) eradication when treated with CIP loaded films. Pure CIP (positive control) and film containing 0.025% CIP (w/v) completely killed *E. coli* after 1.5 and 3 h respectively. Complete eradication of *E. coli* by films containing 0.005% and 0.010% CIP (w/v) was observed at 24 h. *S. aureus* is the most infection causative bacteria present in DFUs, however, all viable cells of *S. aureus* were killed by the CIP loaded films within 24 h. The complete eradication of *P. aeruginosa* was also recorded after 24 h of treatment. Tubes containing only bacteria (negative control) increased in number of cells showing the importance of rapid eradication of bacterial cells to prevent infection progression. It was also noticed that all CIP loaded films exhibited maximum bactericidal effect (99.9% reduction of bacterial cells) within 1.5 h, which correlates well with the *in vitro* drug release data.
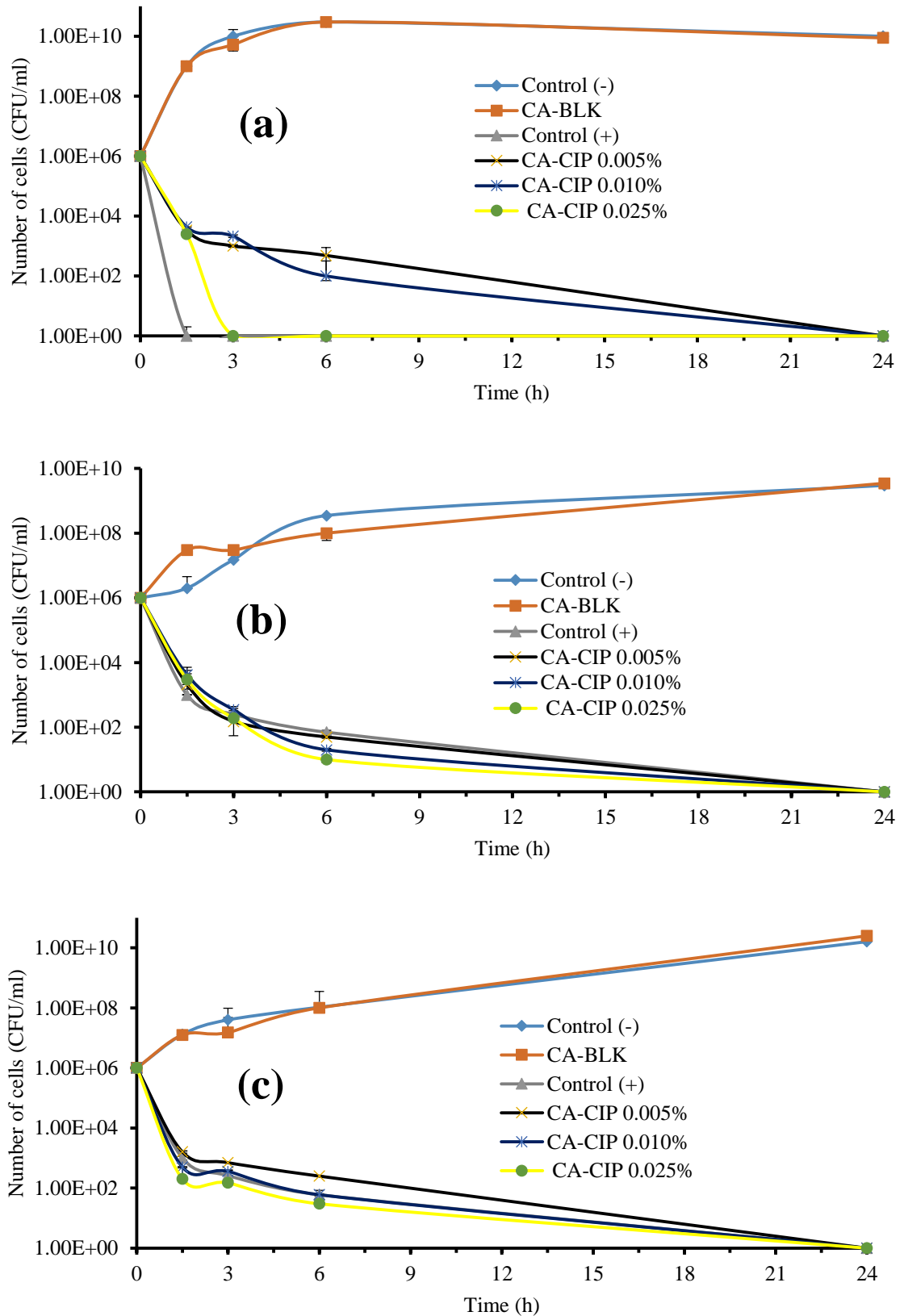
Figure 4.9 Rate of bacterial inhibitions after treating with CA film dressings against: (a) *E. coli*, (b) *S. aureus* and (c) *P. aeruginosa.* Tube containing only bacteria and pure CIP were used as negative control (-) and positive control (+) respectively ($n = 3 \pm$ SD).
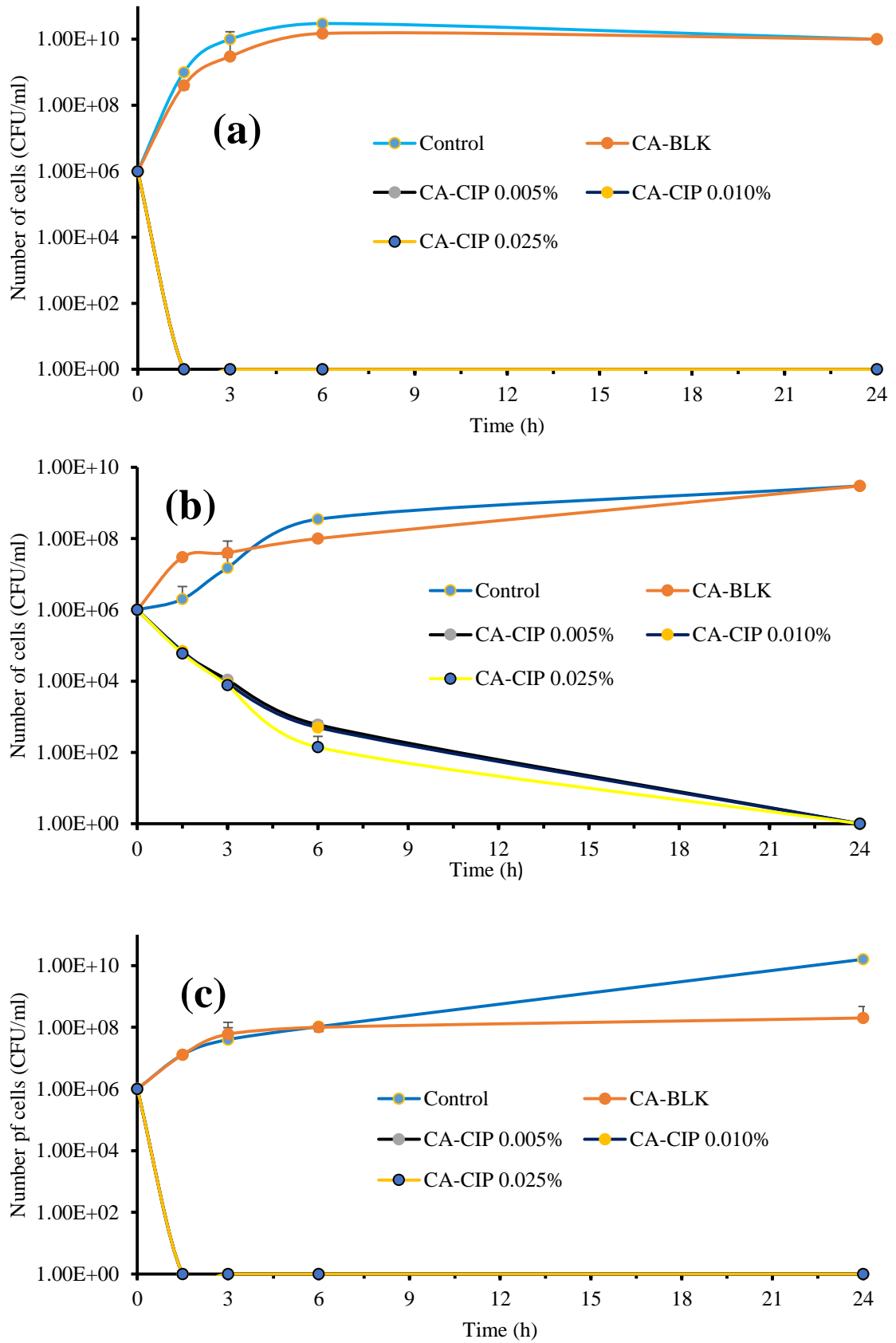
Figure 4.10 Rate of bacterial inhibitions after treating with CIP wafers: (a) *E. coli*, (b) *S. aureus* and (c) *P. aeruginosa*. Tube containing only bacteria was used as control ($n = 3 \pm SD$).

Figure 4.10 also revealed that *E. coli* (**a**) and *P. aeruginosa* (**c**) were completely eradicated within 1.5 h of incubation with the CIP loaded wafers (CA-CIP 0.005%, CA-CIP 0.010% and CA-CIP 0.025%) whilst it took 24 h to kill *S. aureus* (**b**) completely. This suggests that CIP loaded wafers are more effective against *E. coli* and *P. aeruginosa* than *S. aureus*. **Figure 4.11 & Figure 4.12** and **Table 4.1** show the zones and diameter of zone of inhibition (ZOI) respectively of the tested bacteria in the presence of Algisite Ag®, control (+), BLK and CIP loaded films and wafers.
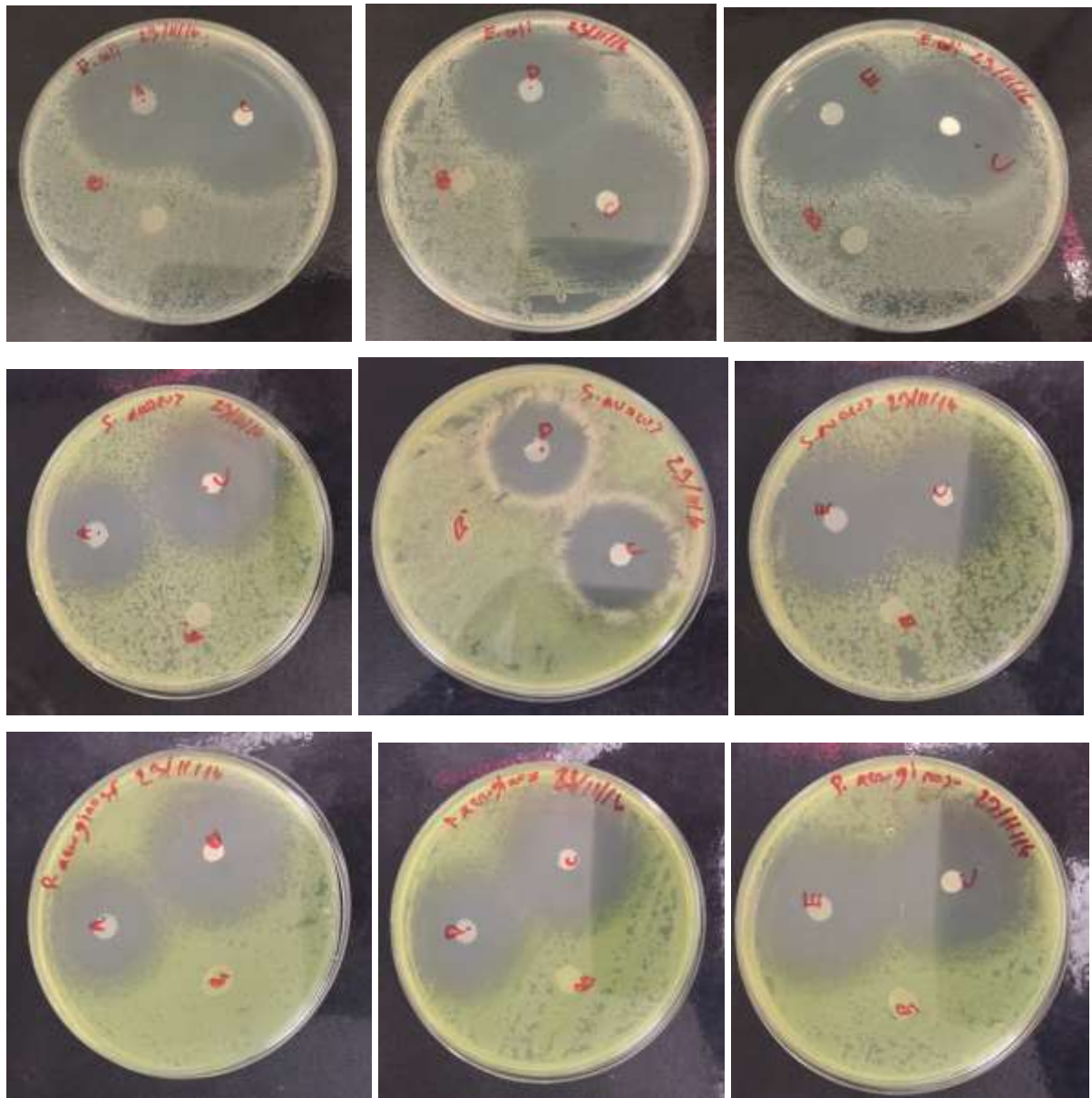
Figure 4.11 Photographic images of ZOI of control (+) (C), BLK (B) and CIP loaded (A= CA-CIP 0.005%, D= CA-CIP 0.010% and C= CA-CIP 0.025%) films tested against *E. coli*, *S. aureus* and *P. aeruginosa*.
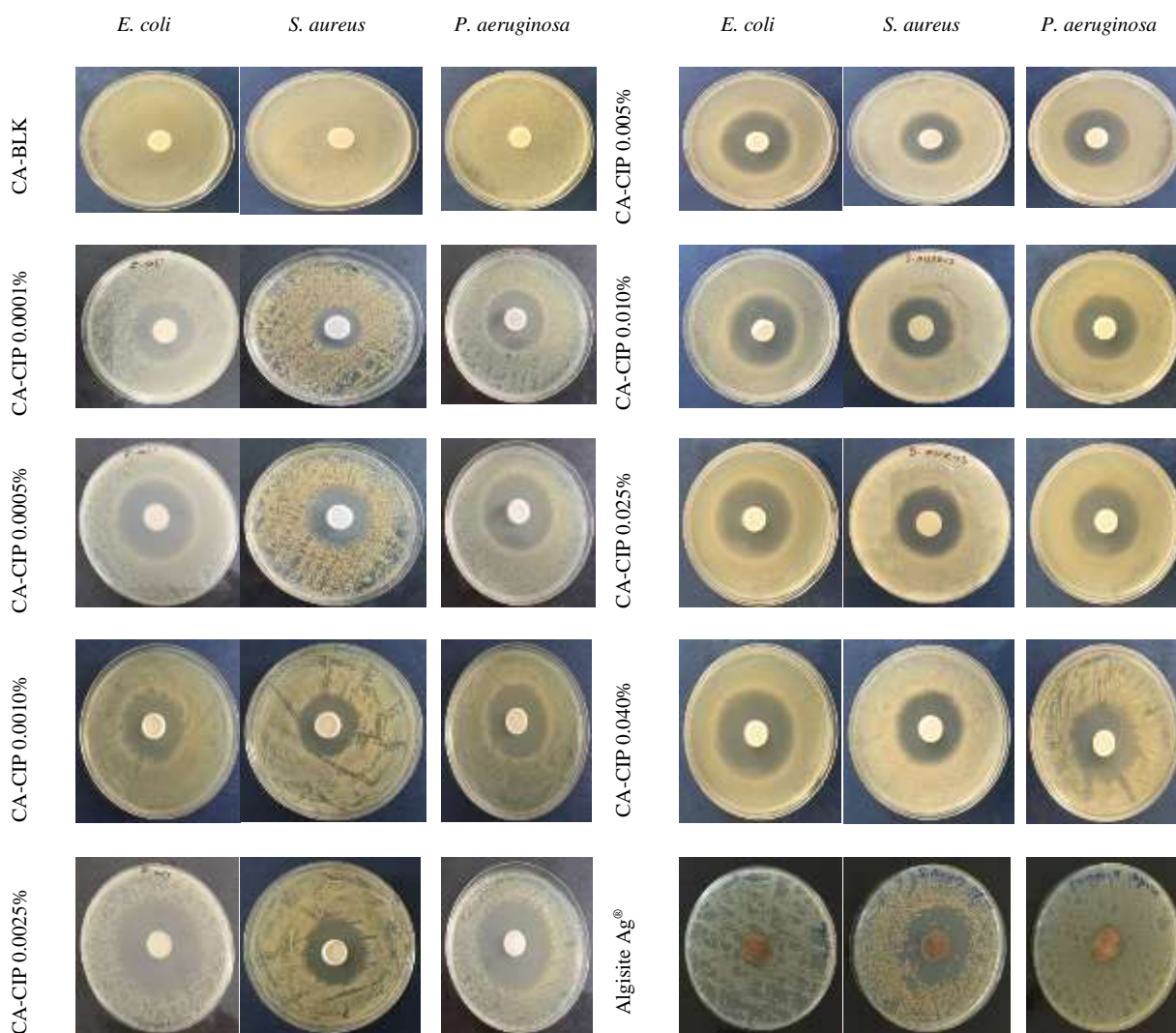
Figure 4.12   Illustrating ZOI of CA-BLK, CIP loaded wafers and commercial product (Algisite Ag®) against *E. coli*, *S. aureus* and *P. aeruginosa*.

ZOIs of the positive control (pure CIP) were 37 ± 0.82, 28.16 ± 1.02 and 34.33 ± 1.31 against *E. coli*, *S. aureus* and *P. aeruginosa* respectively. According to standard guidelines, in disk diffusion technique, 5 μg CIP should have ZOI of 30-40, 22-30 and 25-33 mm against *E. coli*, *S. aureus* and *P. aeruginosa* respectively. (http://www.accessdata.fda.gov/drugsatfda_docs/label/2005/019537s057,020780s019lbl.pdf Accessed: 12 January, 2017). Therefore, this experiment achieved this standardization to justify the tests and the tested films were cut into the same size (6 mm) as the size of positive control to validate the data. All DL films reached this range of ZOI (**Table 4.1**) indicating sensitivity to those causative bacteria.

Table 4.1   Zone of inhibition (ZOI) of CIP loaded films, wafers and Algisite Ag® against *E. coli*, *S. aureus* and *P. aeruginosa* ($n = 3 \pm$ SD).

	E. coli ZOI (mm)	*S. aureus* ZOI (mm)	*P. aeruginosa* ZOI (mm)
Film			
CA-BLK	0.00 ± 0.00	0.00 ± 0.00	0.00 ± 0.00
Control (+)	37.12 ± 0.82	28.16 ± 1.02	34.33 ± 1.31
CA-CIP 0.005%	34.11 ± 0.82	27.33 ± 0.23	29.17 ± 1.54
CA-CIP 0.010%	35.13 ± 0.23	29.06 ± 2.07	33.33 ± 1.69
CA-CIP 0.025%	37.50 ± 1.08	32.00 ± 0.82	33.34 ± 0.62
Wafer			
CA-BLK	0.00 ± 0.00	0.00 ± 0.00	0.00 ± 0.00
CA-CIP 0.0001%	29.67 ± 0.47	20.00 ± 0.82	31.00 ± 0.82
CA-CIP 0.0005%	33.83 ± 0.24	25.67 ± 0.47	35.83 ± 0.43
CA-CIP 0.0010%	34.83 ± 0.65	30.33 ± 0.94	36.83 ± 0.24
CA-CIP 0.0025%	37.17 ± 0.11	31.67 ± 0.23	37.17 ± 0.39
CA-CIP 0.005%	40.47 ± 0.41	33.07 ± 0.09	37.40 ± 0.45
CA-CIP 0.010%	41.43 ± 0.49	33.37 ± 0.29	38.97 ± 0.94
CA-CIP 0.025%	43.43 ± 0.34	34.67 ± 0.47	40.00 ± 0.08
CA-CIP 0.040%	45.07 ± 0.40	36.23 ± 0.34	41.33 ± 0.62
Algiste Ag®	0.00 ± 0.00	33.33 ± 0.49	0.00 ± 0.00

As shown in **Figure 4.11 & Figure 4.12**, BLK films and BLK wafers did not show any zone of inhibition against *E. coli*, *S. aureus* and *P. aeruginosa*, which confirmed that the polymer

has no antibacterial activity on its own. However, clear zones of inhibition were observed in both DL films and wafers for both Gram-positive and Gram-negative bacteria. In addition, the mean diameters (mm) of ZOI for all three microorganisms increased with increasing drug content within the dressings. CIP loaded films showed ZOI of 34.11−37.50, 27.33−32.00 and 29.17−33.34 mm against *E. coli*, *S. aureus* and *P. aeruginosa* respectively (**Table 4.1**). As shown in **Table 4.1** for *E. coli* the mean diameter of ZOI of the wafers with 0.0001% (MIC) and 0.0010% (MBC) CIP was around 29.67 ± 0.47 mm and 34.83 ± 0.65 mm respectively. The largest zone (45.07 ± 0.40 mm) was observed against *E. coli* for the wafer containing 0.040% CIP. In the case of *S. aureus* and *P. aeruginosa*, the ZOI of 0.0005% CIP loaded wafer (MIC for *S. aureus* and *P. aeruginosa*), reached 25.67 ± 0.47 mm and 35.83 ± 0.43 mm. Moreover, the ZOI for wafers loaded with 0.005% (MBC for *S. aureus*) and 0.0010% (MBC for *P. aeruginosa*) CIP were recorded around 33.07 ± 0.09 mm and 36.83 ± 0.24 mm respectively. Overall higher ZOIs as well as maximum killing ability at low concentration confirmed that CIP is more active against *E. coli* and *P. aeruginosa* than *S. aureus*. No bactericidal activity was detected for Algisite Ag® against *E. coli* and *P. aeruginosa* except *S. aureus* as illustrated in **Figure 4.12** with a ZOI value about 33.33 ± 0.49 mm against *S. aureus* (**Table 4.1**). This implies that CIP loaded wafers have better antimicrobial activity than the silver based commercial product.

4.4.3 Antifungal study of FLU loaded dressings

Fungal infections in diabetic foot are often ignored due to lack of research on its pathogenicity and literature substantiation. Therefore, clinicians and surgeons are concentrating on only bacterial infections and prescribing accordingly. However, recent studies have showed the occurrence of a wide range of fungal strains in DFUs (Abilash *et al*., 2015; Challen *et al*., 2010; Chincholikar and Pal, 2002; Nair *et al*., 2006). The development of fungal infections can prolong inflammation and fissuring, leading to breaches in the epidermis and subsequently contribute to the pathogenesis of ulceration and cellulitis in diabetic foot (Chadwick, 2013). The traditional oral antifungal regimens are struggling to treat fungal infected patients with diabetes due to hyperglycaemia, polypharmacy and poor foot hygiene (usually due to obesity, retinopathy, or neuropathy) (Tan and Joseph, 2004). Hence, this study was undertaken to develop FLU loaded dressings that will effectively prevent fungal infections in DFUs. The antifungal activity of the dressings containing different concentrations of FLU (0.05 − 0.40 µg/ml w/v) were investigated against *C. albicans*, one of

the most prevalent fungal strains in DFUs (Abilash *et al*., 2015; Chincholikar and Pal, 2002; Nair *et al*., 2006). The antifungal potential of the dressings was assessed by turbidimetric and ZOI assay.
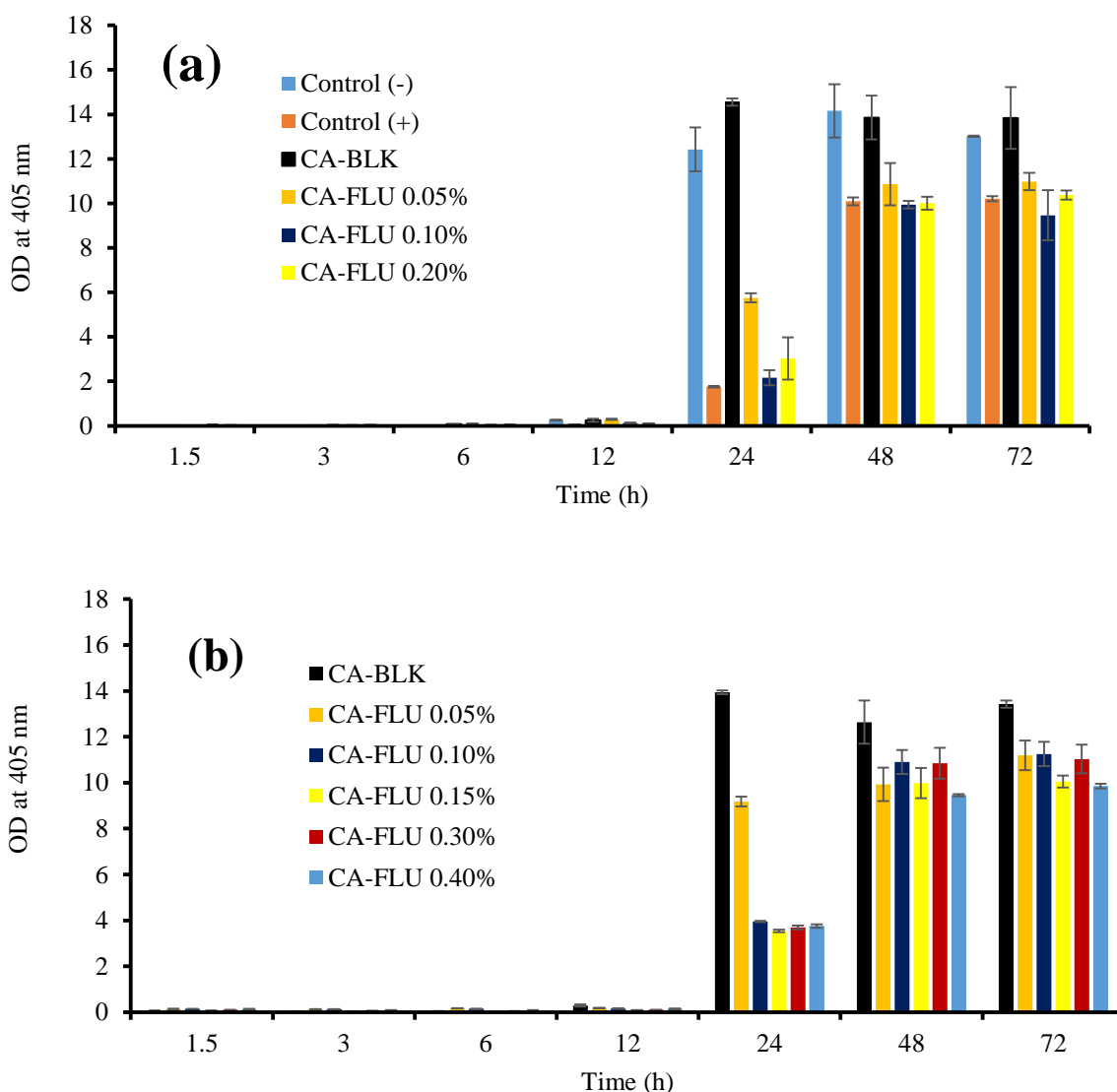
Figure 4.13 Fungal growth evaluations of FLU loaded (a) films and (b) wafers against *C. albicans* by density measurement. Optical density at 405 nm measured after 1.5, 3, 6, 12, 24, 48 and 72 h incubation period. Tube containing only *C. albicans* and pure FLU were used as control (-) and control (+) respectively ($n = 3 \pm$ SD).

Figure 4.13 shows the evaluation of fungal growth in the presence of the formulated FLU loaded films and wafers. The absorbance values remained below 0.29 until 12 h indicating no visible growth until that time. After 24 h, the absorbance values of control (-) (only fungi) and BLK dressings (films and wafers) appeared higher than DL (FLU) dressings. Therefore, the turbidity of the fungal suspension was reduced because of decreasing number of fungal cells

after treating with FLU loaded dressings. It can also be observed that the absorbance values of the DL samples increased with time indicating persistent fungal cell regrowth. The number of cells was counted after different time interval to investigate fungal growth precisely.as shown in **Figure 4.14.**
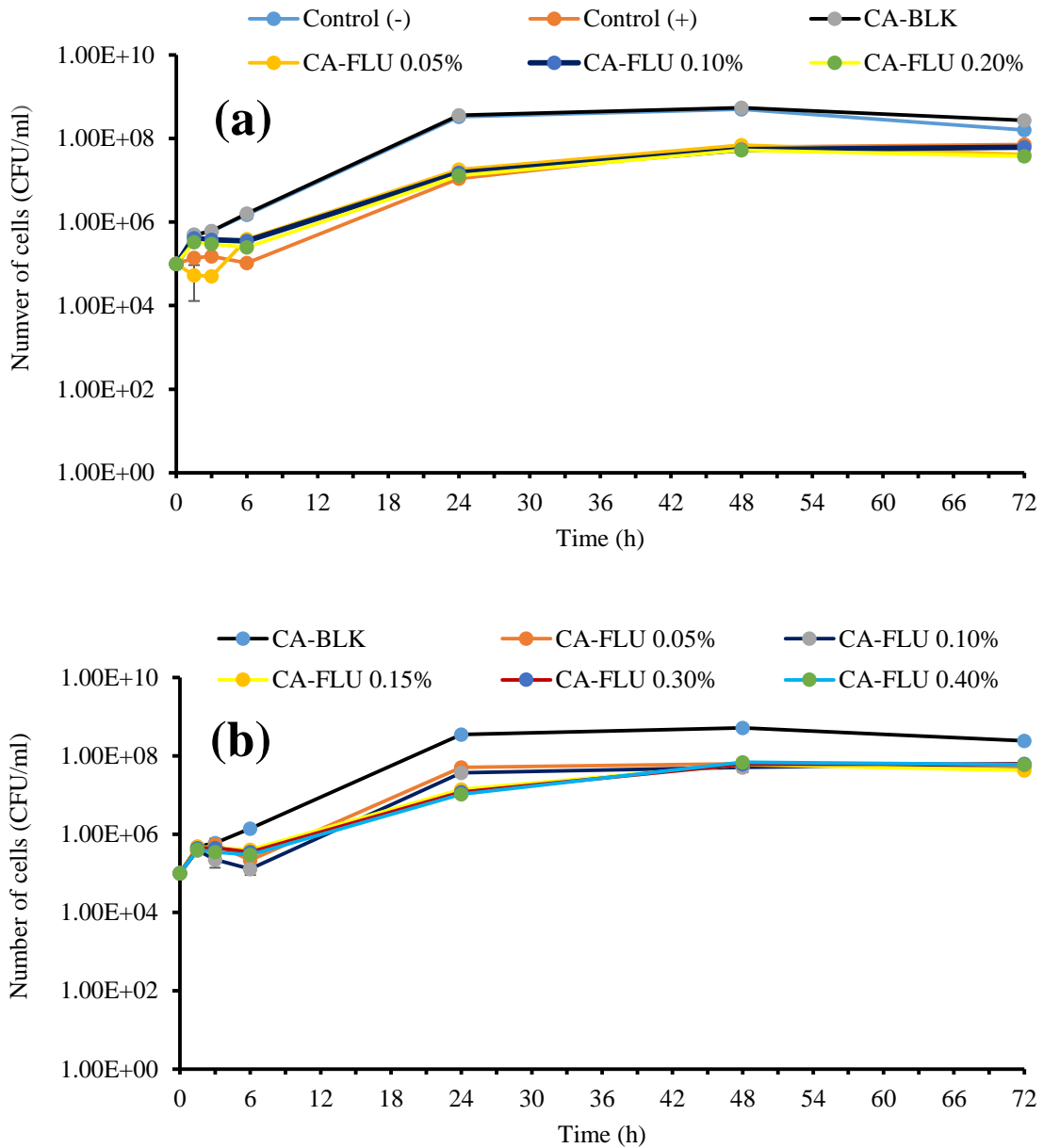
Figure 4.14   Fungicidal kinetic curve of FLU loaded (a) films and (b) wafers against *C. albicans*. Tube containing only *C. albicans* and pure FLU were used as control (-) and control (+) respectively (*n* = 3 ± SD).

The initial cell concentration in every sample was 10^5 CFU/ml. The quantities of survival cells were recorded based on the number of fungal colonies that grew on the SB agar

plates. The kinetic curves (**Figure 4.14**) showed that the number of cells of *C. albicans* in the control (-) and BLK dressings was significantly ($p = 0.007$) increased from 10^5 to 10^8 CFU/ml after 3 to 24 h (log phase/exponential phase) and the cell growth was stabilized (Plateau phase) after 24 h. The growth phase (log phase/exponential phase) of *C. albicans* was 6 to 24 h in the presence of DL dressings. The longer lag phase (0 to 6 h) and shorter growth phase were due to antifungal activity of the FLU loaded dressings. However, a 10-fold reduction in the number of cells as compared to negative control was observed while treating with DL dressings. That means 90% of cells were killed within 24 h after treatment of FLU loaded dressings. A small number of persistent cells started to grow again after 24 h (also supported by turbidity assay) suggesting that the time for changing the dressing is every 24 h. Interestingly the FLU loaded dressings did not show any time and dose-dependent antifungal effect against *C. albicans*. The data suggests that the dressings with low amount of FLU can be used in fungal infected DFUs.

The antifungal activity of FLU loaded dressings was also assessed in terms of ZOI of fungal growth. The results are illustrated in **Table 4.2 and Figures 4.15 & 4.16.** BLK film and wafer did not show any ZOI of growth indicating that the polymer had no antifungal activity. A filter disk containing 25 µg pure FLU was used as a positive control and it showed ZOI about 21.03 ± 0.25 mm. According to National Committee for Clinical Laboratory Standards (NCCLS) method, 25 µg FLU disk should have a ZOI about ≥ 20 mm against *Candida* species to define susceptibility (Kirkpatrick *et al*., 1998). Therefore, this study correlated well with the NCCLS reference method. The growth inhibition zone measured ranged from 27.50 ± 0.41 to 33.10 ± 1.64 and from 28.50 ± 0.41 to 32.53 ± 1.32 for FLU loaded films and wafers respectively. There were no significant differences (*p > 0.05)* in mean diameter of ZOI between and within the dressings demonstrating equal potency against *C. albicans*. Moreover, the dressings containing low amount of FLU can be used in DFUs instead of higher doses.

Table 4.2   Diameter (mm) of ZOI of FLU loaded dressings against *C. albicans.* ($n = 3 \pm$ SD).

	C. albicans ZOI (mm)
Film	
CA-BLK	0.00 ± 0.00
Control (+)	21.03 ± 0.25
CA-FLU 0.05%	27.50 ± 0.41
CA-FLU 0.10%	28.36 ± 2.59
CA-FLU 0.20%	33.10 ± 4.64
Wafer	
CA-BLK	0.00 ± 0.00
CA-FLU 0.05%	28.50 ± 0.41
CA-FLU 0.10%	28.83 ± 0.24
CA-FLU 0.15%	30.00 ± 2.12
CA-FLU 0.30%	30.90 ± 0.45
CA-FLU 0.40%	32.53 ± 1.32

CA-BLK	**Pure FLU**	**CA-FLU 0.05%**

CA-FLU 0.10%	**CA-FLU 0.20%**
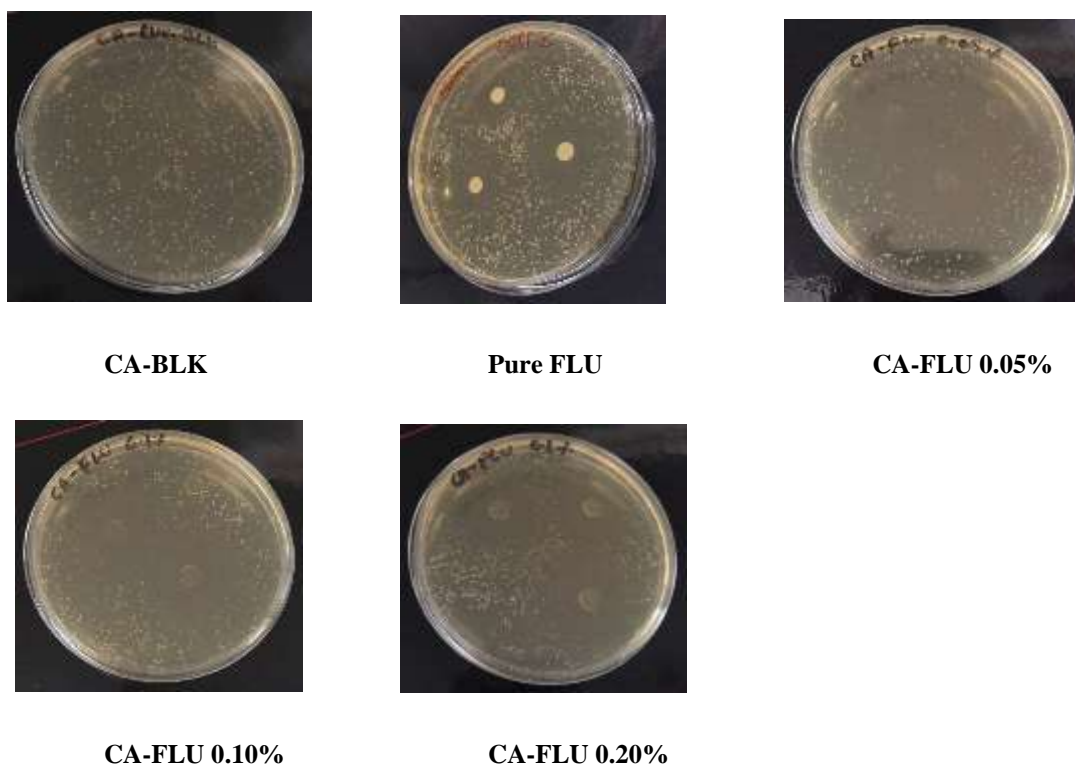
Figure 4.15   25 µg FLU disk (control +) and FLU loaded films on a lawn of 10^5 CFU of C. albicans after 24 h of incubation.

CA-BLK	**CA-FLU 0.05%**	**CA-FLU 0.10%**

CA-FLU 0.15%	**CA-FLU 0.30%**	**CA-FLU 0.40%**
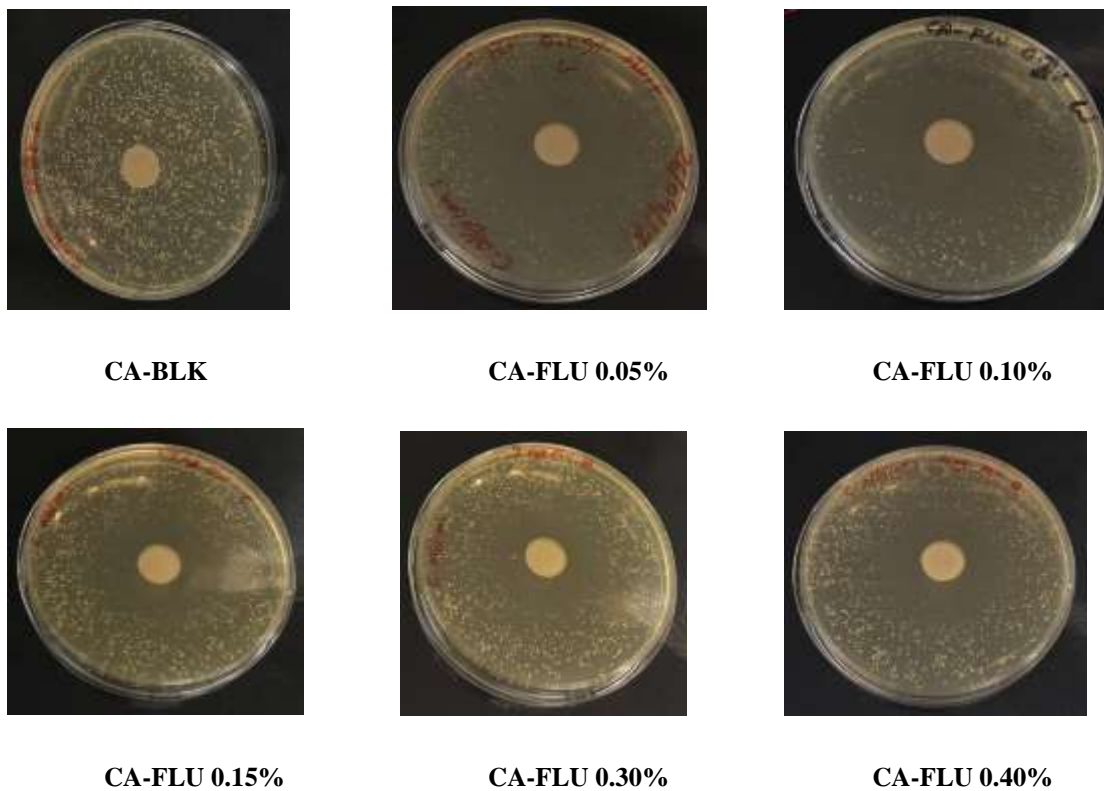
Figure 4.16   BLK and FLU loaded wafers on a lawn of 10^5 CFU of C. albicans after 24 h of incubation.

4.4.4 Mixed infection study of combined drug loaded (CIP and FLU) dressings

Mixed infection studies of combined DL (CIP and FLU) dressings were assessed by turbidimetric method. This study is based on the interaction between DL dressings and the test microorganisms (*E. coli*, *S. aureus*, *P. aeruginosa* and *C. albicans*), followed by changes in turbidity of the mixed microbial suspensions. As shown in **Figure 4.17 a**, the absorbance value of the mixed culture of *E. coli* and *C. albicans* (positive control) was gradually increased from 3h to 24 h demonstrating the log phase of the growth. After 24 h, the absorbance values of the mixed culture (*E. coli* and *C. albicans*) were insignificant ($p = 0.001$). The absorbance values of the BLK dressings and Actiformcool® were also increased with time indicating promotion of microbial growth. The absorbance values of the mixed infection (*E. coli* and *C. albicans*) treated with combined DL dressings were significantly ($p < 0.05$) lower than the positive control and BLK dressings until 12 h. It could be due to suppression of the growth of the mixed culture by releasing both antimicrobials (CIP and FLU) from the dressings. The absorbance value of the mixed culture comprising *S. aureus* and *C. albicans* were gradually increased with the time (**Figure 4.17 b**). This indicated that the *S. aureus* and *C. albicans* grew well together in the BHI broth. The gradual increase in cell densities could be due to interaction between *S. aureus* and *C. albicans* resulting in synergistic effect on the growth (Kean *et al.*, 2017; Harriott and Noverr, 2009). This synergistic effect hinders the healing of DFUs by enhancing microbial tolerance to the antimicrobial agents (Budzynska *et al.*, 2017). It is also reported that the synergistic effect of *S. aureus* and *C. albicans* in mice increased mortality (Carlson, 1983). In this study, the cell densities of the treated mixed culture (*S. aureus* and *C. albicans*) with combined DL dressings were insignificant ($p = 0.82$) after 24 h. Therefore, the synergistic effect of the *S. aureus* and *C. albicans* was overcome by combined DL dressings. In case of the mixed culture of *P. aeruginosa* and *C. albicans,* the cell densities were increased up to 24 h and after that the value decreased from 0.92 to 0.50 until 72 h (**Figure 4.17 c**) and the same observations were observed for the remaining samples.
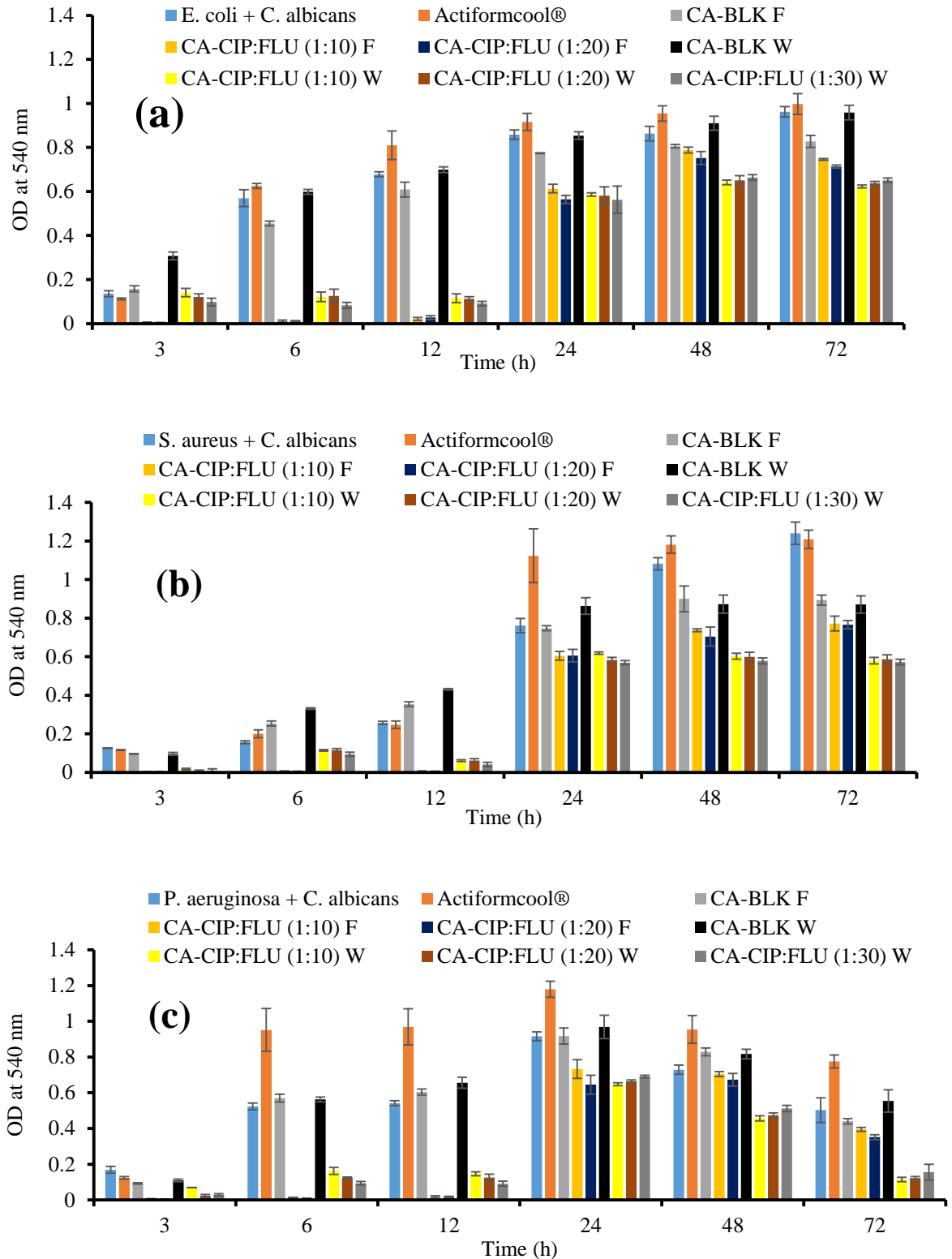
Figure 4.17   Mean reading of increment at 540 nm wavelength optical density measurements of mixed bacterial and fungal strains treated with combined DL dressings and commercial product Actiformcool® ($n = 3 \pm SD$). F: Film; W: Wafer

The reduction in cell densities might be due antagonistic interaction of *P. aeruginosa* and *C. albicans* (Fourie *et al.*, 2016). The interaction of *P. aeruginosa* and *C. albicans* is regulated by releasing of quorum sensing molecules from both organisms (Cugini *et al.*, 2007). *P. aeruginosa* could supress the growth of *C. albicans* by secreting some factors such as 5- methyl-phenazine-1-carboxylic acid (5MPCA) which have anti-fungal properties (Mear *et al.*, 2013). 5MPCA alters the cell wall of *C. albicans* (Kerr *et al.*, 1999). It is also reported, *C. albicans* can inhibit the growth of *P. aeruginosa* by releasing quorum sensing molecules such as farnesol. Farnesol inhibits the production *Pseudomonas* quinolone signal (PQS) that reduces pyochynin synthesis and swarming motility in *P. aeruginosa* (Cugini *et al.*, 2007).

Afterwards, the turbidity of the mixed cultures (either *E. coli* and *C. albicans,* or *S. aureus* and *C. albicans,* or *P. aeruginosa* and *C. albicans*) treated with the dressings containing both CIP and FLU was lower than the untreated mixed cultures. Therefore, potentiality of combined DL dressings in eradicating mixed bacterial and fungal infections can be demonstated. On the other hand, the turbidity of all mixed cultures treated with Actiformcool® were similar to the negative control and BLK dressings. It could probably due to absence of antimicrobial agents in Actiformcool®.

The killing patterns of the dressings containing CIP and FLU are illustrated in **Figures 4.18-4.20**. It can be observed from **Figure 4.18 a, Figure 4.19 a and Figure 4.20 a** that the combined DL dressings exhibited bactericidal activity (99.9% killing) within 3 h. This rapid killing of bacteria (*E. coli, S. aureus* and *P. aeruginosa*) was mediated by the maximum release of CIP from the dressings within a short time (**Chapter 3: Figure 3.21 & Figure 3.24**). The complete eradication of bacterial cells was observed within 24 h in case of the mixed culture of *E. coli* and *C. albicans*, as well as *P. aeruginosa* and *C. albicans.* In the mixed culture of *S. aureus* and *C. albicans,* the complete eradication of bacteria was observed within 72 h. The delayed eradication of *S. aureus* might be due to the synergistic interaction between *S. aureus* and *C. albicans.* Overall, the DL dressings appeared to be highly effective against the causative bacteria present in DFUs. Presence of *C. albicans* did not affect the antibacterial activity of the dressings very much. In terms of killing *C. albicans* from the mixed cultures, combined DL dressings showed 10-fold reduction in cell numbers when compared to the control mixed cultures (untreated). Therefore, the combined DL dressings can reduce 90% of fungal cells from the mixed infections. The highest number of cell survival was observed when the mixed cultures were treated with the commercial product Actiformcool®, confirming no antimicrobial activity. Moreover, the number of the viable cells of *C. albicans* in the presence of *P. aeruginosa* was

10^6 CFU/ml after 72 h (**Figure 4.20 b**). At the same incubation period, the viability of the yeast cells was lower than the cell viability of *C. albicans* either with *E. coli* or *P. aeruginosa*. It suggests that *P. aeruginosa* has suppression (antagonistic) effects against the growth of *C. albicans*. This observation was also supported by the turbidity assay (**Figure 4.17 b**). The number of viable cells of *C. albicans* remained at 10^5 CFU/ml while treating the mixed infection of *P. aeruginosa* and *C. albicans* with combined DL dressings. The viability of Candida cells was lower than the other mixed infections.
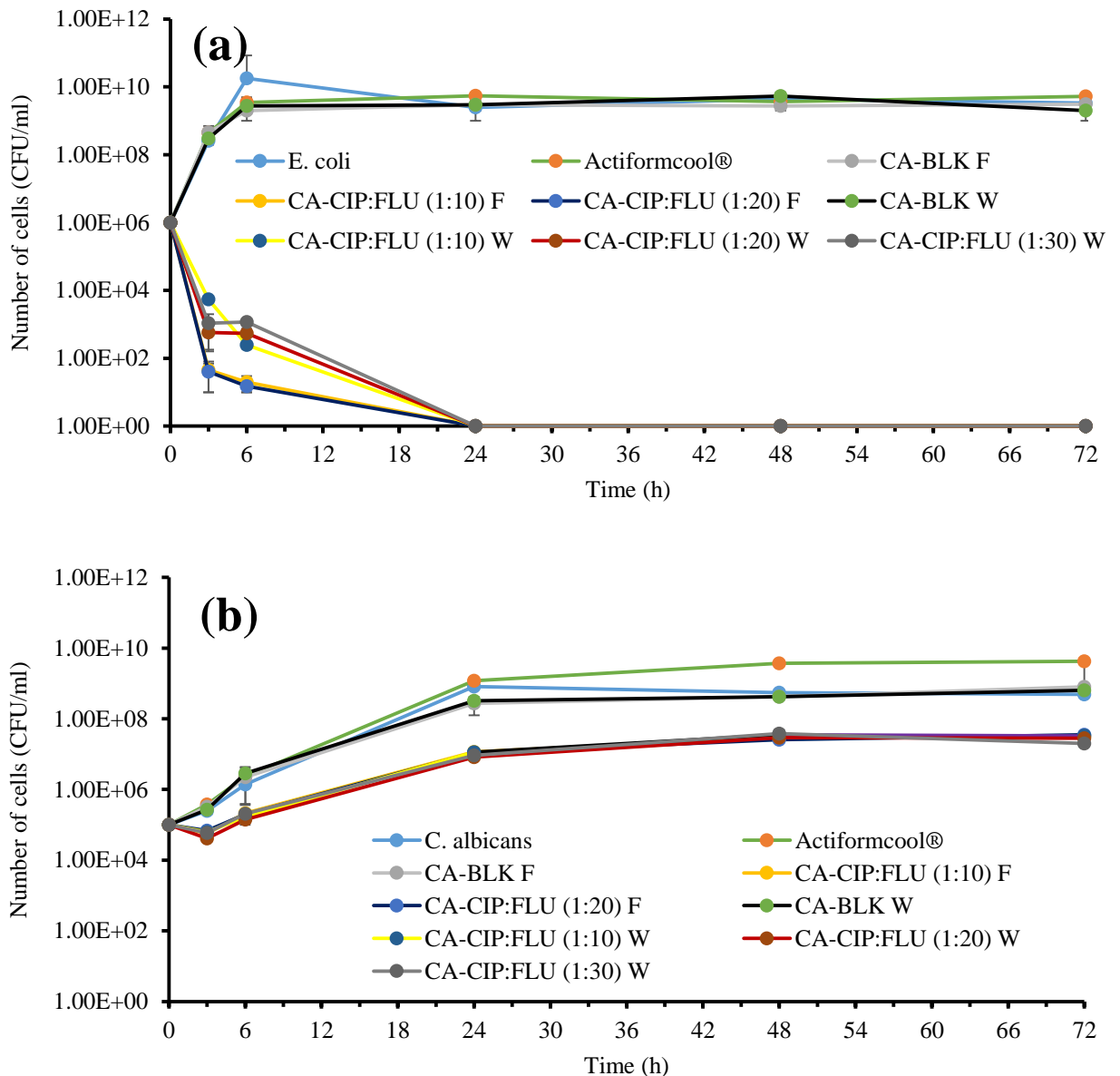
Figure 4.18 Time-kill curves for combined DL dressings and Actiformcool® against the mixed infection of (a) *E. coli* and (b) *C. albicans* ($n = 3 \pm$ SD). F: Film; W: Wafer
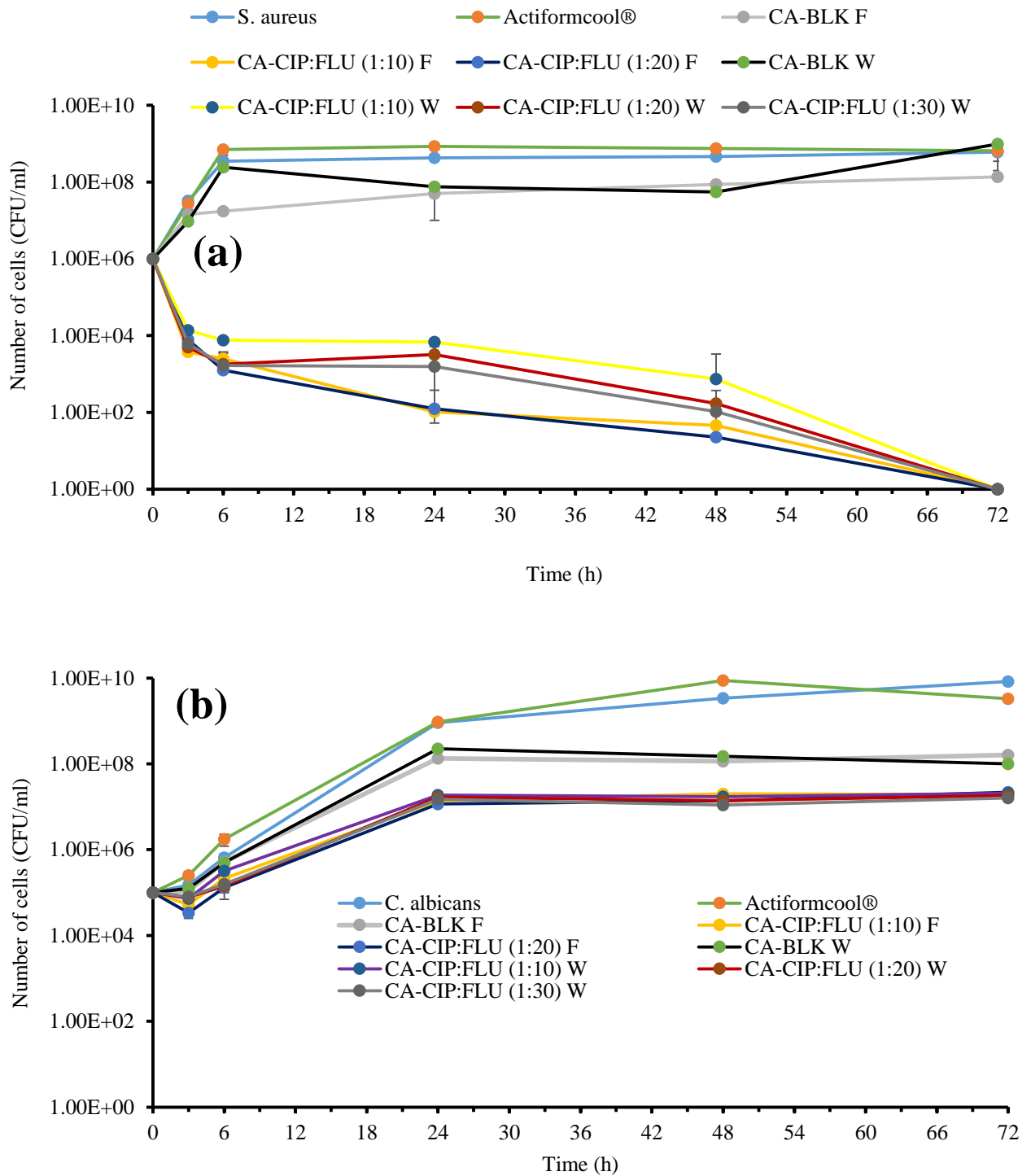
Figure 4.19 Time-kill curves for combined DL dressings and Actiformcool® against the mixed infection of (a) *S. aureus* and (b) *C. albicans* ($n = 3 \pm$ SD). F: Film; W: Wafer
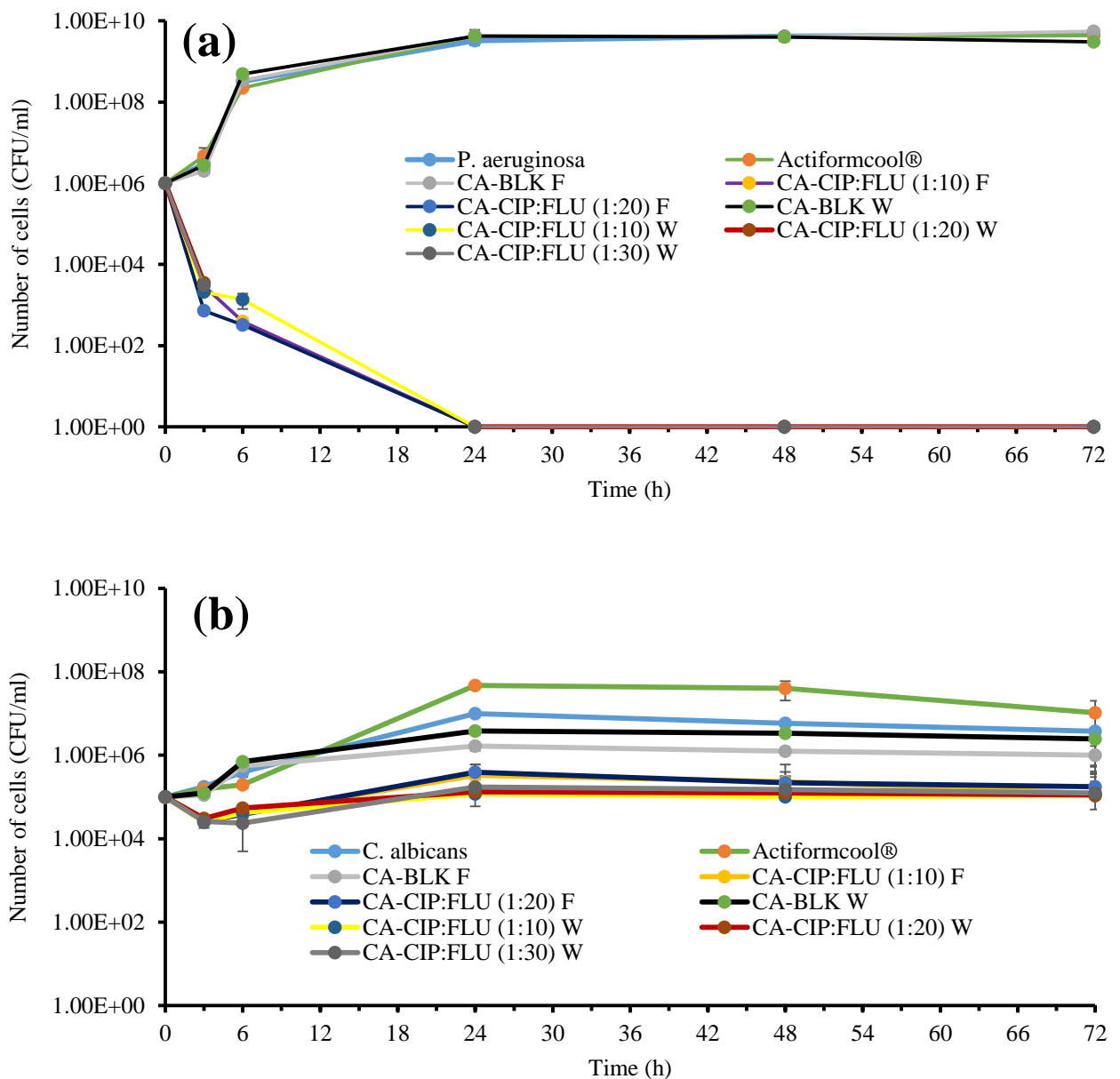
Figure 4.20 Time-kill curves for combined DL dressings and Actiformcool® against the mixed infection of (a) *P. aeruginosa* and (b) *C. albicans* ($n = 3 \pm SD$). F: Film; W: Wafer

To some extent ZOI assay mimics the clinical use of the antimicrobial products and predicts the capability of the dressings to kill or prevent microbial growth in a wound bed. The colonized BHI agar plates represented the infected moist or exuding wounds surface. In order to exhibit antimicrobial activity, the dressings need to absorb moisture from the colonized agar plates to trigger the drug release (in this study CIP and FLU) from its matrix. Thereafter, the drugs need to diffuse back down to the agar to exhibit its antimicrobial effect (Thomas and McCubbin, 2003). **Figure 4.21** and **Table 4.3** show the inhibitory zone diameters of combined

DL dressings mixed placed on the mixed culture of bacteria and fungi. The drug free dressings (BLK) did not show any inhibitory effect on the mixed infections which was also confirmed by the turbidity and time-kill assays.
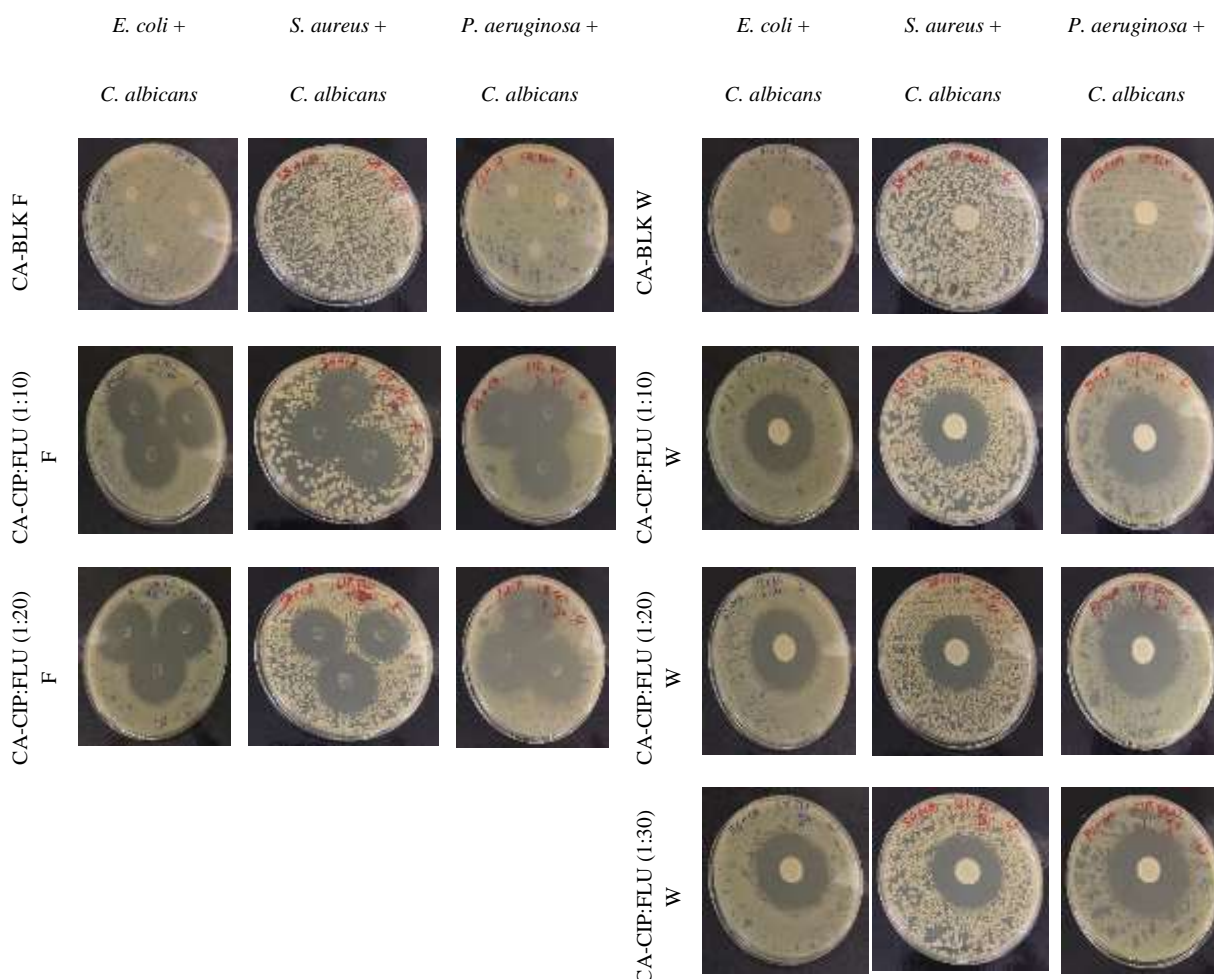
Figure 4.21   Photographic images of ZOI of BLK and combined DL (CIP and FLU) fims and wafers against the mixed culture of bacteria (*E. coli*, *S. aureus* and *P. aeruginosa*) and fungi (*C. albicans*).

The dressings (wafers and films) containing CIP and FLU showed the strongest inhibitory effect (ZOI, 34.00 − 44.83 ± 0.23 nm) against the mixed culture of *P. aeruginosa* and *C. albicans* amongst all other mixed cultures. This high inhibitory effect was also promoted by the antagonistic interaction between *P. aeruginosa* and *C. albicans*. It can also be seen that DL dressings had the lowest ZOI (26.50-36.50 ± 0.41 nm) against the mixed culture of *S. aureus* and *C. albicans* due to synergistic interaction of *S. aureus* and *C. albicans* in resisting drug antimicrobial action. The obtained results also revealed that the wafers showed higher ZOI

(36.67−44.83 ± 0.23 nm) against all mixed cultures than the films (26.50 − 35.60 ± 0.70 nm). This could be due to the higher amount of drugs present in the wafers and could be because the wafers showed the higher drug release (**Chapter 3: Figure 3.24**) than the films (**Chapter 3: Figure 3.21).**

Table 4.3   Zone of inhibition (mm) of the dressings containing various concentrations of drugs (CIP and FLU) on mixed culture of bacteria and fungi ($n = 3 \pm$ SD).

	E. coli + C. albicans	*S. aureus + C. albicans*	*P. aeruginosa + C. albicans*
	ZOI (mm)	**ZOI (mm)**	**ZOI (mm)**
Film			
CA-BLK	0.00 ± 0.00	0.00 ± 0.00	0.00 ± 0.00
CIP : FLU (1:10)	30.50 ± 0.71	28.50 ± 1.08	34.00 ± 0.41
CIP : FLU (1:20)	31.33 ± 0.23	26.50 ± 0.41	35.60 ± 0.70
Wafer			
CA-BLK	0.00 ± 0.00	0.00 ± 0.00	0.00 ± 0.00
CIP : FLU (1:10)	40.43 ± 0.42	36.67 ± 1.43	44.83 ± 0.23
CIP : FLU (1:20)	42.77 ± 0.95	37.17 ± 0.85	44.00 ± 0.82
CIP : FLU (1:30)	42.17 ± 0.23	36.50 ± 0.41	43.33 ± 0.62

4.5 Conclusions

Bacterial, fungal and mixed bacterial/fungal infections are the most common and dangerous sources of complications in the diabetic foot. Therefore, it is vital to identify the type of infection and the microbial load before applying the dressings. The rapid eradication of three common infection causative bacteria; *E. coli*, *S. aureus* and *P. aeruginosa* was attributed to initial burst release of CIP from the dressings which is very important to prevent infection in diabetic foot. Complete eradication of all causative bacteria was observed after 24 h which will be very effective to prevent infection in DFUs. The study also demonstrated the antifungal activity of the FLU loaded dressings against *C. albicans*, with remarkable reduction of fungal

load was observed while treating with FLU loaded dressings. The formulated combined DL dressings containing both CIP and FLU were found to be highly effective against the mixed infections. The time-kill curves against the mixed culture of bacteria and fungi suggest that combined DL dressings are more potent in reducing bacterial load than fungal load. The bactericidal activity was observed within 3 h but the DL dressings did not show corresponding fungicidal (99.9% killing) activity. However, 10-fold reduction of the fungal cells will be high enough in decreasing fungal load in DFUs. The commercial product Algisite Ag® showed effectiveness only against *S. aureus* and the other commercial product Actiformcool® failed to show antimicrobial activity against any mixed infections. Although medicated CA dressings exhibited promising antimicrobial characteristics for wound healing, *in vivo* wound healing study will need to be undertaken in the future to confirm its effectiveness.

CHAPTER 5: *IN-VITRO* CELL VIABILITY AND MIGRATION STUDIES FOR SAFETY AND WOUND SCRATCH ASSAY

5.1 Introduction

Polymeric dressings are easily biodegradable and therefore, host cells can easily accept them without any foreign body reaction (Sannino *et al*., 2009). The molecular domains of biodegradable polymers support and guide cells at different stages of their development by enhancing biological interaction of the polymeric dressings with the host tissue (Asti and Gioglio, 2014) and hence promoting rapid healing without side effects. Porous polymeric dressings have been reported for faster and functional wound healing properties than the nonporous dressings (e.g. hydrogels or hydrocolloids) because micro-porous structures provide high surface area which enables utmost cell-material interactions, material-mediated signalling, enhanced homeostasis and exchange of nutrients and waste (Zhao *et al*., 2017). In addition, stiffness of the dressings also plays a vital role in wound healing. It is reported that cells migrate faster into soft matrices than the rigid matrices because soft matrices enable attraction of nearby fibres of the dressings by active cells, which stimulates cell adhesion and signalling pathways by increasing ligand density on the cell surface and promotes cell migration (Baker *et al*., 2015).

Chronic wound healing is a complex process in which a series of events (such as enhanced vascularization by angiogenic factors, increased cell proliferation and extracellular matrix deposition, and infiltration by inflammatory immune cells) are involved in order to repair the wound bed. Non-healing diabetic wounds are associated with prolonged inflammatory stage characterized by supraphysiological oxidative stress (Xiao *et al*., 2016). The supraphysiological oxidative stress due to high production of reactive oxygen spices and hyperglycaemia can induce keratinocytes dysfunction (Spravchikov *et al*., 2001). Moreover, high level of matrix metalloproteinase (MMPs) production can enhance extracellular matrix (ECM) degradation rate and alter the ECM composition, which obstructs keratinocytes attachment, leading to aberrant cell signalling and impaired migration (Tarnuzzer and Schultz, 1996; Loots *et al*., 1998). Keratinocytes migration from the edge of the wound into the wound bed is very important to re-epithelialize the infected tissue. Therefore, it is highly recommended to test the wound dressings to evaluate the safety and effective keratinocytes migration for potential wound healing.

In vitro cytotoxicity assay is an important method to evaluate safety of biomaterials such as dressings. This assay is based on morphological observation of cell damage and growth after

direct or indirect exposure to the biomaterials (Wiegand and Hipler, 2008). Counting number of cells by haemocytometer after staining with trypan blue is the straightforward technique to evaluate cell viability. However, adherent cells need to be trypsinized before counting. In this method dead cells are stained blue due to loss of membrane integrity (Wiegand and Hipler, 2008). Cytotoxicity study can also be performed by methylthiazolyldiphenyl-tetrazolium bromide (MTT) assay, live/dead cells staining and flow cytometry analysis (Udhayakumar *et al*., 2017, Rottmar *et al*., 2015). There are several commercial kits such as cytotoxicity detection kit (Molecular Probes Inc., OR, USA) and Caspase-Glo assays (Promega GmbH, Mannheim, Germany) available for cytotoxicity study (Wiegand and Hipler, 2008).

Various models and methods have been employed to study cell migration. For example, animal models are often used to study chronic wound healing and delivered important knowledge at the systemic level (Ueck *et al*., 2017). However, their usability is limited by ethical issues and economical aspects (Gonzalez *et al*., 2016). On the other hand, *in vitro* cell based study is simple, inexpensive and reproducible (Gonzalez *et al*., 2016). The wound healing assay also known as scratch assay is a standard *in vitro* technique to evaluate cell migration. In this method, a gap (migration zone) is created after the cells reach optimum confluence (Jonkman *et al*., 2014). There are several methods of creating the gap in confluent monolayer such as direct manipulation through mechanical, electrical, chemical and thermal means, and physical exclusion by placing barriers within cell culture plate (Vedula *et al*., 2013). The most common approach is to create a gap by pipette tips (mechanical means) since it is inexpensive and easy to implement. Different types of pipette tips give different sizes of the migration zone; however, it is difficult to create reproducible wound gap. In addition, scratching by pipette tips may damage the ECM of cells at the edge of the gap, which can affect the rate of cell migration. The physical exclusion can generate consistent gap size and cause minimum cell damage (Jonkman *et al*., 2014), however, this method is more expensive than other scratch methods. After gap creation, the model set up is then observed microscopically over time as cells migrate into the wound gap. The rate of cell migration depends on the type of cells, conditions and size of gap (Jonkman *et al*., 2014, Friedl and Wolf, 2010)

In this chapter, the biocompatibility of the formulated dressings and two commercial products (Algisite Ag® and Actiformcool®) were evaluated with adult human primary epidermal keratinocyte (PEK) cells. The cytotoxicity (cell viability) study was performed by MTT assay while cell migration study was performed by wound scratch assay.

5.2 Materials

Calcium alginate (mannurronic acid:guluronic (59:41), molecular weight: 398.32 g/mol) [CA, (lot number: BCBM8132V)], ciprofloxacin [CIP, (lot number: LRAA6508)], Fluconazole [FLU, (lot number: LRAA6502), Dulbecco's phosphate buffered saline [D-PBS, (lot number: RNBD8494)], trypsin-EDTA solution (lot number: SLBM8412V) and foetal bovine serum [FBS, (lot number: 045M3318)] were purchased from Sigma-Aldrich (Gillingham, UK). Ethanol (batch number: 0933421) and dimethyl sulfoxide [DMSO, (batch number: 0890132)] were ordered from Fisher Scientific (Loughborough, UK). Adult human primary epidermal keratinocytes (PCS-200-011, ATCC), dermal cell basal medium (PCS-200-030, ATCC) and keratinocytes growth kit (PCS-200-040, ATCC) were purchased from LGC standards (Middlesex, UK). Methylthiazolyldiphenyl-tetrazolium bromide [MTT, (lot number: 1721505)] and trypan blue stain, 0.4% (lot number: 1696154) were obtained from Thermo Fisher Scientific (Paisley, UK).

5.3 Method

5.3.1 Optimization of cell concentration for MTT and wound scratch assays

The stock culture of primary epidermal keratinocytes (PEK, adherent cells) were stored in a liquid nitrogen tank (-180 ℃) using dimethyl sulfoxide (DMSO) as a cryopreservative. The frozen cells were thawed according to ATCC recommended protocol. In brief, the stock cryopreserved cells were initially thawed in running tap water for approximately 90 seconds. The vial was wiped with tissue paper and sprayed with 70% IMS (industrial methylated spirits). All of the operations from this point were carried out in laminar flow hood. The vial's content and 5 ml of warmed complete growth medium were transferred to a 15 ml centrifuge tube. The vial was rinsed with 1 ml complete growth medium and transferred to the centrifuge tube to recover any remaining cells left in the vial. After that, 4 ml complete cell growth medium was added to the centrifuge tube to bring the total volume to 10 ml. The cells were spun at 150 x g for 5 min. The supernatant was discarded, and the white pellet was re-suspended in 2 ml of complete growth medium. At this point the number of cells were counted with haemocytometer and seeded into culture flasks at the density of 2500-5000 cells/cm^2 in dermal cell basal medium supplemented with the keratinocyte growth kit for 6−7 days until 80−85% confluence was reached. The cells were detached by trypsin-EDTA solution according to ATCC recommended protocol (**Chapter 8: A.5.2**). One in two serial dilutions (4 x 10^5 to 6.25 x10^3 cells/ml) of cells

were prepared in complete growth medium and seeded in 96-well plate to determine optimal cell counts. Aliquots (100 µl) of each dilution were plated out in triplicate into wells of three separate microtiter plates. After that, MTT assay (thiazolyl blue tetrazolium bromide) was carried out at 24, 48 and 72 h to determine the optimum concentration of cells. Absorbance versus number of cells curve was plotted to identify the liner correlation between MTT absorbance and the number of cells.

5.3.2 Preparation of samples for MTT and wound scratch assays

The tested films (6 mm) and wafers (15 mm) were sterilized in a flow cabinet (NU-437-300E, NUAIRE) with UV light turned on overnight. The sterilized films and wafers were then immersed in 1.5 and 2.5 ml of complete growth medium respectively and placed in the incubator (Heracell 150i CO2 incubator, Thermo Scientific) at 37 ℃ in 5% (v/ v) CO_2 for 24 h. The extracts were collected through filtration using 0.2 µm filter and transferred into sterile Eppendorf tubes.

5.3.3 MTT (cell viability) assay

Cell proliferation was determined by an indirect cytotoxicity assay in which sample extracts were tested instead of direct contact of dressings with the cells. The cells were seeded into 96-well microtiter plates at optimum density (10,000 cells/well). The plates were incubated at 37 ℃ in 5% (v/ v) CO_2 for 5 h to allow cell adherence. After that, media was removed and 100 µl of each sample extract was placed in triplicate into the wells. The plates were left in the incubator at 37 ℃ for up to 72 h. After each time point (24, 48 and 72 h), 10 µl of MTT reagent was added to each well including blank (medium only). The plates were returned to the incubator for 4 h or more until a purple precipitate was clearly visible under the inverted microscope (AE2000, Motic). The media was then removed and 100 µl of DMSO was added to all wells including controls. The plates were again returned to the incubator for 30 min and the absorbance recorded at 492 nm by a microtiter plate reader (Multiskan FC, Thermo scientific) equipped with SkanIt for Multiskan FC 3.1 software (Thermo scientific). Every experiment was carried out in triplicates and repeated three times. The percentage of viable cells was calculated using **Equation 5.1**.

$$\text{Cell viability (\%)} = \frac{At-Ab}{Ac-Ab} * 100 \qquad \qquad \text{(Equation 5.1)}$$

Where At, Ab and Ac are the absorbance of tested samples, blank (medium only) and negative control (untreated cells) respectively.

Additionally, the effect of sample extracts on the cells morphology and adherence was shown microscopically by FLoid® Cell Imaging Station (for CIP loaded dressings) and fluorescence microscopy (Nikon Eclipse Ti-U, UK) (for FLU and combined DL dressings). In this study, the untreated cells and Triton-X-100 (0.01 w/v) treated cells were used as negative (100% viable) and positive controls respectively. Algisite Ag® and Actiformcool® were chosen as representative standard commercial samples for the MTT and wound scratch assays.

5.3.4 Wound scratch (cell migration) assay

The PEK cells were seeded into 24-well tissue culture plates at an initial density of 50,000 cells/well so that they could reach about 80−85% confluence as a monolayer after overnight incubation. However, if the cell layer did not yet confluent, incubation period extended until confluency was reached. The wound gap was created with a sterile 200 μl micropipette tip by scratching in the monolayer vertically (Satish and Korrapati, 2015). To create a consistent gap size, scratching was performed on the centre of the each well with the same size of micropipette tip. The gap distance was equal to the outer diameter (775 μm) of the end of the tip. After scratching, the wells were gently washed twice with D-PBS without affecting monolayer to remove the detached cells (Manoj *et al*., 2009). The sample extracts (see the list of tested samples in **Table 5.1**) were then added in each well. Wells treated with Triton-X-100 (0.01% w/v) and untreated wells were considered as negative and positive control respectively. The migration of cells (representing wound closure) was observed by a fluorescence microscopy (Nikon Eclipse Ti-U, UK) and digital images were captured at the time interval of 0, 1, 2, 3, 7, 8 and 9 days. The images were taken at green bright field mood. To obtain the maximum field of view, a low magnification (4x objective lens) was used whilst capturing images. The wound gaps were evaluated using NIS-Elements software. The percentage of wound closure was calculated based on the length (μm) of wound measured at the specific time as mentioned in **Equation 5.2** (Amin *et al*., 2017).

$$Wound\ closure\ (\%) = \frac{d_0 - d_t}{d_0} \qquad \text{(Equation 5.2)}$$

Here, d_0 represents the length (µm) of the wound was initially created, and d_t refers to the length (µm) of the wound recorded at specific time intervals.

In this study, Triton-X-100 and untreated cells were used as negative and positive control respectively. Moreover, Actiformcool® was chosen as representative standard commercial samples to validate the experiment.

Table 5.1 List of samples tested to evaluate wound healing properties by cell migration study.

Sample	Formulation
Films	CA-BLK
	CA-CIP 0.005%
	CA-FLU 0.05%
	CA-CIP:FLU (1:10)
Wafers	CA-BLK
	CA-CIP 0.005%
	CA-FLU 0.05%
	CA-CIP:FLU (1:10)
Commercial product	Actiformcool®

5.3.5 Statistical analysis

The statistical differences in the result of MTT and wound scratch assays were evaluated using One-way ANOVA test. The differences were considered significant at a 0.05 significance level.

5.4　Results and discussion

5.4.1　Optimization of cell concentration for MTT and wound scratch assays

The colorimetric MTT assay is based on enzymatic conversion in which MTT is converted to purple formazan by the action of dehydrogenase enzymes (Zhou *et al*., 2013) secreted by viable cells. The purple formazan accumulates inside cells as insoluble precipitate. Therefore, solubilizing agent (DMSO, acidified isopropanol, sodium dedoxy sulphate, and dimethylformamide) are used prior to recording absorbance readings (Mosmann, 1983). The quantity of formazan is presumably proportional to the viable cell numbers (Riss *et al*., 2013). The dead cells are unable to convert MTT to purple formazan.

In this study, the concentration of cells for the cell viability and wound scratch studies was optimized by MTT assay. A linear correlation between the concentration of cells and absorbance was detected at 24, 48 and 72 h (**Figure 5.1**). It can be observed that log 10^5 cells/ml was within the linear portion of the curve over 72 h. Therefore, MTT cell proliferation and wound scratch assays of medicated dressings were performed by selecting the optimized number of cells (1 x 10^5 cells/ml).
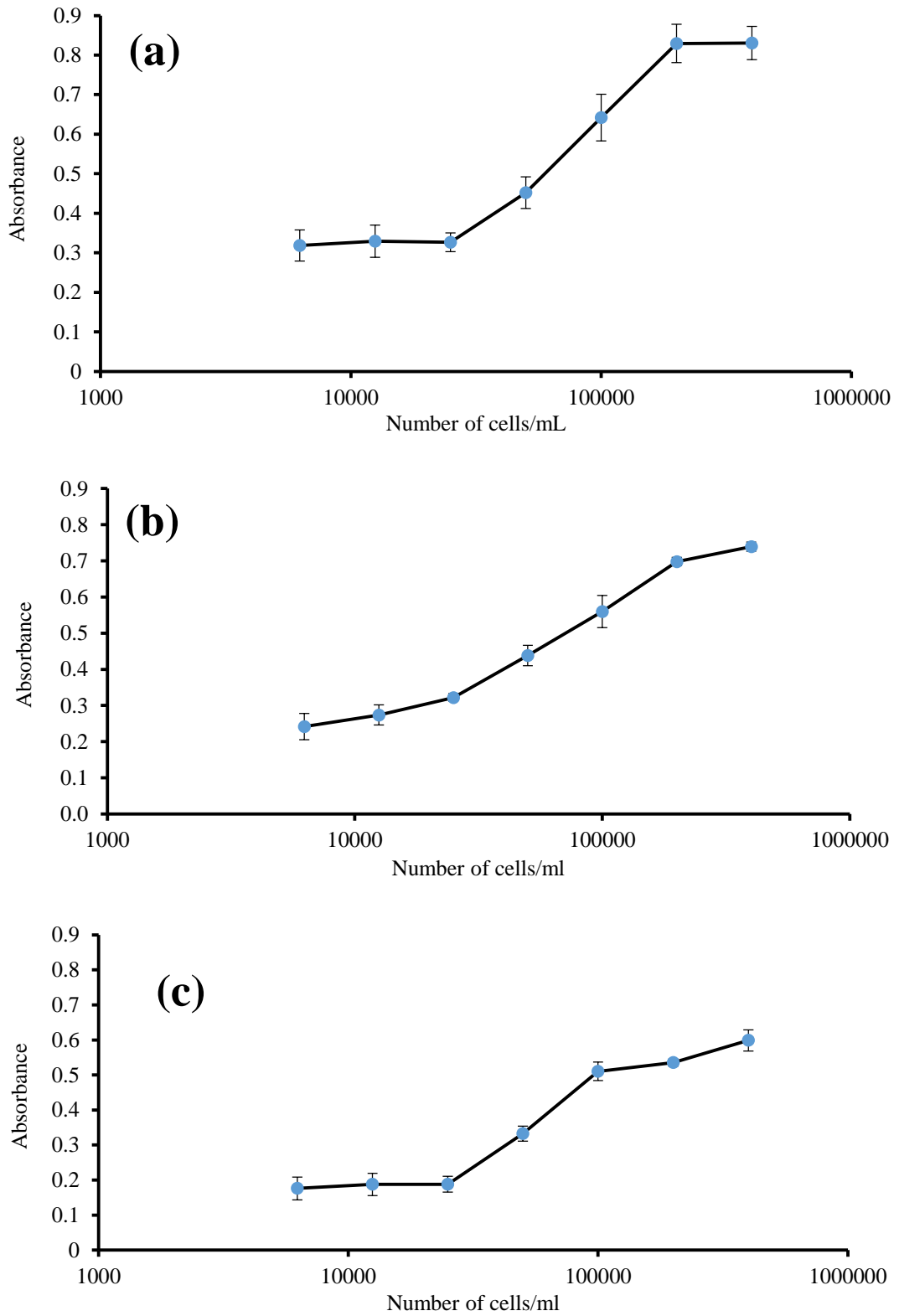
Figure 5.1   Determination of the optimal number of cells for the cell viability assay at (a) 24 h, (b) 48 h and (c) 72 h ($n = 3 \pm$ SD).

5.4.2 MTT assay

Biocompatibility is a vital requirement recommended by the International Organization for Standardization (ISO) for the safe use of medical devices and materials such as drug loaded dressings, which are likely to come into contact with the wounded skin as well as normal skin. Cytotoxicity test is an integral part of biological evaluation, which determines the prevalence of toxic effect and determines the presence of positive influence in terms of biofunctionality that promotes wound healing (Wiegand and Hipler, 2008). The biocompatibility of DL dressings was evaluated using *in vitro* cultures of PEK cell line for 24, 48 and 72h respectively. Keratinocytes are the main cellular component of human skin and therefore, selected as an *in-vitro* model for MTT assay. Moreover, PEK has been investigated as a useful model for testing *in vitro* wound healing activity in the literature (Kim *et al*., 2007; Moritz *et al*., 2014; Sacco *et al*., 2015).

5.4.2.1 CIP loaded dressings

MTT assay revealed that the polymer (CA) used in this study was non-toxic to human keratinocyte cells. The BLK film and wafer were found to be highly biocompatible with the cells, showing the highest percentage of cell viability ($95.27 \pm 2.84\% - 96.57 \pm 2.19\%$) (Figure 5.2 & Figure 5.3). All CIP loaded films showed more than 80% cell viability over 72 h. According to the ISO guideline (DIN EN ISO 10993-5), the *in vitro* cell viability of medical devices and materials after exposure should be $\geq 70\%$ to be considered as non-cytotoxic (Moritz *et al*., 2014). Therefore, according to these guidelines all CIP loaded films exhibited acceptable cell viabilities of PEK. Time dependent cell viability of PEK was also observed when treated with CIP loaded films. The untreated cells were set as 100% viable (negative control) whereas, Triton-X-100 solution (0.01%) was used as positive control for cell cytotoxicity caused a drastic reduction of keratinocytes viability to values <10% after 72 h (**Figure 5.2**). These data correlated well with the findings of other published work describing Triton-X-100 (0.01%) as positive control under in vitro culture of keratinocytes (Moritz *et al*., 2014). The cytotoxicity of Triton-X-100 is associated with the interaction between its monomer and the lipid bilayer present in the cells. The polar head group of Triton-X-100 reacts with lipophilic substances and phospholipids of cell membranes resulting in disruption of compactness and integrity of the lipid membrane, causing breakdown of cellular structure and ultimately leading to cell death (Koley and bard, 2010). Additionally, the keratinocytes were observed microscopically before and after treatment with the samples. In the case of DL dressings, the viable cells appeared as

polygonal structures adhered to the well plates (image not shown). Very few dead non-adherent cells were observed after treating with the dressings, whereas most of the cells were floating when treated with Triton-X-100. There was no reduction of adherent cell numbers in untreated cells. These observations further confirm the non-toxic nature of the DL dressings compared to the known toxic Triton-X-100.
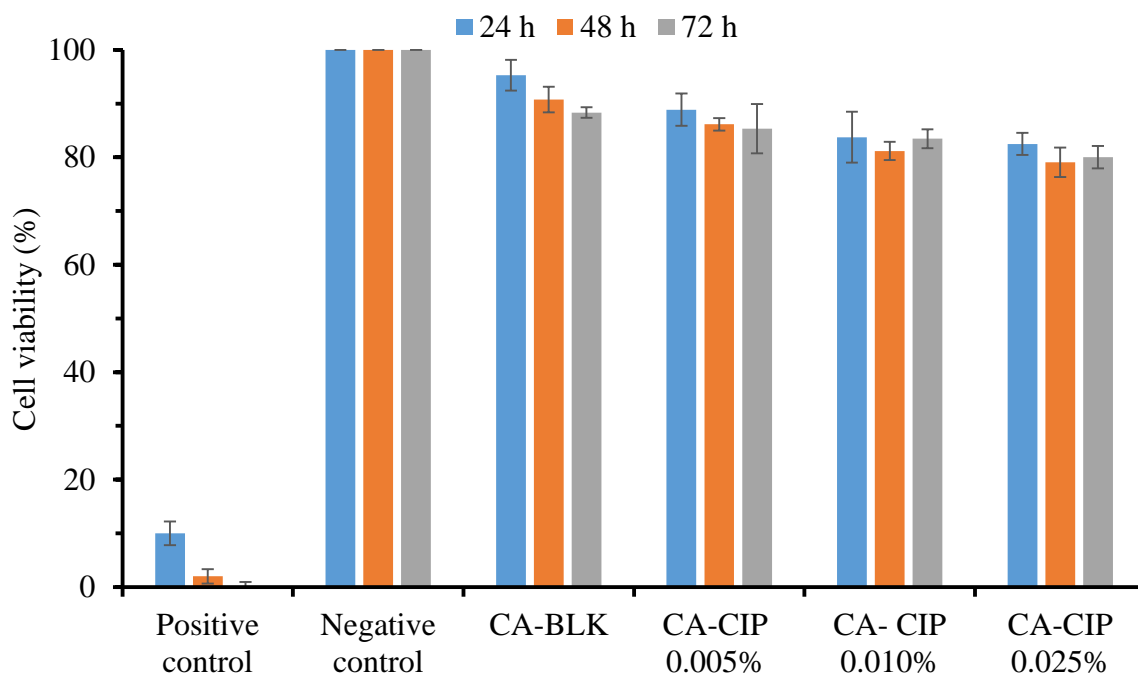
Figure 5.2 Cell viability of human primary epidermal keratinocytes after exposure to the extracts of BLK and CIP loaded films for 24, 48 and 72 h (mean $\pm$ SD, n = 9). In this study Triton-X-100 (0.01% w/v) and untreated cells were used as positive and negative control respectively.

The CIP loaded wafers were found to be highly biocompatible with little influence on the viability of the keratinocytes as shown in **Figure 5.3**. Wafers containing 0.0001 − 0.025% CIP exhibited more than 85% cell viability whereas 0.040% CIP loaded wafer and Algisite Ag® showed just below 80% cell viability over the 72 h incubation period which are acceptable according to ISO (DIN EN ISO 10993-5). The positive control Triton X-100 showed more than 100% cytotoxicity and resulted in a significant reduction in cell viability to values below 0% after 72 h treatment, which was to be expected. A time-dependent toxicity was also observed after treatment of PEK cells with the extracts of CIP loaded wafers and Algisite Ag®. Moreover, dressings containing CIP have been reported safe to fibroblasts (Unnithan *et al*., 2012). However, pure CIP has been reported to exhibit time dependent cytotoxicity on fibroblast cell

lines at concentrations of 0.129 and 0.194 mM, following 48 and 72 h of exposure respectively (Gurbay *et al.*, 2002). On the other hand, none of the literature reviewed reported the cytotoxicity of CIP loaded dressings on PEK cell lines. Therefore, the present work reveals that CIP loaded lyophilized wafers are non-toxic to PEK and appear to be safe dressings for healing of DFUs.
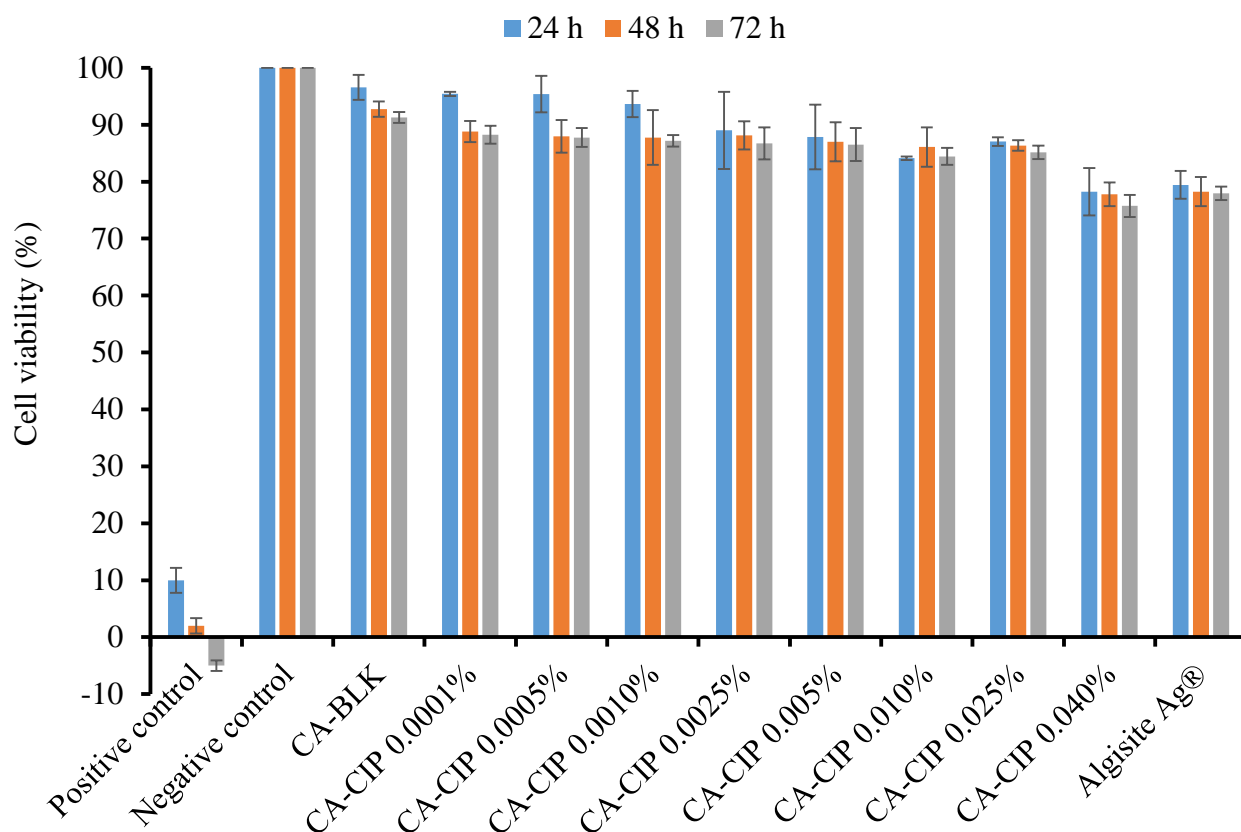
Figure 5.3 Cell viability of human primary epidermal keratinocytes after exposure to the extracts of CIP loaded wafers and fibre mat, Algisite Ag® for 24, 48 and 72 h (mean ± SD, *n* = 9). In this study Triton-X-100 (0.01% w/v) and untreated cells were used as positive and negative control respectively.

Figure 5.4 illustrates the images of cells after treating with extracts of CIP loaded films and wafers respectively. The cells exhibited the lowest confluence after treating with Triton-X-100 as positive control. On the other hand, the untreated cells as negative control were grown as a confluent layer. However, with increasing amount of CIP in dressings and time, the morphology as well as the density of the cells was changed (**Chapter 8: Table A.5.1 & A.5.2**). Further extensive study of cell attachment needs to be done to better understand the changes in morphology of the cells after treating with the dressings. The adherent

cells detached from the surface of culture plates and were floating in the media and appeared as dead cells.

Positive control	Negative control

CA-CIP Film	CA-CIP Wafer
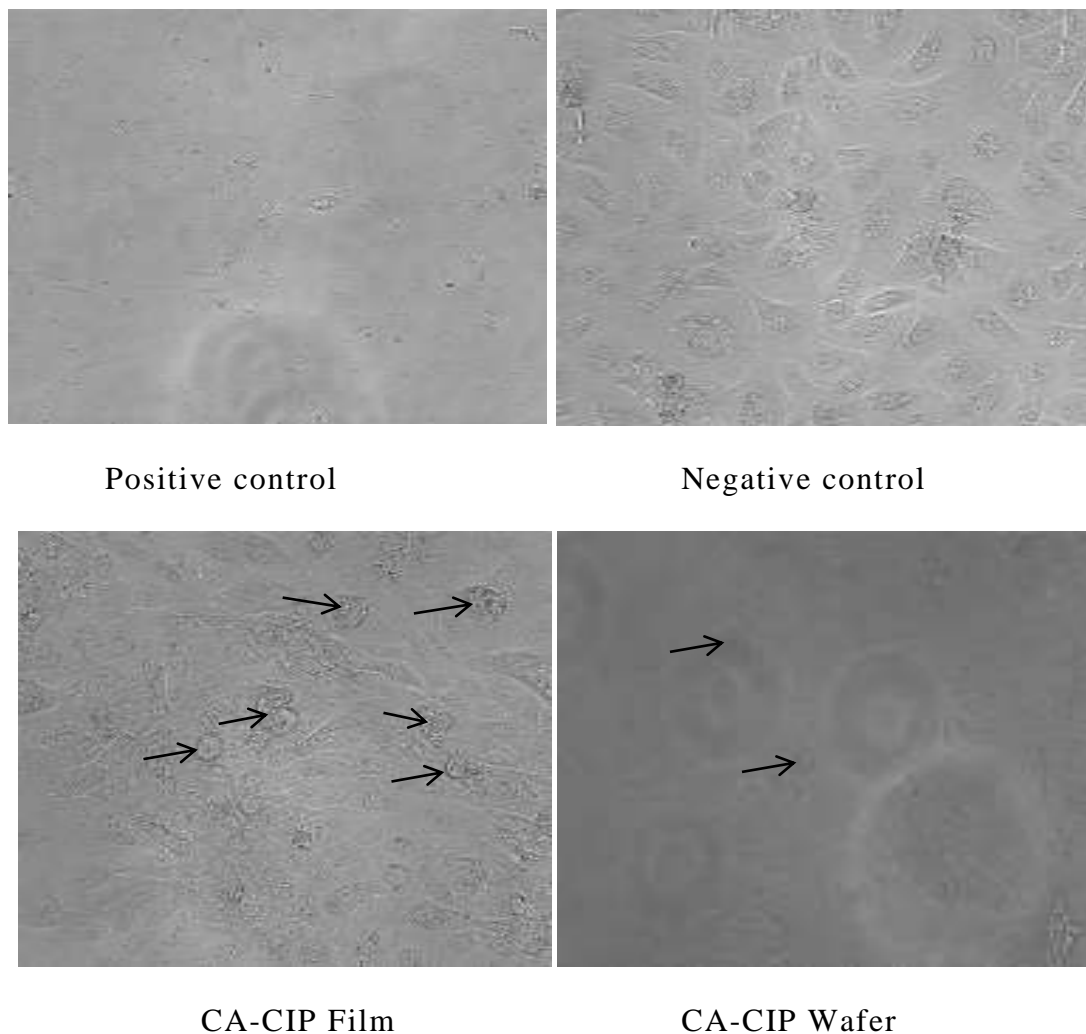
Figure 5.4 The microscopic observations of live/dead cells of human primary epidermal keratinocytes treated with CIP loaded dressings after 72 h of culture. Polygonal shape indicates live cells while black arrows indicate the floating round shape as dead cells. Images were taken by FLoid® Cell Imaging Station with 40x objective lens.

5.4.2.2   FLU loaded dressings

The FLU loaded dressings were treated with human keratinocyte cells to investigate the safety profile of the medicated dressings. In this study, Triton-X-100 (positive control) killed all cells compared to untreated cells (negative control) after 72 h of exposure. FLU loaded dressings exhibited dose and time dependent cytotoxicity on PEK. Wafers containing more than 0.15% FLU showed less than 70% cell viability after 48 and 72 h which failed to comply with the standard cell viability of ISO. FLU is relatively low lipophilic (log P 0.5) in nature due to

presence of hydroxyl groups (Mikamo *et al.*, 2000), therefore high amount of FLU may accumulate in the lipid rich cell membrane and interfere with hydrogen bonding responsible for tight packing of the lipid membrane, resulting in looser packing of cellular integrity (Teixeira *et al.*, 2015). However, the dressings containing up to 0.15% FLU appeared to have more than 80% cell viability over 72 h (**Figure 5.5**), suggesting its low toxicity and can modestly enhance cell proliferation and migration. The concentration and time dependent toxicity of FLU loaded dressings can also be observed in morphological observation (**Table A.5.3**). The cell density appeared to decrease gradually after longer incubation times (24−72 h) and higher dose of FLU (0.30% and 0.40% w/v) in the dressings. **Figure 5.6** clearly demonstrates the keratinocytes growth while treating with FLU loaded dressings and the cell growth was confluent as the negative control. These results showed high biocompatibility and viability of FLU loaded dressings.
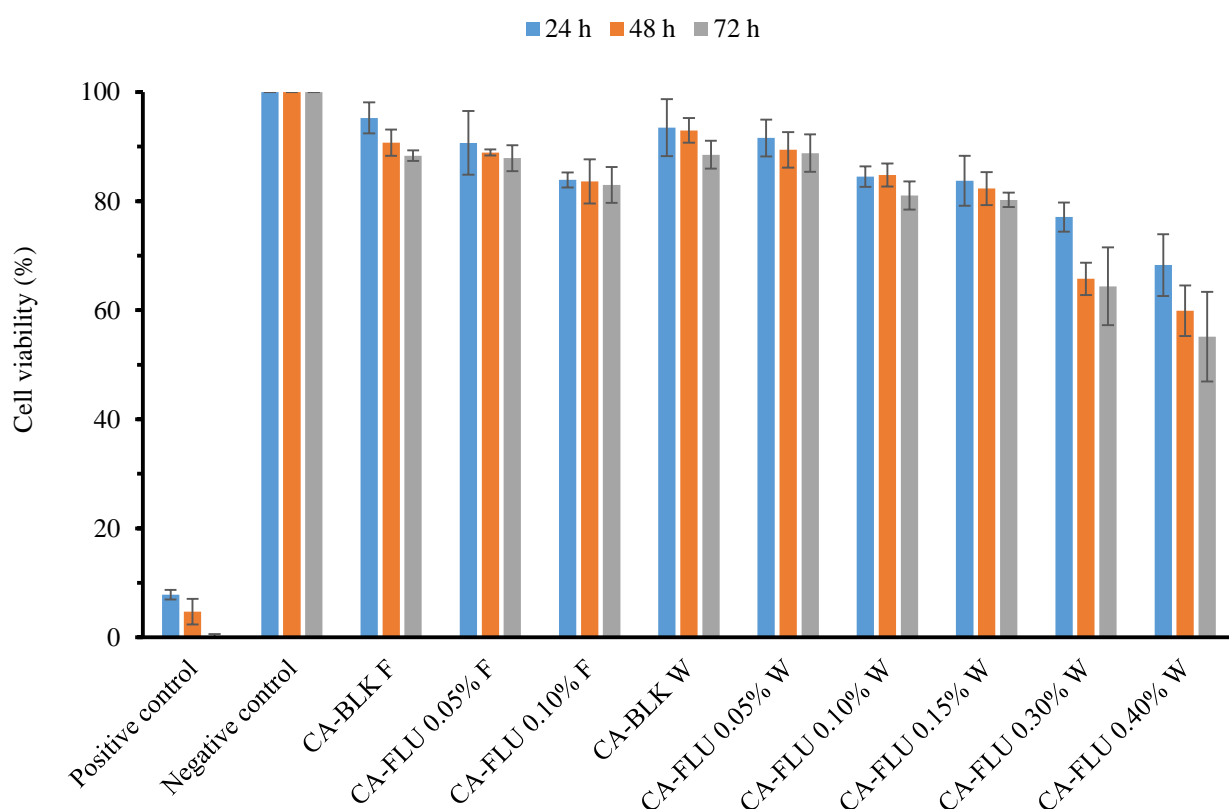
Figure 5.5   Cell viability of human keratinocyte cells incubated with the extracts of FLU loaded dressings. Triton-X-100 and untreated cells were considered as positive and negative controls respectively ($n = 3 \pm$ SD). F: Film; W: Wafer

Positive control   Negative control

CA-FLU Film   CA-FLU Wafer
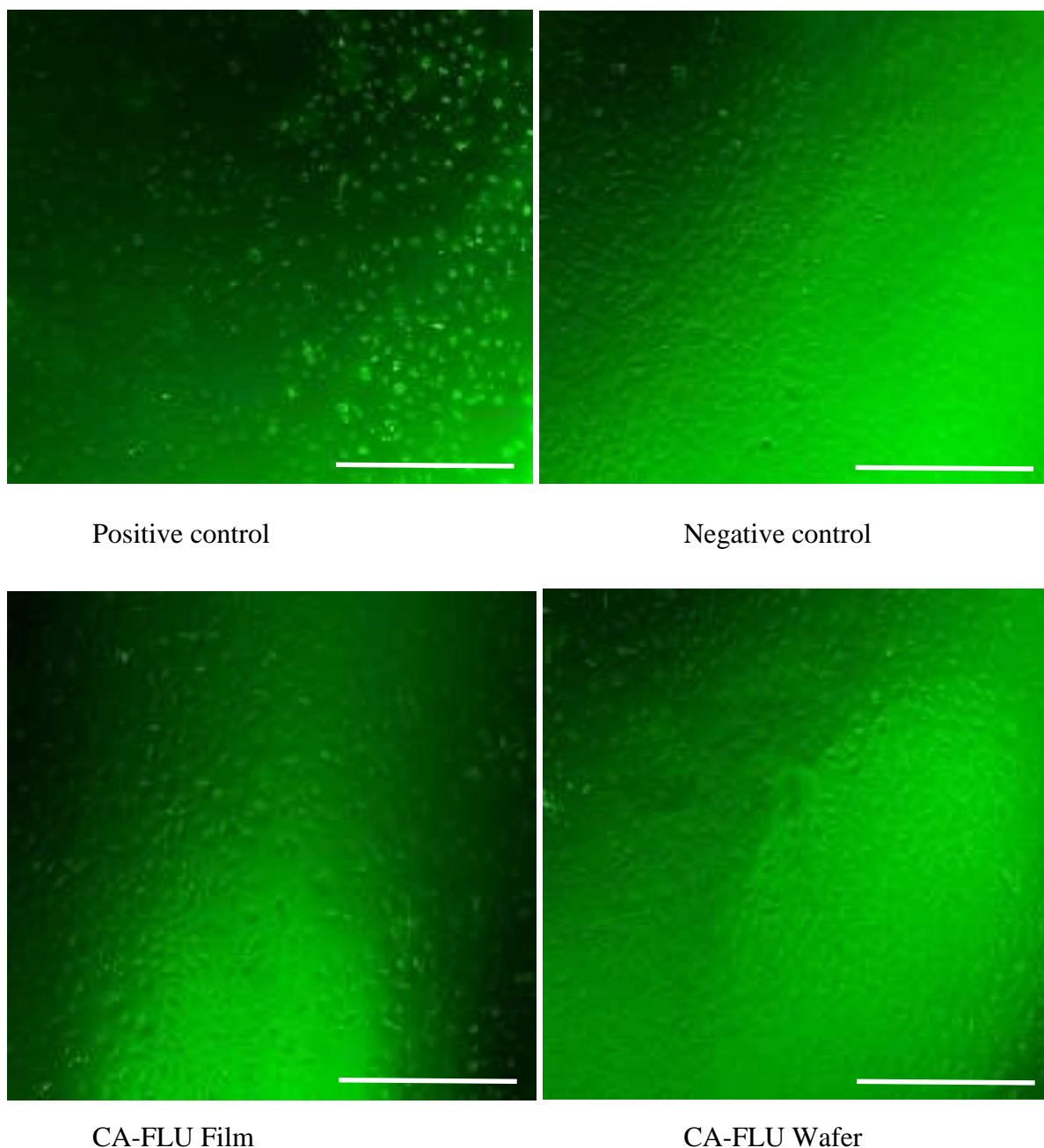
Figure 5.6 Representative photomicrographs (4x) of keratinocyte cells' morphology based on viability test of FLU loaded dressings. Triton-X-100 and untreated cells were considered as positive and negative controls respectively. Scale bar: 500 µm.

5.4.2.3   Combined DL (CIP/FLU) dressings

Figure 5.7 shows the percentage cell viability after treating with the extracts of various combined DL dressings. The untreated cells were considered as 100% viable and Triton-X-100 showed the highest toxicity about 95% after 72 h of incubation. The molecular mechanism of cell toxicity of Triton-X-100 was explained in the previous section (**5.4.2.1**). MTT assay revealed that keratinocyte cells were viable after the exposure of BLK and DL dressings (films

and wafers) with over 90 and 80% respectively after 72 h of culture. It was observed that the cell viability of keratinocytes after exposure to BLK and combined DL dressings decreased with time. In comparison, cells in contact with the different combined DL films and wafers did not show any significant differences ($p = 0.92$) in cell viability between the dressings. The cell viability decreased with increasing amount of FLU in the combined DL dressings. The same trend was also observed in the FLU loaded dressings (**Figure 5.6**) implying that the biocompatibility is dependent on the dose of FLU.
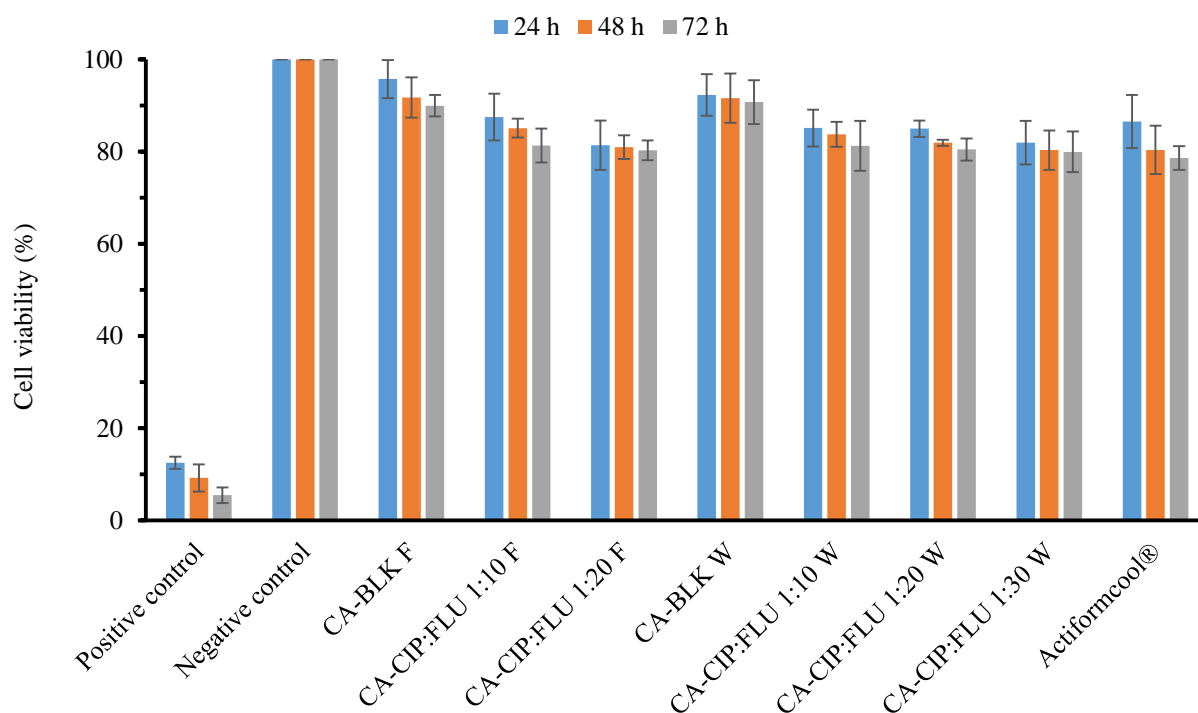
Figure 5.7   Percentage of cell viability of human keratinocyte cells after 24, 48 and 72 h of exposure to combined DL dressings and Actiformcool®. Triton-X-100 and untreated cells were used as positive and negative control respectively ($n = 3 \pm$ SD). F: Film; W: Wafer

However, none of the formulated combined DL dressings were considered as cytotoxic according to ISO standard as all combined DL dressings showed > 70% cell viability. The cell viability of Actiformcool® was recorded to be more than 85% after 24 h and about 80.35 ± 5.78% and 78.61 ± 2.56% after 48 and 72 h respectively.

Positive control	Negative control
CA-CIP:FLU (1:10) Film	CA-CIP:FLU (1:10) Wafer
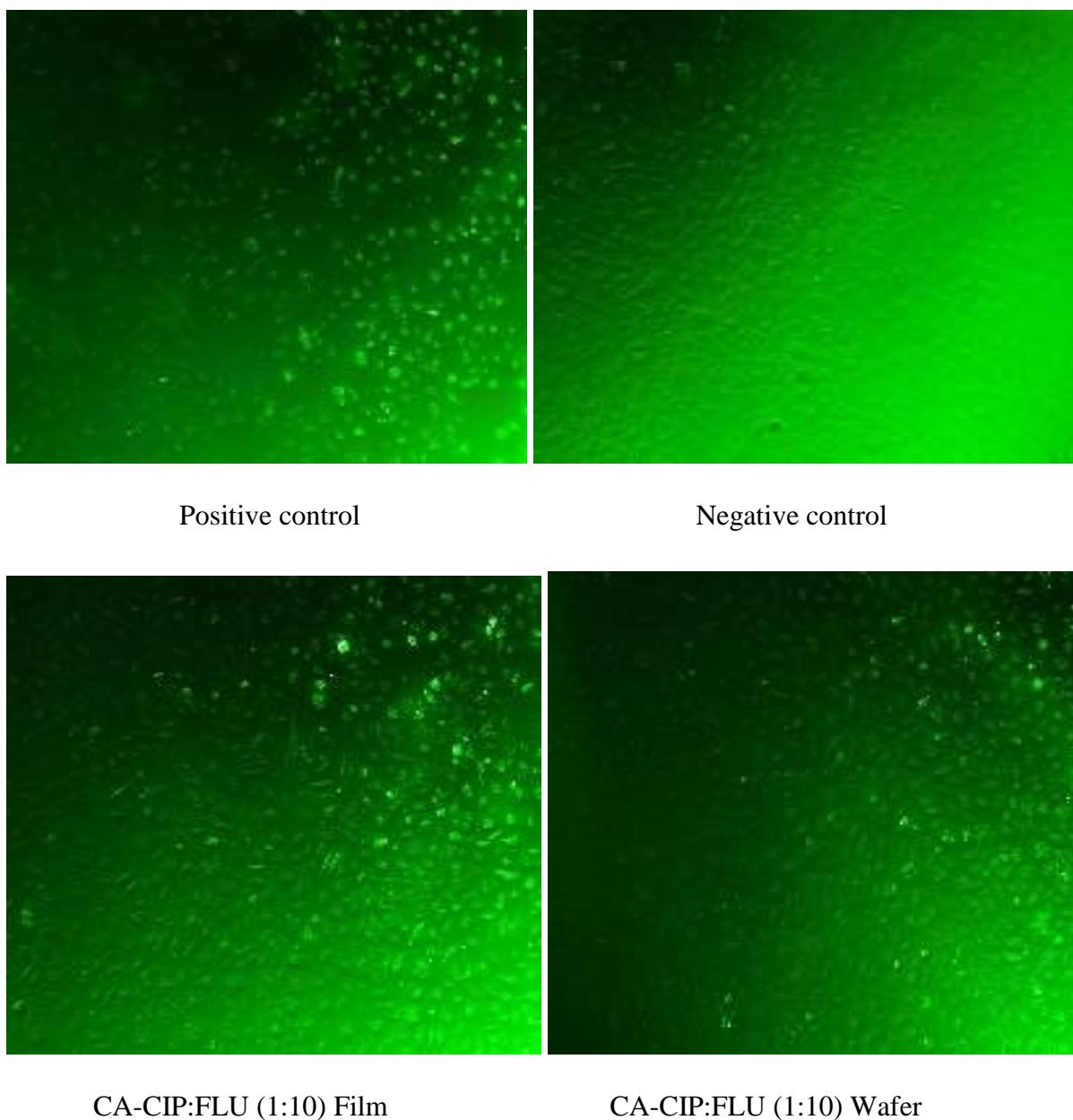
Figure 5.8 Photomicrographs (4x) showing the proliferation of human keratinocyte cells seeded at a density of 1×10^5 cells/ml with the combined DL dressings. Triton-X-100 and untreated cells were considered as positive and negative controls respectively. Scale bar: 500 µm.

The polygonal shaped PEK cells grew confluent as a monolayer when treated with the dressings containing both CIP and FLU. The cells continued to grow uniformly over 72 h. However, the confluence of PEK cells slightly changed after 72 h (**Table A.5.4**). The interaction between drugs and cells might cause cell death resulting in detachment of the cells from the surface of culture plate. There were no significance changes in morphology of PEK cells between combined DL films and wafers, which was also supported by the cell viability assay.

Actiformcool® also demonstrated similar biocompatibility as the prepared dressings thus validated the experiment. PEK cells treated with Triton-X-100 shrunk, became necrotic and detached from the culture plates.

5.4.3 Wound scratch (cell migration) assay

Migration of keratinocytes is important for wound healing, because a wound cannot heal without reepithelialization (Xiao et al., 2016). In chronic DFUs, keratinocytes experience hyperglycaemia and supraphysiological oxidative stress, which challenge keratinocytes viability and migration (Spravchikov et al., 2001; Schafer and Werner, 2008). Therefore, in this study the effect of the various formulated dressings on human keratinocyte cell migration was evaluated by an in vitro wound scratch assay. As shown in **Figure 5.9 a,** keratinocytes barely migrated into the wound gap (about $7.63 \pm 1.99\%$) after 3 days of treating with Triton-X-100 (negative control). After 7 days, no cell migration was observed in case of Triton-X-100, because all the surrounding cells of wound gap died (**Table 5.2**). In the case of untreated cells (positive control) keratinocyte migration (wound closure) was about $81.50 \pm 2.00\%$ after 3 days and complete wound closure (100%) was observed after 7 d. The wound closure of all cells treated with dressings was also completed by 7 days except the cells treated with combined DL dressings (film and wafer) and Actiformcool® (**Figure 5.9, Table 5.2 and Table 5.3**). However, the initial cell migration rate (1-3 days) of untreated cells were higher than any treated cells. This could be due to acclimatization of cells to adapt to the samples that resumed normal growth. Interestingly, cells treated with FLU loaded dressings showed higher rate of initial wound closure than the cells treated with CIP loaded dressings. The possible explanation for the lower initial wound closer by CIP loaded dressings may be a possible zwitterionic effect of CIP (Cavet et al., 1997) that enhanced the interaction with lipophilic substances and phospholipid of cell membrane, leading to disruption of cell membrane and resulting in lower cell proliferation. It has been reported that canine corneal epithelial cells treated with CIP showed high degree of morphological changes (rounding, shrinkage and detachment of cell) which reduced cell migration (Hendrix et al., 2001). It is also reported that CIP has inhibitory effect on tenocytes (tendon cells) migration (Tsai et al., 2009). On the other hand, FLU has high penetration capability into various tissue without affecting the functions of phagocytes (Gurer et al., 1999). FLU has also been reported to be highly biocompatible with human cells and having tolerable erythrocyte haemolysis (Oliveira et al., 2015). There was a clear tendency that keratinocytes treated with combined DL dressings demonstrated a slower wound healing

rate ($70 \pm 2.76\%$ to $78 \pm 1.14\%$ after 8 days of culture) compared to BLK and single (CIP or FLU) DL dressings, and untreated cells (**Figure 5.9 & Table 5.2**).
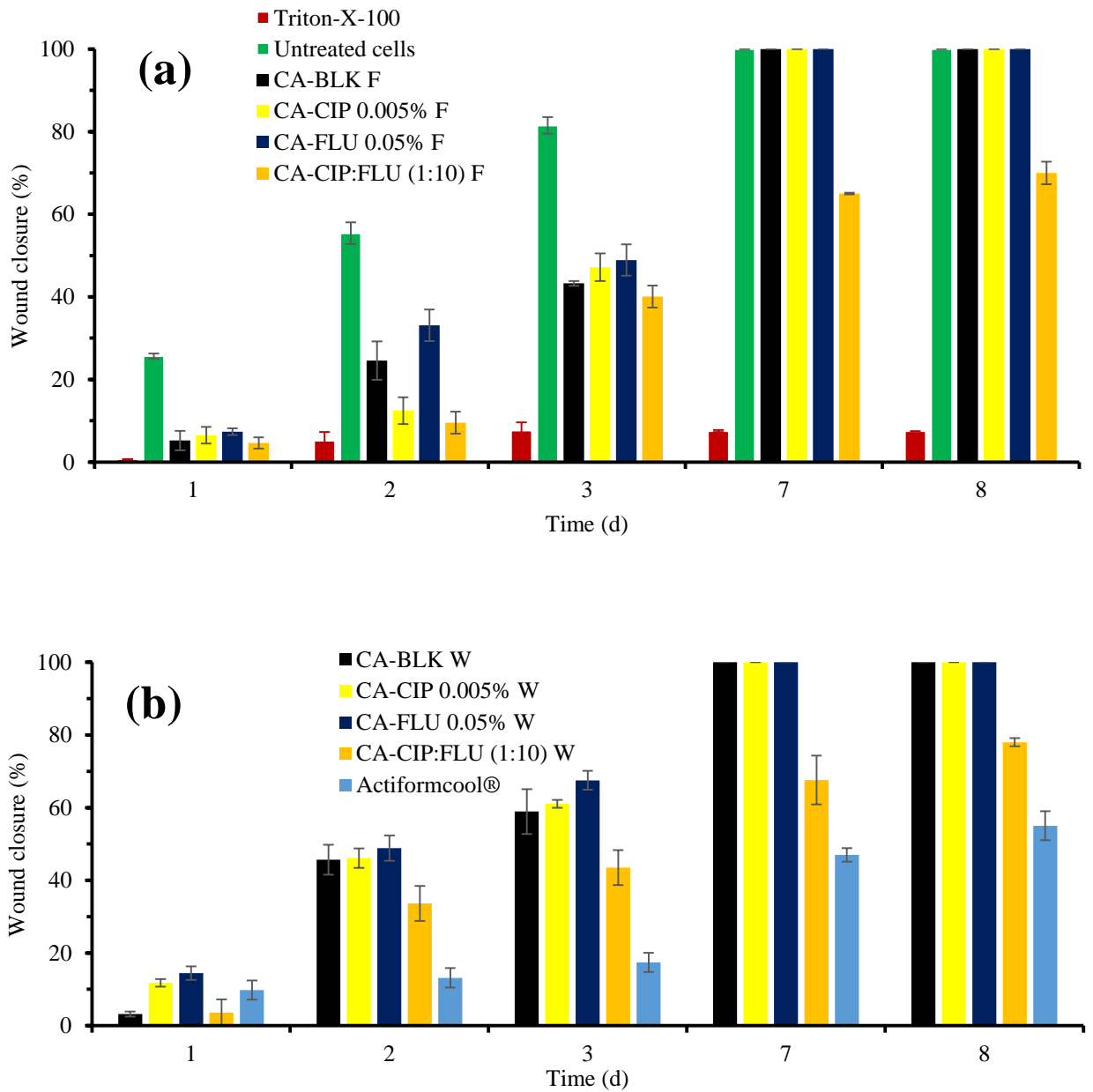
Figure 5.9   *In vitro* wound scratch assay on human keratinocytes treated with medicated (a) films and (b) wafers and Actiformcool® ($n = 3 \pm SD$). F: Film; W: Wafer

Cells treated with the commercial product (Actiformcool®) showed slower rate of migration than the cells treated with formulated dressings. After 8 days of culture, representative wounds treated with Actiformcool® exhibited a wound closure of $55.01 \pm 3.99\%$ compared to the initial wound gap. Overall the results obtained through wound scratch assay revealed that the selected dressings had a positive effect on the *in vitro* wound closure rate and could play a potential role

in wound healing applications. However, *in vivo* wound healing need to be investigated to elucidate the effectiveness of the dressings.

Table 5.2 *In vitro* wound scratch assay on human keratinocyte cells treated with the extracts of medicated films. Triton-X-100 and untreated cells represent as positive and negative control respectively. The blue arrows indicate wound gap (migration zone). Scale bar: 500 μm.
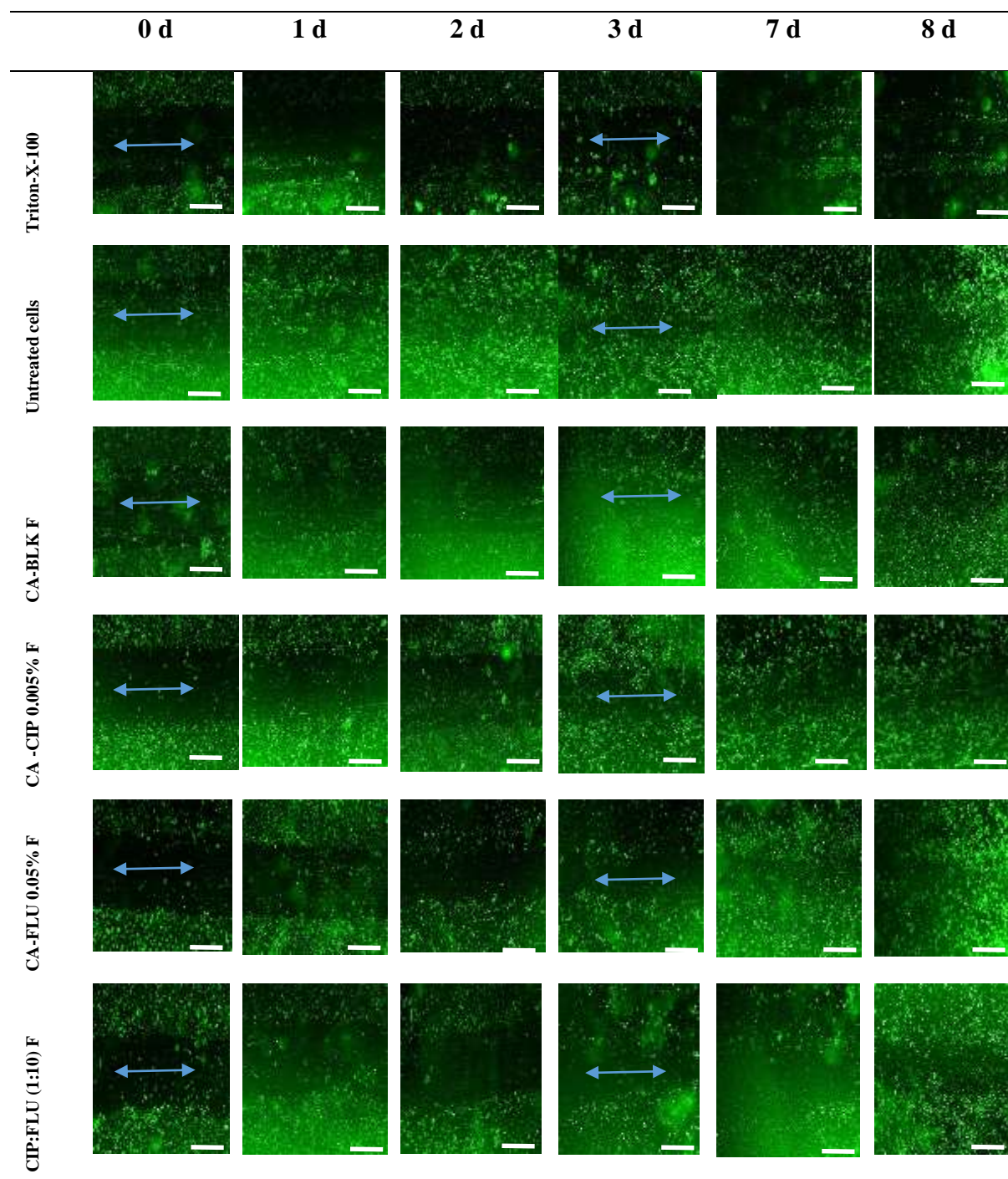
Table 5.3 Representative microscopic images showing the migration pattern of human keratinocyte cells treated with medicated wafers and commercial Actiformcool® dressing at 0, 1, 2, 3, 7 and 8 days. The blue arrows indicate wound gap (migration zone). Scale bar: 500 µm.
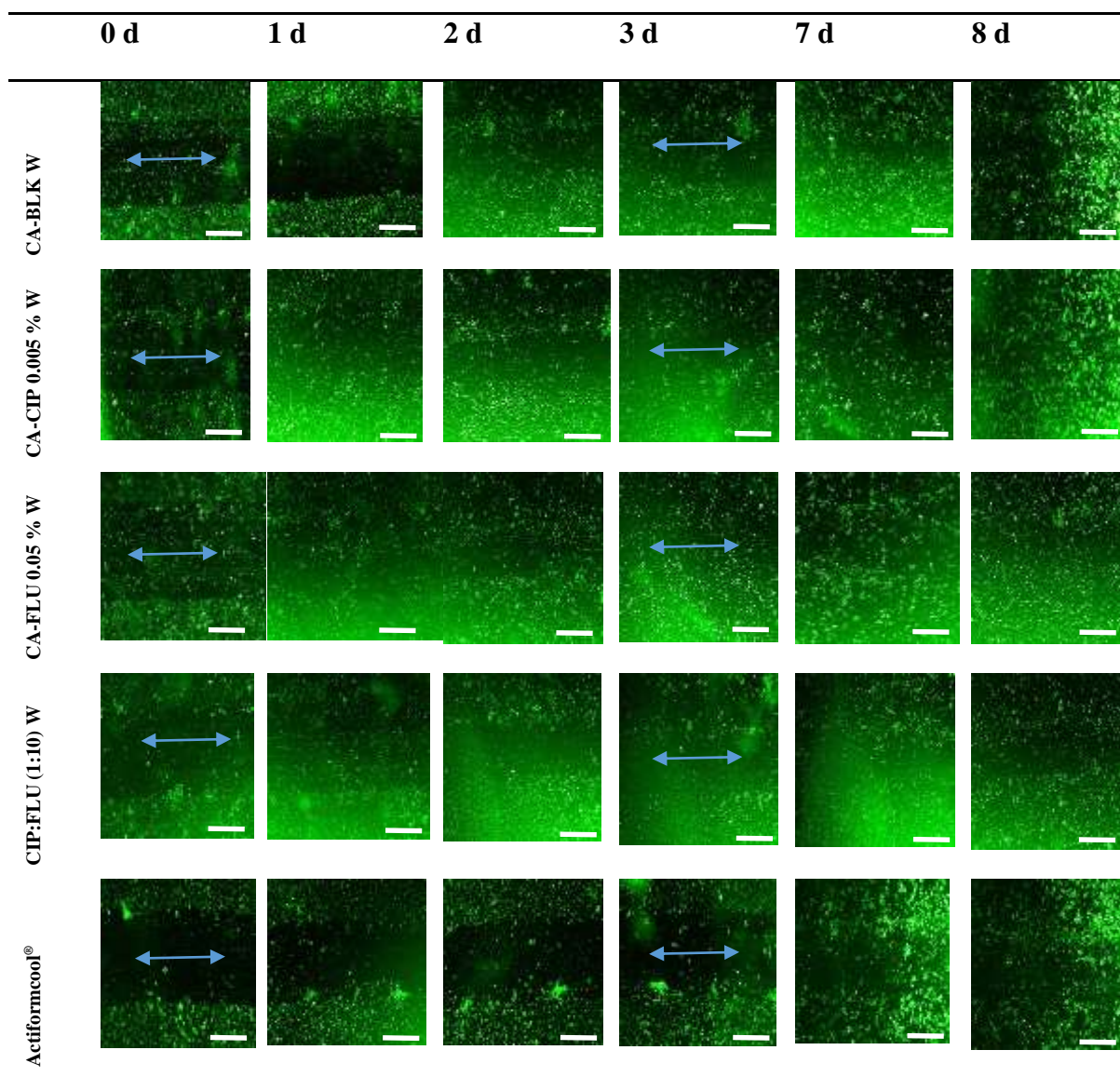
5.5 Conclusions

MTT and wound scratch assay are important experiments to assess wound healing properties of dressings. The effect of medicated films and wafers on the viability and migration of human keratinocytes were studied in this chapter. The results showed that all the dressings except the dressings containing more than 0.15% FLU exhibited acceptable cell viability above 70% with respect to ISO standard. Dose and time dependent cytotoxicity of the DL dressings were observed. The CIP and FLU loaded dressings showed complete wound closure within 7

days, whereas combined DL dressings exhibited more than 65% wound closure in that time. In addition, all the DL dressings showed better wound healing properties in terms of cell viability and migration than Actiformcool® commercial dressing. However, studies of cell attachment and *in vivo* animal testing are needed to elucidate the wound healing action of the prepared dressings.

CHAPTER 6:   SUMMARY DISCUSSION AND FUTURE WORK

6.1   Summary discussion

Treating of mixed infections in chronic leg and diabetic foot ulcers (DFUs) is not well developed. However, the medical and research communities are starting to realize that the chronicity of wounds such as DFUs can in part be attributed to the diversity of microbial populations in such chronic wounds. This project aimed to develop, formulate, characterize and optimize advanced medicated dressings containing broad-spectrum antibacterial (ciprofloxacin) and antifungal (fluconazole) drugs to potentially target mixed infections in DFUs. Polymeric based dressings have advantages of avoiding systemic side effects, obtaining effective drug concentration at the target site and biocompatibility to host cells. Calcium alginate (CA) was chosen as a base polymer due to its haemostatic effects in the initial stage of wound healing. Ciprofloxacin (CIP) was selected as a model antibacterial drug, because it has been reported as a powerful antibiotic used in chronic wounds, which can kill/inhibit the causative bacteria [(e.g. *Escherichia coli* (*E. coli*), *Staphylococcus aureus* (*S. aureus*), *Pseudomonas aeruginosa* (*P. aeruginosa*)] present in DFUs. On the other hand, fluconazole (FLU), a highly effective antifungal agent against the most predominant candida species present in DFUs, was selected as drug for incorporation in the CA based dressings. Solvent cast films and lyophilized wafers were prepared as a potential means of delivering the antimicrobial agents, because they are meant to be multifunctional for preventing microbial infections as well as maintaining a moist wound environment to aid healing. Film dressings have advantages of elasticity that allow application to any part of the body and their transparency allows visualization of the wound bed without removal, thus reduces the chances of traumatizing the wound. On the other hand, wafer dressings can absorb large amounts of wound exudates and allow evaporation of exudates thus preventing fluid accumulation underneath dressings and subsequently reducing skin maceration.

The CA gel (1%) was prepared by ion exchange method in which the divalent calcium ions were exchanged with the monovalent sodium ions. The resultant gels were oven and freeze dried to obtain films and wafers respectively. Interestingly, calcium carbonate ($CaCO_3$) precipitation was observed, confirmed by XRD. However, $CaCO_3$ is reported to have haemostasis properties and have regulatory effect on inflammatory cell filtration, fibroblast proliferation and keratinocyte migration. The unplasticized films were hard, inflexible, non-

elastic and unpliable. Therefore, the films were plasticized with different concentrations of glycerol (GLY) and GLY at 33.33% w/w (based on total dry weight) was found to be optimum concentration to obtain better flexible, tougher and more transparent films than any other plasticized films and was therefore used for drug loading.

CIP loaded films exhibited ideal optical appearance, whereas FLU loaded films did not show ideal transparency. However, the combined drug (CIP and FLU) loaded (DL) films showed better transparency than FLU loaded dressings. The blank (BLK) and all DL wafers were uniform in texture and thickness, soft and pliable in nature. The films were appeared as continuous sheets and wafers appeared as a porous (SEM observation) interconnecting network. FLU and combined DL films exhibited spherulitic crystallization whereas, CIP loaded films showed reduced crystallinity due to plasticizing effects. SEM observation also revealed that the BLK wafer had uniform and circular shaped pores while the uniformity of pores was disturbed after loading drugs. Increasing amount of CIP and FLU resulted in denser pores due to possible crosslinking between drugs and polymer. However, wafers containing up to 0.15% w/v FLU alone and combined CIP and FLU in the ratios of 1:10 and 1:20 showed large circular and uniform pore size distributions.

XRD observation revealed that all dressings retained same peak as of $CaCO_3$. The slight shifting of peaks of all DL dressings to higher diffraction angles indicated the interaction between drug and polymer, which was also confirmed by FTIR. Films containing 33.33% GLY showed the highest mechanical properties amongst all BLK plasticized films. However, none of the DL films as well as BLK exhibited ideal elasticity (30−50%). Texture analysis revealed that addition of CIP reduced rigidity of the films due to its plasticizing effect and addition of FLU increased rigidity of the films due to its antiplasticizing effect. All DL wafers showed lower hardness than BLK wafer due to disturbance in porosity after drug loading. Moreover, the bottom part of the wafer showed lower hardness than the upper part. Therefore, the bottom surface should be the ideal application side, because the lower hardness might reduce the chance of damaging newly formed tissues. All the DL dressings showed lower stickiness as compared to BLK dressings, because in the presence of simulated wound fluid (SWF), drugs precipitated on the surface of the dressings resulting in poor contact between the polymer chains and hence reduced adhesive properties.

The lyophilized wafer dressings, which were highly porous in nature showed better fluid handling properties than films and commercial dressings (Algisite Ag® and Actiformcool®).

All dressings showed high initial (15 min) swelling, which is important to absorb wound fluid quickly. The rapid ingress of fluid into the CA dressings was attributed to the exchange of Ca^{2+} ions in mannuronate units of alginate with Na^+ ions present in SWF. The medicated wafers showed higher water absorption (Aw) (1085 − 2377 %) and holding capacity (EWC, 91 − 95 %) than the medicated films and the commercial products. Therefore, it suggests wafers will absorb more exudates from DFUs than the films and the tested commercial products. CIP loaded dressings showed the highest WVTR (3111.79 ± 16.79−3808.91 ± 48.41 g/m^2day^{-1}) amongst all other dressings due to having the highest in porosity (maximum 98.20 ± 0.56%). In contrast, film dressings exhibited higher WVTR (maximum 3876.53 ± 195.50 g/m^2day^{-1}) than wafer and commercial dressings. This is because, film dressings are semipermeable and thinner and therefore the distance the vapour travels to escape is far less than the wafer and commercial dressings. However, the combined DL wafers and the wafers containing 0.10 and 0.15% w/v FLU showed ideal WVTR values (2000−2500 $g/m^2day^{-}1$) which will be able to maintain moist wound environment effectively. Afterward, film dressings exhibited quicker EWL about 50% within 0.5 h than the wafer and commercial dressings (50% EWL within 2-3 h). This is because the wafer and the commercial dressings were thicker than the film dressings and therefore enabled them to retain more water. Wafers exhibited higher residual moisture content (9 − 17%) than films (8 −12%) because, in the final stage of lyophilization, wafers were dried at lower temperature (20 °C) than films (30 °C). Moreover, the higher residual moisture content of wafers was facilitated by higher porosity of wafers that enabled them to adsorb and retain more bound water. The lower moisture content of films will ensure more stability upon storage and less chance of drug precipitation whereas, higher moisture content of wafers will maintain the wound and the surrounding skin in an optimum state of hydration, implying the wafer dressings will function effectively under compression. The wafers showed greater drug loading capacity than films due to its greater porosity and higher physical volume. CIP loaded wafers showed greater drug loading capacity than FLU loaded wafers, which was also attributed to higher porosity and geometrical shape of the wafers. All formulations retained uniform drug distribution except the films and wafers containing more than 0.05 and 0.15% FLU respectively. FLU was released faster from the dressings (about more than 65-90% within 5 min) than CIP and this was the same in the case of combined DL dressings. The reason behind this, is that FLU might have higher solubility in dissolution medium (SWF), higher affinity to the ions present in SWF and lower molecular weight than CIP. The burst release of FLU from the dressings will be be expected to reduce fungal growth before the next dressings change. On the other hand, sustained amounts of CIP from the dressings up to 6 h can prevent re-infection as

well as the need for frequent dressing change. The drug release from all dressings except CIP loaded films followed Korsmeyer-Peppas model based on the coefficient of linear correlation (R^2).

In this study, the minimum inhibitory concentrations (MIC) of CIP for *E. coli*, *S. aureus* and *P. aeruginosa* were 0.06, 0.5 and 0.125 µg/ml respectively and MIC of FLU for *C. albicans* was 2 µg/ml. Further, the minimum bactericidal concentrations (MBC) of CIP for *E. coli*, *S. aureus* and *P. aeruginosa* were 0.25, 4.0 and 0.5 µg/ml and minimum fungicidal concentration (MFC) for FLU for *C. albicans* was 128 µg/ml. All CIP loaded dressings showed complete eradication of all causative bacteria within 24 h, which will be very effective to prevent infection progression in DFUs. Moreover, a 10-fold reduction (90% killing) in the number of cells of *C. albicans* as compared to negative control (*C. albicans* only) was observed while treating with FLU and combined DL dressings which will be high enough to significantly reduce fungal load in DFUs. In the case of combined DL dressings, the complete eradication of *E. coli* and *P. aeruginosa* from mixed cultures was recorded within 24 h, whereas the complete eradication of *S. aureu*s was observed after 72 h. The slow eradication of *S. aureus* is possibly due to synergistic interaction between *S. aureus* and *C. albicans* in their mixed culture. No fungicidal activity (99.9% killing) of combined DL dressings against all mixed infections (either *E. coli* and *C. albicans,* or *S. aureus* and *C. albicans,* or *P. aeruginosa* and *C. albicans*) was observed. The results obtained from zone of inhibition (ZOI) revealed that wafer dressings had higher ZOI (36.67-44.83 ± 0.23 nm) against all mixed infections than the film dressings (26.50-35.60 ± 0.70 nm) possibly due to higher drug content and drug release of wafers than the films. Algisite Ag® was only effective against *S. aureus* and Actiformcool® was ineffective against all mixed infections.

The optimized concentration of human primary epidermal keratinocyte (PEK) cells was investigated as 1 x 10^5 cells/ml for methylthiazolyldiphenyl-tetrazolium bromide (MTT) and wound scratch assays. MTT assay revealed that all the dressings showed acceptable cell viability above 70% with respect to ISO standard except the dressings containing more than 0.15% FLU. This was because, the high concentration of FLU might accumulate in the lipid rich cell membrane and interfered with hydrogen bonding responsible for tight packing of lipid membranes. Time and dose dependent cytotoxicity was also observed as the longer incubation period and higher dose of drug resulted in lower cell viability. The cell viability of Algisite Ag® and Actiformcool® was recorded about 77.94 ± 1.18% and 78.61 ± 2.56% after 72 h respectively. All the dressings showed effective in vitro wound healing capacity by closing the

gap (wound) within 7 days except the combined DL dressings and Actiformcool®. In contrast, the FLU loaded dressings showed higher rate of initial wound closure than CIP loaded dressings, which was attributed to the higher cell viability of FLU loaded dressing compared to CIP loaded dressings.

Overall, the CIP loaded, FLU loaded and combined DL (CIP-FLU) dressings have potential to be used as medicated dressings to treat DFUs infected with bacteria only, fungi only or both bacteria and fungi respectively.

6.2   Future work

The following further studies will be performed to validate the physico-chemical, functional and biological properties of the developed dressings and also to address some of the limitations of this project.

1. CA is insoluble in water and therefore, different solvent systems, pH, temperature and stirring time were attempted to ensure complete dissolution. Finally, CA was dissolved in sodium carbonate solution and produced sodium alginate (SA) with a byproduct of calcium carbonate in the gels. However, to the best of my knowledge, there has been no research study undertaken on CA as a starting material to produce film and wafer dressings to potentially treat infected DFUs. Therefore, a comparative study between the DL CA dressings and DL SA dressings can be performed to evaluate the differences in physicochemical and functional properties of those dressings.

2. The formulated films did not show ideal elasticity. The elasticity could be improved by blending with other polymers such as gelatin, HPMC, polyox and carrageenan as previously reported by Boateng and co-workers (Boateng *et al*., 2009, 2013a; Pawar *et al*., 2013).

3. IR mapping could be performed on the dressings to confirm the uniform distribution of polymer and drug, and homogeneity of dressings. Furthermore, drug-polymer interaction was investigated by FTIR and XRD analyses. However, further information on drug-polymer interaction and crosslinking can be gathered by Raman spectroscopy, NMR, and molecular and computer modeling.

4. The porosity of the dressings was determined by solvent displacement method. However, the porosity and pore size distribution of the dressings can be further analyzed by Brunauer-Emmett Teller (BET) analysis, mercury intrusion porosimetry,

thermoporommetry, physisorption (physical adsorption), dynamic vapour sorption and imaging methods such as X-ray computed tomography (Lawrence and Jiang, 2017).

5. Prolonged drug release from the dressings could be achieved by increasing percentage of CA in the gels.

6. The microbial activity of the dressings can be further evaluated by visualizing entrapped populations of the microorganisms within the swollen dressing matrix with SEM and confocal microscope. In addition, polymicrobial studies (mixed culture of multiple bacteria) can be performed on CIP loaded dressings. MTT assay can be performed by direct contact of dressings with the PEK cells to mimic real life application. Cytotoxicity of the dressings can also be analyzed by live/deal cells assay and flow cytometry analysis. Studies of cell attachment and *in vivo* animal testing can be performed to elucidate the wound healing action of the dressings. Finally, *in vitro* adhesive test of the dressings can be complemented using i*n vivo* adhesive testing in rat models.

7. *In vivo* mixed infections study could be done in animal model to better elucidate the potential healing of mixed infected *DFUs*.

CHAPTER 7:   REFERENCES

Abdulrazak, A., Ibrahim Bitar, Z., Ayesh Al-Shamali, A., & Ahmed, M. L. (2005). Bacteriological study of diabetic foot infections. *Journal of Diabetes and its Complications*, *19*(3), 138-141.

Abilash, S., Kannan, N., Rajan, K., & Pramodhini, M. (2015). Clinical study on the prevalence of fungal infections in diabetic foot. *International Journal of Currenet Research and Review, 7*(23), 8-13.

Agale, S. V., & Agale, S. V. (2013). Chronic Leg Ulcers: Epidemiology, Aetiopathogenesis, and Management. *Ulcers*, 1-9.

Agren, M. S. (1994). Gelatinase activity during wound healing. *British Journal of Dermatology*, *131*(5), 634–640.

Aguirre, A., Borneo, R., & Leon, A. E. (2013). Properties of triticale protein films and their relation to plasticizing-antiplasticizing effects of glycerol and sorbitol. *Industrial Crops and Products, 50,* 293-303.

Ahmad, J. (2015). The Diabetic Foot. *Diabetes & Metabolic Syndrome: Clinical Research & Review,* 1-39.

Ahmed, A., Getti, G. & Boateng, J.S. (2017). Ciprofloxacin-loaded calcium alginate wafers prepared by freeze-drying technique for potential healing of chronic diabetic foot ulcers. *Drug Delivery and Translation Research,* ISSN 2190-3948, 1-18. https://doi.org/10.1007/s13346-017-0445-9.

Ahn, C., Mulligan, P., & Salcido, R. S. (2008). Smoking-the bane of wound healing: biomedical interventions and social influences. *Advances in Skin & Wound Care*, *21*(5), 227-236.

Alavi, A., Sibbald, R. G., Mayer, D., Goodman, L., Botros, M., Armstrong, D. G., Woo, K., et al. (2014). Diabetic foot ulcers: Part I. Pathophysiology and prevention. *Journal of the American Academy of Dermatology*, *70*(1), 1-18.

Alkhamis, K. A, Obaidat, A. A, & Nuseirat, A. F. (2002). Solid-state characterization of fluconazole. *Pharmaceutical Development and Technology*, *7*(4), 491–503.

Amin, Z. M., Koh, S. P., Tan, C. P., Yeap, S. K., Hamid, N. S. A., & Long, K. (2017). Evaluation of in vitro wound healing efficacy of breadfruit derived starch hydrolysate. *International Food Research Journal*, *24*(4), 1771–1781.

Anderson, K., & Hamm, R. L. (2014). Factors that impair wound healing. *Journal of the American College of Clinical Wound Specialists, 4*, 84-91.

Andrews, J. M. (2001). Determination of minimum inhibitory concentrations. *The Journal of Antimicrobial Chemotherapy*, *48* (Suppl 1), 5-16.

Anisha, B. S., Biswas, R., Chennazhi, K. P., & Jayakumar, R. (2013). Chitosan-hyaluronic acid/nano silver composite sponges for drug resistant bacteria infected diabetic wounds. *International Journal of Biological Macromolecules*, *62*, 310-320.

Armstrong, D. G., Lavery, L. A, van Houtum, W. H., & Harkless, L. B. (1997). The impact of gender on amputation. *The Journal of Foot and Ankle Surgery: Official Publication of the American College of Foot and Ankle Surgeons*, *36*(1), 66–69.

Asadi, M. R., Torkaman, G., Mohajeri-Tehrani, M. R., & Hedayati, M. (2015). Effects of electrical stimulation on the management of ischemic diabetic foot ulcers. *Journal of Babol University of Medical Sciences*, *17*(7), 7-14.

Ashcroft, G. S., Mills, S. J., Shockey, K., Tribble, C., & Kron, I. (2002). Androgen receptor-mediated inhibition of cutaneous wound healing. *The Journal of Clinical Investigation*, *110*(5), 615–624.

Ashcroft, G. S., Greenwell-Wild, T., Horan, M. A., Wahl, S. M., & Ferguson, M. W. (1999). Topical estrogen accelerates cutaneous wound healing in aged humans associated with an altered inflammatory response. *The American Journal of Pathology*, *155*(4), 1137–1146.

Asti, A. & Gioglio, L. (2014). Natural and synthetic biodegradable polymers: different scaffolds for cell expansion and tissue formation. *International Journal of artificial Organs, 37*(3), 187-205.

Ataee, R. A., Derakhshanpour, J., Mehrabi, T. A., & Eydi, A. (2011). Antibacterial effect of calcium carbonate nanoparticles on *Agrobacterium tumefaciens. Iranian Journal of Millitary Medicin, 13*(2), 65-70.

Ayensu, I., Mitchell, J. C., & Boateng, J. S. (2012a). In vitro characterisation of chitosan based xerogels for potential buccal delivery of proteins. *Carbohydrate Polymers*, *89*(3), 935-941.

Ayensu, I., Mitchell, J. C., & Boateng, J. S. (2012b). Development and physico-mechanical characterisation of lyophilised chitosan wafers as potential protein drug delivery systems via the buccal mucosa. *Colloids and Surfaces B: Biointerfaces*, *91*(1), 258-265.

Aziz, Z., Cullum, N., & Flemming, K. (2013). Electromagnetic therapy for treating venous leg ulcers. *Cochrane Database of Systematic Reviews*, *2*(2), CD002933. https://doi.org/10.1002/14651858.CD002933.pub5

Bader, M. S., & Alavi, A. (2014). Management of hospitalized patients with diabetic foot infections. *Hospital practice (1995)*, *42*(4), 111-125.

Baker, B. M., Trappmann, B., Wang, W. Y., Sakar, M. S., Kim, I. L., Shenoy, V. B., & Chen, C. S. (2015). Cell-mediated fibre recruitment drives extracellular matrix mechanosensing in engineered fibrillar microenvironments. *Nature Materials*, *14*(12), 1262–1268.

Balakrishnan, B., Mohanty, M., Umashankar, P. R., & Jayakrishnan, A. (2005). Evaluation of an in situ forming hydrogel wound dressing based on oxidized alginate and gelatin. *Biomaterials*, *26*(32), 6335-6342.

Bandara, H. M. H. N., Yau, J. Y. Y., Watt, R. M., Jin, L. J., & Samaranayake, L. P. (2009). Escherichia coli and its lipopolysaccharide modulate in vitro Candida biofilm formation. *Journal of Medical Microbiology*, *58*(12), 1623–1631.

Banu, A., Hassan M.M.N., Rajkumar, J., & Srinivasa, S. (2015). Spectrum of bacteria associated with diabetic foot ulcer and biofilm formation: A prospective study. *Australasian Medical Journal*, *8*(9), 280-285.

Bajgrowicz, M., Phan, C. M., Subbaraman, L. N., & Jones, L. (2015). Release of ciprofloxacin and moxifloxacin from daily disposable contact lenses from an in vitro eye model. *Investigative Ophthalmology and Visual Science*, *56*(4), 2234–2242.

Beberok, A., Buszman, E., Wrześniok, D., Otręba, M., & Trzcionka, J. (2011). Interaction between ciprofloxacin and melanin: The effect on proliferation and melanization in melanocytes. *European Journal of Pharmacology*, *669*(1-3), 32-37.

Beckmann, K. H., Meyer-Hamme, G., & Schroder, S. (2014). Low level laser therapy for the treatment of diabetic foot ulcers: A critical survey. *Evidence-Based Complementary and Alternative Medicine*, *2014,* http://dx.doi.org/10.1155/2014/626127.

Ben-shalom, N., Nevo, Z., Patchornik, A., & Robinson, D. (2008). Novel injectable chitosan mixtures forming hydrogels. Patent Cooperation Treaty Application, EP2121026.

Blackman, E., Moore, C., Hyatt, J., Railton, R., & Frye, C. (2010). Topical wound oxygen therapy in the treatment of severe diabetic foot ulcers: a prospective controlled study. *Ostomy/wound Management*, *56*(6), 24-31.

Boateng, J. S., & Popescu, A. M. (2016). Composite bi-layered erodible films for potential ocular drug delivery. *Colloids and Surfaces B: Biointerfaces*, *145*, 353-361.

Boateng, J., & Catanzano, O. (2015). Advanced Therapeutic Dressings for Effective Wound Healing—A Review. *Journal of Pharmaceutical Sciences*, *104*(11), 3653-3680.

Boateng, J., Burgos-Amador, R., Okeke, O., & Pawar, H. (2015a). Composite alginate and gelatin based bio-polymeric wafers containing silver sulfadiazine for wound healing. *International Journal of Biological Macromolecules*, *79*, 63-71.

Boateng, J., Pawar, H., & Tetteh, J. (2015b). Evaluation of in vitro wound adhesion characteristics of composite film and wafer-based dressings using texture analysis and FTIR spectroscopy: a chemometrics factor analysis approach. *Royal Society of Chemistry Advances*, *5*(129), 107064-107075.

Boateng, J. S., Pawar, H. V., & Tetteh, J. (2013a). Polyox and carrageenan based composite film dressing containing anti-microbial and anti-inflammatory drugs for effective wound healing. *Pharmaceutics*, *441*(1-2), 181-191.

Boateng, J., Mani, J., & Kianfar, F. (2013b). Improving drug loading of mucosal solvent cast films using a combination of hydrophilic polymers with amoxicillin and Paracetamol as Model Drugs**,** *BioMed Research International, 2013*(198137), 1-8.

Boateng, J. S., Matthews, K. H., Auffret, A. D., Humphrey, M. J., Stevens, H. N., & Eccleston, G. M. (2012). Comparison of the in vitro release characteristics of mucosal freeze-dried wafers and solvent-cast films containing an insoluble drug. *Drug Development and Industrial Pharmacy*, *38*(1), 47-54.

Boateng, J. S., Auffret, A. D., Matthews, K. H., Humphrey, M. J., Stevens, H. N. E., & Eccleston, G. M. (2010). Characterisation of freeze-dried wafers and solvent evaporated films as potential drug delivery systems to mucosal surfaces. *International Journal of Pharmaceutics*, *389*(1-2), 24-31.

Boateng, J. S., Stevens, H. N. E., Eccleston, G. M., Auffret, A. D., Humphrey, M. J., & Matthews, K. H. (2009). Development and mechanical characterization of solvent-cast polymeric films as potential drug delivery systems to mucosal surfaces. *Drug Development and Industrial Pharmacy*, *35*(8), 986-996.

Boateng, J., Matthews, K., Stevens, H., & Eccleston, G. (2008). Wound Healing Dressings and Drug Delivery Systems: A Review. *Journal of Pharmaceutical Sciences*, *97*(8), 2892-2923.

Bourichi, H., Brik, Y., Hubert, P., Cherrah, Y., & Bouklouze, A. (2012). Solid-state characterization and impurities determination of fluconazol generic products marketed in Morocco. *Journal of Pharmaceutical Analysis*, *2*(6), 412–421.

Bowler, G. B. (2003). Bacterial Growth Guideline: Reassessing its Clinical Relevance in Wound Healing. *Ostomy Wound Management*, *49*(1), 1-10.

Bowler, P. G., Duerden, B. I., & Armstrong, D. G. (2001). Wound microbiology and associated approaches to wound management. *Clinical Microbiology Reviews*, *14*(2), 244-269.

Braun, L. R., Fisk, W. A., Lev-Tov, H., Kirsner, R. S., & Isseroff, R. R. (2014). Diabetic foot ulcer: An evidence-based treatment update. *American Journal of Clinical Dermatology*, *15*(3), 267-281.

Brett, D. (2008). A Review of Collagen and Collagen-based Wound Dressings. *Wounds*, *20*(12), 1-11.

Brimson, S., & Nigam, Y. (2012). The role of oxygen-associated therapies for the healing of chronic wounds, particularly in patients with diabetes. Journal of the European Academy of *Dermatology and Venereology*, 1-8.

Budzynska, A., Różalska, S., Sadowska, B., & Różalska, B. (2017). Candida albicans/Staphylococcus aureus Dual-Species Biofilm as a Target for the Combination of Essential Oils and Fluconazole or Mupirocin. *Mycopathologia*, *182*(11–12), 989–995.

Buffo, J., Herman, M. A, & Soll, D. R. (1984). A characterization of pH-regulated dimorphism in Candida albicans. *Mycopathologia*, *85*(1–2), 21–30.

Burns, S and Kuen, Y. Jan. (2012). Diabetic foot ulceration and amputation, Rehabilitation Medicine, Prof. Chong Tae Kim (Ed.), *InTech*, 1-10. DOI: 10.5772/48003.

Caira, M. R., Alkhamis, K. A., & Obaidat, R. M. (2004). Preparation and Crystal Characterization of a Polymorph, a Monohydrate, and an Ethyl Acetate Solvate of the Antifungal Fluconazole. *Journal of Pharmaceutical Sciences*, *93*(3), 601–611.

Callaghan, M. J., Chang, E. I., Seiser, N., Aarabi, S., Ghali, S., Kinnucan, E. R., & Gurtner, G. C. (2008). Pulsed electromagnetic fields accelerate normal and diabetic wound healing by increasing endogenous FGF-2 release. *Plastic and Reconstructive Surgery*, *121*(1), 130–141.

Catanzano, O., Docking, R., Schofield, P., & Boateng, J. (2017). Advanced multi-targeted composite biomaterial dressing for pain and infection control in chronic leg ulcers. *Carbohydrate Polymers*, *172*, 40–48.

Cavet, M. E., West, M., & Simmons, N. L. (1997). Fluoroquinolone (ciprofloxacin) secretion by human intestinal epithelial (Caco-2) cells. *British Journal of Pharmacology*, *121*(8), 1567–1578.

Çerman, A. A., Altunay, I. K., & Karabay, E. A. (2016). Venous Leg Ulceration, Wound Healing - New insights into Ancient Challenges, Dr. Vlad Alexandrescu (Ed.), *InTech*, 289-308. DOI: 10.5772/63962.

Carlson, E. (1983). Effect of strain of Staphylococcus aureus on synergism with Candida albicans resulting in mouse mortality and morbidity. *Infection and Immunity*, *42*(1), 285–292.

Chadwick, P., McCardle, J. (2014). Exudate management using a gelling fibre dressing. *The Diabetic Foot Journal*, *18*(1), 43-48.

Chadwick, P., Edmonds, M., MsCardle, J., Armstrong, D., Apelqvist, J., Botros, M., Clerici, G., et al. (2014). Best Practice Guidelines: *Wound Management in Diabetic Foot Ulcers*. *Wounds International*, *5*(2), 1-23.

Chadwick P. (2013). Fungal infection of the diabetic foot: The often ignored complication. *Diabetic Foot Canada*, *1*(2), 20-24.

Chamarthy, S. P., & Pinal, R. (2008). Plasticizer concentration and the performance of a diffusion-controlled polymeric drug delivery system. *Colloids and Surfaces A: Physicochemical and Engineering Aspects*, *331*(1-2), 25-30.

Chambers, L., Woodrow, S., Brown, A. P., Harris, P. D., Phillips, D., Hall, M., Pritchard, D. I. (2003). Degradation of extracellular matrix components by defined proteinases from the greenbottle larva Lucilia sericata used for the clinical debridement of non-healing wounds. *British Journal of Dermatology*, *148*(1), 14–23.

Chang, K. W., Alsagoff, S., Ong, K. T., & Sim, P. H. (1998). Pressure ulcers--randomised controlled trial comparing hydrocolloid and saline gauze dressings. *The Medical journal of Malaysia, 53*(4), 428-431.

Chellan, G., Neethu, K., Varma, A. K., Mangalanandan, T. S., Shashikala, S., Dinesh, K. R., Sundaram, K. R., et al. (2012). Targeted treatment of invasive fungal infections accelerates healing of foot wounds in patients with Type 2 diabetes. *Diabetic medicine: A Journal of the British Diabetic Association*, *29*(9), 255-262.

Chellan, G., Shivaprakash, S., Ramaiyar, S. K., Varma, A. K., Varma, N., Sukumaran, M. T., Vasukutty, J. R., et al. (2010). Spectrum and prevalence of fungi infecting deep tissues of lower-limb wounds in patients with type 2 diabetes. *Journal of Clinical Microbiology*, *48*(6), 2097-2102.

Chiţa, T., Muntean, D., Badiţoiu, L., Timar, B., Moldovan, R., Timar, R., & Licker, M. (2013). Staphylococcus aureus strains isolated from diabetic foot ulcers. Identification of the antibiotic resistant phenotypes. *Romanian Journal of Diabetes Nutrition and Metabolic Diseases*, *20*(4), 389-393.

Chincholikar, D. A., & Pal, R. B. (2002). Study of fungal and bacterial infections of the diabetic foot. *Indian Journal of Pathology & Microbiology*, *45*(1), 15–22.

Clayton, W., & Elasy, T. A. (2009). A review of the pathophysiology, classification, and treatment of foot ulcers in diabetic patients. *Clinical Diabetes*, *27*(2), 52-58.

Cordeiro, R. A., C Teixeira, C. E., N Brilhante, R. S., E Bora C M Castelo-branco, D. S., N Paiva, M. A., Ã J Giffoni Leite, J. O., Lima, D. T., et al. (2013). Minimum inhibitory concentrations of amphotericin B, azoles and caspofungin against Candida species are reduced by farnesol. *Medical Mycology*, *51*, 53-59.

Cugini, C., Calfee, M. W., Farrow, J. M., Morales, D. K., Pesci, E. C., & Hogan, D. A. (2007). Farnesol, a common sesquiterpene, inhibits PQS production in Pseudomonas aeruginosa. *Molecular Microbiology*, *65*(4), 896–906.

Cutting, K. (2010). Wound dressings: 21st century performance requirements. *Journal of Wound Care*, *19*(Sup1), 4-9.

Daemi, H., & Barikani, M. (2012). Synthesis and characterization of calcium alginate nanoparticles, sodium homopolymannuronate salt and its calcium nanoparticles. *Scientia Iranica*, *19*(6), 2023-2028.

Damir, A. (2011). Why diabetic foot ulcers do not heal? *Journal International Medical Sciences Academy*, *24*(4), 205-206.

Danno, K., Mori, N., Toda, K., Kobayashi, T., & Utani, A. (2001). Near-infrared irradiation stimulates cutaneous wound repair: laboratory experiments on possible mechanisms. *Photodermatology, Photoimmunology & Photomedicine*, *17*(6), 261–265.

Davis, P., Wood, L., Wood, Z., Eaton, A., & Wilkins, J. (2009). Clinical experience with a glucose oxidase-containing dressing on recalcitrant wounds. *Journal of Wound Care*, *18*(3), 114, 116-121.

De Aquino Lemos, J., Costa, C. R., De Araújo, C. R., E Souza, L. K. H., & Do Rosário Rodrigues Silva, M. (2009). Susceptibility testing of candida albicans isolated from oropharyngeal mucosa of HIV+ patients to fluconazole, amphotericin b and caspofungin. killing kinetics of caspofungin and amphotericin b against fluconazole resistant and susceptible isolates. *Brazilian Journal of Microbiology*, *40*(1), 163–169.

Demidova-Rice, T. N., Hamblin, M. R., & Herman, I. M. (2012). Acute and Impaired Wound Healing: Pathophysiology and Current Methods for Drug Delivery, Part 1: Normal and Chronic Wounds: Biology, Causes, and Approaches to Care. *Advances in Skin & Wound Care*, *25*(7), 304–314.

Dhandayuthapani, B., Yoshida, Y., Maekawa, T., & Kumar, D. S. (2011). Polymeric scaffolds in tissue engineering application: A review. *International Journal of Polymer Science*, *2011*(290602), 1-19.

Dhivya, S., Padma, V. V., & Santhini, E. (2015). Wound dressings - a review. *BioMedicine*, *5*(4), 24-28.

Dreifke, M. B., Jayasuriya, A. A., & Jayasuriya, A. C. (2015). Current wound healing procedures and potential care. *Materials Science and Engineering C*, *48*, 651-662.

Donlan, R. M., & Costerton, J. W. (2002). Biofilms: Survival mechanisms of clinically relevant microorganisms. *Clinical Microbiology Reviews*, *15*(2), 167-193.

Dowd, S., Delton Hanson, J., Rees, E., Wolcott, R., Zischau, A., & Sun, Y. et al. (2011). Survey of fungi and yeast in polymicrobial infections in chronic wounds. *Journal of Wound Care*, *20*(1), 40-47.

Dowd, S. E., Wolcott, R. D., Sun, Y., McKeehan, T., Smith, E., & Rhoads, D. (2008). Polymicrobial nature of chronic diabetic foot ulcer biofilm infections determined using bacterial tag encoded FLX amplicon pyrosequencing (bTEFAP). *Public Library of Science ONE*, *3*(10), 1-7.

Dowsett, C., Bielby, A., & Searle, R. (2014). Reconciling increasing wound care demands with available resources. *Journal of Wound Care*, *23*(11), 552, 554, 556-8.

Dumville, J. C., O'Meara, S., Deshpande, S., & Speak, K. (2013a). Hydrogel dressings for healing diabetic foot ulcers (Review). *Cochrane Database of Systematic Reviews (Online)*, *9*(7), 1-48

Dumville, J. C., Deshpande, S., O'Meara, S., & Speak, K. (2013b). Foam dressings for healing diabetic foot ulcers. *Cochrane Database Systematic Reviews*, (6), CD009111. https://doi.org/10.1002/14651858.CD009111.pub3.

Dumville, J. C., O'Meara, S., Deshpande, S., & Speak, K. (2013c). Alginate dressings for healing diabetic foot ulcers. *The Cochrane database of systematic reviews*, *6*(6), CD009110. https://doi.org/10.1002/14651858.CD009110.pub3.

Edmonds, M. (2009). The treatment of diabetic foot infections: Focus on ertapenem. *Vascular Health and Risk Management*, *5*, 949-963.

Edwards, J., & Stapley, S. (2010). Debridement of diabetic foot ulcers. *The Cochrane Database of Systematic Reviews*, (1), CD003556. https://doi.org/10.1002/14651858.CD003556.

El-Azizi, M. A., Starks, S. E., & Khardori, N. (2004). Interactions of Candida albicans with other Candida spp. and bacteria in the biofilms. In *Journal of Applied Microbiology*, *96*(5), 1067–1073.

Elsner, J. J., Shefy-Peleg, A., & Zilberman, M. (2010). Novel biodegradable composite wound dressings with controlled release of antibiotics: Microstructure, mechanical and physical properties. *Journal of Biomedical Materials Research - Part B Applied Biomaterials*, *93*(2), 425–435.

Elsner, J. J., & Zilberman, M. (2010). Novel antibiotic-eluting wound dressings: An in vitro study and engineering aspects in the dressing's design. *Journal of Tissue Viability*, *19*(2), 54-66.

Enoch, S., & Price, P. (2004). Cellular, molecular and biochemical differences in the pathophysiology of healing between acute wounds, chronic wounds and wounds in the aged. *World Wide Wounds*. ISSN: 1369-2607.

Falanga, V. (2005). Wound healing and its impairment in the diabetic foot. *Lancet*, *366*(9498), 1736-1743.

Faria, E., Blanes, L., Hochman, B., Filho, M. M., & Ferreira, L. (2011). Health-related Quality of Life, Self- esteem, and Functional Status of Patients with Leg Ulcers. *Wounds*, *23*, 4-10.

Faries, P. L., Teodorescu, V. J., Morrissey, N. J., Hollier, L. H., & Marin, M. L. (2004). The role of surgical revascularization in the management of diabetic foot wounds. *The American Journal of Surgery*, *187*(5), S34-S37.

Farzamfar, B., Nazari, R., & Bayanolhagh, S. (2013). Diabetic Foot Ulcer, Gangrene Management - New Advancements and Current Trends, Dr. Alexander Vitin (Ed.), *InTech*, DOI: 10.5772/55588.

Feng, S., Nie, L., Zou, P., & Suo, J. (2015). Effects of drug and polymer molecular weight on drug release from PLGA-mPEG microspheres. *Journal of Applied Polymer Science*, *132*(6). https://doi.org/10.1002/app.41431.

Fierer, J., Daniel, D., & Davis, C. (1979). The fetid foot: lower-extremity infections in patients with diabetes mellitus. *Reviews of infectious diseases*, *1*(1), 210-217.

File, T. M., & Tan, J. S. (1983). Amdinocillin plus cefoxitin versus cefoxitin alone in therapy of mixed soft tissue infections (including diabetic foot infections). *The American Journal of Medicine*, *75*(2 PART 1), 100-105.

Fitzsimmons, N., & Berry, D. R. (1994). Inhibition of Candida albicans by Lactobacillus acidophilus: evidence for the involvement of a peroxidase system. *Microbios*, *80*(323), 125-133.

Fonder, M. A., Lazarus, G. S., Cowan, D. A., Aronson-Cook, B., Kohli, A. R., & Mamelak, A. J. (2008). Treating the chronic wound: A practical approach to the care of nonhealing wounds and wound care dressings. *Journal of the American Academy of Dermatology*, *58*(2), 185-206.

Fothergill, A. W. (2012). Antifungal susceptibility testing: clinical laboratory and standards institute (CLSI) methods. In G. S. Hall (Ed.), *Interactions of Yeasts, Moulds, and Antifungal Agents*, 65–74.

Fourie, R., Ells, R., Swart, C. W., Sebolai, O. M., Albertyn, J., & Pohl, C. H. (2016). Candida albicans and Pseudomonas aeruginosa interaction, with focus on the role of eicosanoids. *Frontiers in Physiology*, *7*, 1-15.

Friedl, P., & Wolf, K. (2010). Plasticity of cell migration: A multiscale tuning model. *Journal of Cell Biology*, *188*(1), 11-19.

Frykberg, R. G., Zgonis, T., Armstrong, D. G., Driver, V. R., Giurini, J. M., Kravitz, S. R., Landsman, A. S., et al. (2006). Diabetic Foot Disorders: a Clinical Practice Guideline. *The Journal of Foot & Ankle Surgery*, *45*(5), 1-60.

Fu, Y., & Kao, W. J. (2010). Drug release kinetics and transport mechanisms of non-degradable and degradable polymeric delivery systems. *Expert Opinion on Drug Delivery*, *7*(4), 429–444.

Gabriel, A. J., Jose L. R. A., Ana, M. M. M., & Maria, L. M. H. (2007). Effect of temperature and pH on swelling behavior of hydroxyethyl cellullose-acrylamide hydrogel. *E-Polymers*, *150*, 1-9.

Gardner, S. E., & Frantz, R. A. (2008). Wound bioburden and infection-related complications in diabetic foot ulcers. *Biological Research for Nursing*, *10*(1), 44-53.

Gao, C., Pollet, E., & Averous, L. (2017). Properties of glycerol-plasticized alginate films obtained by thermo-mechanical mixing. *Food Hydrocolloids*, *63*, 414-420

Ghannoum, M. A., & Rice, L. B. (1999). Antifungal agents: mode of action, mechanisms of resistance, and correlation of these mechanisms with bacterial resistance. *Clinical Microbiology Reviews*, *12*(4), 501-517.

Gibas, I., & Janik, H. (2010). Review: Synthetic Polymer Hydrogels for Biomedical. *Chemical Technology*, *4*(4), 297-304.

Gilliver, S. C., Ashworth, J. J., & Ashcroft, G. S. (2007). The hormonal regulation of cutaneous wound healing. *Clinics in Dermatology*, *25*(1), 56–62.

Girmenia, C., Tuccinardi, C., Santilli, S., Mondello, F., Monaco, M., Cassone, A, & Martino, P. (2000). In vitro activity of fluconazole and voriconazole against isolates of Candida albicans from patients with haematological malignancies. *The Journal of Antimicrobial Chemotherapy*, *46*(3), 479–483.

Goldman, R. J. (2009). Hyperbaric Oxygen Therapy for Wound Healing and Limb Salvage: A Systematic Review. *American Academy of Physical Medicine and Rehabilitation*, *1*(5), 471–489.

Gonsalves, W. C., Gessey, M. E., Mainous, A. G., & Tilley, B. C. (2007). A study of lower extremity amputation rates in older diabetic South Carolinians. *Journal of the South Carolina Medical Association*, *103*(1), 4–7.

Gonzalez, A. M., Alonso, P. L., Mauris, J., Cruzat, A., Dohlman, C. H., & Argueso, P. (2016). Establishment of a novel in vitro model of stratified epithelial wound healing with barrier function. *Scientific Reports*, *6*, 1-9.

Grayson, M. L., Gibbons, G. W., Habershaw, G. M., Freeman, D. V., Pomposelli, F. B., Rosenblum, B. I., Levin, E., et al. (1994). Use of ampicillin/sulbactam versus imipenem/cilastatin in the treatment of limb-threatening foot infections in diabetic patients. *Clinical Infectious Diseases: An Official Publication of the Infectious Diseases Society of America*, *18*(5), 683-693.

Grey, J. E., Harding, K. G., & Enoch, S. (2006). Venous and arterial leg ulcers. *British Medical Journal*, *332*, 347-350.

Grinnell, F. (1994). Fibroblasts, myofibroblasts, and wound contraction. *Journal of Cell Biology*, *124*(4), 401-404.

Gombotz, W. R., & Wee, S. (1998). Protein release from alginate matrixes. Advanced Drug *Delivery Reviews*, *31*(3), 267-285.

Gordon, C. R., Rojavin, Y., Patel, M., Zins, J. E., Grana, G., Kann, B., Atabek, U. (2009). A review on bevacizumab and surgical wound healing: an important warning to all surgeons. *Annals of Plastic Surgery*, *62*(6), 707–709.

Gosain, A., & DiPietro, L. A. (2004). Aging and Wound Healing. *World Journal of Surgery*, *28*(3), 321-326.

Gottrup, F., & Jorgensen, B. (2011). Maggot debridement: an alternative method for debridement. *Eplasty*, *11*, 290-302.

Guan, J., Fujimoto, K. L., Sacks, M. S., & Wagner, W. R. (2005). Preparation and characterization of highly porous, biodegradable polyurethane scaffolds for soft tissue applications. *Biomaterials*, *26*(18), 3961–3971.

Gulcelik, M. A., Dinc, S., Dinc, M., Yenidogan, E., Ustun, H., Renda, N., & Alagol, H. (2006). Local granulocyte-macrophage colony-stimulating factor improves incisional wound healing in adriamycin-treated rats. *Surgery Today*, *36*(1), 47–51.

Guo, S., & Dipietro, L. A. (2010). Factors affecting wound healing. *Journal of Dental Research*, *89*(3), 219-229.

Gurbay, A., Garrel, C., Osman, M., Richard, M. J., Favier, A., & Hincal, F. (2002). Cytotoxicity in ciprofloxacin-treated human fibroblast cells and protection by vitamin E. *Human & Experimental Toxicology*, *21*(12), 635-641.

Gurer, S. U., Cevikbas, A., Johansson, C., Derici, K., & Yardimic, T. (1999). Effect of fluconazole on human polymorphonuclear leucocyte functions ex vivo against *Candida albicans*. *Chemotherapy, 45*, 227-283.

Hambleton, I. R., Jonnalagadda, R., Davis, C. R., Fraser, H. S., Chaturvedi, N., & Hennis, A. J. (2009). All-cause mortality after diabetes-related amputation in barbados: A prospective case-control study. *Diabetes Care*, *32*(2), 306–307.

Han, J., Zhou, Z., Yin, R., Yang, D., & Nie, J. (2010). Alginate-chitosan/hydroxyapatite polyelectrolyte complex porous scaffolds: Preparation and characterization. *International Journal of Biological Macromolecules*, *46*(2), 199-205.

Harriott, M. M., & Noverr, M. C. (2009). Candida albicans and Staphylococcus aureus form polymicrobial biofilms: Effects on antimicrobial resistance. *Antimicrobial Agents and Chemotherapy*, *53*(9), 3914–3922.

Heald, A. H., O'Halloran, D. J., Richards, K., Webb, F., Jenkins, S., Hollis, S., Young, R. J. (2001). Fungal infection of the diabetic foot: Two distinct syndromes. *Diabetic Medicine*, *18*(7), 567–572.

Helaine, E. R., Elizabeth, A. C., Robert, L., Susan, J. H., & al., et. (2004). Relation of Lower-Extremity Amputation to All-Cause and Cardiovascular Disease Mortality in American Indians: The Strong Heart Study. *Diabetes Care*, *27*(6), 1286-1293.

Hendrix, D. V., Ward, D. A., & Barnhill, M. A. (2001). Effects of antibiotics on morphologic characteristics and migration of canine corneal epithelial cells in tissue culture. *American Journal of Veterinary Research*, *62*(10), 1664–1669.

Hilton, J. R., Williams, D. T., Beuker, B., Miller, D. R., & Harding, K. G. (2004). Wound dressings in diabetic foot disease. *Clinical Infectious Diseases: An Official Publication of the Infectious Diseases Society of America*, 39 (SUPPL 2), 100-103.

Hinchliffe, R. J., Valk, G. D., Apelqvist, J., Armstrong, D. G., Bakker, K., Game, F. L., Hartemann-Heurtier, A., et al. (2008). A systematic review of the effectiveness of interventions to enhance the healing of chronic ulcers of the foot in diabetes. *Diabetes/Metabolism Research and Reviews 24*, 119-144.

Hoiby, N., Bjarnsholt, T., Givskov, M., Molin, S., & Ciofu, O. (2010). Antibiotic resistance of bacterial biofilms. *International Journal of Antimicrobial Agents*, *35*(4), 322-332.

Houreld, N., & Abrahamse, H. (2010). Low-intensity laser irradiation stimulates wound healing in diabetic wounded fibroblast cells (WS1). *Diabetes Technology & Therapeutics*, *12*(12), 971–978.

Hudzicki, J. (2009). Kirby-Bauer disk diffusion susceptibility test protocol. *Kirby-Bauer-Disk-Diffusion-Susceptibility-Test-Protocol-Library,* 1-22.

Humbert, P., Mikosinki, J., Benchikhi, H., & Allaert, F. A. (2013). Efficacy and safety of a gauze pad containing hyaluronic acid in treatment of leg ulcers of venous or mixed origin: A double-blind, randomised, controlled trial. *International Wound Journal*, *10*(2), 159-166.

Imirzalioglu, C., Sethi, S., Schneider, C., Hain, T., Chakraborty, T., Mayser, P., & Domann, E. (2014). Distinct polymicrobial populations in a chronic foot ulcer with implications for diagnostics and anti-infective therapy. *BioMed Central Research Notes*, *7*(196), 1-7.

Irving, G., & Hargreaves, S. (2009). Venous and arterial leg ulceration. *InnovAiT 2*, 415–422.

Isakov, E., Ring, H., Mendelevich, I., Boduragin, N., Susak, Z., Kupfert, Y., & Marchetti, N. (1996). Electromagnetic stimulation of stump wounds in diabetic amputees. *Journal of Rehabilitation Sciences*, *9*(2), 46–48.

Jain, A. (2012). A new classification of diabetic foot complications: a simple and effective teaching tool. *The Journal of Diabetic Foot Complications*, *4*(1), 1-5.

Jagar, B. Mk., Godhi, A. S., Pandit, A., & Khatri, S. (2012). Efficacy of low level laser therapy on wound healing in patients with chronic diabetic foot ulcers-a randomised control trial. *The Indian Journal of Surgery*, *74*(5), 359–363.

Jannesari, M., Varshosaz, J., Morshed, M., & Zamani, M. (2011). Composite poly(vinyl alcohol)/poly(vinyl acetate) electrospun nanofibrous mats as a novel wound dressing matrix for controlled release of drugs. *International Journal of Nanomedicine*, *6*, 993-1003.

Jeffcoate, W. J., Price, P., & Harding, K. G. (2004). Wound healing and treatments for people with diabetic foot ulcer. *Diabetes/Metabolism Research and Reviews*, *20*(SUPPL 1), 78-89.

Jones, V., Grey, J., & Harding, K. (2006). ABC of wound healing: Wound dressings. *British Medical Journal*, *332*(April), 777-780.

Jonkman, J. E. N., Cathcart, J. A., Xu, F., Bartolini, M. E., Amon, J. E., Stevens, K. M., & Colarusso, P. (2014). An introduction to the wound healing assay using live-cell microscopy. *Cell Adhesion and Migration*. *8*(5), 440-451.

Jurjus, A., Atiyeh, B. S., Abdallah, I. M., Jurjus, R. A., Hayek, S. N., Jaoude, M. A., Gerges, A., et al. (2007). Pharmacological modulation of wound healing in experimental burns. *Burns*, *33*(7), 892-907.

Karthikeyan, K., Sowjanya, R.S., Yugandhar, A.D., Gopinath, S.; Korrapati, P.S. (2015). Design and development of a topical dosage form for the convenient delivery of electrospun drug loaded nanofibers. *Royal Society of Chemistry Advances*, *5*, 52420-52426.

Karu, T. I. (1989). Photobiology of low-power laser effects. *Health Physics*, *56*, 691–704.

Kataria, K., Gupta, A., Rath, G., Mathur, R. B., & Dhakate, S. R. (2014). In vivo wound healing performance of drug loaded electrospun composite nanofibers transdermal patch. *International Journal of Pharmaceutics*, *469*(1), 102-110.

Kavitha, K. V., Tiwari, S., Purandare, V. B., Khedkar, S., Bhosale, S. S., & Unnikrishnan, A. G. (2014). Choice of wound care in diabetic foot ulcer: A practical approach. *World Journal of Diabetes*, *5*(4), 546-556.

Kaviani, A., Djavid, G. E., Ataie-Fashtami, L., Fateh, M., Ghodsi, M., Salami, M., & Larijani, B. (2011). A Randomized Clinical Trial on the Effect of Low-Level Laser Therapy on Chronic Diabetic Foot Wound Healing: A Preliminary Report. *Photomedicine and Laser Surgery*, *29*(2), 109–114.

Kawai, K., Larson, B. J., Ishise, H., Carre, A. L., Nishimoto, S., Longaker, M., & Lorenz, H. P. (2011). Calcium-based nanoparticles accelerate skin wound healing. *Public Library of Science ONE*, *6*(11), 1-13.

Kawai, K., Suzuki, S., Tabata, Y., & Nishimura, Y. (2005). Accelerated wound healing through the incorporation of basic fibroblast growth factor-impregnated gelatin microspheres into artificial dermis using a pressure-induced decubitus ulcer model in genetically diabetic mice. *British Journal of Plastic Surgery*, *58*(8), 1115-1123.

Kaya, E., Ozbilge, H., Kaya, E., & Ozbilge, H. (2012). Determination of the eff ect of fl uconazole against Candida albicans and Candida glabrata by using microbroth kinetic assay* Use of kinetic assay for antifungal activity. *Turkish Journal of Medical Science*, *42*(2), 325–328.

Kean, R., Rajendran, R., Haggarty, J., Townsend, E. M., Short, B., Burgess, K. E., & Ramage, G. (2017). Candida albicans mycofilms support Staphylococcus aureus colonization and enhances miconazole resistance in dual-species interactions. *Frontiers in Microbiology*, *8*(FEB), 1-11.

Kemna, M. E., & Elewski, B. E. (1996). A U.S. epidemiologic survey of superficial fungal diseases. *Journal of the American Academy of Dermatology*, *35*(4), 539-542.

Kerin, H. (2013). Simplifying Venous Leg Ulcer Management. *Wounds international*, 1-10.

Kerr, M. (2012). Foot Care for People with Diabetes: The Economic Case for Change. *NHS Diabetes*, (November), 1-72.

Kerr, J. R., Taylor, G. W., Rutman, A., Hoiby, N., Cole, P. J., & Wilson, R. (1999). Pseudomonas aeruginosa pyocyanin and 1-hydroxyphenazine inhibit fungal growth. *Journal of Clinical Pathology*, *52*(5), 385–387.

Kevin, Y. W., Santos, V., & Gamba, M. (2013). Understanding diabetic foot. *Lippincott Williams & Wilkins*, 36-42.

Khaksar, S., Kesmati, M., Rezaie, A., & Rasekh, A. (2011). Topical estrogen accelerates wound healing in diabetic rats. *Iranian Journal of Endocrinology and Metabolism*, *12*(5). 544-551.

Khaksar, S., Kesmati, M., Rezaie, A., & Rasekh, A. (2010). Effect of estrogen on the process of wound healing in diabetic rats. *Physiology and Pharmacology*, *14*(3), 242–251.

Kianfar, F., Antonijevic, M., Chowdhry, B., & Boateng, J. S. (2013a). Lyophilized wafers comprising carrageenan and pluronic acid for buccal drug delivery using model soluble and insoluble drugs. *Colloids and Surfaces B: Biointerfaces*, *103*, 99-106.

Kianfar, F., Ayensu, I., & Boateng, J. S. (2013b). Development and physico-mechanical characterization of carrageenan and poloxamer-based lyophilized matrix as a potential buccal drug delivery system. *Drug Development and Industrial Pharmacy*, *9045*, 1-9.

Kianfar, F., Chowdhry, B., Antonijevic, M., & Boateng, J. (2011). Novel films for drug delivery via the buccal mucosa using model soluble and insoluble drugs. *Drug Development and Industrial Pharmacy*, *38*(10), 1207-1220.

Kianfar, F., Antonijevic, M. D., Chowdhry, B. Z., & Boateng, J. S. (2011). Formulation Development of a Carrageenan Based Delivery System for Buccal Drug Delivery Using Ibuprofen as a Model Drug. *Journal of Biomaterials and Nanobiotechnology*, *2*(5), 582–595.

Kim, I. Y., Yoo, M. K., Seo, J. H., Park, S. S., Na, H. S., Lee, H. C., Kim, S. K., et al. (2007). Evaluation of semi-interpenetrating polymer networks composed of chitosan and poloxamer for wound dressing application. *International Journal of Pharmaceutics*, *341*(1-2), 35-43.

Kirkpatrick, W. R., Turner, T. M., Fothergill, A. W., McCarthy, D. I., Redding, S. W., Rinaldi, M. G., & Patterson, T. F. (1998). Fluconazole disk diffusion susceptibility testing of Candida species. *Journal of Clinical Microbiology*, *36*(11), 3429–3432.

Koksal, C., & Bozkurt, A. K. (2003). Combination of hydrocolloid dressing and medical compression stocking versus Unna's boot for the treatment of venous leg ulcers. *Swiss Medical Weekly*, *133*(25-26), 364-368.

Koley, D., & Bard, A. J. (2010). Triton X-100 concentration effects on membrane permeability of a single HeLa cell by scanning electrochemical microscopy (SECM). *Proceedings of the National Academy of Sciences of the United States of America*, *107*(39), 16783–16787.

Kondo, S., Niiyama, H., Yu, A., & Kuroyanagi, Y. (2012). Evaluation of a Wound Dressing Composed of Hyaluronic Acid and Collagen Sponge Containing Epidermal Growth Factor in Diabetic Mice. *Journal of Biomaterials Science, Polymer Edition*, 1-12.

Kranke, P., Bennett, M. H., Martyn-St James, M., Schnabel, A., & Debus, S. E. (2012). Hyperbaric oxygen therapy for chronic wounds. *Cochrane Database of Systematic Reviews*, *4*(1), CD004123. 10.1002/14651858.CD004123.pub2.

Krischak, G. D., Augat, P., Claes, L., Kinzl, L., & Beck, A. (2007). The effects of non-steroidal anti-inflammatory drug application on incisional wound healing in rats. *Journal of Wound Care*, *16*(2), 76-78.

Kruse, I., & Edelman, S. (2006). Evaluation and Treatment of Diabetic Foot Ulcers. *Clinical Diabetes*, *24*(2), 91-93.

Kwan, R. L., Wong, W., Yip, S., Chan, K., Zheng, Y., & Cheing, G. L. (2015). Pulsed Electromagnetic Field Therapy Promotes Healing and Microcirculation of Chronic Diabetic Foot Ulcers: A Pilot Study. *Advances in Skin & Wound Care*, *28*(5), 212–219.

Labovitiadi, O., Lamb, A. J., & Matthews, K. H. (2012). In vitro efficacy of antimicrobial wafers against methicillin-resistant Staphylococcus aureus. *Therapeutic Delivery*, *3*(4), 443-455.

Landau, Z., Migdal, M., Lipovsky, A., & Lubart, R. (2011). Visible light-induced healing of diabetic or venous foot ulcers: a placebo-controlled double-blind study. *Photomedicine and Laser Surgery*, *29*(6), 399–404.

Lansdown, A. B. G. (2002). Calcium: A potential central regulator in wound healing in the skin. *Wound Repair and Regeneration*, *10*(5), 271-285.

Lao, L. L., Peppas, N. A., Boey, F. Y. C., & Venkatraman, S. S. (2011). Modeling of drug release from bulk-degrading polymers. *International Journal of Pharmaceutics*, *418*(1), 28-41.

Lauer, G., Sollberg, S., Cole, M., Flamme, I., Stürzebecher, J., Mann, K., Krieg, T., et al. (2000). Expression and proteolysis of vascular endothelial growth factor is increased in chronic wounds. *Journal of Investigative Dermatology*, *115*(1), 12-18.

Lavery, L. A., Van Houtum, W. H., Armstrong, D. G., Harkless, L. B., Ashry, H. R., & Walker, S. C. (1997). Mortality following lower extremity amputation in minorities with diabetes mellitus. *Diabetes Research and Clinical Practice*, *37*(1), 41–47.

Lavery, L. A., Van Houtum, W. H., & Armstrong, D. G. (1997). Institutionalization following diabetes-related lower extremity amputation. *American Journal of Medicine*, *103*(5), 383–388.

Lawrence, M., & Jiang, Y. (2017). Porosity, pore size distribution, micro-structure. *In RILEM State-of-the-Art Reports*, *23*, 39–71.

Leaper, D. (2002). Sharp technique for wound debridement. *World Wide Wounds*, 2002.

LeBel, M. (1988). Ciprofloxacin: chemistry, mechanism of action, resistance, antimicrobial spectrum, pharmacokinetics, clinical trials, and adverse reactions. *Pharmacotherapy*, *8*(1), 3-33.

Lee, K. Y., & Mooney, D. J. (2012). Alginate: Properties and biomedical applications. *Progress in Polymer Science (Oxford),* 37(1), 106-126.

Lee, Y. H., Chang, J. J., Yang, M. C., Chien, C. T., & Lai, W. F. (2012). Acceleration of wound healing in diabetic rats by layered hydrogel dressing. *Carbohydrate Polymers*, *88*(3), 809-819.

Leese, G., Nathwani, D., Young, M., Seaton, A., Kennon, B., Hopkinson, H., Stang, D., et al. (2009). Use of antibiotics in people with diabetic foot disease: A consensus statement. *The Diabetic Foot Journal*, *12*(2), 1-10.

Lemmens, L., Claes, V., & Uzzell, M. (2008). Managing patients with metastatic colorectal cancer on bevacizumab. *British Journal of Nursing (Mark Allen Publishing)*, *17*(15), 944–949.

Leveen, H. H., Falk, G., Borek, B., Diaz, C., Lynfield, Y., Wynkoop, B. J., Mabunda, G. a, et al. (1973). Chemical acidification of wounds. An adjuvant to healing and the unfavorable action of alkalinity and ammonia. *Annals of surgery*, *178*(6), 745-753.

Lim, H., & Hoag, S. W. (2013). Plasticizer Effects on Physical–Mechanical Properties of Solvent Cast Soluplus® Films. *AAPS PharmSciTech*, *14*(3), 903-910.

Lin, S. Y., Lee, C. J., & Lin, Y. Y. (1991). The Effect of Plasticizers on Compatibility, Mechanical Properties, and Adhesion Strength of Drug-Free Eudragit E Films. *Pharmaceutical Research, 8*(9), 1137-1143.

Lipsky, B. A, Holroyd, K. J., & Zasloff, M. (2008). Topical versus systemic antimicrobial therapy for treating mildly infected diabetic foot ulcers: a randomized, controlled, double-blinded, multicenter trial of pexiganan cream. *Clinical infectious diseases: an official publication of the Infectious Diseases Society of America*, *47*(12), 1537-1545.

Lipsky, B. A., & Stoutenburgh, U. (2005). Daptomycin for treating infected diabetic foot ulcers: Evidence from a randomized, controlled trial comparing daptomycin with vancomycin or semi-synthetic penicillins for complicated skin and skin-structure infections. *Journal of Antimicrobial Chemotherapy*, *55*(2), 240-245.

Lipsky, B. A. (2004). Medical Treatment of Diabetic Foot Infections. *Clinical Infectious Diseases*, *39*(Suppl2), 104–114.

Lipsky, A. B., Berendt, A. R., Deery, G. H., Embil, J. M., Joseph, W. S., Karchmer, A. W., LeFrock, J. L., et al. (2004a). *Diagnosis and Treatment of Diabetic Foot Infections. Clinical Infectious Diseases*, *39*, 885-910.

Lipsky, B. A, Itani, K., & Norden, C. (2004b). Treating foot infections in diabetic patients: a randomized, multicenter, open-label trial of linezolid versus ampicillin-sulbactam/amoxicillin-clavulanate. *Clinical Infectious Diseases: An official Publication of the Infectious Diseases Society of America*, *38*, 17-24.

Lipsky, B. A., Baker, P. D., Landon, G. C., & Fernau, R. (1997). Antibiotic therapy for diabetic foot infections: comparison of two parenteral-to-oral regimens. *Clinical Infectious Disease*, *24*(4), 643-648.

Lipsky, B. A, Pecoraro, R. E., Larson, S. A, Hanley, M. E., & Ahroni, J. H. (1990). Outpatient management of uncomplicated lower-extremity infections in diabetic patients. *Archives of Internal Medicine*, *150*(4), 790-797.

Litscher, G., Wang, L., Schikora., D., Rachbauer, D., Schwarz, G., Ropele, S., Huber., E. (2004). Biological effects of painless laser needle acupuncture. *Medical Acupuncture*, *16*(1), 24–29.

Lloyd, L. L., Kennedy, J. F., Methacanon, P., Paterson, M., & Knill, C. J. (1998). Carbohydrate polymers as wound management aids. *Carbohydrate Polymers*, *37*(3), 315-322.

Loots, M. A. M., Lamme, E. N., Zeegelaar, J., Mekkes, J. R., Bos, J. D., & Middelkoop, E. (1998). Differences in cellular infiltrate and extracellular matrix of chronic diabetic and venous ulcers versus acute wounds. *Journal of Investigative Dermatology*, *111*(5), 850–857.

Malafaya, P.B., Silva, G.A. & Reis, R.L., 2007. Natural-origin polymers as carriers and scaffolds for biomolecules and cell delivery in tissue engineering applications. *Advanced Drug Delivery Reviews*, *59*(4-5), 207-233.

Malik, A., Mohammad, Z., & Ahmad, J. (2013). The diabetic foot infections: biofilms and antimicrobial resistance. *Diabetes & Metabolic Syndrome*, *7*(2), 101-107.

Manassa, E. H., Hertl, C. H., & Olbrisch, R.-R. (2003). Wound healing problems in smokers and nonsmokers after 132 abdominoplasties. *Plastic and Reconstructive Surgery*, *111*(6), 2082-2089.

Mannello, F., & Raffetto, J. D. (2011). Matrix metalloproteinase activity and glycosaminoglycans in chronic venous disease: the linkage among cell biology, pathology and translational research. *American Journal of Translational Research*, *3*(2), 149-158.

Mani, R., Gorman, F. W., & White, J. E. (1986). Transcutaneous measurements of oxygen tension at edges of leg ulcers: preliminary communication. *Journal of the Royal Society of Medicine*, *79*(11), 650-4.

Manoj, K., Debasish Mishra, B., Tapas Maity, B. K., & Snehasish Dutta Gupta, B. (2009). Screening Wound-Healing Potential of Different Aloe vera L. Germplasms at the Cellular Level. *Medicinal and Aromatic Plant Science and Biotechnology*, *3*(1), 62–64.

Markuson, M., Hanson, D., Anderson, J., Langemo, D., Hunter, S., Thompson, P., Rustvang, D. (2009). The relationship between hemoglobin A(1c) values and healing time for lower extremity ulcers in individuals with diabetes. *Advances in Skin & Wound Care*, *22*(8), 365–372.

Matthews, K. H., Stevens, H. N. E., Auffret, A. D., Humphrey, M. J., & Eccleston, G. M. (2008). Formulation, stability and thermal analysis of lyophilised wound healing wafers containing an insoluble MMP-3 inhibitor and a non-ionic surfactant. *International Journal of Pharmaceutics*, *356*(1-2), 110-120.

Matthews, K. H., Stevens, H. N. E., Auffret, A. D., Humphrey, M. J., & Eccleston, G. M. (2006). Gamma-irradiation of lyophilised wound healing wafers. *International Pharmaceutics*, *313*(1-2), 78-86.

Mauriello, C. T., Hair, P. S., Rohn, R. D., Rister, N. S., Krishna, N. K., & Cunnion, K. M. (2014). Hyperglycemia inhibits complement-mediated immunological control of S. aureus in a rat model of peritonitis. *Journal of Diabetes Research*, *2014*, 1-11.

Mayet, N., Choonara, Y. E., Kumar, P., Tomar, L. K., Tyagi, C., Du Toit, L. C., & Pillay, V. (2014). A comprehensive review of advanced biopolymeric wound healing systems. *Journal of Pharmaceutical Sciences*, *103*(8), 2211-2230.

McArdle, C., Lagan, K. M., & McDowell, D. A. (2014). The pH of wound fluid in diabetic foot ulcers -- the way forward in detecting clinical infection? *Current Diabetes Reviews*, *10*(3), 177-181.

Mear, J. B., Kipnis, E., Faure, E., Dessein, R., Schurtz, G., Faure, K., & Guery, B. (2013). Candida albicans and Pseudomonas aeruginosa interactions: More than an opportunistic criminal association? *Medecine et Maladies Infectieuses*. *43*(4), 146-151.

Medina, EL., Fan, D., Coughlin, L. A., Ho, E. X., Lamont, I. L., Reimmann, C., & Koh, A. Y. (2015). Candida albicans Inhibits Pseudomonas aeruginosa Virulence through Suppression of Pyochelin and Pyoverdine Biosynthesis. *Public Library of Science Pathogens*, *11*(8), 1-34.

Mendes, J. J., Marques-Costa, A., Vilela, C., Neves, J., Candeias, N., Cavaco-Silva, P., & Melo-Cristino, J. (2012). Clinical and bacteriological survey of diabetic foot infections in Lisbon. *Diabetes Research and Clinical Practice*, *95*(1), 153–161.

Menke, N. B., Ward, K. R., Witten, T. M., Bonchev, D. G., & Diegelmann, R. F. (2007). Impaired wound healing. *Clinics in Dermatology*, *25*(1), 19-25.

Mikamo, H., Hua, Y. X., Hayasaki, Y., Sato, Y., & Tamaya, T. (2000). Effects of fluconazole on viable cell count in experimental intraperitoneal Candida abscesses. *Journal of Infection and Chemotherapy*, *6*(3), 144–147.

Minatel, D. G., Frade, M. A. C., Franca, S. C., & Enwemeka, C. S. (2009). Phototherapy promotes healing of chronic diabetic leg ulcers that failed to respond to other therapies. *Lasers in Surgery and Medicine*, *41*(6), 433–441.

Missoni, E. M., Kalenic, S., Vukelić, M., De Syo, D., Belicza, M., Kern, J., & Babić, V. V. (2006). Role of yeasts in diabetic foot ulcer infection. *Acta medica Croatica: casopis Hravatske akademije medicinskih znanosti*, *60*(1), 43-50.

Missoni, E. M., Kalenic, S., Vukelić, M., De Syo, D., Belicza, M., & Vazić-Babić, V. (2005). Candida infections of diabetic foot ulcers. *Diabetologia Croatica*, *34*(1), 29-35.

Mohamed Ali, E. (2013). Ozone application for preventing fungal infection in diabetic foot ulcers. *Diabetologia Croatica*, *42*(1), 3-22.

Momoh, F. U., Boateng, J. S., Richardson, S. C. W., Chowdhry, B. Z., & Mitchell, J. C. (2015). Development and functional characterization of alginate dressing as potential protein delivery system for wound healing. *International Journal of Biological Macromolecules*, *81*, 137-150.

Monfre, M. J. (2016). Pressure Ulcers, Wound Healing - New insights into Ancient Challenges, Dr. Vlad Alexandrescu (Ed.), *InTech,* 329-340.

Morales, D. K., & Hogan, D. A. (2010). Candida albicans Interactions with Bacteria in the Context of Human Health and Disease. *Public Library of Science Pathogens*, *6*(4), 1-4.

Morales, J. O., & McConville, J. T. (2011). Manufacture and characterization of mucoadhesive buccal films. *European Journal of Pharmaceutics and Biopharmaceutics*, *77*(2), 187-199.

Morgan, D. (2002). Wounds - what should a dressing formulary include? *Hospital Pharmacist*, *9*, 261-266.

Moritz, S., Wiegand, C., Wesarg, F., Hessler, N., Müller, F. A., Kralisch, D., Hipler, U. C., et al. (2014). Active wound dressings based on bacterial nanocellulose as drug delivery system for octenidine. *International Journal of Pharmaceutics, 471*(1-2), 45-55.

Mosmann, T. (1983). Rapid colorimetric assay for cellular growth and survival: Application to proliferation and cytotoxicity assays. *Journal of Immunological Methods*, *65*(1–2), 55–63.

Moura, L. I. F., Dias, A. M. A., Carvalho, E., & De Sousa, H. C. (2013). Recent advances on the development of wound dressings for diabetic foot ulcer treatment - A review. *Acta Biomaterialia*, *9*(7), 7093-7114.

Mousley, M. (2007). Understanding diabetic foot ulcers. 1: Pathophysiology. *Nursing Times*, *103*(31), 28-29.

Nagesh, G., Santosh, J., Audumbar, M., & Manojkumar, P. (2016). A review on recent trends in oral drug delivery- lyophilized wafer technology. *International Journal of Research in Pharmacy and Pharmaceutical Sciences*, *1*(2), 5-9.

Nair, N., Biswas, R., Gotz, F., & Biswas, L. (2014). Impact of Staphylococcus aureus on pathogenesis in polymicrobial infections. *Infection and Immunity*, *82*(6), 2162-2169.

Nair, S., Peter, S., Sasidharan, A., Sistla, S., & Unni, A. K. K. (2006). Incidence of mycotic infections in diabetic foot tissue. *Journal of Culture Collections*, *5*(2006-2007*)*, 85-89.

Nawazz, Bentley, G. (2011). Surgical incisions and principles of wound healing. *Surgery, 29*(2), 59–62.

Negoro, T., Thodsaratpreeyakul, W., Takada, Y., Thumsorn, S., Inoya, H., & Hamada, H. (2016). Role of Crystallinity on Moisture Absorption and Mechanical Performance of Recycled PET Compounds. *In Energy Procedia*, *89*, 323–327.

Ng, S. F., & Jumaat, N. (2014). Carboxymethyl cellulose wafers containing antimicrobials: A modern drug delivery system for wound infections. *European Journal of Pharmaceutical Sciences*, *51*(1), 173-179.

Nicholas, E. (2016). Wound assessment: exudate. *Wound International, 7*(3), 30-33.

Nicks, B. A., Ayello, E. A., Woo, K., Nitzki-George, D., & Sibbald, R. G. (2010). Acute wound management: Revisiting the approach to assessment, irrigation, and closure considerations. *International Journal of Emergency Medicine*, *3*(4), 399-407.

Nigam, Y., Bexfield, A., Thomas, S., & Ratcliffe, N. A. (2006). Maggot therapy: The science and implication for CAM part II - Maggots combat infection. *Evidence-based Complementary and Alternative Medicine*, *3*(3), 303-308.

Nireesha, G., Divya, L., Sowmya, C., Venkateshan, N., Niranjan Babu, M., & Lavakumar, V. (2013). Lyophilization/Freeze Drying - An Review. *International Journal of Novel Trends in Pharmaceutical Sciences*, *3*(4), 87-98.

Nithyalakshmi, J., Nirupa, S., & Sumathi, G. (2014). Diabetic foot ulcers and Candida co-infection : a single centered study. *International Journal of Current Microbiology and Applied Sciences*, *3*(11), 413–419.

Oh, D. M., & Phillips, T. J. (2006). Sex Hormones and Wound Healing. *Wounds*, *18*, 8–18

Okoye, E. I. & Okolie, T.A., 2015. Development and *in vitro* characterization of ciprofloxacin loaded polymeric films for wound dressing. *International Journal of Health & Allied Sciences, 4*(4), 234-42.

Oliveira, M. B., Calixto, G., Graminha, M., Cerecetto, H., Gonzalez, M., & Chorilli, M. (2015). Development, characterization, and in vitro biological performance of fluconazole-loaded microemulsions for the topical treatment of cutaneous leishmaniasis. *Biomed Research International*, *2015*(96894), 1-12.

O'Loughlin, A., McIntosh, C., Dinneen, S. F., & O'Brien, T. (2010). Basic concepts to novel therapies: a review of the diabetic foot. *The International Journal of Lower Extremity Wounds*, *9*, 90-102.

Ong S, Y., Wu, J., Moochhala S, M., Tan M, H., & Lu, J. (2008). Development of a chitosan-based wound dressing with improved hemostatic and antimicrobial properties. *Biomaterials*. *29*(32), 4323-4332.

Otiniano, M. E., Du, X., Ottenbacher, K., Black, S. A., & Markides, K. S. (2003). Lower extremity amputations in diabetic Mexican American elders - Incidence, prevalence and correlates. *Journal of Diabetes and Its Complications*, *17*(2), 59–65.

Ozturk, E., Agalar, C., Keçeci, K., & Denkbas, E. (2006). Preparation and characterization of ciprofloxacin-loaded alginate/chitosan sponge as a wound dressing material. *Journal of Applied Polymer Science*, *101*(3), 1602-1609.

Panda, B., Parihar, A. S., & Mallick, S. (2014). Effect of plasticizer on drug crystallinity of hydroxypropyl methylcellulose matrix film. *International Journal of Biological Macromolecules*, *67*, 295–302.

Panomsuk, S. P., Hatanaka, T., Aiba, T., Katayama, K., & Koizumi, T. (1996). A study of the hydrophilic cellulose matrix: Effect of drugs on swelling properties. *Chemical & Pharmaceutical Bulletin*, *44*(5), 1039–1042.

Parenteau, B. R., Gauvin, R., & Berthod, F. (2010). Collagen-based biomaterials for tissue engineering applications. *Materials*, *3*(3), 1863-1887.

Patra, C. N., Swain, S., Sruti, J., Patro, A. P., Panigrahi, K. C., Beg, S., & Rao, M. E. B. (2013). Osmotic drug delivery systems: basics and design approaches. *Recent Patents on Drug Delivery & Formulation*, *7*(2), 150–61.

Pawar, H. V., Boateng, J. S., Ayensu, I., & Tetteh, J. (2014). Multifunctional medicated lyophilised wafer dressing for effective chronic wound healing. *Journal of Pharmaceutical Sciences*, *103*(6), 1720-1733.

Pawar, H. V., Tetteh, J., & Boateng, J. S. (2013). Preparation, optimisation and characterisation of novel wound healing film dressings loaded with streptomycin and diclofenac. *Colloids and Surfaces B: Biointerfaces*, *102*, 102-110.

Peek, M. E. (2011). Gender differences in diabetes-related lower extremity amputations. In *Clinical Orthopaedics and Related Research*, *469*, 1951–1955.

Peleg, A. Y., Hogan, D. A., & Mylonakis, E. (2010). Medically important bacterial-fungal interactions. *Nature reviews. Microbiology*, *8*(5), 340-349.

Pendse, S. P. (2010). Understanding diabetic foot. *International Journal of Diabetes in Developing Countries*, *30*(2), 75-79.

Percival, S., McCarty, S., Hunt, J., & Woods, E. (2014). The effects of pH on wound healing, biofilms, and antimicrobial efficacy. *Wound Repair and Regeneration*, *22*(2), 174-186.

Peters, B. M., & Noverra, M. C. (2013). Candida albicans-staphylococcus aureus polymicrobial peritonitis modulates host innate immunity. *Infection and Immunity*, *81*(6), 2178–2189.

Peters, B. M., Jabra-Rizk, M. A., O'May, G. A., William Costerton, J., & Shirtliff, M. E. (2012). Polymicrobial interactions: Impact on pathogenesis and human disease. *Clinical Microbiology Reviews*, *25*(1), 193-213.

Peterson, L. R., Lissack, L. M., Canter, K., Fasching, C. E., Clabots, C., & Gerding, D. N. (1989). Therapy of lower extremity infections with ciprofloxacin in patients with diabetes mellitus, peripheral vascular disease, or both. *The American Journal of Medicine*, *86*(6), 801-808.

Phoudee, W., & Wattanakaroon, W. (2015). Development of Protein-Based Hydrogel Wound Dressing Impregnated with Bioactive Compounds. *Natural Science*, *49*(1), 92-102.

Posnett, J., & Franks, P. J. (2008). The burden of chronic wounds in the UK. *Nursing Times*, *104*(3), 44-45.

Prete, P. E. (1997). Growth effects of Phaenicia sericata larval extracts on fibroblasts: Mechanism for wound healing by maggot therapy. *Life Sciences*, *60*(8), 505-510.

Puoci, F., Piangiolino, C., Givigliano, F., Parisi, O. I., Cassano, R., Trombino, S., Curcio, M., et al. (2012). Ciprofloxacin-collagen conjugate in the wound healing treatment. *Journal of Functional Biomaterials*, *3*(2), 361-371.

Pyorala, K., Laakso, M., & Uusitupa, M. (1987). Diabetes and atherosclerosis: An epidemiologic view. *Diabetes/Metabolism Reviews*, *3*(2), 463–524.

Queen, D., Gaylor, J. D. S., Evans, J. H., Courtney, J. M., & Reid, W. H. (1987). The preclinical evaluation of the water vapour transmission rate through burn wound dressings. *Biomaterials*, *8*(5), 367–371.

Rattanaruengsrikul, V., Pimpha, N., & Supaphol, P. (2009). Development of gelatin hydrogel pads as antibacterial wound dressings. *Macromolecular Bioscience*, *9*(10), 1004-1015.

Ravaghi, H., Flemming, K., Cullum, N., & Olyaee Manesh, A. (2006). Electromagnetic therapy for treating venous leg ulcers. *Cochrane Database Systematic Reviews*, *28*(2), CD002933. doi: 10.1002/14651858.CD002933.pub5.

Ravichandran, P., & Chitti, S P. (2015). Antimicrobial Dressing for Diabetic Foot Ulcer Colonized with MRSA. *Online Journal of Biological Sciences, 15*(4), 282-291.

Rezvanian, M., Tan, C. K., & Ng, S. F. (2016). Simvastatin-loaded lyophilized wafers as a potential dressing for chronic wounds. *Drug Development and Industrial Pharmacy*, *42*(12), 2055–2062.

Rhim, J., Gennadios, A., Weller, C., & Hanna, M. (2002). Sodium dodecyl sulfate treatment improves properties of cast films from soy protein isolate1. *Industrial Crops and Products*, *15*(3), 199-205.

Richard, J. L., Lavigne, J. P., & Sotto, A. (2012). Diabetes and foot infection: More than double trouble. *Diabetes/Metabolism Research and Reviews*, *28*(SUPPL 1), 46-53.

Riss, T. L., Moravec, R. A., Niles, A. L., Duellman, S., Benink, H. A., Worzella, T. J., & Minor, L. (2013). Cell Viability Assays. *Assay Guidance Manual*, *114*(8), 785–796.

Roca Jalil, M. E., Baschini, M., & Sapag, K. (2015). Influence of pH and antibiotic solubility on the removal of ciprofloxacin from aqueous media using montmorillonite. *Applied Clay Science*, *114*, 69–76.

Rodriguez, P. G., Felix, F. N., Woodley, D. T., & Shim, E. K. (2008). The role of oxygen in wound healing: A review of the literature. *Dermatologic Surgery*, *34*(9), 1159-1169.

Rohl, J & Murray, R. Z. (2013). Matrix metalloproteinases during wound healing – a double edged sword. *Wound Practice and Research*, *21*(4), 174-182.

Romanelli, M., Vowden, K., & Weir, D. (2010). Exudate management made easy. *Wounds International*, *1*(2), 1-6.

Rottmar, M., Richter, M., Mder, X., Grieder, K., Nuss, K., Karol, A., Bruinink, A. (2015). In vitro investigations of a novel wound dressing concept based on biodegradable polyurethane. *Science and Technology of Advanced Materials*, *16*(3), 1-5.

Roudbary, M., Razi, F., Mohammadi, S. R., Annabestani, Z., & Esfahani, E. N. (2014). Distribution of mycotic and bacterial infections among the patients with diabetic foot ulcers referred to diabetes and metabolic disorder clinic, Tehran, Iran 2011-2012. *European Journal of Experimental Biology, 4*(4), 20-25.

Roy, D. C., Tomblyn, S., Burmeister, D. M., Wrice, N. L., Becerra, S. C., Burnett, L. R., Saul, J. M., et al. (2015). Ciprofloxacin-Loaded Keratin Hydrogels Prevent Infection and Support Healing in a Porcine Full-Thickness Excisional Wound. *Advances in Wound Care*, *4*(8), 457-468.

Rubio, P. A. (1991). Use of semiocclusive, transparent film dressings for surgical wound protection: Experience in 3637 cases. *International Surgery*, *76*(4), 253-254.

Ruszczak, Z., & Friess, W. (2003). Collagen as a carrier for on-site delivery of antibacterial drugs. *Advanced Drug Delivery Reviews*, *55*(12), 1679-1698.

Sakharam, S. S., Shete, A. S., Patil Manisha, V., & Varne Bhushan, S. (2012). Different binary polymer mixture for solubility enhancement of poorly water-soluble drug by solid dispersion technique. *International Journal of PharmTech Research*, *4*(3), 1159–1166.

Sanniyasi, S., Balu, J., & Narayanan, CD. (2015). Fungal Infection: A Hidden Enemy in Diabetic Foot Ulcers. *Ankle Surg (Asia-Pacific)*, *2*(2), 74–76.

Sannino, A., Demitri, C., & Madaghiele, M. (2009). Biodegradable cellulose-based hydrogels: Design and applications. *Materials*, *2*(2), 353-373.

Santana, A. A., & Kieckbusch, T. G. (2013). Physical evaluation of biodegradable films of calcium alginate plasticized with polyols. *Brazilian Journal of Chemical Engineering*, *30*(4), 835–845.

Sarheed, O., Ahmed, A., Shouqair, D & Boateng, J. (2016). Antimicrobial Dressings for Improving Wound Healing, Wound Healing - New insights into Ancient Challenges, Dr. Vlad Alexandrescu (Ed.), *InTech*, 377-402., DOI: 10.5772/63961.

Satish, A., & Korrapati, P. S. (2015). Fabrication of a triiodothyronine incorporated nanofibrous biomaterial: its implications on wound healing. *RSC Advances*, *5*, 83773–83780.

Schafer, M., & Werner, S. (2008). Oxidative stress in normal and impaired wound repair. *Pharmacological Research: The Official Journal of the Italian Pharmacological Society*, *58*(2), 165–171.

Schreml, S., Szeimies, R.-M., Prantl, L., Landthaler, M., & Babilas, P. (2010). Wound healing in the 21st century. *Journal of the American Academy of Dermatology*, *63*(5), 866-868.

Schroeckh, V., Scherlach, K., Nutzmann, H.-W., Shelest, E., Schmidt-Heck, W., Schuemann, J., Martin, K., et al. (2009). Intimate bacterial-fungal interaction triggers biosynthesis of archetypal polyketides in Aspergillus nidulans. *Proceedings of the National Academy of Sciences*, *106*(34), 14558-14563

Schultz, G. S., Ladwig, G., & Wysocki, A. (2005). Extracellular matrix: Review of its roles in acute and chronic wounds. *World Wide Wounds*.

Semenza, G. L. (2000). HIF-1 and human disease: One highly involved factor. *Genes and Development*, *14*(16), 1983-1991.

Sgariglia, M. A., Soberón, J. R., Quiroga, E. N., Sampietro, D. A., & Vattuone, M. A. (2006). Evaluation of the antibacterial activity of different extractive forms of Guayacán ritidome. *Molecual Medicinal Chemistry, 11,* 21-23.

Shanmugam, P., M, J., & Susan S, L. (2013). The bacteriology of diabetic foot ulcers, with a special reference to multidrug resistant strains. *Journal of Clinical and Diagnostic Research*, *7*(3), 441–445.

Sharma, S., Rana, S., Thakkar, A., Baldi, A., Rsr, M., & Rk, S. (2016). Physical, chemical and phytoremediation technique for removal of heavy metals. *Journal of Heavy Metal Toxicity and Diseases*, *1*(2), 1–15.

Sharma, V. K., Khadka, P. B., Joshi, A., & Sharma, R. (2006). Common pathogens isolated in diabetic foot infection in Bir Hospital. *Kathmandu University Medical Journal*, *3*(15), 295-301

Sherman, R. A. (2003). Maggot therapy for treating diabetic foot ulcers unresponsive to conventional therapy. *Diabetes Care*, *26*(2), 446-451.

Shi, Y., Truong, V., Kulkarni, K., Qu, Y., Simon, G., & Boyd, R. et al. (2015). Light-triggered release of ciprofloxacin from an in situ forming click hydrogel for antibacterial wound dressings. *Journal of Materials Chemistry B*, *3*(45), 8771-8774.

Shilpa, A., Agrawal, S. S., & Ray, A. R. (2003). Controlled Delivery of Drugs from Alginate Matrix. *Journal of Macromolecular Science, Part C: Polymer Reviews*, *43*(2), 187-221.

Singh, N., Armstrong, D. G., & Lipsky, B. A. (2005). Preventing foot ulcers in patients with diabetes. *The Journal of the American Medical Association*, *293*(2), 217-228.

Singer, A. J., & Clark, R. A. (1999). Cutaneous wound healing. *The New England journal of medicine*, *341*(10), 738-46.

Skorkowska, T. K., Czemplik, M., Kulma, A., & Szopa, J. (2013). The local treatment and available dressings designed for chronic wounds. *Journal of The American Academy of Dermatology*, *68*(4), 117-126.

Smith, S. C., Faxon, D., Cascio, W., Schaff, H., Gardner, T., Jacobs, A., et al. (2002). Prevention conference VI: diabetes and cardiovascular disease: writing group VI: revascularization in diabetic patients. In: Proceeding of the American Heart Association; 18–20 January 2001; *Circulation*, *105*(18), 165–169.

Sood, A., Granick, M. S., & Tomaselli, N. L. (2014). Wound Dressings and Comparative Effectiveness Data. *Advances in wound care*, *3*(8), 511-529.

Sorensen, L. T., Jørgensen, S., Petersen, L. J., Hemmingsen, U., Bülow, J., Loft, S., & Gottrup, F. (2009). Acute Effects of Nicotine and Smoking on Blood Flow, Tissue Oxygen, and Aerobe Metabolism of the Skin and Subcutis. *Journal of Surgical Research*, *152*(2), 224–230.

Sotto, A., Lina, G., Richard, J.-L., Combescure, C., Bourg, G., Vidal, L., Jourdan, N., et al. (2008). Virulence potential of Staphylococcus aureus strains isolated from diabetic foot ulcers: a new paradigm. *Diabetes care*, *31*(12), 2318-24.

Spravchikov, N., Sizyakov, G., Gartsbein, M., Accili, D., Tennenbaum, T., & Wertheimer, E. (2001). Glucose Effects on Skin Keratinocytes Implications for Diabetes Skin Complications. *Diabetes*, *50*(7), 1627–1635.

Speak, K. (2014). Management of highly exuding diabetic foot ulcers. *Diabetic Foot Canada, 2*(3), 28-33.

Spichler, A., Hurwitz, B. L., Armstrong, D. G., & Lipsky, B. A. (2015). Microbiology of diabetic foot infections: from Louis Pasteur to "crime scene investigation". *BioMed Central Medicine*, *13*(2), 1-13.

Stewart, P. S. (2002). Mechanisms of antibiotic resistance in bacterial biofilms. *International journal of medical microbiology*, *292*(2), 107-113.

Stout, E. I., & McKessor, A. (2012). Glycerin-Based Hydrogel for Infection Control. *Advances in wound care*, *1*(1), 48-51.

Tan, J. S., & Joseph, W. S. (2004). Common Fungal Infections of the Feet in Patients with Diabetes Mellitus. *Drugs and Aging*. *21*(2), 101-112.

Taskin, A. K., Yasar, M., Ozaydin, I., Kaya, B., Bat, O., Ankarali, S., Yildirim, U., et al. (2013). The hemostatic effect of calcium alginate in experimental splenic injury model. *Turkish Journal of Trauma & Emergency Surgery*, *19*(3), 195-199.

Tarnuzzer, R. W., & Schultz, G. S. (1996). Biochemical analysis of acute and chronic wound environments. *Wound Repair and Regeneration*, *4*(3), 321–325.

Tarun, K., & Gobi, N. (2012). Calcium alginate/PVA blended nano fibre matrix for wound dressing. *Indian Journal Of Fibre & Textile Research*, *37*(2), 127-132.

Teixeira, K. I. R., Denadai, A. M. L., Sinisterra, R. D., & Cortes, M. E. (2015). Cyclodextrin modulates the cytotoxic effects of chlorhexidine on microrganisms and cells in vitro. *Drug Delivery*, *22*(3), 444–453.

Tentolouris, N., Petrikkos, G., Vallianou, N., Zachos, C., Daikos, G. L., Tsapogas, P., Markou, G., et al. (2006). Prevalence of methicillin-resistant Staphylococcus aureus in infected and uninfected diabetic foot ulcers. *Clinical Microbiology and Infection*, *12*(2), 186-189.

Thein, Z. M., Samaranayake, Y. H., & Samaranayake, L. P. (2006). Effect of oral bacteria on growth and survival of Candida albicans biofilms. *Archives of Oral Biology*, *51*(8), 672–680.

Thomas, S., & McCubbin, P. (2003). An in vitro analysis of the antimicrobial properties of 10 silver-containing dressings. *Journal of Wound Care*, *12*(8), 305–308.

Thomas, S.; Fear, M.; Humphreys, J.; Disley, L.; Waring, M. (1996). The effect of dressing on the production of exudate from venous leg ulcers. *Wounds*, *8*, 145–150.

Tiwari, S., Pratyush, D. D., Dwivedi, A., Gupta, S. K., Rai, M., & Singh, S. K. (2012). Microbiological and clinical characteristics of diabetic foot infections in northern India. *Journal of Infection in Developing Countries*, *6*(4), 329–332.

Trengove, N. J., Stacey, M. C., McGechie, D. F., & Mata, S. (1996). Qualitative bacteriology and leg ulcer healing. *Journal of Wound Care*, *5*(6), 277-280.

Tsai, W. C., Hsu, C. C., Chen, H. C., Hsu, Y. H., Lin, M. S., Wu, C. W., & Pang, J. H. S. (2009). Ciprofloxacin-mediated inhibition of tenocyte migration and down-regulation of focal adhesion kinase phosphorylation. *European Journal of Pharmacology*, *607*(1–3), 23–26.

Tsou, T. L., Tang, S. T., Huang, Y. C., Wu, J. R., Young, J. J., & Wang, H. J. (2005). Poly(2-hydroxyethyl methacrylate) wound dressing containing ciprofloxacin and its drug release studies. *Journal of Materials Science: Materials in Medicine*, *16*(2), 95-100.

TVL, H. B., Vidyavathi, M., K, K., Sastry, T., RV, S. kumar, Hima, B. T., Vidyavathi, M., et al. (2010). Preparation and evaluation of ciprofloxacin loaded chitosan-gelatin composite films for wound healing activity. *International Journal of Drug Delivery*, *2*(2), 173-182.

Udhayakumar, S., Shankar, K. G., Sowndarya, S., & Rose, C. (2017). Novel fibrous collagen-based cream accelerates fibroblast growth for wound healing applications: in vitro and in vivo evaluation. *Biomaterials Science*, *9*, 1–44.

Ueck, C., Volksdorf, T., Houdek, P., Vidal-Y-Sy, S., Sehner, S., Ellinger, B., & Brandner, J. M. (2017). Comparison of in-vitro and ex-vivo wound healing assays for the investigation of diabetic wound healing and demonstration of a beneficial effect of a triterpene extract. *Public Library of Science ONE*, *12*(1), 1-16.

Unnithan, A. R., Barakat, N. A. M., Tirupathi Pichiah, P. B., Gnanasekaran, G., Nirmala, R., Cha, Y. S., Jung, C. H., et al. (2012). Wound-dressing materials with antibacterial activity from electrospun polyurethane-dextran nanofiber mats containing ciprofloxacin HCl. *Carbohydrate Polymers*, *90*(4), 1786-1793.

Varma, M. V. S., Kaushal, A. M., Garg, A., & Garg, S. (2004). Factors affecting mechanism and kinetics of drug release from matrix-based oral controlled drug delivery systems. *American Journal of Drug Delivery*, *2*(1), 43–57.

Varsha TK, Rahul W, Bothikar ST, Vijay A, Bhate VM. (2016). Study of fungal infections in diabetic foot Ulcer. *Indian Journal of Microbiology Research*, *3*(4), 458–463.

Vedula, S. R. K., Ravasio, A., Lim, C. T., & Ladoux, B. (2013). Collective Cell Migration: A Mechanistic Perspective. *Physiology*, *28*(6), 370–379.

Vieira, M. G. A., Da Silva, M. A., Dos Santos, L. O., & Beppu, M. M. (2011). Natural-based plasticizers and biopolymer films: A review. *European Polymer Journal*, *47*(3), 254-263.

Vishal, G. N., Shivakumar, H. G. (2012). Investigation of Swelling Behavior and Mechanical Properties of a pH-Sensitive Superporous Hydrogel Composite. *Iranian Journal of Pharmaceutical Research*, *11*(2), 481–493.

Wang, S., Tu, Y., Wan, R., & Fang, H. (2012). Evaporation of tiny water aggregation on solid surfaces with different wetting properties. *Journal of Physical Chemistry B*, *116*(47), 13863–13867.

Wang, W., Lin, S., Xiao, Y., Huang, Y., Tan, Y., Cai, L., & Li, X. (2008). Acceleration of diabetic wound healing with chitosan-crosslinked collagen sponge containing recombinant human acidic fibroblast growth factor in healing-impaired STZ diabetic rats. *Life Sciences*, *82*(3-4), 190-204.

Wang, Q., Dong, Z., Du, Y., & Kennedy, J. F. (2007). Controlled release of ciprofloxacin hydrochloride from chitosan/polyethylene glycol blend films. *Carbohydrate Polymers*, *69*(2), 336–343.

White, R., & Cutting, K. F. (2006). Modern exudate management: a review of wound treatments. *World Wide Wounds*, 1-10.

Wibawa, T., Nurrokhman, Baly, I., Daeli, P. R., Kartasasmita, G., & Wijayanti, N. (2015). Cyclosporine A decreases the fluconazole minimum inhibitory concentration of candida albicans clinical isolates but not biofilm formation and cell growth. *Tropical Biomedicine*, *32*(1), 176–182.

Wiegand, C. & Hipler, U. (2008). Methods for the measurement of cell and tissue compatibility including tissue regeneration processes. *GMS Krankenhaushygiene Interdisziplinär*, *3*(1), 1-9.

Winston, J. A., & Miller, J. L. (2006). Treatment of onychomycosis in diabetic patients. *Clinical Diabetes*, *24*(4), 160-166.

Wiranidchapong, C., Ruangpayungsak, N., Suwattanasuk, P., Shuwisitkul, D., & Tanvichien, S. (2015). Plasticizing effect of ibuprofen induced an alteration of drug released from Kollidon SR matrices produced by direct compression. *Drug Development and Industrial Pharmacy*, *41*(6), 1037–1046.

Xiao, Y., Reis, L. A., Feric, N., Knee, E. J., Gu, J., Cao, S., & Radisic, M. (2016). Diabetic wound regeneration using peptide-modified hydrogels to target re-epithelialization. *Proceedings of the National Academy of Sciences*, *113*(40), 5792–5801.

Xu, R., Xia, H., He, W., Li, Z., Zhao, J., Liu, B., Wang, Y., et al. (2016). Controlled water vapor transmission rate promotes wound-healing via wound re-epithelialization and contraction enhancement. *Scientific Reports*, *6*(24596), 1-12.

Yazdanpanah, L., Nasiri, M., & Adarvishi, S. (2015). Literature review on the management of diabetic foot ulcer. WJD 5 th Anniversary Special Issues (4): Diabetes-related complications. *World Journal of Diabetes*, *6*(1), 37-53.

Zhang, H., Qadeer, A., & Chen, W. (2011). In situ gelable interpenetrating double network hydrogel formulated from binary components: Thiolated chitosan and oxidized dextran. *Biomacromolecules*, *12*(5), 1428-1437.

Zhang, Y., & Zhang, M. (2001). Microstructural and mechanical characterization of chitosan scaffolds reinforced by calcium phosphates. *Journal of Non-Crystalline Solids*, *282*(2–3), 159–164.

Zhao, X., Sun, X., Yildirimer, L., Lang, Q., Lin, Z. Y. (William), Zheng, R., Khademhosseini, A. (2017). Cell infiltrative hydrogel fibrous scaffolds for accelerated wound healing. *Acta Biomaterialia*, *49*, 66–77.

Zhou, C., Heath, D. E., Sharif, A. R. M., Rayatpisheh, S., Oh, B. H. L., Rong, X., Beuerman, R., et al. (2013). High water content hydrogel with super high refractive index. *Macromolecular Bioscience*, *13*(11), 1485-1491.

Zibaeenezhad, M. J., Aslani, A., Moniri, A., Kheiri, M. A., Heydari, S. T., Amanat, A., & Daneshvar, Z. (2012). Interventional revascularization of coronary artery lesions in diabetic patients; in-hospital and one year follow up. *International Cardiovascular Research Journal*, *6*(4), 113-117. Ulcers. *Clinical Diabetes*, *24*(2), 91-93.

Zubair, M., Malik, A., Ahmad, J., Rizvi, M., Farooqui, K. J., & Rizvi, M. W. (2011a). A study of biofilm production by gram-negative organisms isolated from diabetic foot ulcer patients. *Biology and Medicine*, *3*(2), 147-157.

Zubair, M., Malik, A., & Ahmad, J. (2011b). Clinico-microbiological study and antimicrobial drug resistance profile of diabetic foot infections in North India. *Foot (Edinburgh, Scotland)*, *21*(1), 6-14.

Web references:

Chronic Wound Care Guidelines (Abridged version). (2006). The Wound Healing society. http://woundheal.org/files/2017/final_pocket_guide_treatment.pdf. [Accessed: 16 December, 2016].

CIPRO® (ciprofloxacin hydrochloride) TABLETS CIPRO® (ciprofloxacin*) ORAL SUSPENSION.
http://www.accessdata.fda.gov/drugsatfda_docs/label/2005/019537s057,020780s019lbl.pdf [Accessed: 12 January, 2017].

Diabetes UK. (2016). Facts and Stats. https://www.diabetes.org.uk/About_us/What-we-say/Statistics/ [Accessed: 09 January, 2017].

Dissolving films. (2010). http://www.particlesciences.com/news/technical-briefs/2010/dissolving-films.html [Accessed: 03 January, 2017].

Kerr M. Diabetic Foot Care in England: an Economic Study. *Insight Heal Econ*. (2017). https://www.diabetes.org.uk/Upload/Shared practice/Diabetic footcare in England, An economic case study (January 2017).pdf. [Accessed: 16 December, 2017].

Moore, K. (2006). The interaction of a 'second generation' hydrogel with the chronic wound environment. Poster Presentation, EWMA Conference, Prague. Available at http://lohmann-rauscher.co.uk/downloads/clinical-evidence/AFC014-Keith-Moore-The-interaction-of-a-2nd-generation-h.pdf. [Accessed 29 January, 2018].

National Pressure Ulcer Advisory Panel. Educational and Clinical Resources/NPUAP Pressure Injury Stages [Internet]. Available from: http://www.npuap.org/resources/educational-and-clinical-resources/npuap-pressure-injury-stages/ [Accessed: 16 December , 2016].

Pressure ulcers. http://www.webmd.com/skin-problems-and-treatments/four-stages-of-pressure-sores [Accessed: 16 December, 2016].

Thomas S. The role of dressings in the treatment of moisture-related skin damage. World Wide Wounds 2008. http://www.worldwidewounds.com/2008/march/Thomas/Maceration-and-the-role-of-dressings.html [Accessed: 04 January, 2017].

Thomas S. (2007). Fluid Handling Properties of Allevyn Dressing. Wound Management Communication. http://www.dressings.org/TechnicalPublications/PDF/S+N-Allevyn-March-2007/Allevyn-Fluid-Handling-Properties-April-2007.pdf. [Access: 04 January, 2017].

Wound Source. http://www.woundsource.com/product-category/dressings/ antimicrobial-dressings. [Accessed: 29 December, 2016].

CHAPTER 8: APPENDIX

A.1 GENERAL INTRODUCTION AND LITERATURE REVIEW

Table A1.1 List of commercially available dressings indicated for chronic leg and DFUs treatment (Sarheed *et al*., 2016; Moura *et al*., 2013; Wound Source (web), 2017).

Dressing type	Brand Name	Manufacturer	Composition
Contact layer dressings	Acticoat* Flex 3	Smith & Nephew, UK	Elemental silver
	Acticoat* Flex 7		
	KerraContact™ Ag	Crawford Healthcare, US	Two non-adherent polyethylene mesh wound contact layers and one absorbent core made of polyester and all three layers are coated with silver
	SilverDerm 7®	DermaRite Industries, LLC, US	Non-adherent knitted nylon plated with approximately 99% elemental silver and 1% silver oxide.
	Therabond® 3D Antimicrobial Systems with Silvertrak™ Technology	Alliqua Biomedical, US	Silver-plated nylon three-dimensional fabric
Foams	RTD®	Keneric Healthcare, US	Silver zirconium phosphate (7mg/g), methylene blue

		(0.25mg/g), gentian violet (0.25mg/g)
Restore® Non-Adhesive Foam with Silver and Triact™ Technology	Hollister Incorporated-Wound Care, US	Non-adhesive foam containing silver
Ligasano®	Ligasano	Honeycomb-polyurethane foam
Algidex Ag®	DeRoyal, US	Ionic silver, alginate, and maltodextrin
Acticoat* Moisture Control Allevyn* Ag	Smith & Nephew, UK	Polyurethane foam coated with silver Silver sulfadiazine incorporated hydrocellular absorbent pad
Aquacel® Ag Duoderm®	ConvaTec, US	CMC with ionic silver Polyurethane foam

Biatain® Ag Biatain® Silicone Ag	Coloplast Corp, US	Silver
		Silicone-bordered foam dressing containing silver
HydraFoam/Ag™ Bordered Foam/Ag™	DermaRite Industries, LLC, US	Silver
		The inner layer consists of polyethylene net containing silver ions and an outer layer of breathable polyurethane film
MediPlus™ Comfort Border Foam Ag+	MediPurpose INC, US	Hydrocellular tri-layer coated with silver
Mepilex® Ag	Molnlycke Health Care, LLC, US	Polyurethane foam incorporated with silver sulphate
Optifoam® Ag	Medline Industries, Inc. US	Ionic silver

	V.A.C.® Granufoam Silver™	KCl, US	Silver
	Kendall™ AMD	Medtronic, US	Hydrophilic foam Impregnated with 0.5% polyhexamethylene biguanide (PHMB).
	IodoFoam®	Progressive Wound Care Technologies, US	Ansorbent foam complexed with iodine
Traditional dressings (Gauze, fibres, clothes, mats, pads, others)	Absorbent Dermanet® Ag+ Border (DagB)	DeRoyal, US	Silver containing multi-layered polyurethane pad
	TheraHoney® Sheet	Medline Industries, Inc. US	100% Manuka honey impregnated gauze dressing
	Manukahd®	ManukaMed USA, LLC	Absorbent gelling fiber with high amount of Manuka honey
	Medihoney®	Derma Sciences, Inc. US	Calcium alginate pad incorporated with 100% active Leptospermum honey

Aquacel® Ag Extra™ Hydrofiber®	ConvaTec, US	Ionic Silver with two layers of Hydrofiber® Technology
Actisorb™ Silver 220 Silvercel™	KCl, US	Silver loaded in a non-adherent nylon sleeve
		High G (guluronic acid) alginate, carboxymethylcellulose (CMC) and silver-coated nylon fibers.
Durafiber* Ag	Smith & Nephew, UK	Ionic silver containing fibre
Algisite Ag®		Calcium alginate and silver
Iodoflex*		Pad containing 0.9% cadexomer iodine
3M™ Tegaderm™ Ag Mesh	3M Health Care, US	Silver sulphate containing gauze dressing
Exsalt™ SD7	Crawford Healthcare, US	Silver

	Silverlon® Calcium Alginate	Argentum Medical, LLC, US	Calcium alginate and silver
	Silverlon® Island Wound & Surgical Dressings		Incorporating a silver wound contact layer, an absorbent rayon pad covered with a film transparent (urethane) layer and an adhesive border.
	Simpurity™ Silver Alginate Dressing Pads	Safe n' Simple, US	Alginate and silver particles
Biological dressings (Alginate, collagen and hyaluronic acid based dressings)	DermaGinate/Ag™ DermaCol™ Ag	DermaRite Industries, LLC, US	Alginate and silver
	SilvaKollagen® Gel		Collagen, sodium alginate, CMC, ethylenediamine tetraacetic acid (EDTA) and silver chloride Collagen gel added with silver
	Kaltostat®	ConvaTec, US	Sodium alginate and/or calcium alginate
	Bionect®	Dara VioScience, UK	Hyaluronic acid sodium salt, 0.2%

Unite® Biomatrix	Synovis Orthopedic and WoundCare, Inc, US	Non-reconstituted collagen
Dermanet® Ag+	DeRoyal, US	Ionic silver, alginate, and maltodextrin
Regranex® Gel	Healthpoint Biotherapeutics, US	Rh PDGF-BB loaded in sodium CMC
Maxorb® ES Ag+ Maxorb™ Extra Ag+	Medline Industries, Inc. US	CMC, alginate and silver
Opticell Ag+		Silver sodium hydrogen, zirconium phosphate, CMC and alginate
Arglaes® Powder		Alginate and ionic silver
Puracol Plus Ag+ MicroScaffold Collagen		Ionic silver in alginate powder
		Silver incorporated in a three-dimensional collagen microscaffold
Algicell® Ag	Derma Sciences, UK	Alginate and silver

Gentell Calcium Alginate Ag®	Gentell Wound and Skin Care, USA	Calcium alginate and silver sulfadiazine
CalciCare™	Hollister Incorporated - Wound Car, UK	high G (guluronic acid) calcium/sodium alginate and silver zirconium
Restore Calcium Alginate Dressing with Silver®		Calcium alginate and ionic silver
Promogran prisma™ Matrix	KCl, US	Oxidized regenerated cellulose (44%), collagen (55%) and silver (1%)
Sorbalgon Ag®	Hartman, USA	Calcium alginate and ionic silver
Suprasorb A + Ag Calcium Alginate®	L&R Inc, USA	Calcium alginate and silver
Askina Calgitrol Ag®	B. Braun Hospicare Ltd, Ireland	Calcium alginate and silver alginate with 10% of bounded water
Melgisorb® Plus	Mölnlycke Health Care, LLC, US	Calcium alginate
BGC Matrix®		Collagen based dressing with advanced carbohydrate beta-glucan

	SeaSorb Ag®	Coloplast, UK	Calcium alginate and ionic silver
Hydrogels	SilvaSorb® SilverMed™	Medline Industries, Inc. US	Hydrogel sheet with Ionic silver
			Amorphus hydrogel with silver
	DermaSyn/Ag™ Silver	DermaRite Industries, LLC, US	Hydrogel containing ionic silver
	Resta™ SilverGel®	SteadMed Medical, LLC, US	Ionic silver in hydrogel
	Solosite®	Smith & Nephew, UK	Polyethylene and polyurethane hy
	Silver-Sept®	Anacapa Technologies, Inc. US	Amorphous hydrogel with silver salt
	Silverseal®	Alliqua Biomedical, US	Hydrogel sheet with silver
	SilvrSTAT®	ABL Medical, LLC, US	Amorphous hydrogel with silver nanoparticles
	Actiformcool®		Alginate

		Activa Healthcare Ltd, UK	
Films	Silverlon®	Argentum Medical, LLC, US	Silver loaded polyurethane film
	OPSITE*	Smith & Nephew, UK	Transparent adhesive film dressing
Hydrocolloids	Silverseal® Hydrocolloid	Derma Sciences, US	Silver containing hydrocolloids
	Medihoney®		100% active leptospermum honey in combination with a hydrocolloid gelling agent
	GranuDerm™ Sentry™	Acute Care Solutions, LLC, US	Alginate hydrocolloid with polyurethane
	Granuflex®	ConvaTec, US	Hydrocolloid matrix bonded onto a vapour permeable film or foam backing
	Comfell®PlusUlcer	Coloplast, UK	Sodium-CMC and Calcium alginate hydrocolloid matrix layered with polyurethane film

Table A1.2 Summary of empirical antibiotic regimens for the treatment of infection in the diabetic foot (Leese *et al.*, 2009).

Severity or extent of infection	Recommended therapy	Susceptible pathogens
Mild (Treatment duration: 1 to 2 weeks)	**Primary** Flucloxacillin 1g orally four times a day **Oral alternatives** Doxycycline 100 mg orally twice per day, or Clindamycin 300-450 mg orally three times a day, or Cephalexin 500 mg orally four times a day.	*S. aureus*
Moderate (Treatment duration: 2 to 4 weeks, depending on the response to oral administration or parenterally followed by orally)	**Primary** Flucloxacillin 1g orally or parenterally (IV) four times a day **Oral alternatives** Co-trimoxazole 960 mg orally twice a day, or Co-amoxiclav 625 mg orally three times a day **If Allergic to penicillins**	*S. aureus* or Beta-haemolytic *Streptococci* Methicillin-resistant *S. aureus* (MRSA) Enterococcus

	Clindamycin 300-450 mg orally four times a day, or	*S. aureus* or
	Ciprofloxacin 500-750 mg orally twice a day	Beta-haemolytic *Streptococci*
	-Add metronidazole 400 mg orally three times a day if anaerobes present	
		Anaerobes
	Alternatives	
	Ciprofloxacin 400 mg and metronidazole 500 mg IV three times a day, or	
	Gentamicin 500 mg and metronidazole mg IV three times a day	*P. aeruginosa*
		Anaerobes
	-Add vancomycin IV if MRSA infection suspected	
		MRSA
Severe (Treatment duration: 2 to 4 weeks depending on response; administered parenterally then switch to orally. If osteomyelitis is present, then treatment is continued for at least 4-6 weeks.)	**Primary**	
	Co-amoxiclav 1.2g IV three times a day	*Enterococcus*
	Oral switch	
	Co-amoxiclav 625 mg three times a day, or	*Enterococcus*
	Co-trimoxazole 960 mg twice a day	MRSA

If allergic to Penicillin

Ciprofloxacin 400 mg IV twice a day and metronidazole 500 mg three times a day, or	*P. aeruginosa*
Gentamicin IV (minor serum concentration) and metronidazole 500 mg IV three times a day	Anaerobes
-Add vancomycin IV (minor serum concentration) if MRSA present.	*P. aeruginosa*
	Anaerobes

Alternatives

MRSA

Ciprofloxacin 500-750 mg orally twice a day and metronidazole 400 mg orally

three times a day

If continued MRSA cover required

P. aeruginosa

Linezolid 600 mg orally twice a day, or

Anaerobes

Rifampicin 300 mg orally twice a day with either:

-Doxycycline 100 mg orally twice a day

MRSA

-Trimethoprim 200 mg twice a day

	-Fusidic acid 500 mg three times a day	MRSA
	In case of osteomyelitis	MRSA
	Sodium fusidate 500 mg orally three times a day, or	
	Rifampicin 600 mg orally twice a day	

A.2   FORMULATION DEVELOPMENT AND PHYSICO-CHEMICAL CHARACTERIZATION OF CALCIUM ALGINATE BASED DRESSINGS

A.2.1   Solvent casting of films

Solvent casting method involves several manufacturing steps such as preparation of gel, removal of air bubbles, transferring the appropriate amount of gel onto the casting surface, drying at a particular temperature, cutting the final dosage form to get adequate amount of drug and packing (Bala *et al*., 2013). Some important factors need to be considered during the entire manufacturing process including homogeneity and viscosity of the gel, entrapped air bubbles, content uniformity and residual solvent content in the final dosage form (Morales and McConville, 2011). During the preparation of gel, it needs to be stirred with or without applying heat that depends on the solvent, polymer and drug. Vigorous stirring creates air bubbles and these entrapped air bubbles can be removed by vacuum. Gentle stirring creates low air bubbles which can be withdrawn by keeping the gel steady state before pouring onto the casting surface. Solvent casting requires relatively lower temperature compared to hot-melt extrusion and therefore this method is ideal for manufacturing heat sensitive API (active pharmaceutical ingredient). The final dosage form can be cut into desired dimensions as it is an excellent advantage for wound dressing.

Solvent cast technique has some drawbacks. Proteins or any biological API cannot be incorporated into polymeric matrix by solvent cast technique because of long manufacturing time and heat. Biological API may degrade or denature due to prolonged production time. Sometimes it is difficult to remove entrapped air bubbles due to homogeneity reasons and that also affects the content uniformity along the casting surface. Additionally slow solvent evaporation process retards manufacturing speed and therefore requires high energy and costs (Morales and McConville, 2011).

A.2.2   Lyophilization

Lyophilization or freeze drying is a technique in which water or another solvent is frozen, followed by its removal from the frozen sample by sublimation and then by desorption (Nireesha *et al*., 2013). Freeze drying involves three steps such as freezing, primary drying and secondary drying. In the freezing stage, some part of the liquid sample becomes ice crystal and the remaining part is freeze concentrated into the glassy state where the viscosity is too high to allow further crystallization. The next step is primary drying wherein the ice cake formed during

the freezing cycle is removed by sublimation under vacuum at low temperatures, resulting in a highly porous structure in the remaining amorphous solute that is typically 30% water. The final step is secondary drying, wherein most of the remaining water is desorbed from the glass as the temperature of the sample gradually is increased while maintaining low pressures. Ideally, the final dosage form is a dry, easily reconstituted cake with high surface area (Beaty, 2004).

There are some advantages and limitations of freeze drying technique. Biological products such as vaccines or other injectable which are heat sensitive can be easily incorporated into the polymeric matrix as the method involves operating at lower temperature. The residual moisture content of final dosage is very low that enhancing stability and shelf-life of the products. The volatile compounds are difficult to freeze dry as it may be removed by the vacuum. Moreover, due to increased handling and processing time it loses acceptability. The cost may also an issue depending on the product (Nireesha *et al.*, 2013).

A.2.3 Texture analysis

Texture analysis is used to characterize the tensile properties and mucoadhesion of the solvent cast films and lyophilized wafers. It is important to measure the tensile properties such as tensile strength, Young's modulus, % elongation at break and hardness to achieve soft, durable, elastic, pliable, flexible and stress resistant dressings (Boateng *et al.*, 2008). In addition, the dressings should have adequate adhesive properties such as stickiness, cohesiveness and work of adhesion (WOA) to adhere with the wound surface. The American Society for Testing and Materials (ASTM) states that the film's thickness should be less than 1 mm (ASTM, 1997).

Tensile strength of a film is the maximum force applied to a point at which the film tears apart and describes how brittle and hard the film is (Boateng *et al.*, 2008). The maximum peak from stress-strain curve (force vs distance curve) is recorded as maximum force. *Young's modulus* is the measurement of rigidity or stiffness of the film. It is calculated from the slope of the initial linier portion of stress-strain curve. *Percentage elongation at break* is determination of elasticity or flexibility of the film. It is the measurement of maximum length before tearing apart from the original length when a tensile force is applied. Plasticizers such as GLY, sorbitol or polyethylene glycol (PEG) have effect on the above mechanical properties (Vieira *et al.*, 2011; Lim and Hoag, 2013; Chamarthy and Pinal, 2008).

Compressive test is applied to the sample of a greater thickness than film such as lyophilized wafer to characterize hardness by texture analysis. Hardness is the resistance of the sample to the compressive force (N) of deformation and ease of recovery (Boateng *et al*., 2008). Hardness is measured to check the brittleness and uniformity of texture. *Adhesive test* is also performed by texture analysis for stickiness, cohesiveness and total work of adhesion of the dosage forms. Stickiness is the maximum force (N) required to detach the sample from the model surface (gelatine gel or agar gel). This is also known as adhesive strength. The adhesive strength of wafer as a wound dressing is essential in wound healing where dressings should adhere with the wound bed and painless removal (Boateng *et al*., 2008). Cohesiveness is the ability of the sample to repel the detachment from the model surface. Inadequate cohesiveness of the sample leads to easy separation from the wound site. It is calculated by recording the distance travelled (mm) before detaching from the simulated wound surface (Momoh *et al*., 2015). The total WOA indicates the amount of total energy involved in the probe during the separation from the simulated wound surface. It is computed by taking the area under the force versus distance curve (Boateng *et al*., 2015).

A.2.4   Scanning electron microscopy (SEM)

SEM is used to observe the surface morphology and topography of the dressings (Momoh *et al*., 2015). Lyophilized wafers are usually porous and this can be confirmed by SEM analysis. The uniformity, size and shape of the pores within the polymeric matrix can also be observed by SEM. In case of films the homogeneity of the polymer and drugs may be assumed with SEM observation. The homogenous surface indicates homogenous mixture of polymers and drugs (Boateng *et al*., 2013). Rough surface of the films indicate crystallization or recrystallization (Boateng *et al*., 2013). SEM observation is very important to understand the fact of fluid handling properties of the dressings.

A.2.5   X-ray diffraction (XRD)

XRD is performed to determine the physical form of the dressings, pure drugs and polymers. This analysis reveals whether the pure drugs and polymers are amorphous or crystalline. The changes in characteristic peaks of drugs or polymers can also be observed (Boateng *et al*., 2013). It also tells the changes in crystallinity after final formulation.

A.2.6 Fourier transform infrared (FTIR) spectroscopy

FTIR is used to identify the characteristic functional groups present in the starting material (polymers and drugs) and their incorporation into polymeric matrix. It also confirms the possibility of interaction of chemical bonds between the drug and polymer. The peak absorption at specific wavenumber indicates the nature of peak assignment/vibration type such as asymmetric, symmetric bending etc. (Sahoo *et al.*, 2012). FTIR is also helpful in identifying unknown sample with quality, purity and consistency of the sample (Sahoo *et al.*, 2011).

A.3 FLUID HANDLING FUNCTIONAL CHARACTERIZATION OF CALCIUM ALGINATE BASED DRESSINGS

A.3.1 Porosity

The ideal measurement of porosity of the dressings can be done by Brunauer-Emmett Teller (BET) analysis. The actual pore size can be determined by this method. Though in the project, solvent displacement method has been used to measure the percentage porosity. In this method ethanol is used as a solvent.

A.3.2 Water absorption, EWC and swelling index

Water absorption and EWC tests are performed to investigate the maximum water uptake and water holding capacities respectively of the dressings. In addition, swelling studies are undertaken to investigate the rate of water uptake capacity of the dressings. These tests are important to determine the appropriate dressings (Boateng *et al.*, 2008).
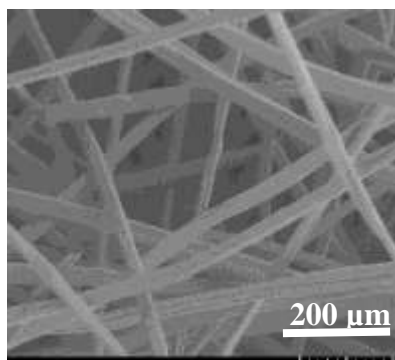
Algisite Ag®

Figure A.3.1 SEM images of Algisite Ag® captured at x200 magnification.

A.3.3   Water vapour transmission rate (WVTR)

WVTR indicates the ability of dressings to absorb fluid and draw it out from the wound bed across the materials into the atmosphere. Wound dressings require an adequate level of moisture transmission to keep the wound area comfortable and promote the healing process. Dry wounds exhibit the most water loss thus decrease body temperature and rate of metabolism. Therefore, the wound dressing should not reduce the body fluid significantly. The wound dressings should provide adequate moisture content by maintaining a balance between water absorption and transmission as well as humidity in the affected site (Kim *et al*., 2007. Higher water vapour transmission rate promotes epithelization process of wound healing. On the other hand, lower WVTR delays the healing process by accumulating excess wound exudates (Xu *et al*., 2016) and leads to skin maceration, excoriation and microbial growth.

A.3.4   Evaporative water loss (EWL)

EWL of the dressings is recorded to determine the behaviour of the dressings when exposed to air. The dressings should be able to take up and hold more exudate and oedema fluid quickly from the wound bed into its matrix by an active upward-directed process (Balakrishnan *et al*., 2005). After holding exudates, the dressings should promote evaporation of wound fluid from its surface to maintain moist wound environment.

A.3.5   Moisture content

After freeze drying or solvent casting the final dosage forms retain some moisture. This residual moisture content of the dressings is determined by thermogravimetric analysis (TGA). High residual water content into the dressings is susceptible to microbial growth and also retards stability by accelerating crystallization of the drug upon storage (Kianfar *et al*., 2013). Therefore, it is important to maintain low moisture content. However, high moisture content of the dressings can maintain the wound and surrounding skin in an optimum state of hydration thus implies the dressings to functions efficiently under compression (Thomas, 2008).

A.3.6   Drug release

Drug release depends on the type of polymer, drug and also type of delivery system. It also depends on the amount of drug and polymer. Higher amount of polymer decreases rate of drug release due to increase in mechanical strengths resulting slow hydration and dissolution. The wafers seem to higher rate of drug release than films because of porosity. The highly porous

wafers allow rapid water ingress than film. Therefore, the rate of swelling, dissolution and diffusion of drug from the resulting gel is faster from the wafers than films (Boateng *et al.*, 2009). The drug release mechanism of films and wafers involves water uptake and subsequent swelling to form a gel layer which controls drug release by viscous resistance to drug diffusion (Boateng *et al.*, 2009).
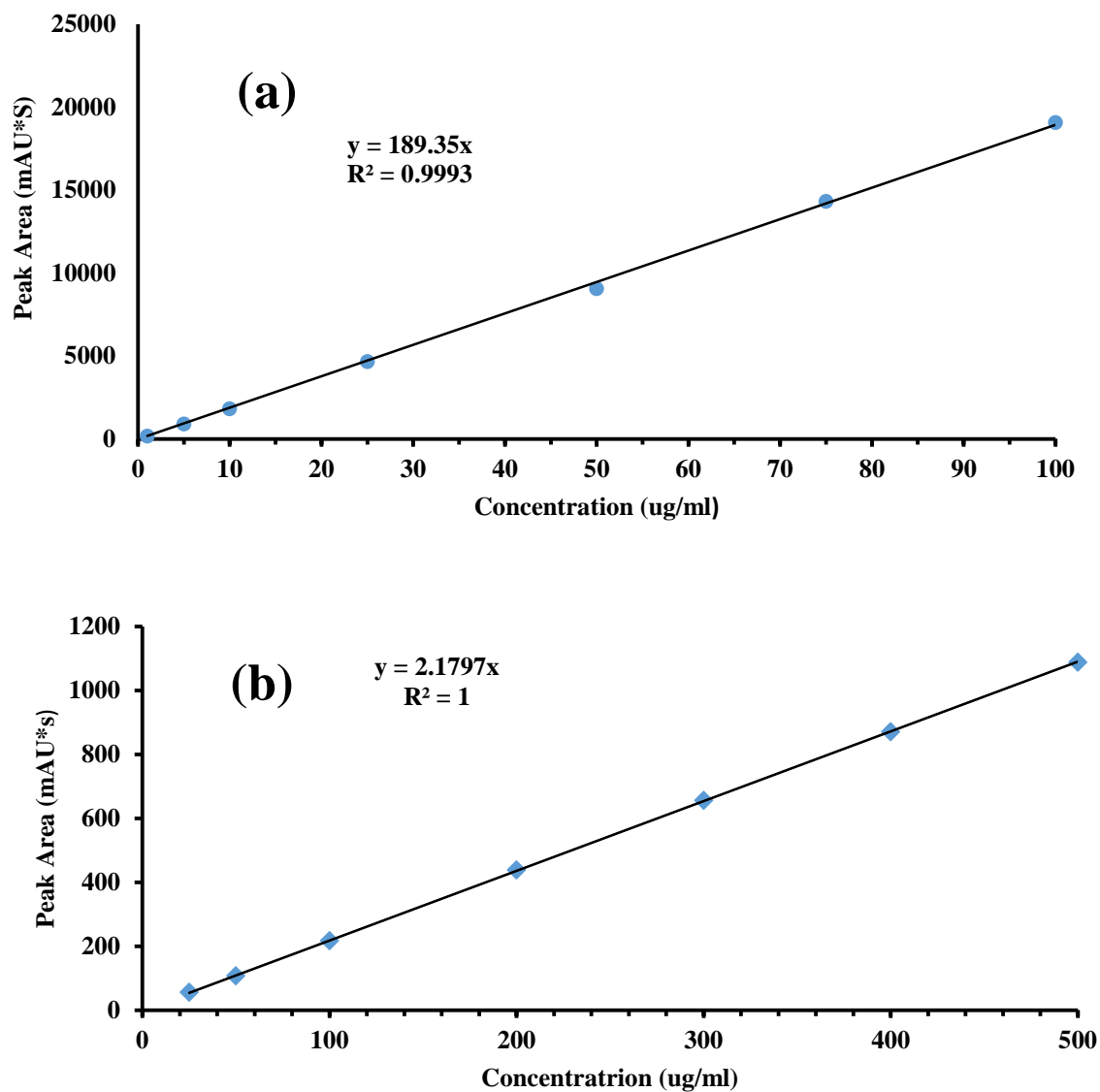

Figure A3.2   Standard calibration curve of CIP (a) and FLU (b) obtained by HPLC method.

Table A3.1   Surface pH of formulated dressings and commercial products ($n = 3 \pm$ SD).

Films	pH
CA-0.00% GLY	9.61 ± 0.10
CA-9.09% GLY	9.59 ± 0.13
CA-20.00% GLY	9.61 ± 0.19
CA-33.33% GLY	9.53 ± 0.18
CA-42.86% GLY	9.43 ± 0.19
CA-50.00% GLY	9.45 ± 0.11
CA-CIP 0.005%	7.36 ± 0.04
CA-CIP 0.010%	7.17 ± 0.17
CA-CIP 0.025%	7.22 ± 0.10
CA-FLU 0.05%	7.17 ± 0.19
CA-FLU 0.10%	6.61 ± 0.07
CA-FLU 0.20%	6.61 ± 0.05
CA-CIP:FLU (1:10)	6.71 ± 0.02
CA-CIP:FLU (1:20)	7.01 ± 0.07
Wafers	
CA-BLK	9.24 ± 0.09
CA-CIP 0.005%	6.94 ± 0.20
CA-CIP 0.010%	7.30 ± 0.20
CA-CIP 0.025%	7.42 ± 0.20
CA-FLU 0.05%	7.07 ± 0.07

CA-FLU 0.10%	6.90 ± 0.13
CA-FLU 0.15%	7.05 ± 0.09
CA-FLU 0.30%	7.61 ± 0.13
CA-FLU 0.40%	8.17 ± 0.18
CA-CIP:FLU (1:10)	7.07 ± 0.20
CA-CIP:FLU (1:20)	7.39 ± 0.18
CA-CIP:FLU (1:30)	7.44 ± 0.09
Algisite Ag®	6.04 ± 0.04
Actiformcool®	5.91 ± 0.20

A.4   ANTIMICROBIAL PROPERTIES OF DRUG LOADED CALCIUM ALGINATE DRESSINGS TARGETTING BACTERIAL, FUNGAL AND MIXED INFECTIONS IN CHRONIC LEG AND DIABETIC FOOT ULCERS

A.4.1   Antimicrobial study

Antimicrobial study is carried out to test the release of the drugs from the dressings in enough quantities to inhibit or kill microorganisms. The antimicroobial assay is done by turbidimetric and Kirby-Bauer disc diffusion methods. The CIP loaded dressings were tested against *E. coli, S. aureus and P. aeruginosa*. The FLU loaded dressings were tested against *C. albicans*. The combined DL (CIP and FLU) dressings were tested against the mixed infections (either *E. coli* and *C. albicans,* or *S. aureus* and *C. albicans,* or *P. aeruginosa* and *C. albicans*). In the broth dilution method, the cloudiness of the bacterial suspension is observed visually and spectroscopically after suspending the dressings into it. In this method, the number of cells can be counted after different times of incubation (Time-kill assay) to check how quickly the dressings eradicate microbial load. In Kirby-Bauer disc diffusion method zone of inhibition (ZOI) is measured.

A.5 *IN-VITRO* CELL VIABILITY AND MIGRATION STUDIES FOR SAFETY AND WOUND SCRATCH ASSAY

A.5.1 Cell viability and migration study

When the dressing is applied onto the wound site, it also touches the normal healthy skin. Therefore, cell viability study is important to check whether the dressings are safe to normal healthy skin. The test is done by methyl thiazolyldiphenyl-tetrazolium bromide (MTT) assay. The dressings should be biocompatible with the human keratinocytes (skin cells) and should induce cell migration which is essential for complete wound closure. The cell migration study was performed by wound scratch assay.

A.5.2 Procedure for cell trypsinization

The cells were trypsinized when they had reached about 80-85% confluence. In the first step the cells were rinsed with Dulbecco's phosphate buffered saline (D-PBS) (5 and 15 ml for 25 and 75 cm^2 culture flasks respectively). The D-PBS was discarded from the flask and the required amount of pre-warmed trypsin- EDTA solution (1 and 3 ml for 25 and 75 cm^2 culture flasks respectively) was added to the flask. The flask was gently rocked to ensure complete coverage of the trypsin-EDTA solution over the cells. After that, the flask was incubated at 37°C for 6 - 7 min. At this stage, the adherent cells started to detach from the surface of the flask. To ensure maximum detachment of cells, the flask was gently tapped from several sides. When the majority of the cells appeared to have detached, the same volume of trypsin neutralizing solution as trypsin-EDTA solution was added to the flask. The dissociated cells were transferred into a sterile centrifuge tube. At this point, the flask was microscopically observed to see any remaining cells in the flask, and any such additional cells were collected by adding D-PBS in the flask. After that, the cells were centrifuged at 150x g for 5 minutes. The neutralized dissociation solution was aspirated from the cell pellet and re-suspended cells in 2-8 ml fresh pre-warmed complete growth medium. The number of cells were counted with haemocytometer and seeded at the required density for the experiments.

Table A5.1 The microscopic observations of live/dead cells of human primary epidermal keratinocytes treated with CIP loaded films over 72 h of culture. Polygonal shape indicates live cells while black arrows indicate the floating round shape as dead cells. Images were taken by FLoid® Cell Imaging Station with 40x objective lens.

Table A5.2   The microscopic observations of live/dead cells of human primary epidermal keratinocytes treated with CIP loaded wafers over 72 h of culture. Polygonal shape indicates live cells while black arrows indicate floating round shapes as dead cells. Images were taken by FLoid® Cell Imaging Station with 40x objective lens.

Table A5.3   Representative photomicrographs (4x) of keratinocyte cells' morphology based on viability test of FLU loaded dressings. Triton-X-100 and untreated cells were considered as positive and negative controls respectively. Scale bar: 500 μm.
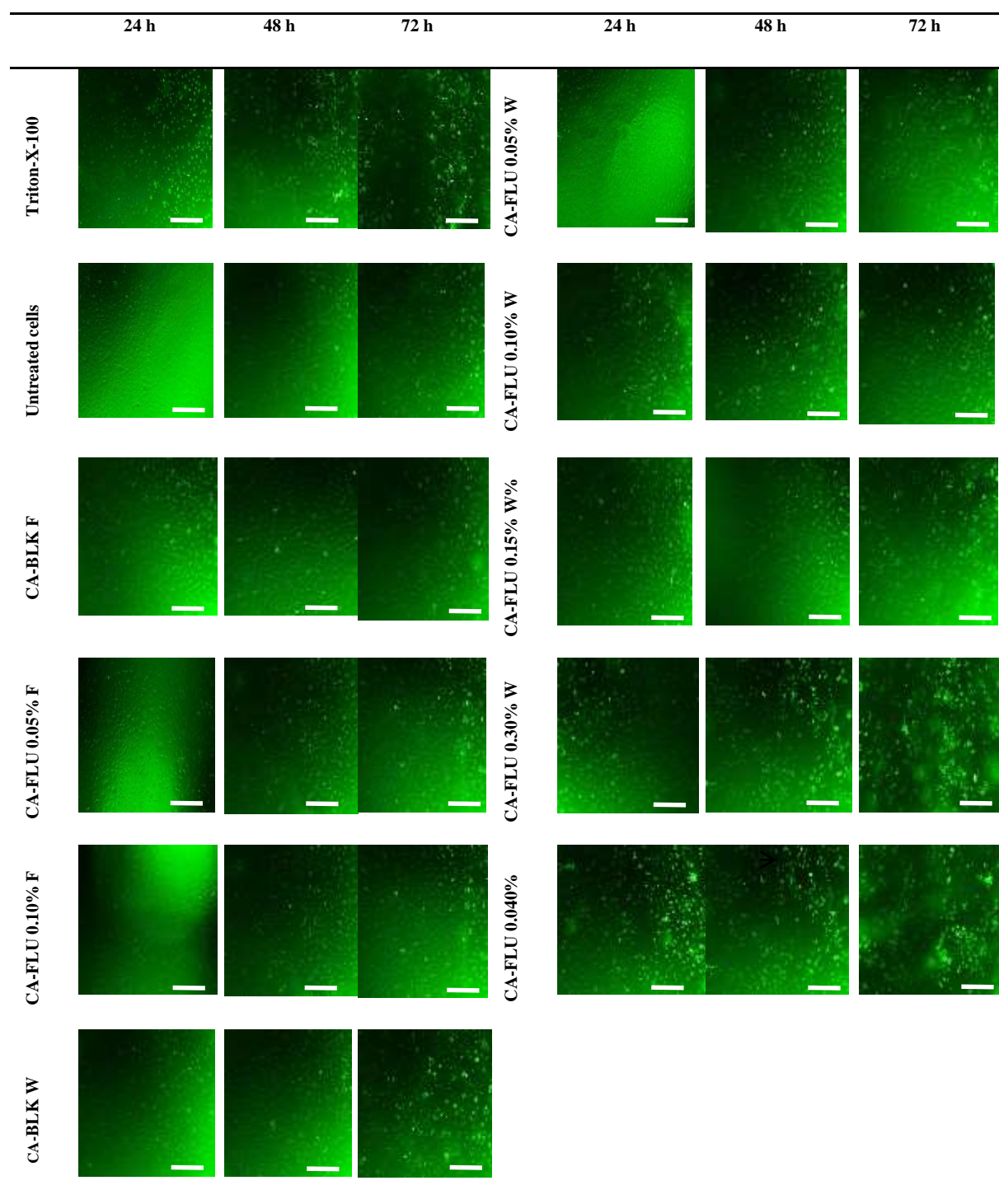
F: Film; W: Wafer

Table A5.4   Photomicrographs (4x) showing the proliferation of human keratinocyte cells seeded at a density of 1 x 10^5 cells/ml with the combined DL dressings. Scale bar: 500 μm.
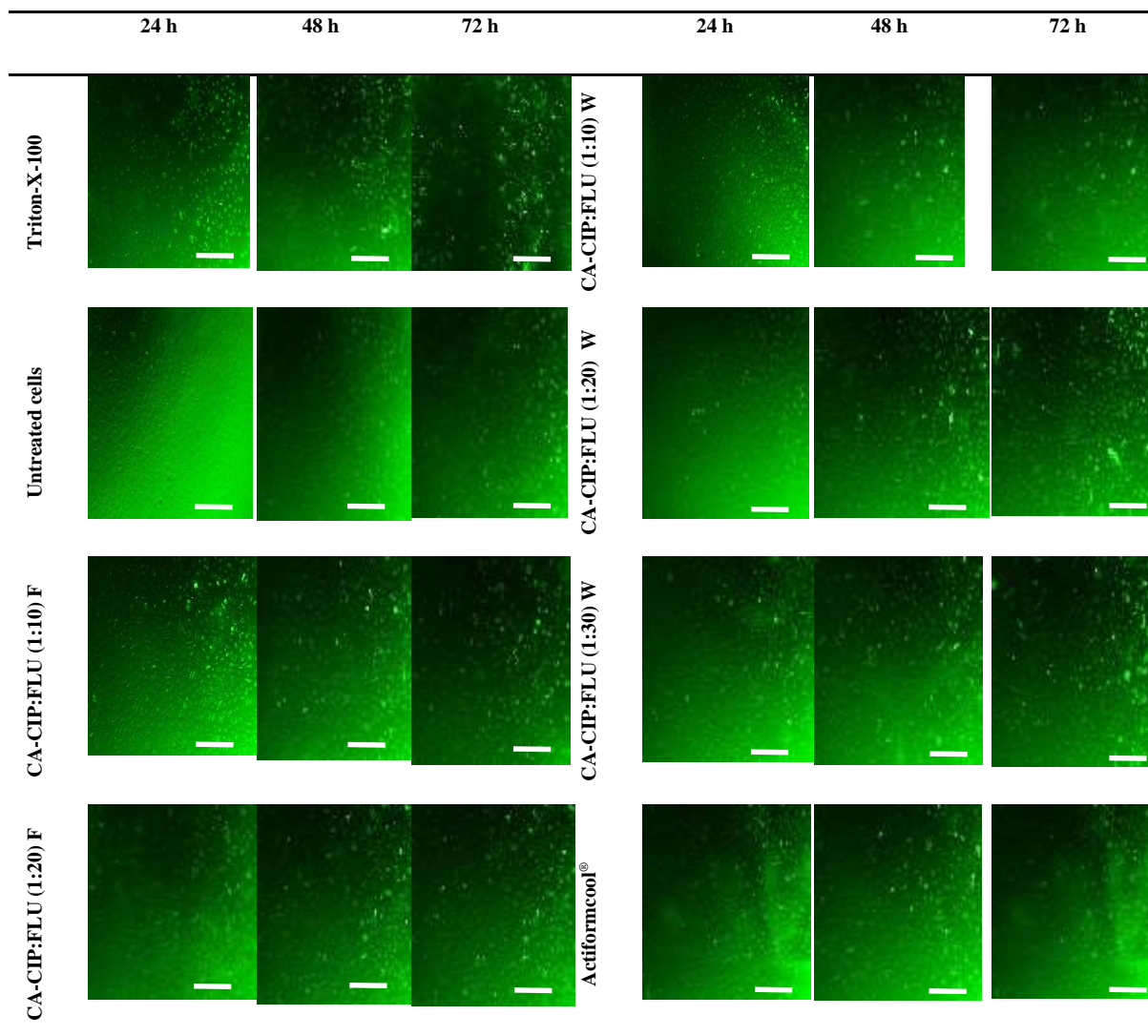
F: Film; W: Wafer

A7 References

Bala, R., Khanna, S., Pawar, P., & Arora, S. (2013). Orally dissolving strips: A new approach to oral drug delivery system. *International Journal of Pharmaceutical Investigation*, *3*(2), 67.

Balakrishnan, B., Mohanty, M., Umashankar, P. R., & Jayakrishnan, A. (2005). Evaluation of an in situ forming hydrogel wound dressing based on oxidized alginate and gelatin. *Biomaterials*, *26*(32), 6335-6342.

Beaty, N. B. (2004). Lyophilization. *Journal of Pharmaceutical Sciences*, *93*(9), 1-34.

Boateng, J., Pawar, H., & Tetteh, J. (2015). Evaluation of in vitro wound adhesion characteristics of composite film and wafer based dressings using texture analysis and FTIR spectroscopy: a chemometrics factor analysis approach. *Royal Society of Chemistry Advances*, *5*(129), 107064-107075.

Boateng, J. S., Pawar, H. V., & Tetteh, J. (2013). Polyox and carrageenan based composite film dressing containing anti-microbial and anti-inflammatory drugs for effective wound healing. *Pharmaceutics*, *441*(1-2), 181-191.

Boateng, J. S., Stevens, H. N. E., Eccleston, G. M., Auffret, A. D., Humphrey, M. J., & Matthews, K. H. (2009). Development and mechanical characterization of solvent-cast polymeric films as potential drug delivery systems to mucosal surfaces. *Drug Development and Industrial Pharmacy*, *35*(8), 986-996.

Boateng, J., Matthews, K., Stevens, H., & Eccleston, G. (2008). Wound Healing Dressings and Drug Delivery Systems: A Review. *Journal of Pharmaceutical Sciences*, *97*(8), 2892-2923.

Chamarthy, S. P., & Pinal, R. (2008). Plasticizer concentration and the performance of a diffusion-controlled polymeric drug delivery system. *Colloids and Surfaces A: Physicochemical and Engineering Aspects*, *331*(1-2), 25-30.

Hifumi, H., Ewing A, V., Kazarian, S. G. (2016). ATR-FTIR spectroscopic imaging to study the drying and dissolution of pharmaceutical polymer-based films. *International Journal of Pharmaceutics*. *515*(1-2), 57-68.

Kianfar, F., Ayensu, I., & Boateng, J. S. (2013). Development and physico-mechanical characterization of carrageenan and poloxamer-based lyophilized matrix as a potential buccal drug delivery system. *Drug Development and Industrial Pharmacy*, *9045*, 1-9.

Kim, I. Y., Yoo, M. K., Seo, J. H., Park, S. S., Na, H. S., Lee, H. C., Kim, S. K., et al. (2007). Evaluation of semi-interpenetrating polymer networks composed of chitosan and poloxamer for wound dressing application. *International Journal of Pharmaceutics*, *341*(1-2), 35-43.

Leese, G., Nathwani, D., Young, M., Seaton, A., Kennon, B., Hopkinson, H., Stang, D., et al. (2009). Use of antibiotics in people with diabetic foot disease: A consensus statement. *The Diabetic Foot Journal*, *12*(2), 1-10.

Lim, H., & Hoag, S. W. (2013). Plasticizer Effects on Physical–Mechanical Properties of Solvent Cast Soluplus® Films. *AAPS PharmSciTech*, *14*(3), 903-910.

Limban C, Missir AV, Grumezescu AM, et al. Bioevaluation of novel anti-biofilm coatings based on PVP/Fe 3O4 nanostructures and 2-((4-Ethylphenoxy)methyl)-N-(arylcarbamothioyl)benzamides. *Molecules*. 19(8), 12011-12030 (2014).

Momoh, F. U., Boateng, J. S., Richardson, S. C. W., Chowdhry, B. Z., & Mitchell, J. C. (2015). Development and functional characterization of alginate dressing as potential protein delivery system for wound healing. *International Journal of Biological Macromolecules*, *81*, 137-150.

Morales, J. O., & McConville, J. T. (2011). Manufacture and characterization of mucoadhesive buccal films. *European Journal of Pharmaceutics and Biopharmaceutics*, *77*(2), 187-199.

Moura, L. I. F., Dias, A. M. A., Carvalho, E., & De Sousa, H. C. (2013). Recent advances on the development of wound dressings for diabetic foot ulcer treatment - A review. *Acta Biomaterialia*, *9*(7), 7093-7114.

Nireesha, G., Divya, L., Sowmya, C., Venkateshan, N., Niranjan Babu, M., & Lavakumar, V. (2013). Lyophilization/Freeze Drying -An Review. *International Journal of Novel Trends in Pharmaceutical Sciences*, *3*(4), 87-98.

Sahoo, S., Chakraborti, C. K., & Behera, P. K. (2012). Spectroscopic investigations of a Ciprofloxacin/HPMC mucoadhesive suspension. *International Journal of Applied Pharmaceutics*, *4*(3), 1-8.

Sahoo, S., Chakraborti, C. K., Mishra, S. C., Nanda, U. N., & Naik, S. (2011). FTIR and XRD investigations of some fluoroquinolones. *International Journal of Pharmacy and Pharmaceutical Sciences*, *3*(3), 165-170.

Sarheed, O., Ahmed, A., Shouqair, D & Boateng, J. (2016). Antimicrobial Dressings for Improving Wound Healing, Wound Healing - New insights into Ancient Challenges, Dr. Vlad Alexandrescu (Ed.), *InTech* , 377-402., DOI: 10.5772/63961.

Thomas S. The role of dressings in the treatment of moisture-related skin damage. World Wide Wounds 2008. http://www.worldwidewounds.com/2008/march/Thomas/Maceration-and-the-role-of-dressings.html [Accessed: 04 January, 2017].

Vieira, M. G. A., Da Silva, M. A., Dos Santos, L. O., & Beppu, M. M. (2011). Natural-based plasticizers and biopolymer films: A review. *European Polymer Journal*, *47*(3), 254-263.

Xu, R., Xia, H., He, W., Li, Z., Zhao, J., Liu, B., Wang, Y., et al. (2016). Controlled water vapor transmission rate promotes wound-healing via wound re-epithelialization and contraction enhancement. *Scientific Reports*, *6*(24596), 1-12.